Autoimmunity in idiopathic epilepsies and encephalopathies of childhood

Dr Sukhvir Wright
Linacre College
University of Oxford

Thesis submitted for degree of Doctor of Philosophy
Michaelmas Term 2014

Medical Sciences Division
University of Oxford

Abstract

Immune mechanisms are thought to be involved in the pathological disease process in a number of childhood epileptic syndromes and encephalitis. Of particular interest is the occurrence of autoantibodies to essential neuronal proteins, for example the N-methyl-D-aspartate receptor (NMDAR), in the blood and spinal fluid in some of these patients. The aims of this study were: to examine the sera of newly diagnosed paediatric epilepsy patients for specific neuronal autoantibodies, correlate to epilepsy phenotype and disease outcomes; to investigate the pathogenicity and epileptogenicity of central nervous system (CNS) autoantibodies *in vivo*; and to test new therapies *in vitro* and *in vivo* based on the potential pathogenic mechanisms.

In 290 paediatric patients with new-onset epilepsy and seizures tested for CNS autoantibodies, 11.4% were positive (33/290 versus 8/112 in controls; p=0.01, Fisher's exact test). Previously unreported contactin-2 antibody positive and contactin-associated-protein 2 (CASPR2) antibody positive epilepsy patients were described. Patients with 'focal epilepsy of unknown cause' were more likely to be antibody positive.

To test the pathogenicity and epileptogenicity of these antibodies, a novel *in vivo* telemetry system was used to continuously record electroencephalogram (EEG) in mice injected into the cerebral lateral ventricle with NMDAR antibody (NMDAR-Ab) positive immunoglobulin (IgG). Although no spontaneous seizures were seen, mice challenged with the pro-convulsant pentylenetetrazole (PTZ) had increased seizure susceptibility, and more epileptiform "spikes" in the EEG after PTZ compared to healthy control (HC) IgG injected mice. Seizure susceptibility strongly correlated with binding intensity of NMDAR-Ab IgG analysed in post-mortem tissue. Given the hypothesis this epileptogenic effect was mediated by NMDAR-Abs internalising cell surface NMDARs, and to try and rescue this deficit, a neurosteroid, pregnenolone sulphate (PregS) known to increase NMDAR cell surface expression, was therapeutically used. This approach worked *in vitro*, and although *in vivo* effects were not yet established, treatment with neurosteroids may be beneficial for autoantibody mediated neurological disease.

Acknowledgements

I have been privileged to have had two truly inspirational women, Professor Angela Vincent and Dr Louise Upton, as my mentors and supervisors. Angela, your enthusiasm for science, extensive knowledge and relentless energy has amazed me throughout this process. I am grateful for your support and all you have taught me. Louise, your unrivalled expertise, remarkable patience and wonderful sense of humour enabled me to really enjoy the world of basic science, thank you.

Kevin Hashemi, for the incredible support with the EEG system, as well as Professor Walker and the UCL group. For laboratory work in Oxford, special thanks to Teresa Moloney, as well as Beth Lang, Leslie Jacobson, Patrick Waters, Mark Woodhall, Linda Clover, Anjan Nibber, and Rosie Pettingill for invaluable help with assays, teaching and support. Great thanks to Dr Tony McShane for allowing me to do clinics, the highlight of my month, and to Yael Hacohen for always insightful clinical expertise, and collection of clinical data. Dr Karri Lamsa, Dimitrios Kotzadimitriou, Kathryn Newton and Dr Lorenz Muller, thanks to all for assistance with the ex-vivo electrophysiology experiments. Julian Bartram and Lucasz Stasiak from DPAG, thank you for initial work with the in-vivo studies. Thanks to all the staff in the BMS for expert advice, professionalism, support and guidance.

Thanks to Professor Brouwer and the Dutch Study of Epilepsy Group, Associate Professor Russell Dale and Dr Jehan Suleiman, and Dr Pierre Szepetowski and colleagues for generously collaborating in this work, and Dr Arjune Sen for invaluable advice.

Thanks to the patients and families who consented to be part of this work. I am also grateful to the Wellcome Trust for my funding award and the Neurology consultants at Birmingham Children's Hospital for giving me that first nudge into research.

Finally thanks to all my friends and family. To Kim for being there no matter what, and your always perfect advice. To Susan for a friendly, warm home-away-from-home in Oxford, thank you. To Dylan and Daisy, for putting up with me working and keeping me totally grounded, focussed and smiling. To Ben, the biggest thanks of all, as without your hard work, support and humour none of this would have been possible.

Abbreviations

Ab	antibody
AchR	acetylcholine receptor
ACTH	adrenocorticotrophic hormone
ADAM	Disintegrin And Metalloprotease domain
ADLTE	autosomal dominant lateral temporal lobe epilepsy
AED	anti-epileptic drug
AMPA	alpha amino-3-hydroxy-5-methyl-4-isoxazolepropionic acid
BBB	blood brain barrier
BSA	bovine serum albumin
CAE	childhood absence epilepsy
CASPR	contactin-associated-protein-2
CNS	central nervous system
CSF	cerebrospinal fluid
CSWS	continuous spike and wave in slow-wave sleep
DAPI	4',6-diamidino-2-phenylindole
DIV	day in vivo
DLAP5	DL-2-Amino-5-phophonopentanoic acid
DMSO	dimethylsulfoxide
DMEM	Dulbecco's modified Eagle's medium
DSCE	Dutch Study of Childhood Epilepsy
DTX	dendrotoxin
EEG	electroencephalogram
ECP	event classification processor
EFGP	enhanced green fluorescent protein
EPSC	excitatory post-synaptic current
GABA	gamma amino butyric acid
GAD	glutamic acid decarboxylase
GluR	glutamate receptor
GLUT1	glucose-transporter-1
GTC	generalised tonic clonic
HBSS	Hank's balanced salt solution
HEK	human embryonic kidney cells
HEPES	4-(2-hydroxyethyl)-1-piperazineethanesulfonic acid
HF	high frequency
HFP	high-frequency power
HLA	human leucocyte antigen
HP-β-CD	2-Hydroxypropyl-β-cyclodextrin
HRP	horseradish peroxidase
HSV	herpes simplex virus
Hz	hertz
ICV	intracerebroventricular
IGE	idiopathic generalised epilepsy
IgG	immunoglobulin
IL	interleukin
ILAE	international league against epilepsy

Int	intermittency
IPSC	inhibitory post-synaptic current
ITU	intensive therapy unit
IVIG	intravenous immunoglobulins
Kv	voltage gated potassium channel subunit
LD	learning difficulties
LE	limbic encephalitis
LGI1	leucine-rich-glioma-inactivated-1
LKS	Landau-Kleffner syndrome
LRP4	lipoprotein receptor-related protein 4
LTD	long-term depression
LTP	long-term potentiation
MAP-2	microtubule-associated protein 2
MBP	myelin basic protein
MDT	multi-disciplinary team
MEM	minimal essential medium
MG	myasthenis gravis
MRI	magnetic resonance imaging
MuSK	muscle specific kinase
NB	neurobasal
NBQX	2,3-dihydroxy-6-nitro-7-sulfamoyl-benzo[f]quinoxaline-2,3-dione
NGS	normal goat serum
NMDA	N-methyl-D-aspartate
NMJ	neuromuscular junction
NMO	neuromyelitis optica
NMT	neuromyotonia
OCB	oligoclonal bands
OMS	opsoclonus myoclonus syndrome
PBS	phosphate buffered saline
PCDH19	protacadherin 19
PERM	progressive encephalomyelitis
PET	positron emission topography
PFA	paraformaldehyde
PICU	paediatric intensive care unit
PLEX	plasma exchange
PLL	poly-L-lysine
pM	picomole per litre
PNS	peripheral nervous system
PREGS	pregnenolone sulphate
PTZ	pentylenetetrazol
RIA	radioimmunoassay
SCLC	small cell lung carcinoma
SLE	systemic lupus erythematous
SE	status epilepticus
Sp	spikeyness
SPS	stiff person syndrome
SW	Sukhvir Wright
TIDM	type 1 diabetes mellitus
TNF	tumour necrosis factor
TP	transient power
TUNEL	terminal deoxynucleotidyl transferase dUTP

UCL	University College London
UKISS	United Kingdom infantile spasms study
VGCC	voltage gated calcium channel
VGKC	voltage gated potassium channels
WT	wild type
YFP	yellow fluorescent protein

Table of contents

List of Tables

List of Figures

CHAPTER 1 - Introduction

1.1 "Autoimmune disease" - a recent discovery

When antibodies were first discovered in blood by Jules Bordet at the turn of the 20th century, early researchers believed antibodies and the immune system were solely designed to protect us from disease. The concept of *autoimmune* disease, where the immune system itself becomes a destructive pathological force acting against the host's own cells, was coined 'horror autotoxicus' by Paul Ehrlich, meaning the immune system could never turn on itself. This was following experiments where he failed to show the production of autoantibodies in goats who were immunized with their own red blood cells (Mackay 2010, Chang 2014). Ehrlich's condemnation of autoimmunity overshadowed the interpretation of results of important discoveries over the next 30 years, including early models of experimental autoimmune encephalomyelitis (EAE) relevant to multiple sclerosis (Rivers and Schwentker 1935). Here, the authors made no reference to autoantibody autosensitisation as the underlying pathogenesis in monkeys injected with extracts of rabbit brain. This was despite them developing central nervous system (CNS) disease, with inflammatory histological lesions including myelin destruction. Instead, they focused on the possible transfer of an infectious agent, even though proving sterility of the injected extracts!

The mainly incidental discoveries of the Coombs test in autoimmune haemolytic anaemia, anti-nuclear antibodies in systemic lupus erythematosus, rheumatoid factor and thyroid receptor antibodies during the 1940s and 1950s (Roitt, Doniach et al. 1956) heralded the beginning of the acceptance of autoimmunity as a pathological process. These discoveries were translated into animal models and improvements in microscopy

enabled detection of immunological deposits in frozen sections of tissues and detection of antibodies in serum of patients with suspected autoimmune diseases (Mackay 2010).

In 1957, guidelines to establish whether a human disease was autoimmune in origin were published (Witebsky, Rose et al. 1957), modelled on Koch's postulates to define microbiological pathogenicity. These defining criteria for autoantibody pathogenicity were recently revised in light of advances in molecular biology and require evidence from the three main areas listed below (Rose and Bona 1993) .

1. Reproduction of disease in a normal recipient by direct transfer of autoantibody.
    - An example is transplacental transmission of pathogenic autoantibodies from an affected mother to foetus in utero. This also applies to direct infusion of pathogenic human autoantibodies to experimental animals.
2. Reproduction of autoimmune diseases in experimental animal models.
    - Here, once the antigen is identified in the human disease, the essential features of the disease are reproduced by active immunization.
3. Circumstantial evidence from clinical clues.
    - These include clinical history of other autoimmune diseases in the same individual or family members, lymphocytic infiltration of target organ, human-leucocyte-antigen (HLA) association and favourable response to immunotherapy.

This thesis is concerned with the presence, relevance, and pathogenicity of the recently discovered CNS autoantibodies in paediatric epilepsy. Autoimmune diseases of the *peripheral* nervous system (PNS) were identified in the 1970s with pathogenic

autoantibodies described in Myasthenia Gravis (MG) and Lambert-Eaton myasthenic syndrome (LEMS). These classical autoantibody-mediated diseases fulfil Witebsky's criteria and form the basis of our understanding for CNS autoantibody diseases (Vincent 2002), and are therefore considered first below.

1.2 Peripheral Nervous System Autoantibodies

Both the pre- and post-synaptic regions of the neuromuscular junction (NMJ) harbour potential targets for pathogenic autoantibodies in myasthenic syndromes. The autoantibodies target the extracellular domain of the membrane protein in the target tissue. MG, generally considered a paradigm of organ specific autoimmune disease, is associated with antibodies to three post-synaptic proteins at the NMJ, the acetylcholine receptor (AChR), muscle-specific kinase (MuSK) and low-density lipoprotein receptor-related protein 4 (LRP4). Autoantibodies to the pre-synaptic voltage-gated calcium channels (VGCC; P/Q type) cause LEMS. These autoantibodies can all be readily measured in the serum using radioimmunoassays and cell-based assays (Vincent, Waters et al. 2012). Common to both diseases is the progressive muscle weakness, association with underlying malignancy, symptom improvement with plasma exchange (PLEX) (removal of circulating antibodies), and HLA association (Newsom-Davis 2005).

In MG, autoantibody-induced AChR loss at the NMJ reduces neuromuscular transmission, ultimately leading to the characteristic muscle weakness. This AChR loss is mediated through three different mechanisms: autoantibody mediated complement-dependent lysis of AChRs and post-synaptic membrane damage; cross-linking of the AChRs by divalent antibodies (IgG1 and IgG3) causing internalization and reduced

surface expression; and direct competition of AChR antibodies with AChR on receptor binding sites preventing receptor activation and ion channel opening. Passive transfer of MG human IgG into mice reproduced typical electrophysiological features of the disease and reduced the number of AChRs at the NMJ (Toyka, Brachman et al. 1975, Toyka, Drachman et al. 1977), thereby confirming the autoantibody pathogenicity. Further proof of this came from the first use of PLEX in a MG patient with AChR antibodies which produced remarkable improvement (Newsom-Davis, Vincent et al. 1978).

The study of autoantibodies in PNS disorders has led to a greater understanding of the role of autoantibodies in neurological disease overall. As described, these autoantibodies bind to the extracellular domain of membrane proteins, can be measured easily in serum, cause pathologically relevant effects *in vivo* and *in vitro*, and affected patients show substantial improvements with immunotherapy. Many of these features can also be applied to the increasingly recognised CNS autoantibodies in patients suffering from encephalitis and epilepsy. The main CNS target antigens in these diseases include the N-methyl-D-aspartate receptor (NMDAR), the voltage-gated potassium channel complex (VGKC-complex) and associated proteins (leucine-rich-glioma-inactivated-1 (LGI1), contactin-associated-protein-2 (CASPR2), contactin-2), the α-amino-3-hydroxy-5-methyl-4-isoxazolepropionic acid receptor (AMPAR) receptor, Gamma-aminobutyric acid B ($GABA_B$) receptors and the intracellular glutamic-acid decarboxylase (GAD) enzyme. The characteristic features of these antigens and autoantibodies, their related neurological diseases and relevance to epilepsy will now be discussed.

1.3 Central Nervous System Autoantibodies

1.3.1 N-methyl-D-aspartate receptor (NMDAR)

The NMDAR is a voltage-dependent ionotropic glutamate receptor which is essential for normal synaptic function. It is made up of GluN1 (NR1) and GluN2 (NR2) subunits, each of which contain a large N-terminal extracellular domain, three transmembrane domains, a re-entrant transmembrane domain and intracellular C-terminus. The NR1 subunit is obligatory in the heteromeric assembly of the receptor and, with the four NR2 subunits (NR2A-D), different combinations form functional channels with specific pharmacological and physiological properties. NMDARs are inactive at resting membrane potential as there is a voltage-dependent block of the channel pore with magnesium ions. Activation of the NMDAR also requires the binding of a co-agonist (glycine or D-serine) to the glycine modulatory site. Activated NMDARs allow Ca^{2+} influx into the cell which is required for activation of signalling cascades essential to the processes of long-term potentiation (LTP) and long-term depression (LTD) that are thought to underlie learning and memory. The functional importance of NMDARs in normal brain function is best illustrated by human disease where the NMDAR is implicated in an underlying pathogenic process.

1.3.2 NMDAR-Ab encephalitis

Autoantibodies to the NMDAR were first identified in a case series of 12 young females (14-44 years) who developed severe encephalopathy with specific clinical features, including psychiatric symptoms, seizures, cognitive and autonomic dysfunction, movement disorder and decreased level of consciousness, often requiring ventilatory support (Dalmau, Tuzun et al. 2007). Given that 11 of the patients had a teratoma of the ovary and one a mature teratoma in the mediastinum, and the patients responded

symptomatically to a combination of tumour removal and immunotherapy, this disorder was initially reported as a paraneoplastic encephalitis affecting young women. However, many studies since have reported cases that include males, children and patients with no underlying malignancy (Dalmau, Gleichman et al. 2008, Florance, Davis et al. 2009, Davies, Irani et al. 2010, Armangue, Titulaer et al. 2013, Titulaer, McCracken et al. 2013, Viaccoz, Desestret et al. 2014).

Even though the characteristic symptoms described above, that define NMDAR-Ab encephalitis, are seen during the illness in both adults and children, there is some debate as to the symptom presentation of disease in these two groups of patients (Rosenfeld, Titulaer et al. 2012). In adults, the most common presenting symptoms are delusions, hallucinations, abnormal behaviour, and psychosis, i.e. neuropsychiatric. Some studies have suggested that in children, a more neurological phenotype including abnormal movements, seizures and focal or sensory deficits are more commonly the first symptoms (Armangue, Titulaer et al. 2013). However, in a prospective study of 31 children in the United Kingdom (UK) with NMDAR-Ab encephalitis, behavioural change and/or neuropsychiatric symptoms were reported in 90% of children at presentation (Wright, Hacohen et al. 2014 *in press*). The recognition of bizarre behaviour is an important pathognomonic feature of NMDAR-Ab encephalitis that needs to be actively sought in the clinical history, even in the youngest patients. In the UK study, nine patients (31%) presented under the age of 3 years confirming recent reports that NMDAR-Ab encephalitis is relatively common even in very young children (Goldberg, Titulaer et al. 2014). Studies in both adults and children have expanded the clinical phenotype of NMDAR-Ab encephalitis to include disease with a predominance of a single symptom, for example movement disorders (Hacohen, Dlamini et al. 2014), psychiatric features (Kayser, Titulaer et al. 2013), or seizures (Niehusmann, Dalmau et al. 2009). In paediatric NMDAR-Ab encephalitis, seizures are seen in 68% (21/31) of

cases, the second most common symptom after behavioural change and/or neuropsychiatric features (Wright, Hacohen et al. 2014 *in press*). A recent observational study describing 13 adult male patients, found 61.5% (8/13) presented initially with a seizure which was focal in five (Viaccoz, Desestret et al. 2014). By contrast, only 8/58 female cases presented with seizures initially, and these were mostly generalized. A similar study in a large cohort of 577 patients, found that even though seizures as an initial symptom were more common in men than women (27% vs 11%); in both groups psychiatric features were still the most frequent initial symptom (Titulaer and Dalmau 2014). An associated tumour with NMDAR-Ab encephalitis is predominantly found in female patients (14-45 years), and nearly all (96%) are ovarian teratomas (Titulaer, McCracken et al. 2013), as described in the first case series. Other malignancies have rarely been found in NMDAR-Ab encephalitis patients, but include testicular teratomas, Hodgkin's lymphoma, small cell carcinoma, glioblastoma and neuroblastoma (Zandi, Irani et al. 2009, Irani, Bera et al. 2010, Fujii, Kubo et al. 2013). Tumours are much less common in young children, the youngest reported patient with NMDAR-Ab encephalitis and a tumour was 7 years old (Titulaer, McCracken et al. 2013).

In terms of investigations for NMDAR-Ab encephalitis, magnetic resonance imaging (MRI) brain findings are often non-specific but CSF abnormalities are seen in up to 79% of patients, and the EEG is abnormal in over 90% of patients (Armangue, Titulaer et al. 2013, Titulaer, McCracken et al. 2013). These are often reported as encephalopathic with or without epileptiform discharges. A unique electroencephalogram (EEG) pattern has been reported in up to 30% of hospitalized adult NMDAR-Ab encephalitis patients known as, "extreme delta brush", (Schmitt, Pargeon et al. 2012). This pattern of generalized slowing in the delta range (1-3Hz) has superimposed rhythmic fast activity (beta range, 20-30Hz) and is similar to "delta brush" waveforms seen in premature infants. These changes are seen rarely in paediatric

patients and may in fact just be a feature of severe prolonged illness and intensive care admission (Armangue, Titulaer et al. 2013). Recent reports suggest that in paediatric patients, early and longitudinal EEG patterns can be pathognomonic and can aid in the differentiation between epileptiform and non-epileptiform movements (Gitiaux, Simonnet et al. 2013, Nosadini, Boniver et al. 2014) .

As in most autoantibody-mediated diseases, treatment of NMDAR-Ab encephalitis is aimed at removal of circulating antibodies (PLEX) and suppression of the immune system with steroids or intravenous immunoglobulin (IVIG) (often referred to as "1st line" immunotherapy) or reducing production of antibodies (using Rituximab and other immunomodulatory agents, referred to as "2nd line" treatment). The removal of an associated tumour if present, and any additional oncological therapy, is essential and correlates with improved outcome overall (Dalmau, Gleichman et al. 2008). With early recognition and prompt treatment, a significant neurological improvement is seen in 81% of patients (Titulaer, McCracken et al. 2013). There is no controlled trial to provide high quality evidence on the optimal therapeutic strategy, but a large cohort analysis appears to suggest the additional benefits of second line therapy when first line therapy fails (Titulaer, McCracken et al. 2013). Relapses occur in 12-23% of patients, are often less severe than the original disease episode and respond to immunotherapy (Irani, Bera et al. 2010, Titulaer, McCracken et al. 2013).

The average time of hospital stay for paediatric NMDAR-Ab encephalitis in the UK cohort was 60 days, higher than other form of acquired encephalopathies (Granerod, Ambrose et al. 2010), with 42% requiring admission to ITU. Appropriate management of these patients is challenging and frequently requires input of a multi-disciplinary team (MDT). Speech and language therapists, physiotherapists and occupational therapists form the mainstay of this fundamental support team and should be engaged

early in disease presentation for maximal benefit to the patients (Wright, Hacohen et al. 2014 *in press*).

NMDAR-Ab encephalitis is a well-characterised, treatable form of encephalitis, and given the incidence has exceeded viral encephalitis in some epidemiological studies (Gable, Sheriff et al. 2012), it is more commonly seen in acute Neurology. Nevertheless, further studies of larger prospective cohorts and randomised treatment trials are still needed to establish the role of second line immunotherapy and the duration of treatment needed for this condition.

1.3.3 NMDAR-Abs and epilepsy

Four out of the five cases of temporal lobe epilepsy in young women presented by Niehusmann et al., had prominent associated features of NMDAR-Ab encephalitis, which included psychiatric disturbance, speech dysfunction, and decreased level of consciousness. Four out of five responded to immunotherapy (Niehusmann, Dalmau et al. 2009). In an adult epilepsy study of neuronal antibodies, the seven positive NMDAR-Ab patients were from new patient and follow-up adult epilepsy clinics (n=416) and had no other clinical evidence of NMDAR-Ab encephalitis. Five out of seven had been previously classified as focal epilepsy of unknown cause (Brenner, Sills et al. 2013). This supports the idea that antibodies may be clinically significant in idiopathic epilepsy as well as encephalitis, although whether they can be directly epileptogenic is still unknown. Moreover, NMDAR-Abs have been found in up to 10% of serum samples in adult healthy controls, however these studies used a fixed rather than live cell based assay which is designed to detect only pathogenic antibodies that bind to extracellular epitopes (Dahm, Ott et al. 2014, Hammer, Stepniak et al. 2014).

1.4 The VGKC-complex

The Shaker family of VGKCs are composed of four transmembrane α subunits and four intracellular β subunits. The large number of different α subunits (Kv1.1- Kv1.7) and their ability to combine both homotypically and heterotypically leads to a wide variety of VGKCs functioning to control membrane excitability.

VGKC autoantibodies are measured by radioimmunoassay, where antibodies immunoprecipitate the VGKC as a complex from solubilised mammalian brain membranes. They were originally described in both PNS (cramp fasciculation syndrome, neuromyotonia (Hart, Maddison et al. 2002) and CNS hyperexcitability limbic encephalitis (LE) disorders (Buckley, Oger et al. 2001). However, the question arose as to how autoantibodies to the same antigenic target (the VGKC) caused such a variety of neurological syndromes. It was subsequently shown that the antigenic targets were in fact the extracellular domains of proteins complexed to the VGKC, i.e. CASPR2, contactin-2 and LGI1 (Irani, Alexander et al. 2010, Lai, Huijbers et al. 2010).

CASPR2 is a transmembrane protein with a large extracellular sequence localised at the juxtaparanodes of myelinated axons (Poliak, Gollan et al. 1999), and is essential for clustering of the VGKCs (Poliak, Salomon et al. 2003). The protein contactin-2 (also called TAG-1 in mice) is a member of the immunoglobulin superfamily, and functions as a cell-adhesion molecule (Tsiotra, Karagogeos et al. 1993). It is also expressed in the juxtaparanode of myelinated fibres and acts in association with CASPR2.

LGI1 is a secreted synaptic protein that organises a trans-synaptic complex with the ADAM22/23 proteins, an important interaction that has been shown to regulate AMPAR mediated synaptic transmission (Fukata, Adesnik et al. 2006). The LGI1 protein also prevents inactivation of the VGKC through the cytoplasmic regulatory protein Kvβ (Schulte, Thumfart et al. 2006).

1.4.1 VGKC-complex antibody associated neurological disease

VGKC-complex Ab associated LE patients present with sub-acute onset of cognitive impairment, including memory loss, disorientation, confusion, and seizures; hyponatraemia is seen in up to 60% of patients (Buckley, Oger et al. 2001, Vincent, Buckley et al. 2004). VGKC-complex antibody titres are often over 1000pM (less than 100pM is normal), with MRI findings of high signal in the hippocampus reported in up to 75% of cases; EEG shows either focal or generalised slow wave abnormalities, sometimes with an epileptogenic focus (Vincent, Buckley et al. 2004). In occasional cases, there is an association with thymoma (Buckley, Oger et al. 2001).

Prior to the identification of VGKC-complex Abs, LE was thought to be predominantly a paraneoplastic condition associated with malignancies such as SCLC, thymoma or testicular cancer. Paraneoplastic LE can be difficult to distinguish clinically from VGKC-complex Ab associated LE (Gultekin, Rosenfeld et al. 2000), but hyperintensity on the brain MRI scan is often seen in several limbic areas and may extend to the brainstem, hyponatraemia is rare. Patients often have non-pathogenic paraneoplastic antibodies to intracellular targets (Hu, CV2, CRMP5, Ma2) and associated SCLC or other tumours. Treatment of the tumour is more effective on the neurological outcome than immune modulation (Turkay, Baskin et al. 1996).

In non-paraneoplastic LE, the commonest target within the VGKC-complex is LGI1 (80-90%) (Irani, Alexander et al. 2010, Lai, Huijbers et al. 2010). A case series of LGI1 antibody encephalitis found the disease to be more common in males, with a median age of onset of 63 years (Irani, Alexander et al. 2010). All 64 patients had amnesia and/or confusion and 92% (59/63) had seizures. MRI changes of temporal lobe inflammation were seen in 62%, and hyponatraemia in 59% (38/63). No tumours were seen in this group and most responded well to immunotherapies as previously described

(Irani, Alexander et al. 2010). In the same study 19 CASPR2 antibody positive patients were also described, and half of them had amnesia, confusion and neuropsychiatric features similar to the LGI1-Ab positive patients, but they were significantly less likely to have seizures. Ten patients had neuromyotonia and six had tumours; neuropathic pain, insomnia, dysautonomia and weight loss were also more common (Irani, Alexander et al. 2010). Three of the positive CASPR2 patients had Morvan syndrome, a syndrome characterised by neuromyotonia, dysautonomia, encephalopathy and insomnia but equally treatment responsive (Irani, Pettingill et al. 2012). CASPR2-Abs are more commonly associated with Morvan syndrome than LE. In 29 cases of Morvan syndrome recently characterised, CASPR2 antibodies were found in 19 out of 27 samples available for testing (Irani, Pettingill et al. 2012). Half of patients also had antibodies to LGI1, which could explain some aspects of the clinical phenotype (Irani, Pettingill et al. 2012).

Contactin-2 antibodies are found rarely in LE. They have been described in some patients with multiple sclerosis (Boronat, Sepulveda et al. 2012), and are also present in a proportion of patients with neuromyotonia or Morvan syndrome. A recent study looking at outcomes of limbic encephalitis with VGKC-antibodies, found that hippocampal atrophy was more common in LGI1-Ab LE (7/9) patients than those with CASPR2-Abs (0/3) or with VGKC-complex Abs only (0/6) (Malter, Frisch et al. 2014). The LGI1-Ab patients were also left with significantly poorer memory that the other two subgroups.

1.4.2 VGKC-complex antibodies and epilepsy

VGKC-complex antibodies have also been reported in adult epilepsy (McKnight, Jiang et al. 2005, Majoie, de Baets et al. 2006, Brenner, Sills et al. 2013) , and a few paediatric cases (Suleiman, Brenner et al. 2011, Suleiman, Brenner et al. 2011).

McKnight et al., first reported VGKC-complex antibodies in 11% (16/139) cases of adult epilepsy. A good response to immunotherapy was seen in ten out of 16 patients, although five of these actually had LE and the highest VGKC-complex Ab titres. Two positive cases with a median age of onset of 14 years had drug resistant focal epilepsy (McKnight, Jiang et al. 2005). A further study concentrating on drug resistant adult epilepsy cases found a VGKC-complex Ab positivity rate of 6% (Majoie, de Baets et al. 2006). Antibodies to the VGKC-complex were the most commonly found in the Brenner study, screening new and follow-up epilepsy patients (20 patients; 4.8% of total) (Brenner, Sills et al. 2013); 14 of these patients had focal epilepsy, nine of unknown cause. Another study of 144 adult patients with unexplained adult onset epilepsy identified VGKC-complex Abs in 4.2% (6/144), one positive for LGI1 and another for CASPR2 antibodies, although no control group was similarly tested (Lilleker, Jones et al. 2013). All experienced focal seizures (two with generalised-tonic clonic seizures) and showed improvement in seizure control with immunotherapy.

Similar screening studies have not been performed in large paediatric epilepsy cohorts. However, elevated VGKC-complex Abs (titres between 107 - 640pM) were identified in 4/10 children with unexplained encephalitis presenting with encephalopathy and status epilepticus (SE) (Suleiman, Brenner et al. 2011). The samples were taken within the first week of their illness, with antibody tests retrospectively done on the stored samples. Additionally, low levels of VGKC-complex Abs (201pM) also tested retrospectively, were reported in one case of infantile-onset epileptic spasms and developmental delay. The patient showed a partial response to steroid treatment, but this was only started late in the disease course (Suleiman, Brenner et al. 2011).

Febrile-Infection Related Epilepsy Syndrome (FIRES), describes a devastating epileptic encephalopathy that occurs in normal children following a fever or infection.

Children develop acute or subacute refractory status epilepticus and the chronic seizure disorder which develops is also extremely treatment resistant (Kramer, Chi et al. 2011, van Baalen, Hausler et al. 2012). MRI and CSF examination are often normal, with mild inflammatory changes only that are non-specific. VGKC-complex antibodies were described in one case (Illingworth, Hanrahan et al. 2011), but this finding has not been replicated (van Baalen, Hausler et al. 2012). Immunotherapy is not often associated with a positive outcome in FIRES patients, although symptomatic response has been seen with the ketogenic diet (Nabbout, Mazzuca et al. 2010).

Some adult patients with a specific phenotype of multiple daily brief dystonic seizures have LGI1 antibodies and develop a seizure syndrome, known as "faciobrachial dystonic seizures" (FBDS), during LE or before the onset of LE (Irani, Michell et al. 2011). In the initial stages of FBDS, patients have normal sodium levels and brain MRI, and the EEG is abnormal in a minority of patients (7-25%) (Irani, Michell et al. 2011, Irani, Stagg et al. 2013). Anti-epileptic drugs (AEDs) are often ineffective, and associated with cutaneous reactions, often severe, in 41% of patients. This included a localised rash in 8 patients (carbamezepine in 4, phenytoin in 2, lamotrigine in 1 and levetiracetam in1), erythroderma in 2 patients (both phenytoin) and Stevens-Johnson syndrome in 2 after receiving carbamezapine (one patient require intensive care unit admission) (Irani, Michell et al. 2011). Immunotherapy produced a clear reduction in seizures, and in further studies was shown to prevent subsequent development of poor cognitive outcome (Irani, Stagg et al. 2013). FBDS demonstrates how some CNS autoantibodies can be directly associated with an adult epilepsy syndrome. Additionally, genetic mutations in LGI1 have been identified in patients with autosomal dominant lateral temporal lobe epilepsy (ADTLE) (Kalachikov, Evgrafov et al. 2002).

CASPR2 antibodies have been found in three adult epilepsy patients within LE studies (Irani, Alexander et al. 2010, Lancaster, Huijbers et al. 2011). In humans,

homozygous mutations in the CASPR2 gene (CNTNAP2) were described in a group of Amish children with cortical dysplasia focal epilepsy (CDFE) syndrome (Strauss, Puffenberger et al. 2006). These children have intractable focal seizures beginning in early childhood with all developing autistic regression.

Deletions in the contactin-2 (CNTN2) gene have also been described in focal epilepsy (Stogmann, Reinthaler et al. 2013). Copy number variants in both CASPR and contactin-2 among other cell adhesion molecules, have also been found in 20% of the paediatric epilepsy syndromes, continuous spike and wave in slow-wave sleep (CSWS) and Landau-Kleffner syndrome (LKS) (Lesca, Rudolf et al. 2012).

1.5 The α-amino-3-hydroxy-5-methyl-4-isoxazolepropionic acid receptor (AMPAR) receptor

The AMPA receptor (AMPAR) is an ionotropic transmembrane glutamate receptor that mediates the majority of fast synaptic transmission throughout the CNS. Most AMPARs are heteromeric composed of four types of subunits (GluA1-4). Autoantibodies to this receptor are rare; in a case series of ten patients all presented with a form of LE, four patients had seizures, and seven had an underlying malignancy (Lai, Hughes et al. 2009). The median age of presentation was 60 years and nine out of the ten cases were female. Nine received immunotherapy and responded to this treatment alongside oncological therapy when required. There was a tendency towards frequent relapse.

1.5.1 AMPAR-Abs and epilepsy

Antibodies to the GluA3 subunit were identified in early research studies investigating the pathogenesis underlying Rasmussen's encephalitis (Rogers, Andrews et al. 1994), a rare neurological disorder characterized by progressive unihemispheric inflammation of

the cerebral cortex causing cognitive deterioration, hemiplegia, hemianopia and drug-resistant focal epilepsy (Varadkar, Bien et al. 2014). Further studies were unable to reproduce this finding of potentially pathogenic GluA3 receptors (Watson, Jiang et al. 2004) and given the lack of response to PLEX seen in patients with this disease, it is unlikely that CNS autoantibodies are causative. However, AMPAR-Abs have been identified in serum of two patients with Rasmussen's encephalitis suggesting that CNS autoantibodies can be found and may be secondary to the disease process (Nibber et al. 2014, *in preparation*).

1.6 Gamma-aminobutyric acid B ($GABA_B$) receptors

GABA receptors are the main inhibitory receptors throughout the CNS. The G-protein coupled $GABA_B$ receptors are composed of two subunits $GABA_B1$ and $GABA_B2$, and mediate pre- and post-synaptic inhibition. Autoantibodies to the $GABA_B$ receptor have been reported in two case series (Lancaster, Lai et al. 2010, Hoftberger, Titulaer et al. 2013). Patients presented with symptoms of LE, although in one series, all patients had early or prominent seizures (Lancaster, Lai et al. 2010). 50% of all cases had an underlying SCLC. Immunotherapy and oncological treatment resulted in a full or partial improvement in 24/29 (83%) treated cases. In a recent case series of five patients, four patients had small-cell lung cancer; in three, the identification of the lung cancer was *after* the diagnosis of $GABA_B$ encephalitis, the antibody positivity prompting the search for this specific tumour (Kim, Lee et al. 2014). In this case series there was a partial response to therapy, however patients received first-line immunotherapy only.

$GABA_B$ receptor antibodies ($GABA_B$R-Abs) are accompanied by other autoantibodies in some cases, including those to the VGCC (Lancaster, Lai et al. 2010, Dogan Onugoren, Rauschka et al. 2014). VGCC-Abs cause paraneoplastic Lambert

Eaton myasthenic syndrome by reduction of presynaptic VGCC's; SCLC is also the most common underlying malignancy in these patients (Titulaer, Lang et al. 2011). They are not usually associated with epilepsy of LE. $GABA_BR$-Abs have also been reported in a case with opsoclonus-myoclonus syndrome (OMS) and LE (DeFelipe-Mimbrera, Masjuan et al. 2014). OMS or Dancing-eye syndrome is a rare neurological disorder, which associates with neuroblastoma in approximately 50% of cases; neuronal cell line surface binding of patient IgG has previously demonstrated the presence of potentially pathogenic antibodies (Blaes, Pike et al. 2008).

Overall the $GABA_BR$-Ab patients who respond best to immunotherapy are those with LE in the context of SCLC (Jeffery, Lennon et al. 2013). $GABA_BR$-Abs have not yet been reported in epilepsy patients.

1.7 Glutamic acid D-carboxylase (GAD)

GAD is a rate-limiting cytosolic enzyme of GABA synthesis. In neurological disease, antibodies to GAD (GAD-Abs) are mainly associated with stiff-person syndrome (SPS), a rare disorder in which patients suffer from rigidity and cramps (Solimena, Folli et al. 1990). However, GAD-Abs have also been reported in some cases of cerebellar ataxia (Honnorat, Saiz et al. 2001, Saiz, Blanco et al. 2008) and LE (Malter, Helmstaedter et al. 2010). A LE study in children and adolescents found four out of ten patients were positive for GAD-Abs (Haberlandt, Bast et al. 2011), two of whom also had low titre of VGKC-complex antibodies. Despite immunotherapy, these patients had a poor outcome (Haberlandt, Bast et al. 2011). While in some GAD-Ab associated disease, such as SPS, immunotherapy is beneficial (Dalakas 2005), the treatment responses of other cases is variable and limited to case reports.

1.7.1 GAD-Abs and epilepsy

GAD-Abs have been reported in adult epilepsy which is often drug-resistant (Peltola, Kulmala et al. 2000, McKnight, Jiang et al. 2005, Yoshimoto, Doi et al. 2005, Brenner, Sills et al. 2013). All seven positive GAD-Ab patients in a recent epilepsy screening study had focal epilepsy (Brenner, Sills et al. 2013). A further study also found high GAD-Ab serum titres in 5.4% (6/112) of adult patients with unexplained adult onset focal epilepsy, CSF analysis revealed oligoclonal bands and intrathecal GAD Abs in all patients (Lilleker, Biswas et al. 2014). Immunotherapy did not result in sustained symptomatic improvement in any of the patients, with one patient eventually requiring epilepsy surgery for seizure control. Histological analysis of the resected brain tissue revealed no evidence of active inflammation and GAD-Abs persisted with high serum titres following surgery (Lilleker, Biswas et al. 2014). This case highlights the controversy that exists over the pathological significance of GAD-Abs. However, studies investigating GAD-Abs and their relevance in neurological disease have often tested samples many years after the start of disease and the patients may not have been adequately treated at presentation.

One study examining serum GAD-Abs in paediatric epilepsy found 14/208 patients were positive (Veri, Uibo et al. 2013), but levels of positivity were taken as 5 U/ml on the ELISA testing technique used. Only high serum titres over 50,000 U/ml are generally considered to be of neurological significance, casting doubt on the relevance of these antibodies to the disease process. More long-term prospective trials are needed to clarify the clinical significance of GAD antibodies in epilepsy.

It is apparent that antibodies against multiple different CNS proteins have been described in cases of epilepsy, even without encephalitis. Given the importance of these proteins in normal synaptic transmission, disruption of their function is pathologically significant, and considered in more detail in section 1.8.

1.8 Pathological and epileptogenic potential of CNS autoantibodies and antigens

In order to consider the potential pathological significance of CNS autoantibodies within the framework of epilepsy aetiology, it is important to consider first existing evidence on the role of the immune system in the pathogenesis of seizure disorders.

1.8.1 Epilepsy and the immune system

(1) Experimental evidence

The CNS used to be considered ‘immunoprivileged’ and safe from immunological attack due to the presence of the blood-brain-barrier (BBB), the lack of a conventional lymphatic drainage, and low levels of circulating lymphocytes and monocytes. It has now become clear, however, that immune and inflammatory reactions do occur in the CNS, either intrinsically from the brain itself or acquired from systemic circulation through a damaged BBB. These two inflammatory processes can each precipitate and sustain seizure activity (Vezzani, French et al. 2011, Marchi, Granata et al. 2014). Seizures induce cytokine release from glial cells which increases calcium influx into neurons precipitating excess glutamate release and increased neuronal hyperexcitability. The BBB becomes impaired allowing infiltration of albumin and leucocytes into the brain which results in further inflammatory cytokine release from glial cells, These inflammatory reactions and resultant neuronal hyperexcitability lead to recurrent spontaneous seizures with the eventual development of refractory epilepsy (Shimada and Takemiya 2014).

Inflammatory changes within the brain are seen in Rasmussen’s encephalitis, a chronic focal epilepsy syndrome characterized by unilateral inflammation of the cerebral cortex (Rasmussen, Olszewski et al. 1958). Febrile seizures, mainly seen in

children between the ages of 3 months to 5 years, are thought to be a consequence of systemic activation of the immune system by fever (Patterson, Carapetian et al. 2013). Recent studies in animal models, have identified a role for the cytokine interleukin-1 β (IL-1β), in the pathogenesis of prolonged febrile seizures and febrile SE (Dube, Ravizza et al. 2010). Other inflammatory mediators such as tumour necrosis factor (TNF), interleukin-6 (IL-6), prostaglandin E2 and the complement cascade (Xiong, Qian et al. 2003) have also been shown to induce or exacerbate seizures (Vezzani, French et al. 2011). Seizure threshold is also lowered in animals systemically injected with lipopolysaccharide, a powerful inducer of peripheral and brain inflammation (Sayyah, Javad-Pour et al. 2003).

(2) Clinical evidence

A causal role of inflammation in epilepsy comes primarily from the association between seizures/ epilepsy and systemic autoimmune and inflammatory conditions, for example systemic lupus erythromatous and Hashimoto's thyroiditis (Palace and Lang 2000). In fact, a recent population based study found the risk of epilepsy was significantly heightened among patients with autoimmune disease and especially pronounced in children (Ong, Kohane et al. 2014).

Patients with specific childhood epilepsy syndromes are known to respond well to immunotherapy, in particular steroids, but the reason for this is still the subject of active research. West syndrome/ Infantile spasms is an electroclinical epileptic syndrome, characterized by epileptic spasms and a "hysparrythmic" pattern on the EEG. The underlying aetiology may be structural, metabolic, or genetic, but in a proportion of cases, the cause is unknown (Riikonen 2014). A recent Cochrane review of the treatment suggested that hormonal treatment (prednisolone or tetracoside) led to resolution of spasms faster and in more infants than vigabatrin, and improved the long-

term developmental outcome in infants with no underlying cause (Hancock, Osborne et al. 2013).

CSWS is another childhood epileptic encephalopathy characterized by focal or generalised seizures occurring during sleep, atypical absences when awake, cognitive regression and an EEG pattern of electrical status epilepticus in sleep (ESES) (Sanchez Fernandez, Chapman et al. 2013). Epileptic seizures are often treatable and some children never have overt clinical seizures. When referring to the epileptic encephalopathy with predominantly language regression, the term LKS is often used. In LKS, symptoms begin in early childhood following initial normal language development before the progressive deterioration of language function; seizures may not appear until several years later, if at all. There is also electroclinical overlap of these syndromes with Rolandic epilepsy which is the most common focal epilepsy of childhood. Historically thought to be a 'benign' epilepsy, recent studies have highlighted the co-existing mild cognitive deficits and language problems which may be long-term (Monjauze, Broadbent et al. 2011). All these syndromes form part of a spectrum of epilepsy associated with speech, language, cognitive, neurodevelopmental and behavioural disorders (Deonna and Roulet-Perez 2010) .The main aetiologies are likely to be structural and genetic (Lesca, Rudolf et al. 2012). Recently, a number of groups have identified de novo and inherited mutations in the NR2A subunit in approximately 20% of cases (Carvill, Regan et al. 2013, Lemke, Lal et al. 2013, Lesca, Rudolf et al. 2013).

Although standard AEDs are used effectively in the treatment of CSWS, corticosteroid treatment can also lead to complete resolution. In a study of 44 children with ESES, corticosteroid treatment led to reductions of seizures or neuropsychological improvement in 34/44 (77%), with 34 achieving complete seizure control, and a normal EEG in 21 patients (Buzatu, Bulteau et al. 2009). IVIG treatment has also been

associated with some success in the treatment of these patients, although this evidence is limited to case reports only (Mikati, Saab et al. 2002, Arts, Aarsen et al. 2009).

In view of this response to immunotherapy, an autoimmune aetiology has been suspected in CSWS/ LKS, with some studies demonstrating staining of sagittal rat brain sections with serum from affected patients (Boscolo, Baldas et al. 2005). However, some of the brain regions stained (brainstem, auditory cortex and cerebellum) may not be related to disease pathogenesis. Other studies have looked at brain-derived neurotrophic factor, autoantibodies to myelin basic protein (MBP) and endothelial cells (Connolly, Chez et al. 1999, Connolly, Chez et al. 2006) in the serum and found altered levels in affected patients as compared to controls. However the studies are small, not conclusive and again the relevance of these antibodies to pathogenesis is questionable (Granata, Cross et al. 2011).

1.8.2 Pathogenicity of NMDAR-Abs

As well as the favourable clinical response to immunotherapy, *in vitro* and *in vivo* studies provide further evidence of the pathogenicity of NMDAR-Abs. Incubation of dissociated rodent hippocampal neurons with patient NMDAR-Abs *in vitro,* causes a selective reduction in surface membrane NMDARs (Hughes, Peng et al. 2010). This is reversible on removal of the NMDAR-Abs, and mediated by autoantibody cross-linking of the receptors and internalisation, similar to the effect described of AChR-Abs in MG. Recent studies have shown this internalisation is seen on neuronal cultures within 12 hours of incubation with patient NMDAR-Abs, and affects NMDARs on both excitatory and inhibitory neurons (Moscato, Peng et al. 2014). A marginal reduction of GABAergic terminals synapsing onto excitatory neurons was also reported within 24 hours of NMDAR-Ab application onto neuronal cultures. However, the distributions of

both glutamatergic and GABAergic synapses on target neurons are not homogeneous in dissociated neuronal cultures and changes in synaptic densities when measured under these conditions need careful interpretation (Ito, Komatsu et al. 2013). NMDAR receptor expression was also reduced in the hippocampus of rats infused *in vivo* with NMDAR-Abs, similar to post-mortem brain histological studies of NMDAR-Ab encephalitis patients (Hughes, Peng et al. 2010). NMDAR-Abs have been shown to influence the trafficking of the NR2 subunit-containing NMDARs *in vitro* (Mikasova, De Rossi et al. 2012). Following incubation of hippocampal neurons with NMDAR-Abs, the surface NR2A-NMDARs were laterally displaced out of the synapse and synaptic plasticity was inhibited as evidenced by the failure of an LTP protocol to upregulate surface AMPARs. This was prevented by activation of the receptor tyrosine kinase EPHB2; expression of this receptor has been shown to regulate NMDAR synaptic content. Injection of Ephrin B2 ligand (which activates the EPHB2 receptor) *in vivo* into CA1 along with patient NMDAR-Ab IgG prevented the reduction of NMDAR cell surface expression induced by the patient IgG (Mikasova, De Rossi et al. 2012). This study confirmed that the antibodies internalise NMDARs and suggest a possible associated mechanism which may have future therapeutic applications.

The functional effect of NMDAR-Abs on the synapse and neuronal network has been investigated *in vivo* and *in vitro*. Some studies report an acute *pharmacological* action of the NMDAR-Abs, including an increase in the extrasynaptic concentration of glutamate within 30 minutes of an infusion of NMDAR-Abs *in vivo* into the CA1 area of rats (Manto, Dalmau et al. 2010); and suppression of LTP induction in *ex-vivo* mouse hippocampal slices following a five minute application of NMDAR-Abs (Zhang, Tanaka et al. 2012). Application of NMDAR-Ab CSF to *in vitro* neuronal networks of dissociated primary rat cortical culture acutely suppressed the global activity of the neuronal network as recorded by the microelectrode (MEA) system (Jantzen, Ferrea et

al. 2013). In contrast to these studies, another group have shown a complete lack of effect of NMDAR-Abs on NMDAR-mediated current amplitudes in hippocampal neurons when treated for only 30 minutes (Moscato, Peng et al. 2014), as opposed to the dramatic reduction resulting from 24 hours of treatment when the NMDARs are internalised. Given the reduction of NMDAR expression seen in patients post-mortem, it is more likely that NMDAR-Ab mediated internalisation is the cause of NMDAR hypofunction rather than direct pharmacological blockade of the receptor. However, whether this loss of surface NMDARs in an animal model can recapitulate all the clinical features of the patients that are thought to be a consequence of NMDAR hypofunction has not yet been demonstrated.

In vivo experiments in this laboratory by Dr Phillipa Pettingill have shown that passive transfer of NMDAR-Ab IgG into the cerebral lateral ventricle of C57BL/6 mice can induce mild behavioural disturbance and reduced working memory, as measured by spontaneous alternation (Pettingill et al. 2014, *in preparation*). Additionally, abnormal clasping movements were seen in mice injected with NMDAR-Ab positive IgG more frequently than those injected with control IgG. Unfortunately, without any neurophysiology, it was impossible to determine if these were epileptiform movements or dystonic posturing. Although these results represent the first evidence that symptoms of NMDAR-Ab mediated neurological disease can be induced in an experimental animal, further work is needed to firmly establish the exact pathophysiological mechanisms underlying the disease.

(1) Pathological effects of NMDAR hypofunction

NMDAR dysfunction has been implicated in schizophrenia since the observation that use of NMDAR antagonists mimic the spectrum of positive, negative and psychotic symptoms seen in the disease, and provoke further symptoms in stable schizophrenia

patients (Lahti, Koffel et al. 1995, Coyle 1996). Mice with reduced NR1 expression (up to 95%) survived to adulthood but displayed behavioural abnormalities, including increased motor activity and stereotypy, consistent with a schizophrenia phenotype (Mohn, Gainetdinov et al. 1999). They also showed increased seizure susceptibility to kainate-induced seizures with lethal seizures in 100% of the mutant mice, compared to none in the WT mice, at a dose of 20mg/kg (Duncan, Inada et al. 2010). These results were intriguing, as despite a genetic reduction in a major excitatory signalling pathway, there was an increase in intrinsic excitability of the neuronal network in these mice as evidenced by the behaviours seen. Further studies of this NR1 hypomorphic mouse model demonstrated a selective disruption of parvalbumin-expressing interneurons (Gandal, Sisti et al. 2012). Post-mortem brain studies of schizophrenia patients have also shown a reduced expression of NMDARs particularly in parvalbumin-expressing interneurons (Bitanihirwe, Lim et al. 2009). This suggests it is specifically the NMDARs on GABAergic inhibitory interneurons that are reduced causing a disruption of the normal feedback inhibition of pyramidal cells, and allowing total excitatory output to be increased. In support of this, selective NR1 reduction in parvalbumin-expressing interneurons reproduced the schizophrenia phenotype in a mouse model (Belforte, Zsiros et al. 2010). Theoretically, NMDARs could act in a similar manner causing internalisation of NMDARs on interneurons (Figure 1.1).

Studies of NMDAR hypofunction in disease are of particular relevance to the pathogenicity of NMDAR-Abs and may help form hypotheses on further, or more specific treatments for NMDAR-Ab encephalitis.

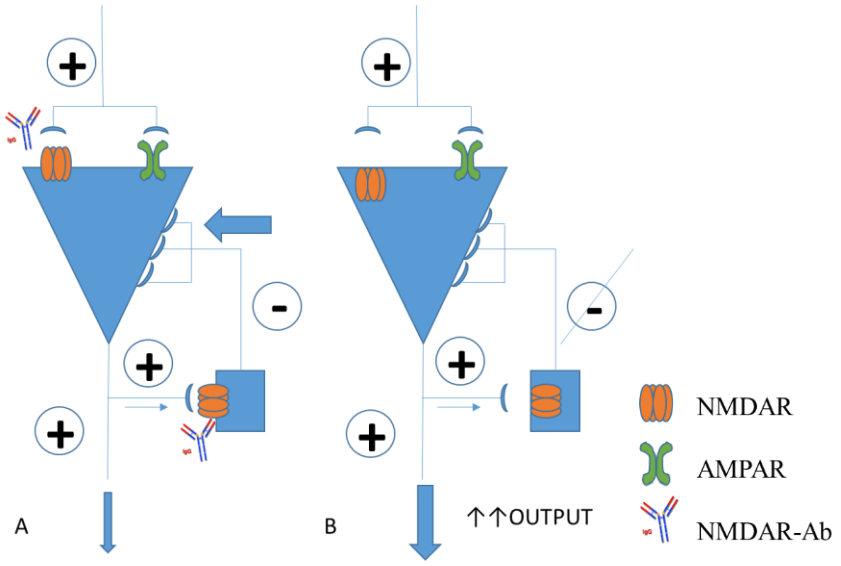

Figure 1-1 Schematic of proposed action of NMDAR-Abs on neuronal circuits

A. The GABAergic interneuron (blue rectangle) receives input from the pyramidal cell (blue triangle) and exerts inhibitory control by recurrent projections to the pyramidal cell.
B. Internalisation of the NMDARs by the NMDAR-Ab disrupts the local feedback inhibition, however the excitatory output is sustained through the AMPAR. The total excitatory output is increased

*Adapted from Rujescu, D., et al. (2006). "A pharmacological model for psychosis based on N-methyl-D-aspartate receptor hypofunction: molecular, cellular, functional and behavioral abnormalities." Biol Psychiatry **59**(8): 721-729*

(2) Treatment of NMDAR hypofunction in disease

Using schizophrenia as a paradigm of pathological NMDAR hypofunction in disease, can any lessons be learned in terms of treatment and applied to NMDAR-Ab mediated neurological disease?

Drugs that are known to modulate the NMDAR have been used as adjunctive treatments in schizophrenia and their efficacy was recently the subject of a meta-analysis study (Singh and Singh 2011). D-serine, glycine, N-acetyl-cysteine (NAC), and sarcosine had therapeutic benefits in the treatment of negative and total symptoms of schizophrenia when the patient was not being treated with clozapine (Singh and Singh 2011). D-serine and glycine are NMDAR co-agonists, sarcosine is a glycine transporter inhibitor, and NAC increases levels of glutathione which can potentiate the activity of the NMDAR (Lavoie, Murray et al. 2008). These agents act to enhance the activity of

existing NMDARs but do not increase the number of functional NMDARs so may not be beneficial in the acute stages of NMDAR-Ab encephalitis when we assume active internalization of NMDARs is taking place.

An alternative drug that has been used as effective adjunct therapy in the treatment of schizophrenia is a neurosteroid, pregnenolone (Figure 1.2). Neurosteroids are derived from cholesterol and are precursors to gonadal steroid hormones and the adrenal corticosteroids. They are produced de novo by glial cells and principal neurons, hence the term 'neurosteroid' (Baulieu 1997), and modulate brain excitability primarily by interaction with receptors and ion channels on the membrane surface rather than intracellularly (Zheng 2009). Pregnenolone treatment elevates levels of two other

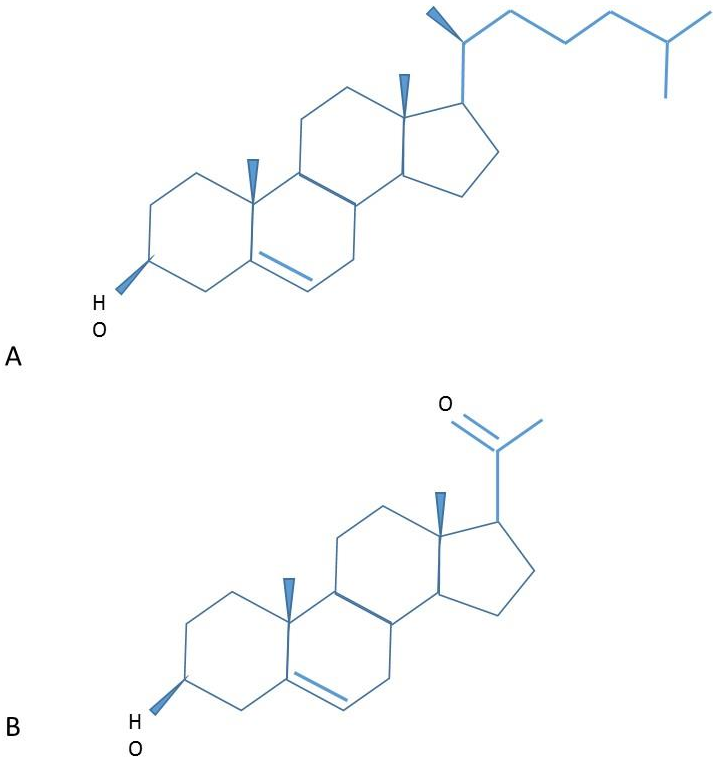

Figure 1-2 The structure of the neurosteroid pregnenolone

A. Steroids are a specific class of lipid with the common structure of four fused hydrocarbon rings. Cholesterol, shown here, is a precursor for steroid hormone.
B. Pregnenolone is a 21-carbon steroid derived from cholesterol and found in steroid hormone-producing tissues. It can be produced from precursor steroids *de novo* by glial cells and principal neurons.

neurosteroids; allopregnanalone, a neurosteroid that enhances $GABA_A$ receptor responses, and pregnenolone sulphate, a positive NMDA receptor modulator.
A recent randomized controlled trial of adjunctive pregnenolone in schizophrenia showed the drug was well tolerated and improved functional capacity in participants with schizophrenia (Marx, Lee et al. 2014). *In vivo*, pregnenolone was found to reduce the hyperlocomotion, stereotypic bouts and prepulse inhibition (PPI) deficits in a mouse model of schizophrenia acutely, and improved impaired cognitive deficits with chronic treatment (Wong, Chang et al. 2012).

Pregnenolone sulphate (PregS), a sulfated ester of pregnenolone, is a positive NMDAR modulator (Partridge and Valenzuela 2001, Adamusova, Cais et al. 2013) with recent studies showing the mechanism of action is to increase surface expression of functional NMDARs (Kostakis, Smith et al. 2013). This membrane delimited effect occurred within ten minutes of application to cortical neurons. PregS has been shown to prevent cognitive deficits in mouse models of Alzheimer's disease (Yang, Chen et al. 2012) and prevent learning and memory deficits induced by NMDAR antagonists *in vivo* (Mathis, Paul et al. 1994). In addition to the effect of PregS on NMDARs, other CNS targets have been described, including the $GABA_A$ receptor, glycine receptor, and more recently the TRPM3 channel (Harteneck 2013) and Kir2.3 channel (Smith, Gibbs et al. 2014). This needs careful consideration in experimental and clinical use.

Knowledge of the basic underlying pathogenic mechanism of NMDAR-Abs can direct future treatments hypotheses, however further work *in vitro* and *in vivo* will need to prove the usefulness of these novel agents in NMDAR-Ab mediated neurological disease.

1.8.3 VGKC-complex Ab pathogenicity

The pathogenicity of VGKC-complex Abs is demonstrated clinically by the correlation of symptom improvement with a fall in VGKC-complex-Abs (Buckley, Oger et al. 2001, Vincent, Buckley et al. 2004, Irani, Buckley et al. 2008). Additionally LE and NMT patient sera binds to specific brain regions implicated in the disease process, particularly the hippocampus (Vincent, Buckley et al. 2004, Irani, Pettingill et al. 2012). A post-mortem histological study of four autoimmune VGKC-complex-Ab LE patients found T-cell infiltrates, presence of human IgG and deposition of complement factors in the hippocampus and cortex. This suggests antibody-mediated complement activation as a pathogenic mechanism for VGKC-complex Abs; these changes were not seen in similar specimens of patients with GAD or NMDAR-Abs (Bien, Vincent et al. 2012). In a knockout genetic mouse model, loss of the LGI1 protein causes frequent spontaneous seizures in the second postnatal week (Chabrol, Navarro et al. 2010). Mice do not survive beyond day 20, most likely due to the frequent seizures interrupting a normal feeding pattern. Heterozygous littermates show increased seizure susceptibility to auditory stimuli, but no spontaneous seizures. Many of the LGI1 mutations reported in ADTLE patients prevent the secretion of the LGI1 protein *in vitro*, suggesting that LGI1 "hypofunction" is the neurobiological effect caused by the epileptogenic mutation.

In terms of LGI1-Ab pathogenicity, *ex-vivo* electrophysiology studies have shown that one patient's IgG containing LGI1 antibodies induced epileptiform activity in CA3 pyramidal cells in rat hippocampal slices, similar to that induced by the VGKC inhibitor dendrotoxin (Lalic, Pettingill et al. 2011). A more detailed *in vitro* study showed that LGI1 autoantibodies inhibited the interaction of LGI1 with ADAM22 and caused synaptic AMPAR reduction (Ohkawa, Fukata et al. 2013), a potentially

pathogenic and epileptogenic effect. Both pre- and postsynaptic mechanisms are likely to play a role in LE.

Interestingly, it has recently been shown that feline complex partial seizures with orofacial movement (FEPSO) in cats can be associated with VGKC-complex and LGI1-Abs (Pakozdy, Halasz et al. 2013). Similar to humans, post-mortem hippocampal lesions show marked IgG infiltration and complement deposition, confirming the same potential pathogenic mechanism (Klang, Schmidt et al. 2014).

Severe adult-onset epilepsy is also observed in the CASPR2 knockout mouse model (Penagarikano, Abrahams et al. 2011). *In vitro* studies of CASPR2-Abs pathogenicity by Dr Philippa Pettingill in Oxford, have shown reduction of surface CASPR2 protein levels on cortical and hippocampal culture neurons following incubation with the antibodies (Pettingill et al. 2014, *in preparation*).

1.8.4 AMPAR-Ab and $GABA_BR$-Ab pathogenicity

Incubation of live hippocampal neurons with AMPAR-Abs caused a reduction in surface AMPAR numbers, an effect reversed on removal of the antibodies (Lai, Hughes et al. 2009). Therefore, similar to NMDAR-Abs, AMPAR-Abs are thought to mediate their pathogenic effect through internalization of the receptor. In a different study, application of AMPAR-Ab IgG to live hippocampal neurons also caused a reduction in the amplitude and frequency of miniature excitatory postsynaptic currents (mEPSCs) (Gleichman, Panzer et al. 2014).

Unlike in NMDAR-Ab encephalitis and with NMDAR-Abs, there was no reduction of $GABA_BR$ levels on *in vitro* hippocampal neurons exposed to $GABA_BR$ antibodies (Lancaster, Lai et al. 2010). Preliminary electrophysiological studies with $GABA_B$ IgG on *ex-vivo* mouse brain slices show $GABA_B$ antibodies may have a direct pharmacological effect on the receptor itself (Nibber et al. 2014, *in preparation*).

1.8.5 GAD-Abs pathogenicity

In Type 1 insulin dependent diabetes, where GAD-Abs are also often found, these are thought to be markers of pancreatic destruction rather than directly pathogenic (Ellis and Atkinson 1996). Given the response to immunotherapy is variable in GAD-Ab neurological disorders, the pathogenic effect of GAD-Abs has been investigated. Repetitive intrathecal passive transfer of GAD-Abs into mice from a patient with SPS and profound anxiety, resulted in an anxious phenotype on behavioural testing (Geis, Weishaupt et al. 2011). There was no change in muscle stiffness prompting the question as to whether another unspecified autoantibody in the purified patient IgG was mediating the behavioural changes seen (Geis, Weishaupt et al. 2011). Nevertheless, this passive transfer of neuronal autoantibodies directly into the CNS was partially successful. The comparison of this versus systemic passive transfer and active immunization in recapitulating CNS disease *in vivo* is further considered in section 1.8.6.

1.8.6 Passive transfer models of CNS disease

As well as autoantibodies to GAD in SPS, less commonly some patients have antibodies to amphiphysin, an intracellular protein involved in the synaptic vesicle cycle; disruption of function leads to synaptic transmission failure (Evergren, Marcucci et al. 2004). Knockout mice display learning deficits and an increased susceptibility to seizures (Di Paolo, Sankaranarayanan et al. 2002).

Amphiphysin antibodies and other onconeural antibodies (anti-Hu, anti-Yo) were not thought to be directly pathological as their targets were inaccessible, within the cell. In 2005, Sommer at al., demonstrated that peripheral, intraperitoneal injections of human amphiphysin antibody positive IgG into rats that had an artificially disrupted

BBB, developed stiffness and spasms resembling SPS (Sommer, Weishaupt et al. 2005). This pathogenic effect was dose-dependent but the motor signs were intermittent and short-lived, limiting the electrophysiological studies. However, they found that some of the antibodies were able to perfuse through the leaky BBB into CNS tissue. In order to define the pathophysiology of these antibodies, the same group then infused purified IgG (12 injections of 10µl over 3 weeks) from two SPS patients with amphiphysin antibodies (including the same patient from the previous experiments) directly into the intrathecal compartment in rats to circumvent the BBB (Geis, Weishaupt et al. 2010). The rats displayed features of SPS, including stiffness and muscle spasms; *in vivo* electrophysiology recordings experiments implicated reduced inhibitory synaptic function as the cause. In additional *in vitro* studies, amphiphysin antibodies bound to CNS neurons with subsequent internalization, leading to disturbance of synaptic vesicle endocytosis and diminished release of the inhibitory neurotransmitter GABA. The exact mechanism of how the internalization of amphiphysin antibodies occurred *in vivo* is still unknown. However, this intrathecal model demonstrated successfully CNS effects of CNS autoantibodies through passive transfer, and provided evidence of the pathogenic mechanism.

The same group repeated their experiments with GAD antibodies (section 1.8.5) to try and reproduce the motor symptoms of SPS (Hansen, Grunewald et al. 2013), using IgG from a patient with predominant motor symptoms and no anxiety. On this occasion, 15 intracerebroventricular (ICV) 10µl injections of purified IgG were administered over a three week period, and compared to intrathecal injections. They found that ICV injections of GAD-Abs produced motor dysfunction in awake rats that were not seen in the intrathecal model of passive transfer. However, despite the huge amount of IgG used, stiffness and spasms were not seen.

These experiments demonstrate that passive transfer of neuronal autoantibodies systemically (with BBB breakdown) or directly into the CSF compartments can reproduce symptoms of CNS disease. The experiments by Dr Philippa Petingill using NMDAR-Ab IgG showed for the first time that the newly recognized CNS autoantibodies that bind to the extracellular surface can also show pathogenic effects, even after one ICV injection into mice. A single intrathecal injection of IgG from a patient with paraneoplastic cerebellar degeneration and LEMS containing VGCC-Abs, also produced a marked ataxia in injected mice (Martín-García, Mannara et al. 2013).

Importantly all the models employed methods to circumvent the BBB to allow the antibodies access to the brain parenchyma and replicate the natural history of the human disease. The binding pattern *in vivo*, can aid understanding of the pathological processes with regards to the specific receptor/ and or regional binding localization. However, direct intracerebral injections of autoantibodies can also give an insight into the underlying pathological mechanisms of CNS autoantibodies on the brain parenchyma.

Aquaporin-4 autoantibodies, which bind this glial water channel protein, are found in neuromyelitis optica (NMO), an inflammatory demyelinating disease of the CNS (Lennon, Kryzer et al. 2005). Intracerebral injection of IgG from NMO patients with the addition of human complement into mice, caused loss of aquaporin-4 expression, glial cell oedema, and myelin destruction within 12 hours, with eventual neuronal death and extensive inflammatory cell infiltration at seven days (Saadoun, Waters et al. 2010). Mice injected into the right hemisphere with IgG and complement showed preferential right turning behaviour which was not seen in the control injected mice. None of these effects were seen without the addition of complement to the NMO IgG suggesting that both are essential for the formation of NMO lesions. Given the

direct intracerebral injection gives reproducible lesions, this mouse model of passive transfer would be useful for testing novel therapies and studying other factors involved in the different stages of NMO pathogenesis. However, for other CNS autoantibodies, the lesional effect of the intracerebral injection may make interpretation of behavioural data difficult.

1.8.7 Active immunization models of CNS disease

The induction of an autoimmune disorder by active immunization forms one of Witebsy's criteria for autoimmune disease. One report published, relevant to autoimmune epilepsy, involved the active immunization of mice with a GluR3 peptide followed by kindling with the proconvulsant pentylenetetrazole (PTZ) (Ganor, Goldberg-Stern et al. 2014). GluR3 antibodies were only found in six out of ten of the Glu-R3B-immunised mice (and not in the control injected mice), and these mice showed increased seizure susceptibility with repeated PTZ doses, increased anxiety and subtle motor deficits on behavioural testing. The main problem with this study is the use of the peptide to produce antibodies. This is unlikely to produce CNS-autoantibodies that bind to the extracellular surface of the native receptor and therefore very unlikely to be pathogenic. The peptide used was similar to that in the original Rasmussen's encephalitis animal studies that were subsequently disproven (Rogers, Andrews et al. 1994).From the available evidence, it appears that the most effective way to reproduce the pathogenic effects of CNS autoantibody mediated disease *in vivo* is by passive transfer, circumventing the BBB by systemic, intrathecal, intracerebroventricular or intracerebral injection, and on occasion with additional factors, e.g. complement.

1.8.8 Animal models of epilepsy

Producing an optimal model of seizures and epilepsy is also challenging. Acute animal models of epilepsy display seizures induced either by chemoconvulsants, electrical, metabolic and sound stimuli. These models are most useful and appropriate for investigating mechanisms of epileptogenesis. Often, these seizures are provoked in a normal brain, so long-term and interictal epileptogenic changes cannot be studied. However, chronic epilepsy models have recurrent spontaneous seizures and enable both anatomical and electrophysiological characterisation of ictogenesis. Despite this advantage, they are more expensive and time-consuming in experimental practice.

Recent advances have led to the use of 'optogenetics' in the experimental investigation of epileptogenesis (Boyden, Zhang et al. 2005, Tonnesen, Sorensen et al. 2009). Through the expression and stimulation of opsins (light-sensitive proteins) in selected cell-types, the "optogenetic approach" allows the experimenter to have control over neuronal excitability both *in vivo* and *in vitro.* This technique is also being investigated as a treatment for epilepsy (Wykes, Heeroma et al. 2012, Sukhotinsky, Chan et al. 2013).The main experimental models of epilepsy used, and their relative advantages and disadvantages are summarized in Table 1.1.

Model	Epileptogenic stimulus	Effect	Uses/Advantages	Limitations
Pilocarpine SE	Systemic or intrahippocampal injection	Limbic SE; chronic seizures, *cf* TLE in humans with HS	Spontaneous seizures AED screening Mechanisms epileptogenesis and SE Study of co-morbidities	High mortality, age dependent severity and frequency of spontaneous seizures
Kainic acid SE	Systemic or intrahippocampal injection	Limbic SE; chronic seizures, *cf* TLE in humans with HS	Spontaneous seizures AED screening Mechanisms epileptogenesis	High mortality, age dependent severity and frequency of spontaneous seizures
Acute chemical models, e.g. PTZ, strychnine, NMDA	Systemic or intrahippocampal injection	Nonconvulsive absence or generalised tonic-clonic seizures	Acute, repetitive seizures Rapid screening of AEDs	No neuropathological changes Lack of spontaneous seizures
Electroshock-induced seizures	Current stimulation through corneal or auricular electrodes	Generalised tonic-clonic seizures	AED screening Studying molecular effects of epileptogenesis	Must be used in conjunction with other seizure models as can give conflicting results when applied to AED effects on human epilepsy
Afterdischarges (AD)	Focal electrical stimulation in specific brain regions, e.g. limbic structures	Complex partial seizures (limbic stimulation) Myoclonic seizures (sensorimotor cortex)	Study of ictal spread to other regions. Kindling, treatment studies of refractory epilepsy	Unable to manipulate subgroups of neurons Difficulty studying electrophysiological changes during focal stimulation due to electrical artefact. Kindling is time-consuming and costly.
Hyperthermic seizures	Heated airstream to increase body temperature in immature rodents	Mimics febrile seizures	Mechanisms of epileptogenesis	No evidence of hippocampal neuronal loss
Hypoxia model	Unilateral carotid ligation or global hypoxia in airtight chamber in immature rodents	Brief, repetitive, tonic-clonic seizures	Recurrent seizures Model of neonatal hypoxic encephalopathy AED screening Mechanisms epileptogenesis	Varied seizure susceptibility
Brain pathology	Fluid percussion injury	Generalised tonic-clonic seizures	Post TBI epilepsy AED screening Mechanisms of epileptogenesis	Initial mild seizures, long latency periods
Audiogenic models	Acoustic stimulation in genetically prone rodents	Tonic-clonic and wild running seizures	TLE and reflex epilepsy studies Mechanisms epileptogenesis Study of co-morbidities	No spontaneous recurrent seizures
Optogenetic models	Targeted light stimulation of selected neuronal subtypes expressing opsins	Controllable epileptic oscillations (excitatory and inhibitory)	Mechanisms of epileptogenesis Control of *in vivo* induced epileptiform activity	Technical issues regarding gene delivery, miniaturisation of sources for light stimulation. Complex interactions from light stimulation can be difficult to interpret/predict.

Table 1-1 The most commonly used experimental rodent models of acute and chronic epilepsy.

Abbreviations: SE status epilepticus; TLE temporal lobe epilepsy; HS hippocampal sclerosis; AED anti-epileptic drug; PTZ pentylenetetrazol; TBI traumatic brain injury

Refs: Seizures and Epilepsy, Jerome Engel, Jr. Published 2013;Kandratavicius, L., et al. (2014). "Animal models of epilepsy: use and limitations." Neuropsychiatr Dis Treat **10**: 1693-1705; Auvin, S., et al. (2012). "Novel animal models of pediatric epilepsy." Neurotherapeutics **9**(2): 245-261; Kokaia, M., et al. (2013). "An optogenetic approach in epilepsy." Neuropharmacology **69**: 89-95.

Given the compelling evidence of the association between the immune system, seizures, and CNS autoantibodies, the importance of investigating the presence and pathogenicity of autoantibodies in paediatric epilepsy is clear. In a recent study of the new epilepsy classification scheme in paediatric epilepsy, almost one-third of children were classified as having an "unknown aetiology". (van Campen, Jansen et al. 2013), It is tempting to hypothesise that some of these patients may harbour pathogenic antibodies and have a potentially treatable cause for their epilepsy. In adults, 'autoimmune epilepsy' has been used to define epilepsy patients likely to have an immune-mediated cause for their epilepsy. This has enabled studies of treatment and outcomes in these cases, the results of which may be applied to paediatric autoimmune epilepsy cases.

1.8.9 Management of autoimmune epilepsy in adults

The first study to evaluate treatment responses in adult 'autoimmune epilepsy' looked retrospectively at cases presenting to an autoimmune neurology clinic and epilepsy clinic within a five year period (Quek, Britton et al. 2012). Cases were defined as 1) epilepsy as the exclusive (n=11) or predominant (n=21) presenting concern and 2) autoimmune pathogenesis suspected by the treating clinician based on detection of a neural antibody, inflammatory CSF, or inflammation on MRI. Focal seizures were the most common seizure type seen in 84% (27 out of 32 cases). Most patients had received at least 2 AEDs at time of presentation and 81% still had daily seizures. Additional clinical features of LE were seen in 20 patients (63%). Most patients (28/31) had an abnormal EEG, epileptiform changes were seen in 63%; 22 patients had MRI changes, 20 of these were 'probable inflammatory changes'. Neural antibodies were identified in 91% of patients but included those to intracellular antigens (CRMP-5, Ma2). VGKC-

complex Abs were the most commonly found CNS autoantibody to a membrane protein (n=18).

Immunotherapy treatment was given to 27 out of 32 of these patients for the treatment of seizures, in addition to their AEDs. This was either intravenous steroids (methylprednisolone) alone, IVIG alone, or a combination of methylprednisolone, IVIG, cyclophosphamide and PLEX. At last follow-up (median 17 months, range 3-72 months), 22 out of 27 (81%) patients clinically improved, as judged by the treating clinician and patient reports of seizure frequency. Strikingly, 67% of patients achieved seizure freedom.

Autoimmune epilepsy as defined in this group of patients, clearly included a large number of patients with LE and VGKC-complex Abs, a phenotype known to respond well to immunotherapy (Vincent, Buckley et al. 2004). The study was also limited in the retrospective design and concurrent AED treatment. Some patients had changes to the AEDs alongside the immunotherapy, which may have given a false impression of the potential effectiveness of immunotherapy.

On the basis of this study, the following clinical features suggestive of autoimmune epilepsy were presented (Toledano, Britton et al. 2014):

- Acute to subacute onset (maximal seizure frequency < 3 months)
- Multiple seizure types or facio-brachial dystonic seizures (FBDS)
- AED resistance
- Personal or family history of autoimmunity
- History of recent or past neoplasia
- Viral prodrome
- Evidence of CNS inflammation (CSF/ MRI / PET scans)
- Detection of neural antibody

Most of these could equally apply to a diagnosis of autoimmune encephalitis and are not specific to “autoimmune epilepsy”. Nevertheless, this type of guidance can help inform treatment decisions in autoimmune encephalitis patients where seizures are the most frequent and severe symptom. This particularly applies to the use of immunotherapy which is not often used as a standard epilepsy treatment in any existing adult epilepsy syndromes, apart from the recently described FBDS (section 1.8.1). Even in prospective studies of epilepsy patients without encephalitis, newly diagnosed adult epilepsy patients with co-existing CNS surface membrane protein autoantibodies have a tendency towards standard AED treatment resistance (Brenner, Sills et al. 2013). The pattern of autoimmune epilepsy as defined above will also alert the clinician to the possibility of an underlying tumour, more common in adult patients with autoantibodies.

Can similar guidelines be applied to children with epilepsy that is thought to be autoimmune? Paraneoplastic syndromes are rare in children, and a viral prodrome is non-discriminatory given the higher levels of non-specific viral infections in children on a regular basis. Some of the investigations, including PET scans are not often useful in the paediatric population.

Sulieman et al., (Suleiman, Brilot et al. 2013), proposed a set of clinical criteria for the recognition of paediatric ‘autoimmune epilepsy’ modified from an existing guideline on recognition, testing and treatment of suspected CNS autoimmune disorders (Zuliani, Graus et al. 2012). To support the diagnosis of autoimmune epilepsy in children, they had to have an acute/ subacute presentation (<12 weeks) and exclusion of CNS infection, toxic and metabolic causes. Supportive features, one of which was needed in addition, included presence of a well-defined clinical syndromes such as NMDAR-Ab encephalitis or LE, evidence of CNS inflammation (MRI/CSF/inflammatory neuropathology on biopsy) or presence of other autoimmune

disorders (Suleiman, Brilot et al. 2013). A positive response to immunotherapy increased the likelihood of autoimmune epilepsy.

With the lack of large prospective cohort studies in paediatric autoimmune epilepsy, these guidelines can be useful in making a retrospective diagnosis of autoimmune epilepsy, but this is based on the presence of CNS autoantibodies and response to immunotherapy. Some paediatric autoimmune encephalitis patients without CNS autoantibodies can make a significant clinical response to immunotherapy (Hacohen, Wright et al. 2013), and this is acknowledged within the guidelines. However, it has been shown that early treatment and diagnosis is associated with a better outcome in CNS autoantibody related disease (Titulaer, McCracken et al. 2013). As with adult autoimmune epilepsy, these paediatric guidelines worked well with autoimmune encephalitis patients (three NMDAR-Ab encephalitis and two VGKC-complex Ab LE patients were given a ‘definite’ or ‘probable’ autoimmune epilepsy classification). However the guideline falls down in the diagnosis of epilepsy patients. One case of a one year old with epileptic encephalopathy and epileptic spasms who had VGKC-complex antibodies (201pM) and responded to steroids, was given a definite diagnosis of autoimmune epilepsy. The testing of VGKC-complex Abs was at 13 months, onset of epilepsy was at 4 months. This case was previously presented in a case report (Suleiman, Brenner et al. 2011), and it could be argued this child had a diagnosis of cryptogenic West syndrome. She had modified hypsarrythmia on EEG and had been treated with vigabatrin, and enrolled on the UK Infantile Spasms Study (UKISS) where she received oral prednisolone. She responded to this treatment but this is standard treatment in West syndrome and infantile spasms. The problem is that diagnosing this child with definite autoimmune epilepsy may have treatment implications. Would the next step then be PLEX, intravenous steroids, cyclophosphamide or rituximab if there was a relapse of spasms, as these treatment options would be used in autoimmune CNS

disease? In West syndrome, it is more likely that other AEDs would be tried that are known to help in this disease, for example topiramate or nitrazepam, which are generally safe and well-tolerated in children. This case demonstrates both the importance and difficulty in the classification of any epilepsy syndrome, including autoimmune epilepsy (Berg, Berkovic et al. 2010).

From both guidelines, it is apparent that patients with CNS autoantibodies are the most responsive to treatment, and of all available criteria to define autoimmune epilepsy, identification of these in paediatric epilepsy patients may be most relevant.

1.8.10 Summary

Epilepsy and the immune system are integrally related in the production, pathogenesis, and sustainment of seizure activity. The identification of CNS autoantibodies in seizure-related disorders such as NMDAR-Ab encephalitis has prompted the search for these autoantibodies in patients with epilepsy. Prompt recognition and removal of these autoantibodies is associated with a good outcome in most patients with the full clinical syndrome and resolution of seizure activity. The identification of CNS autoantibodies in epilepsy patients has both diagnostic and therapeutic implications, particularly in those with no known aetiology who may be resistant to standard therapies. This has been recently demonstrated in adult screening studies of new-onset and follow-up patients in epilepsy out-patient clinics, and limited treatment/ outcome reports.

There is a pressing need for large cohort studies of new-onset paediatric epilepsy patients to improve the identification and clinical phenotyping of autoimmune epilepsy. There are many unanswered questions in paediatric autoimmune epilepsy. Does the finding of a CNS autoantibody in paediatric epilepsy have prognostic implications? What is the short- and long-term outcome? Is this different to CNS autoantibody negative patients? Should all paediatric epilepsy patients be tested? However, even the

presence of CNS autoantibodies in paediatric epilepsy does not necessarily mean they are the cause of epilepsy. The epileptogenic potential of some CNS autoantibodies has been demonstrated *in vitro*, but these effects have not yet been demonstrated *in vivo*, as required by Witebsky's criteria. This thesis attempts to directly answer these questions.

The aims of the work described in this thesis were threefold;

1. Screen new-onset paediatric epilepsy cohorts for the presence of disease relevant CNS autoantibodies and relate these findings to the epilepsy phenotype, treatment regimes, and outcomes of the patients.
2. Investigate the pathogenicity, and in particular epileptogenicity, of CNS autoantibodies *in vivo.*
3. Investigate new potential therapies for CNS autoantibody –related neurological diseases based on underlying pathogenic mechanisms.

CHAPTER 2 - Materials and methods

2.1 Clinical material

Serum samples from two paediatric epilepsy cohorts with control groups were tested for the presence of CNS autoantibodies. All collaborating groups had local ethical consent for participation in this research. Additionally, ethical approval for sample testing was obtained from the Oxfordshire Regional Ethics Committee (07/Q1604/28). Samples were tested blinded to the clinical details, with clinical information only exchanged upon completion of antibody testing. A third cohort of serum from patients with CSWS was also tested for specific antibodies relevant to the disease (French CSWS cohort).

2.1.1 Dutch Study of Childhood Epilepsy

The Dutch Study of Childhood Epilepsy (DSCE) recruited 494 children (aged 1 month to 16 years) with new-onset epilepsy between 1988 and 1992. Children were enrolled from four participating centres in the Netherlands (Arts, Geerts et al. 1999). The cohort comprised approximately 75% of the expected incidence within the referral area. The study was approved by the medical ethical committees of all participating hospitals. Parents or caregivers gave their written informed consent. The recruiting paediatric Neurologist completed an extensive questionnaire which included details of seizure semiology, possible provoking factors, previous medical history and family history. Confirmation of the diagnosis of epilepsy and inclusion in the study was made by a committee of three paediatric Neurologists, using predefined diagnostic criteria. Newly diagnosed epilepsy was defined as two or more unprovoked seizures within a one year period. Children with acute symptomatic seizures were excluded. The aetiology was

classified according to the definitions of the International League Against Epilepsy (ILAE) guidelines at the time (Guidelines for epidemiologic studies on epilepsy. Commission on Epidemiology and Prognosis, International League Against Epilepsy, 1993).

Blood samples were taken from some of the patients at onset, and during the first year of disease at either six or 12 month intervals. Owing to sample depletion from previous serological studies (Callenbach, Jol-Van Der Zijde et al. 2003), only 178 samples had sufficient remaining material and were made available for testing for this study. In addition, 114 age and sex-matched control samples from sibling donors for recipients of a bone marrow graft were also provided by the group for testing. All of the samples had been stored at -20^{o}C since collection. At enrolment, classification of the seizures and epilepsy syndromes was made after discussion by three participating paediatric Neurologists according to the 1989 ILAE criteria. This was revised after two years and at the end of the most recent intractability study (Geerts, Brouwer et al. 2012) as some children proved to have neurological brain-related morbidities. In view of the new terminology published in the most recent reorganization of the ILAE seizure and epilepsy classification, and to facilitate interpretation of the new serological data with the historical clinical data, we have provided definitions of the terms used in this study in Table 2.1.The serum samples used from this study and the other two cohorts (French and Australian) were all collected and stored as part of a clinical research study with standard operating procedures according to study protocol. However, transport of the samples from overseas may have subjected them to a freeze-thaw cycle, despite use of appropriate delivery services and transport containers. In order to minimise this, aliquots were taken and frozen separately to avoid repeated sample handling. Further samples from antibody positive patients were sent for re-testing by the Dutch

collaborators to confirm the results so it is unlikely that transporting the samples affected the results.

Terminology	Definition
Idiopathic epilepsy (IE)	Epileptic syndromes with particular clinical characteristics and specific EEG findings. Unknown origin but presumed genetic aetiology.
Remote symptomatic epilepsy (RSE)	Epilepsies considered the consequence of a known or suspected disorder of the central nervous system resulting in a static encephalopathy. All children with mental retardation (MR) with epilepsy of unknown cause were classified as RSE.
Cryptogenic epilepsy (CE)	Epilepsies of unknown origin that do not conform to the criteria for IE or RSE.
Terminal remission	Interval between the very last seizure and the end of follow-up.
Fast response to medication	6 months of remission starting within 2 months after initiation of anti-epileptic drug (AED).
Intractability	No remission exceeding 3 months (at least one seizure per 3 months) during a minimum period of 1 year of observation despite adequate treatment (Arts 2004). Early onset intractability: onset of intractability within the first 5 years of follow-up. Late onset intractability: onset after the first 5 years of follow-up.
Description of patterns of seizures before enrollment	Continuous - intervals between seizures < 1 week Intermittent - intervals between seizures > 1 week Multiple bursts - clusters of seizures within 1 week with >1 week between clusters

Table 2-1 Definitions of terminology used from the pre-existing clinical database of the Dutch Study of Epilepsy in Childhood.

2.1.2 Australian cohort

The second cohort was also collected prospectively by Dr Jehan Suleiman and Dr Russell Dale at Sydney Children's Hospital, Westmead, from September 2009 to

November 2011. Children were recruited between two months and 16 years of age. Patients with new onset seizures of any types or aetiology were included except;

- Neonates (0-60 days) as many of the causes for seizures are age specific and have different aetiological factors
- Patients with a clear cause for seizures, i.e. bacterial meningitis, stroke, traumatic brain injury and brain tumours
- Patients whose serum was collected more than 6 months from onset of first seizure
- Patients with non-epileptic paroxysmal events

The patients were all either inpatients or outpatients at The Children's Hospital at Westmead. In this study, a seizure was defined as per ILAE guidelines;
" the clinical manifestation consists of sudden and transitory abnormal phenomena which may include alterations of consciousness, motor sensory, autonomic, or psychic events, perceived by the patient or observer" (Guidelines for epidemiologic studies on epilepsy. Commission on Epidemiology and Prognosis, International League Against Epilepsy, 1993). The clinical and paraclinical information was collected by Dr Jehan Suleiman.

The serum samples from 112 patients were provided for antibody testing. A disease control cohort of 68 patients was also provided. These samples had also been stored at -20^{o}C pre-testing. Ethics approval was obtained in August 2009 from the Ethics Committee at the Children's Hospital, Westmead (HREC reference number 09/CHW/57).

2.1.3 French CSWS cohort

Serum from children with CSWS were collected by four French medical centres from 2009. To be included in the study, children with CSWS had to have at least one EEG compatible with an ESES pattern. The diagnosis of LKS was made in patients presenting with severe language impairment and language regression (acquired aphasia) associated with epileptiform activity (Lesca, Rudolf et al. 2012). All experiments were conducted in accordance with the Declaration of Helsinki and all procedures were carried out with the adequate understanding and written informed consent that were obtained from the parents for their children and for themselves, according to the appropriate bioethics law and ethical committees (n° 05/78, CPP Strasbourg Alsace 1). Serum samples (n=53), were provided from patients and relatives, and included ten serum samples from unaffected family members, 25 from patients with CSWS, 12 with Rolandic epilepsy, four with LKS, one with epilepsy and autism and one with dyspraxia. The serum samples were all coded at the time of testing. The clinical details were only released after completion of all antibody testing.

2.2 Autoantibody detection methods

2.2.1 Cell-based assays

A cell-based assay (CBA) was used to detect the presence of known antibodies against cell surface expressed antigenic targets, namely the NMDA-, AMPA-and $GABA_B$-receptors, and the VGKC-complex associated proteins LGI1, CASPR2 and contactin-2 proteins. These assays had been previously validated and are in routine clinical use (Leite, Jacob et al. 2008, Irani, Bera et al. 2010). All assays were performed by SW unless otherwise stated.

Human embryonic kidney cells (HEK293) were cultured in Dulbecco's modified Eagle's medium (DMEM) with 10% foetal calf serum (FCS) and 1% penicillin-streptomycin-amphotericin (PSA) at 37ºC in 5% CO_2 at 90% humidity. For the CBA, cells were resuspended in 0.25% trypsin/ 1mM EDTA solution and plated at a density of approximately 40,000 cells/cm^2 in 6 well plates containing poly-L- lysine (PLL) coated glass coverslips. Twenty-four hours later, each well was transiently transfected with a total of 3 µg of plasmid DNA of the antigen of interest using polyethylenimine (PEI) (ratio of 2:1 pDNA:PEI). 48 hours post-transfection, HEK cells expressed the antigenic protein at sufficient levels to use for antibody screening. The LGI1 and CASPR2 plasmid constructs included an enhanced green fluorescent protein (EGFP) tag which allowed for visual confirmation of successful cell transfection and protein expression. For all other constructs, a plasmid encoding EGFP was co-transfected to indicate successful cell transfection. For NMDAR transfected cells, the media was supplemented with 500 µM of ketamine to prevent cell death due to activation of NMDARs by glutamate in the media. To test patient serum for the presence of antibodies, HEK cells on coverslips were incubated with patient sera (dilution 1:20 or 1:100) in 1% BSA diluent (DMEM supplemented with 1% bovine serum albumin and buffered with 20 mM HEPES) for 60 minutes at room temperature. Cells were washed three times with HEPES-buffered DMEM and fixed in 3% formaldehyde for 10 minutes. Following a further 3 washes, Alexa Fluor 568-conjugated goat anti-human IgG secondary antibody (A-21090, Invitrogen) was applied for 45 minutes at room temperature (1:750 diluted in 1% BSA diluent). Cover slips were washed with PBS (phosphate buffer solution), mounted using aqueous mounting medium (Dako, Cambridge, UK) containing 4',6-diamidino-2-phenylindole (DAPI) as a nuclear counterstain. Cells were visualised using a Leica DM2000 fluorescence microscope. Binding was scored on a scale from 0-4 where 0 is "no-binding" and 4 is

"strong binding" and was conducted by two independent observers blinded to clinical details, with good consistency between final scores (Figure 2.1) (Leite, Jacob et al. 2008, Waters and Vincent 2008, Irani, Bera et al. 2010).

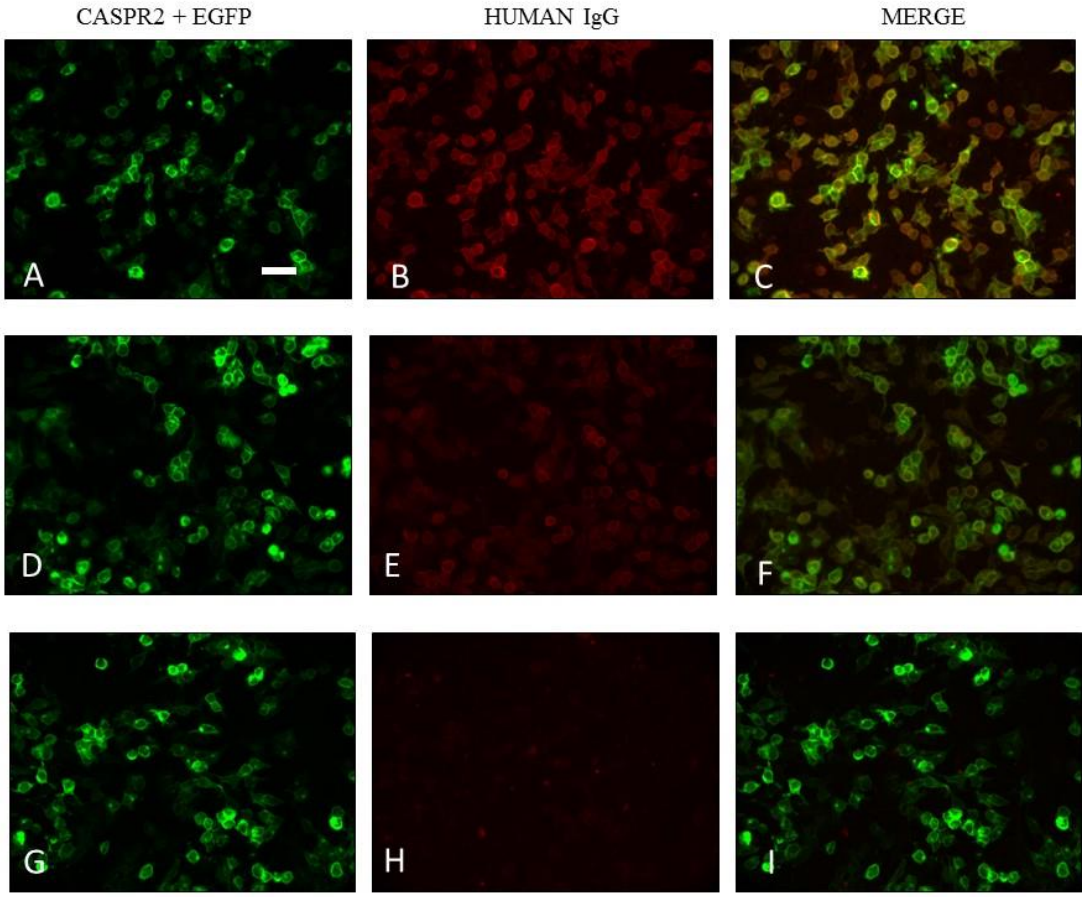

Figure 2-1 Scoring of cell based assay for detection of CASPR2 antibodies.

A-C. The CASPR2 transfected HEK cells are seen by means of the EGFP tag, indicating good positive transfection of HEK cells (green). Application of human sera (at a dilution of 1 in 100) containing CASPR2 antibodies binds to the CASPR2 protein expressed on the cell surface of the transfected HEK cells (B). These human antibodies are labelled with a red fluorescent secondary antibody. In the merge photomicrograph (C), the red IgG human CASPR2 antibodies co-localise with the transfected HEK cells indicating specific binding and a positive result. This serum would score a positive CBA score of 3. Scale bar 50µm, same for all photomicrographs.

D-E. Less bright staining of human IgG (red, E) with co-localization seen in F but this is less than C. This assay would score a 1.5.

G-H. There is good transfection of CASPR2+EGFP in the HEK cells (green, G). However, this human serum is negative for CASPR2 antibodies as there is no human IgG staining (red, H) confirmed on the merge photomicrograph. This assay would score negative (0).

2.2.2 Radioimmunoprecipitation assay (RIA)

(1) VGKC-complex antibodies

To detect VGKC-complex antibodies in patient sera a radioimmunoprecipitation (RIA) assay was performed as previously described (Hart, Waters et al. 1997, Vincent, Buckley et al. 2004). In brief, digitonin solubilized VGKC complexes were generated from rabbit brain membrane extract and were radioactively labelled with ^{125}I-α-Dendrotoxin (DTX)**.** 50µl of a 1 in 10 dilution of patient serum (with PTX, 0.02M phosphate buffer and 0.1% Triton x100, pH7.2) was incubated with 50µl of I^{125}-αDTX-labelled extract overnight at 4^{o}C. Next day, VGKC immunocomplexes were immunoprecipitated by adding sheep anti-human IgG. The precipitates were pelleted by centrifugation, the pellet was washed three times with Phosphate buffered saline containing triton-X 100 and the radioactivity counted using the Wallac Wizard 1470 Automatic Gamma Counter. The level of radioactivity detected (calculated in pM) is proportional to the antibody level in the sample (normal < 100pM, high positive >400pM). To negate the effects of non-specific binding, a 'hot-cold' assay was also performed on the samples. This assay subtracted non-specific surface-bound ^{125}I-αDTX from total surface-bound ^{125}I-αDTX to estimate specific surface-bound ^{125}I-αDTX. To achieve this, patient samples were incubated with unlabelled DTX to saturate binding of VGKC-complex receptors before addition of labelled extract as above. Serum samples with high titres of VGKC antibodies were tested at serial dilutions to obtain accurate titres.

(2) GAD antibodies

GAD antibodies were measured using a commercial radioimmunoassay (RSR Ltd., Cardiff, United Kingdom). 50µl of a 1 in 10 dilution of patient serum was incubated with 50µl I^{125}-GAD overnight at 4^{o}C as per the manufacturer's instructions. Serum

samples with GAD antibodies exceeding 10 units/ ml were considered positive and tested at serial dilutions to obtain accurate titres.

2.2.3 Primary neuronal cultures

(1) Hippocampal neurons

Primary hippocampal neuronal cultures were prepared by SW from P0 Wistar rat pups as described previously (Kaech and Banker 2006, Beaudoin, Lee et al. 2012). In brief, P0 pups were decapitated, brains removed and the hippocampi were dissected into Hanks Balanced Salts Solution (HBSS) dissection medium. Following 20 minutes incubation with 0.25% trypsin/EDTA solution at 37^{o}C, hippocampi were washed three times in MEM buffer (Minimal Essential Medium with 10% FCS and 1% PSA) and triturated to form a homogenous single cell suspension. After gentle centrifugation, cells were resuspended and plated at a density of 50,000 cells cm^{-2} in MEM buffer into wells containing PLL coated glass coverslips. Four hours later, media was replaced with serum free medium (Neurobasal medium supplemented with B-27 nutrient factor, 200mM glutamine and PSA) and cells were maintained at 37^{o}C in 5% CO_2 at 90% humidity. Twice weekly half of the media was replaced by fresh Neurobasal media. Neuronal cells were assayed between days *in vitro* (DIV) 14-17.

(2) Cerebellar granule neurons

Cerebellar granule neurons were prepared by SW as previously described (Parizad et al., 2008). In brief, P6 Sprague-Dawley pups were euthanized by decapitation and the cerebella dissected into HHGN dissection solution (1 x HBSS, 2.5 mM HEPES (pH 7.4), 35mM glucose, 4mM $NaHCO_3$). Meninges were removed and cerebellae were washed three times with HHGN solution. Cerebella were incubated in trypsin-DNase solution for 10 minutes at 37^{o}C. Following a further three washes in HHGN solution,

the cerebellae were triturated and dissociated into a single cell suspension in a Basal Medium Eagle (BME) buffer containing DNase. Cells were seeded at a density of 500, 000 cells per cm^{-2}. Cells were maintained by adding a final concentration of 10 µM cytosine arabinoside (AraC) on DIV1. On DIV 3 glucose was added to a final concentration of 25 mM. Cerebellar neurons were assayed at DIV 7.

2.2.4 Neuronal assay for detection of cell-surface antibodies

To determine if patient sera contained antibodies that reacted with unknown surface expressed neuronal antigenic targets, primary hippocampal and cerebellar cultures were incubated for one hour with patient serum at a dilution of 1 in 100 in the respective neuronal culture medium supplemented with HEPES and 1% BSA. Cells were washed and fixed in formaldehyde 4% for 10 minutes. After washing, cells were incubated with anti-human IgG-Alexa Fluor 488-conjugated secondary antibody (A-11013) at 1:1000 for 45 minutes. To visualize the neuronal cultures, cells were permeabilised with 0.25% Triton X 100 in PBS and incubated in mouse anti-MAP2 (Sigma; 1:1000 for hippocampal cultures) or mouse anti-beta-3-tubulin (Sigma; 1 in 1000 for cerebellar cultures) primary antibody for 1 hour at room temperature. After washing, cells were incubated with anti-mouse IgG-Alexa Fluor 568-congugated secondary antibody at dilution 1:1000. Cover slips were washed with PBS, mounted using aqueous mounting medium (Dako, Cambridge, UK) containing DAPI as a nuclear counterstain. Cells were visualised using a Leica DM2000 fluorescence microscope.

2.2.5 In vivo pathogenesis experiments

All in-vivo pathogenesis experiments were performed by SW, unless specifically stated otherwise.

(1) Purification of patient IgG

IgG was purified from the plasma of three NMDA receptor antibody positive patients and from the serum from two healthy controls using Protein G Sepharose beads (Sigma, UK). Following centrifugation and heat inactivation (65^{o}C for 30 minutes), the plasma was diluted 1:1 with Hartmann's solution and incubated with the Protein G Sepharose column beads overnight at 4^{0}C on a roller for optimal binding of IgG. The sample was loaded and passed through a chromatography column to allow other plasma proteins to pass through. The IgG was eluted from the column beads with 0.1M glycine solution (pH 2.3) and immediately neutralised with 100µl of 1M Tris pH 8. Protein concentration of eluted fractions was measured using a Coomassie Plus assay kit (Pierce, USA). The peak protein fractions were pooled and dialysed against Hartmann's physiological solution six times over 36 hours. The IgG was concentrated using Amicon ultra-4 10KDa filter units, and filter-sterilised. The concentration was determined using NanoDrop 3300 (ThermoScientific, UK), and IgG stored at 4^{o}C. To confirm positivity and determine end point dilutions, purified IgG preparations were tested for immunoreactivity on brain sections, CBAs and on hippocampal neurons.

(2) Preadsorption of NMDAR antibodies

Similar to the protocol for the CBA, PLL coated T-175 flasks of HEK cells were transfected with expression vectors encoding the NR1 and NR2B NMDA receptor subunits. 48 hours later, cells were resuspended in 0.25% trypsin/ 1 mM EDTA solution and centrifuged to yield individual cell pellets. Patient plasma was incubated with the NMDA receptor expressing cell pellets for 45 minutes at room temperature with gentle rotation. The adsorbed samples were retrieved for re-testing on the cell based assay.

(3) Implantation of telemetric transmitters

Transmitter A3019A, weight 2.4g was used in all animals (Figure 2.2). The operating life is 3.6 weeks at a sampling rate of 512 SPS. The high-pass filter consists of a zero at 0.7Hz and low-pass filter is a 3-pole filter with 160Hz cut-off frequency (http://www.opensourceinstruments.com/Electronics/A3019/M3019.html).

Female C57/BL6 mice were used in all experiments. All surgery was conducted under isofluorane gaseous anaesthesia (2–4% in oxygen). Depth of anaesthesia was monitored by observing breathing rate and paw-pinch reflex. The level of isofluorane was adjusted to maintain surgical anaesthesia. Vetergesic (Sogeval, UK) and Metacam© (Boehringer Ingelheim) were used as peri- and post-operative analgesia. Temperature was controlled using a homeothermic blanket (Harvard Apparatus). Mice were placed in a stereotaxic frame for all surgeries. A 2 cm incision was made caudally over the skull surface. A subcutaneous pocket was formed over the right flank by blunt tissue dissection, and the transmitter (Open Source Instruments, weight 2.4 g) was then inserted in to it (Figure 2.2). The rubber-ensheathed electrode wires with screws attached were left anteriorly exposed prior to fixation to the skull surface. Two holes were drilled through the skull at co-ordinates 1mm lateral and 1mm caudal from bregma (to leave enough space for subsequent ICV injections). Electrode screws were fixed into the drilled holes with dental cement to hold them in place. Mash and a heat pad were provided during recovery. The animals recovered for a minimum of 5 days before any further surgery. Daily records of weight, appearance, wound healing, spontaneous and provoked behaviour were kept throughout the experimental period.

A.

B.

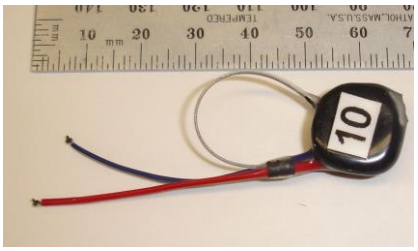

Figure 2-2 Schematic demonstrating EEG transmitter placement *in vivo* and actual transmitter.

A. The transmitter is implanted to lie subcutaneously over the flank. The two transmitter screws are fixed into the skull to give one reference and one reading electrode.
B. Subcutaneous Transmitter A3019A with Screw Electrodes (courtesy of OSI). The antenna is stranded wire coated with silicone. The leads are helical wire insulated with silicone and screws are M0.5, 1-mm long with binding heads.

(4) Stereotaxic intracerebroventricular injection of human IgG

C57BL/6 female mice were housed in single sex cages in a vivarium at 21^{o}C, with 58 % humidity and a 12 hour light-dark cycle. Animals had free access to food and water. All surgery and experiments were performed in accordance with the UK Home Office Licence Regulations under the Animal Scientific Procedures Act, 1986, and personal licence stipulations. All surgery was conducted under isofluorane gaseous anaesthesia (2–4 % in oxygen) in a stereotaxic frame. Body temperature was maintained using a heating pad. The skull surface was exposed and a single burr hole made at the appropriate stereotaxic co-ordinates for targeting the lateral ventricle on the left side: 1 mm lateral and 0.45 mm caudal from bregma. 8µl of purified IgG from either NMDAR-Ab positive patient or HC was slowly injected to a depth of -1.85 mm from dura over 20 minutes using a Hamilton syringe with a 33 gauge needle. 300 nl of fluorescent beads

(Lumaflour Inc.) were simultaneously injected with the IgG to verify the position of injection post-mortem. Following completed IgG infusion, the Hamilton syringe was left in place for an additional five minutes to allow for diffusion and withdrawn slowly. The skin was sutured and the animal was allowed to recover in a warm chamber before being replaced in its home cage. Animals were singly housed post transmitter implantation.

(5) EEG data acquisition and analysis

Freely moving mice implanted with telemetric EEG devices were housed in a Faraday cage containing an aerial to collect the EEG signals. Transmitter signals (512 samples/ second) were continuously received and decoded by a Data Receiver which passes them to Neuroarchiver software for storage and playback;
(http://www.opensourceinstruments.com/Electronics/A3018/Neuroarchiver.html (OpenSource Instruments (OSI)) for up to 28 days (Chang, Hashemi et al. 2011).
The raw EEG was analysed by observing the EEG trace during playback of the archived files alongside the Event Classifier application in Neuroarchiver. Using the Event Classifier:
(http://www.opensourceinstruments.com/Electronics/A3018/Seizure_Detection.html), short segments of EEG were classified according to six metrics (Table 2.2). Similar events cluster together when these metrics are plotted against each other. A library of distinctive and potentially pathological events was established allowing fast identification of abnormal EEG events by automated comparison of a test event to the library. The power of oscillation of the EEG trace at different frequencies was calculated by subjecting it to a Fourier transform and then dividing it up into pre-defined frequency bands (delta 1-4 Hz, theta 4-8 Hz, alpha 8-12 Hz, beta 12-30 Hz, low

gamma 30-50 Hz, high gamma 50-70 Hz, high frequency 70-120 Hz), using a Power Band Average script provided by OSI.

Metric	Definition
Event power	Power between 4 and 160 Hz An 'event power' of five times the baseline is the threshold for an 'event'
Transient power	Ratio of power between 1 and 4 Hz to 'event power' Measure to separate movement artefact in low frequency spectrum from 'event power'
High frequency power	Ratio of power between 60 and 160 Hz to 'event power' Measure to capture high frequency oscillation component of seizures
Spikeyness	Measure for the concentration of signal power in time (this is high for sudden large amplitude changes that occur with spikes)
Asymmetry	Measure for the bias of the signal to the positive or negative side of the average signal
Intermittency	Measure for how intermittent the high frequency signal is within a given interval, indicative of a train of sharp spikes or short bursts of high frequency power

Table 2-2 Definition of metrics extracted by Event Classification Processor from the EEG

(6) Seizure induction

A single dose of between 40 to 50 mg/kg of PTZ was given intraperitoneally (i.p.) for seizure induction (injections of PTZ given by Dr Louise Upton). Mice were marked on the tail by Dr Louise Upton to distinguish between them when observed in pairs. Mice were observed for the next 60 minutes while recording seizure events (all by SW, blinded to the IgG injected into the mouse). These were classified according to previously published seizure scoring systems (Weiergraber, Henry et al. 2006, Luttjohann, Fabene et al. 2009). Video examples of Stage 2 (Video 1) and Stage 3 (Video 2) seizures are attached, and details are listed in Table 2.3. Frequency of seizures, time latency to onset of convulsive seizures and total seizure score were recorded. Total seizure score was calculated at the end of the 60 minute observation

period, with a score of two or three given for each stage two or three seizure respectively. Mice were observed singly or in pairs with the observer blinded to the IgG previously injected. Seizure induction was carried out 48 hours after ICV injection. The observation period was videoed to allow subsequent video-EEG matching of observed events with EEG signatures.

Stage	Phenotype seen
1	Non seizure activity Non convulsive state Hypoactive Prone posture with direct contact of abdomen with the cage bottom
2	Partial clonus Partial clonic activity affecting face, head, vibrissae and forelimbs Short 1-2 seconds, can be repetitive over time
3 a, b, c	Generalised myoclonus Generalised (whole-body) clonus involving all four limbs and tail. Further subdivisions of Stage 3 were defined as follows; a) Whole-body clonus without loss of upright posture b) Whole-body clonus with loss of upright posture c) Whole-body clonus with a complete loss of motoric control (wild running and jumping) Can last up to 30 seconds followed by postical depression
4	Generalised (maximal) tonic-clonic seizure Tonic extension of hindlimbs Normally a pre-morbid event due to respiratory insufficiency

Table 2-3 Modified Rancine seizure rating scale used for seizure induction observation period (Weiergraber, Henry et al. 2006)

2.2.6 Immunofluorescence and tissue analysis

For post-mortem brain analysis mice were transcardially perfused with ice cold PBS. The brain was removed, flash frozen in isopentane at -40^{o}C, and stored at -80^{o}C. Sagittal brain sections were cut at 12 µm thickness using a Leica CM1900 cryostat, and stored in four separate series (Figure 2.3). For determination of the level of human IgG bound, the sections were rinsed with PBS and blocked with 10% normal goat serum (NGS) for 45 minutes. Sections were then incubated in anti-human IgG alexa-fluor-488 at 1 in 1000 (Invitrogen, UK) overnight at 4^{o}C. Sections were washed and mounted with

aqueous mounting medium containing DAPI. Slides were visualised using a Leica DM2000 microscope as previously, and photographs taken with the connected Rolera-XR Fast 1394 digital CCD camera coupled with Q-Capture Pro software. Photographs of sections were analysed with ImageJ using a previously designed macro for fluorescence intensity analysis (Appendix 1).

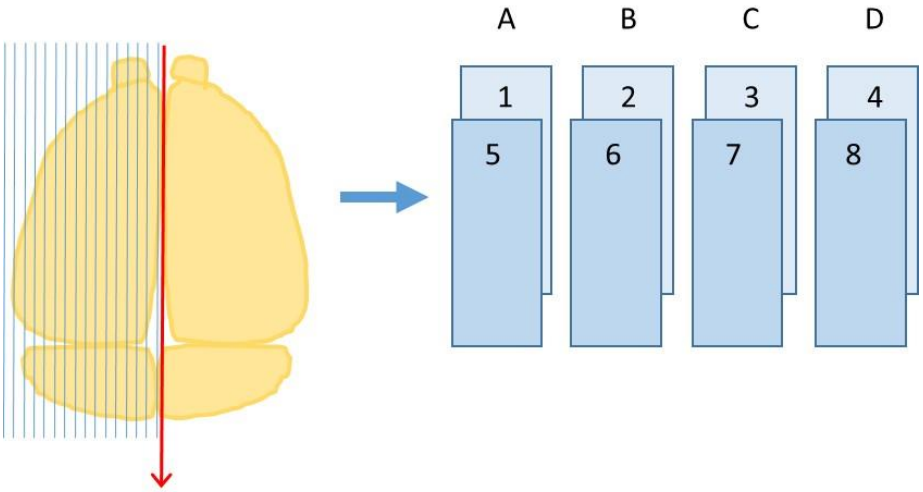

Figure 2-3 Schematic to demonstrate sectioning of injected mouse brains

Each hemisphere was sectioned in the sagittal plane on the cryostat at a thickness of 12µm (thin blue lines on left hemispheres, red arrow indicates separation of hemispheres). Each slide contained two sagittal sections which were then stored in four series as demonstrated in A to D in the schematic. This method of collection and storage facilitated immunohistochemical analysis of IgG spread throughout the injected hemisphere.

For NR1 staining two different commercial antibodies were used; purified mouse anti-NR1 (556308, BD Pharmingen) and mouse anti-NR1 (75-272, NeuroMab). With the BD Pharmingen antibody, sections were fixed for 5 minutes with 3% formaldehyde and washed in PBS. Tissue sections were blocked and permeabilised using 1% Triton in PBS with 10% NGS for 45 minutes. The primary antibody was incubated overnight at 4^{o}C at a dilution of 1:250 in PBS with 5% NGS. Sections were then incubated in anti-mouse IgG alexa-fluor-488 or alexa-fluor 568 at 1 in 1000 (Invitrogen, UK) for one hour, washed in PBS three times, and mounted as previously.

The Neuromab anti-NR1 antibody was used at the same dilution of 1:250 with the same protocol except that sections were not fixed or permeabilised.

Rabbit anti-parvalbumin antibody (ab11427, Abcam) was used for co-localisation of NR1 with this calcium binding protein. With this antibody, sections were fixed as previously then blocked with 0.2% Triton and 10% NGS for 45 minutes, before overnight incubation at 4^{o}C. Sections were then incubated in anti-rabbit IgG alexa-fluor-488 at 1 in 1000 (Invitrogen, UK) for one hour, washed in PBS, and mounted as previously.

Rabbit Anti-c-fos (Ab-5, 4-17, Calbiochem) was used for detection of c-fos protein in post-fixed 12 µm frozen sections of the NMDAR-Ab and HC IgG injected mice. Sections were permeabilised with 0.2% Triton at room temperature, then transferred to PBS for one minute. The sections were blocked with 10% NGS in 0.2% PBS Triton (PBST). Incubation with the primary at 1:250 was overnight at 4^{o}C. Slides were washed PBS 0.5% tween four times for five minutes each wash. The secondary antibody (goat-anti rabbit 568) was diluted at 1:1000 in PBS with 0.2% Triton and 2.5% NGS for two hours at room temperature. Slides were then washed in PBS 0.05% Tween as previously with a last wash in distilled water, before mounting as previously with DAPI.

2.2.7 Quantification of c-fos labelling

Sagittal sections stained for c-fos were coded prior to immunostaining and quantification. For each animal four photomicrographs from two sections of the post-fixed right hemisphere were taken of the cortex at magnification x 40. The location of the areas was guided by the atlas of Franklin and Paxinos and kept consistent for each animal (Figure 2.4). Cells exhibiting nuclear staining for c-fos were counted using the Image J cell counter tool. On completion of quantification, the slides were decoded to

allow analysis of the relationship between c-fos expression and seizure score, and IgG injected.

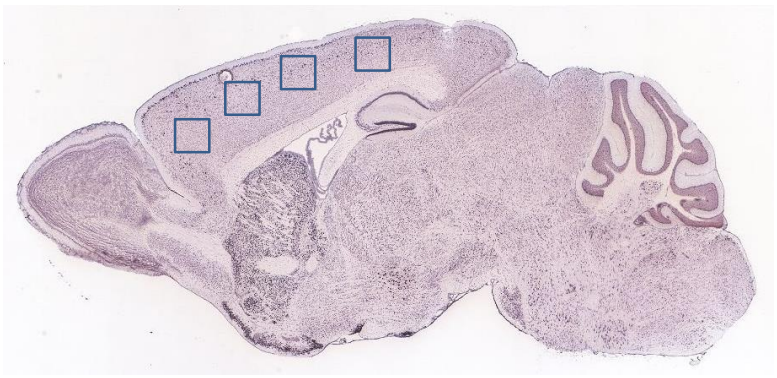

Figure 2-4 Determination of c-fos labelling (image courtesy of Allen Brain Atlas online)

Representative sagittal mouse section demonstrating areas of cortex analysed in each section for c-fos labelling (indicated by blue squares).

2.2.8 TUNEL staining

In situ cell death was detected using a TUNEL (TdT-mediated dUTP nickend labelling) assay kit conjugated to tetramethylrhodamine (TMR) red (TUNEL Apoptosis Detection Kit (Millipore, UK)). 12 µm sections were fixed for thirty minutes in 4% formaldehyde, then permeabilised for 15 minutes at room temperature in TBS containing 0.25% Triton X-100. Sections were incubated in 50 µl of TUNEL reaction mixture (terminal deoxynucleotidyl-transferase enzyme plus TMR red labelled nucleotides) for 1 hour at 37°C in a humidified atmosphere in the dark. Slides were rinsed 3 times with TBS and coverslipped using mounting medium containing DAPI. As a positive control for the assay, permeabilised sections were treated with 5 units/ ml DNase I recombinant (Roche Diagnostics) for 10 minutes at room temperature to induce DNA strand breakages prior to the labelling procedure. Sections incubated in label solution only (without terminal deoxynucleotidyltransferase enzyme) served as a negative control.

2.2.9 Optogenetics experiments

These experiments were performed with the assistance of Dr Lorenz Muller (LM) and Ms Kathryn Newton (KN), indicated by abbreviations.

(1) Intracerebral injection of virus

CAMKIIa-Cre homozygous mice were housed and prepared in an identical manner to C57BL/6 mice for ICV injections (section 2.2.5). Mice were injected with a cre-recombinase AAV2-ChR2-eYFP construct into the left dorsal CA1 (all injections performed by SW). Co-ordinates for the craniotomy were 1.6mm caudal and 1.4mm lateral from bregma. A total of 800 nL of the virus particle construct (titre of $4x10^{12}$/ ml) was injected (300 nL at 1.6mm depth, 300 nL at 1.4 mm and 200 nL at 1.2mm). The wound was sutured and mice recovered as previously. Mice were left for up to three weeks to allow optimal virus expression before injection of IgG into the left lateral ventricle as described previously (SW).

(2) Ex-vivo electrophysiology

48 hours after injection of IgG, the CAMII-Cre homozygous mice were anaesthetised with sodium pentobarbitone (20% w/v, 0.2mg/g) and decapitated (SW). The brain was quickly removed and acute sagittal slices (250µm) were prepared (LM) in high sucrose artificial CSF at 0-4^{o}C, containing in nM: 75 sucrose, 87 NaCl, 2.5 KCl, 7 $MgCl_2$, $0.5CaCl_2$, 1.25 NaH_2P0_4, 25 $NaHC0_3$, 20 glucose (solutions prepared by SW). Slices were submerged in high sucrose solution at 32^{o}C for 20 minutes to recover, before being transferred to an interface chamber for one hour, which contained Earle's balanced solution (in mM, 117.24 NaCl, 5.33 KCl, 1.01 $NaH_2PO_4.H_20$, 26.19 $NaHCO_3$, 3 Mg^{2+}, 1 Ca^{2+}, 5.56 D-glucose) at room temperature. Recordings were performed in a submerged recording chamber at 29-32^{o}C; the recording ACSF contained in mM: 119

NaCl, 2.5 KCl, 1.3 $MgSO_4$, 2.5 $CaCl_2$, 1.25 Na_2HPO_4, 25 $NaHCO_3$, 11 glucose. Solutions were all oxygenated continuously at every experimental stage (95% O_2, 5% CO_2). Whole cell voltage clamp recordings were made using a 20 X immersion objective (LM). Patching pipettes (6-8MΩ) were made from borosilicate glass capillaries (SW, LM). The pipette solution contained in mM; 145 Cs-Methanesulfonate, 20 HEPES, 10 CsOH, 8NaCl, 0.2 CsOH-EGTA, 2 Mg-ATP, 0.3 GTP-Na, 5 QX-314, 0.2-0.4% neurobiotin. A Multiclamp 700 B patch-clamp amplifier was used for recordings, signals were low pass filtered at 2 kHz, digitized at 10 kHz and analysed using pClamp 10.2 software. For optogenetic experiments, pyramidal cells expressing ChR2 were selectively activated by a laser light spot of 20 µm diameter (wavelength of 473nm) and postsynaptic currents were recorded in putative CA1 pyramids (LM, SW). This protocol has been used successfully in Dr Karri Lamsa's laboratory (Figure 2.5). A CAMKII inhibitor KN-62 (3µM, Abcam) and group 1 metabotropic glutamate receptor antagonist RS-MCPG (200 µM, Abcam) were added to the storage solution to inhibit plasticity related phenomena.

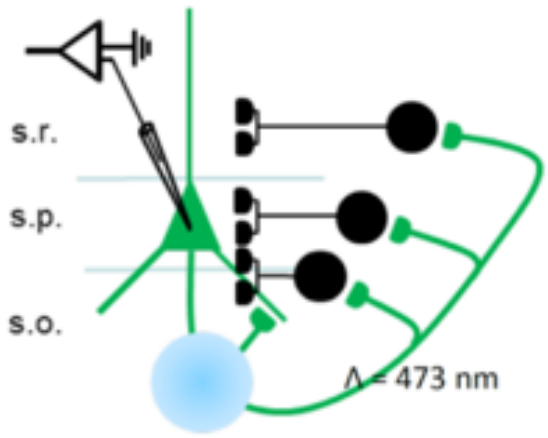

Figure 2-5 Experimental design of optogenetic stimulation to test GABAergic neuronal NMDAR contribution to recurrent inhibition of pyramidal cells.

Optogenetic stimulation (fixed spot 473nm laser light stimulation in blue) of channelrhodopsin-2 expressed in CA1 pyramidal cell glutamatergic fibres. Stimuli (5 pulses) were applied at 20Hz "low gamma frequency" to activate glutamatergic axons (green) and initiate monosynaptic EPSCs and to drive GABAergic interneurons (black) to evoke recurrent GABAergic IPSCs.

Figure courtesy of D.Kotzadimitriou in Dr K Lamsa's laboratory, Dept of Pharmacology, Oxford.

(3) Immunocytochemistry

Neurobiotin in the pipette solution diffuses in to patched cells during recording (LM). To confirm that they were pyramidal cells, slices with neurobiotin-filled cells were fixed in 4% paraformaldehyde and 0.05% glutaraldehyde fixative overnight at 4^{o}C (SW). Slices were washed with 0.1 M phosphate buffer (PB), embedded in 20% gelatin and resectioned (60µm) on an ice-cold microtome (SW). For cell visualization, sections were permeabilised with 50 nM Tris-buffered saline and 0.3% Triton x-100 solution, incubated overnight with Alexa-Fluor Cy5 conjugated streptavidin (Invitrogen, UK) at 4^{o}C, then washed and mounted with Vectashield (SW). Labelled cells were evaluated by confocal laser microscopy (SW with assistance from Ms Kathryn Newton, lab technician).

2.2.10 Pregnenolone sulphate (PregS) experiments

All PregS experiments were performed by SW.

(1) *In vitro*: Hippocampal neurons

Hippocampal neurons were cultured in six-well plates as previously described, and used on DIV 13. A 500 µM solution of PregS (Sigma, UK) was prepared in 0.5% dimethlysulfoxide (DMSO, Sigma, UK). Cells were treated for ten minutes at 37^{o}C with 500µM PREGS, vehicle alone (0.5% DMS0) or no treatment. All cells were then assayed with NMDAR-Ab IgG (1:300) as previously described.

(2) *In vitro* internalisation studies on HEK cells

For testing the effect of PregS on NMDAR-Ab induced internalisation, an in-vitro preparation of transfected HEK cells was prepared as for NMDAR-Ab CBA (section 2.2.1). Coverslips were incubated for one hour at 37^{o}C with NMDAR-Ab serum, after which a proportion were washed and stained immediately for surface anti-human IgG

binding, and surface NR1 expression with NR1 commercial antibody (BD Pharmingen), before fixing with 3% formaldehyde. The remaining coverslips were left in the incubator for 24 hours, additional ketamine was added to prevent the excitotoxic effects of glutamate release on the remaining NMDAR transfected HEK cells.

At 24 hours, some coverslips were again removed and immediately stained for surface human IgG and NR1 expression as previously in order to verify that internalisation of NMDARs by the NMDAR-Abs had taken place. The remaining coverslips were treated with 500μM PregS, vehicle alone or no-treatment for ten minutes at room temperature. The cells were then stained for NR1 expression, washed, fixed and mounted as previously.

(3) Preparation of PregS solution for in-vivo studies

Mice were treated with i.p. injections of PregS for *in vivo* experiments. In order to achieve a 10 mg/ ml solution concentration of PregS, the solvent 2-Hydroxypropyl-B-cyclodextrin solution (cyclodextrin, Sigma, UK) was used. Animals received 60 mg/kg doses of either PregS in solution with cyclodextrin or cyclodextrin (vehicle) alone in line with the experimental protocol.

2.2.11 Statistical analysis

Data were analysed using Graphpad Prism 6 for Windows (San Diego, USA). Descriptive statistics were used to summarise patient data. Fisher's exact test was used to compare categorical data and the Mann-Whitney test to compare continuous data variables. The correlation between seizure score and fluorescence intensity of bound IgG was assessed by linear correlation. The Komolgorav-Smirnov test was used to compare distributions of IgG intensity.

CHAPTER 3 - Autoantibodies in paediatric epilepsy cohorts and correlation with clinical features

3.1 Introduction

It is becoming clear that autoantibodies to CNS proteins are found in epilepsy patients who may not have evidence of encephalitis. In adults, facial-brachial dystonic seizures (FBDS) can precede the development of encephalitis and early treatment with immunotherapy may prevent the progression to encephalitis in some patients (Irani, Michell et al. 2011, Irani, Stagg et al. 2013). These patients have antibodies to the VGKC-complex protein LGI1. A similar specific phenotype has not yet been identified in children, which is surprising given that immunotherapy (e.g. steroids) is used as first-line treatment in some paediatric epilepsy syndromes (Lux, Edwards et al. 2005, Hussain, Shinnar et al. 2014). Case reports and short series of paediatric epilepsy patients with positive autoantibodies, including a small number with West syndrome and paediatric SE, have been published. Unfortunately these studies have been confounded by testing samples late in the disease, an overlap with the phenotype of patients tested with encephalitis, and a lack of control subject testing (Suleiman, Brenner et al. 2011, Suleiman, Brenner et al. 2011).

Here, two paediatric epilepsy cohorts were screened for several autoantibodies and their presence correlated to clinical and paraclinical features as well as to short and long-term outcomes. In addition, two control cohorts and a candidate antigen approach to look for novel antigens in specific paediatric epilepsy patient groups were investigated.

3.2 Autoantibody screening of paediatric epilepsy patients and controls

In order to examine the presence and prevalence of CNS autoantibodies in paediatric epilepsy, sera from two cohorts of paediatric patients with new-onset epilepsy and healthy controls were screened. Sera from the first paediatric epilepsy cohort (Australian) were prospectively collected from children attending the Children's Hospital at Westmead Hospital in Sydney between September 2009 and November 2011 (n=112). A disease control (DC) cohort was also provided from the same hospital (n=68). Sera from the second paediatric epilepsy cohort were collected for the Dutch Study of Childhood Epilepsy between 1988 and 1992. This Dutch cohort contained 178 serum samples and 114 additional sera from age and sex matched HCs.

Sera from a total of 290 paediatric epilepsy patients and 180 controls were screened using the routine techniques of CBA and RIA as described in section 2.2.1. and 2.2.2.

An example of a positive CASPR2 CBA assay, is shown in Figure 3.1.

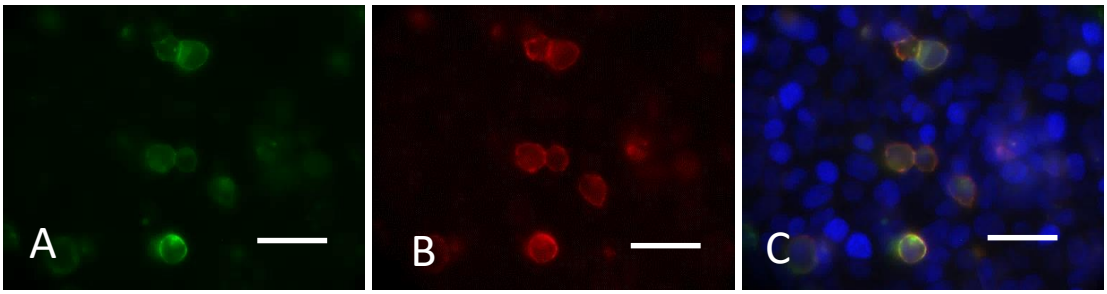

Figure 3-1 Positive CASPR2 CBA result.

A. The transfected CASPr2-EGFP tagged transfected HEK cells (green). Scale bar 40μm in all photomicrographs.
B. Serum from Patient 21 bind to the surface of the CASPR2 transfected cells, seen with anti-human IgG labelling (red).
C. The transfected cells (A) and anti-human IgG labelled cells (B) colocalise indicating a positive result with a CASPR2 CBA score of 1.5 for this patient.

Autoantibodies to the VGKC-complex, the VGKC-complex associated proteins contactin-2, CASPR2, (but not LGI1) and the NMDAR, were found in both the Dutch (DSCE) and Australian (AUS) paediatric epilepsy cohorts (Figure 3.2 A-D). Serum dilutions of 1:20 were used for the LGI1, NMDAR and AMPAR CBA, and 1:100 for CASPR2, contactin-2 and $GABA_B$. The routine laboratory cut-off values for positivity on the assays were used (shown as red dotted lines in Figure 3.2), although some of the control results fell above this. Autoantibodies to GAD, AMPA receptors and $GABA_B$ receptors were not detected. However, in total eight controls were positive (DC n=3; HC n=5). In the disease control cohort, two were positive for VGKC-complex antibodies and one positive for NMDAR-Abs. The healthy control cohort had three positive VGKC-complex antibody patients, one NMDAR-Ab positive and one positive for both VGKC-complex and NMDAR-Abs.

The number of autoantibody positive patients in the two paediatric epilepsy cohorts (33/290; 11.4%) was significantly higher than in the control patients (8/182; 4.4%) (p= 0.01, Fisher's exact test; Figure 3.2E-F). The positive samples in the Dutch epilepsy cohort were also tested on hippocampal and cerebellar neurons (Table 3.1). Positive staining on hippocampal neurons was seen in 47% of the samples, this low percentage may be a due to the relatively low titres seen. Further analysis of all the antibody positive patients, including clinical correlation is separated between the two cohorts (DSCE and HC; AUS and DC) as they were collected independently.

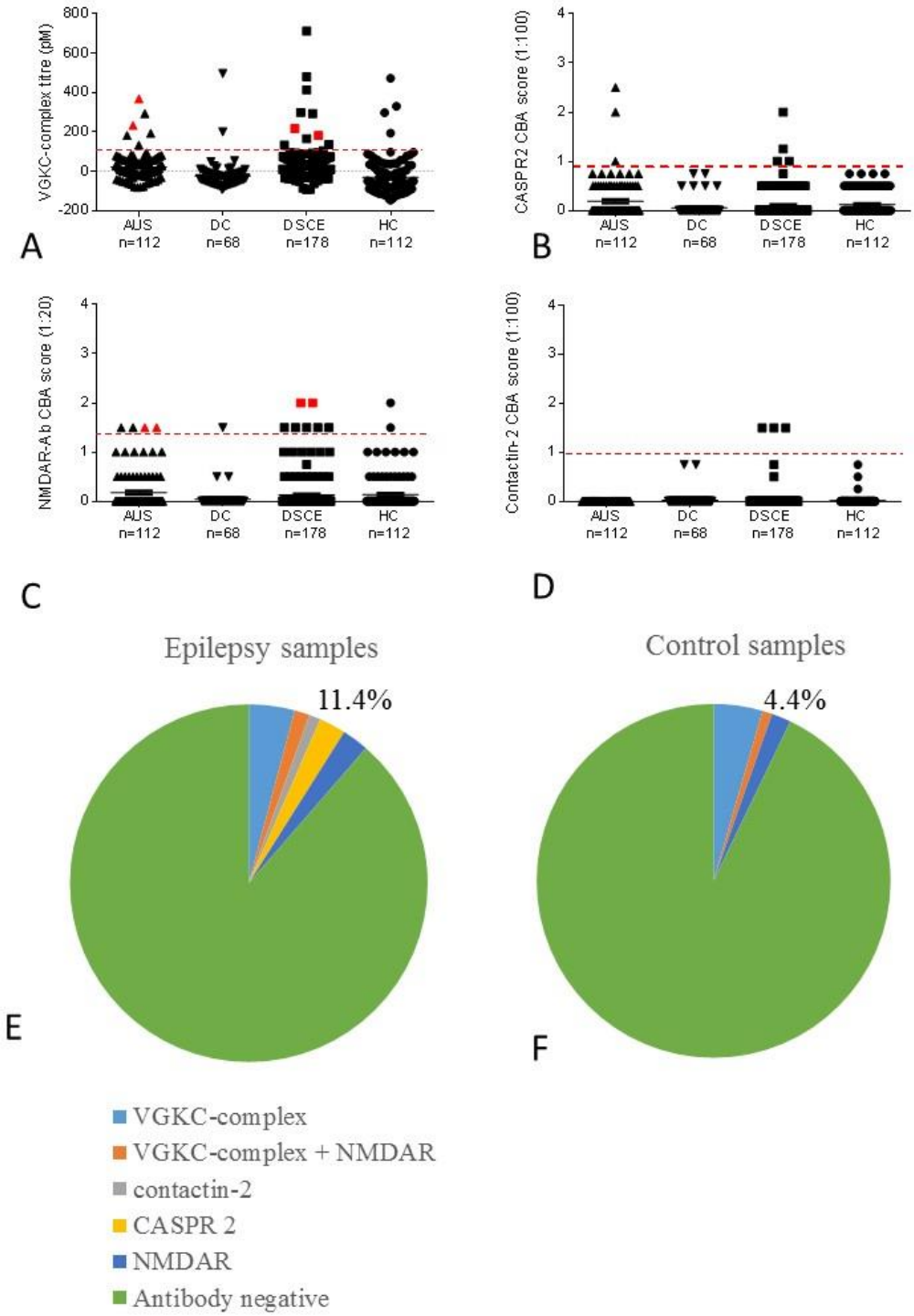

Figure 3-2 Autoantibody positivity in paediatric epilepsy

A-D. The scatter diagrams show the titres and CBA scores of positive tests for each antigen; VGKC-complex (A), CAPSR2 (B), NMDAR (C) and Contactin-2 (D). Double positives seen in the patient group are highlighted in red. The red dashed line indicates the positive cut-off used routinely in the Oxford laboratory. AUS Australian, DC disease control, CSCE Dutch Study of Childhood Epilepsy, HC Healthy control.

E-F. The pie charts show the prevalence of positive antibodies in the epilepsy patient groups (E) and in control samples (F). Antibodies to the VGKC-complex and the associated proteins were the most common. The number of autoantibody positive patients in the epilepsy group is significantly higher than in the controls (11.4% vs 4.4%, p=0.01, Fisher's exact test).

Antigen	Assay	DSCE Sample number	Result pmol/L for RIA 0-4 for CBA	Hippocampal neurons	Cerebellar neurons
VGKC-COMPLEX	RIA (POSITIVE IF >100)	KJ 166	104	+	-
		KL 168	135	++	-
		KD 256	166	ND	ND
		KJ 84	182	-	-
		KJ 190	217	ND	ND
		KJ 157	293	+	-
		KD 290	299	-	-
		KJ 75	414	-	-
		KD 227	480	+	-
		KJ 58	712	+	-
CASPR2	CBA (1in 100, POSITIVE>1)	KW 80	1	+	-
		KL 141	1	+	-
		KL 173	1.25	-	-
		KW 19	2	ND	ND
CONTACTIN-2	CBA (1 in 100, POSITIVE>1)	KW 52	1.5	-	-
		KW 51	1.5	++	-
		KW 85	1.5	-	-
NMDA R	CBA (1 in 20, POSITIVE>1.5)	KD 376	1.5	+	-
		KD 221	1.5	+	-
		KD 321	1.5	-	-
		KD 336	1.5	-	-
		KL 125	1.5	++	-
		KJ 190	2	ND	ND
		KJ 84	2	-	-

Table 3-1 Neuronal assay results for antibody positive epilepsy patients in Dutch cohort

A positive test is indicated by ++, a weak positive by +, and a negative test result with -; ND indicates when the sample was not done/ tested due to no serum sample remaining for testing.

3.3 Australian cohort and disease control results

3.3.1 Clinical features of whole cohort and controls

This epilepsy cohort was collected prospectively from 112 children aged between two months and 16 years, who presented with a well described paroxysmal episode compatible with a clinical seizure, and had serum collected within six months of seizure onset. Full clinical data were available from 108 patients. The 68 disease controls consisted of hospital patients who had serum collected as part of their routine investigations (for infectious and immunological tests). The classification of seizure types, epilepsy and electroclinical syndrome and aetiology was performed by Dr Jehan Suleiman and Dr Deepak Gill (Sydney Children's Hospital) and was only released after the antibody testing had been completed. Both Dr Suleiman and Dr Gill were blinded to the results of the antibody testing at the time of classification.

Ninety-five patients (95/108; 88%) were admitted to the hospital during their initial presentation or during the first six months after seizure onset (median length of stay 4.5 days, range 1 to 360 days); 13 patients required admission to ITU. Pre-existing developmental, motor or psychiatric abnormalities were seen in 30 patients. There was a positive family history of seizures (including febrile seizures) or of epilepsy in at least one first degree relative of 18 patients (16.7%).

Fifty-five patients presented with focal seizures (51%); 13 presented in status epilepticus. Twenty-five patients had an intercurrent illness at the time of presentation and 17 patients were recorded to be febrile. Twenty-nine patients had associated encephalopathy, 22 had behavioural or psychiatric alteration and eight were thought to have cognitive impairment. Motor impairment was seen in 16, and an associated movement disorder was seen in five patients. EEG findings were abnormal in 81/108 patients, with MRI abnormalities seen in 47/98. The most common abnormality

reported was structural, for example polymicrogyria or focal cortical dysplasia. Non-specific high signal changes were also described. CSF was collected in 61 patients, and pleocytosis seen in eight samples. No CSF antibody testing had been performed on these samples. CSF oligoclonal bands were positive in two out of 40 samples analysed; serum oligoclonal bands were negative in one of these cases and paired in the other.

Forty-five patients received acute seizure treatment and 84 required continuing (more than seven days) antiepileptic drugs (AEDs). Eighteen patients required immunotherapy (oral prednisolone, intramuscular synthetic ACTH and intravenous methyl prednisolone, IVIG); four patients were treated with oral prednisolone alone, 12 in conjunction with other AEDs and two with IV steroids, IVIG and AEDs. In all cases the decision to treat with immunotherapy was made on the basis of a clinical presentation suggestive of an immune-mediated cause; a recognised immunotherapy responsive seizure syndrome (e.g. West syndrome); or as adjunctive treatment in intractable epilepsy, prior to and independent of autoantibody test results which were not done at the time of treatment/ presentation. A positive clinical response, seen in 15 out of 18, was defined as clinical improvement in seizures and/or encephalopathy as judged by the treating clinician. The responders included those with West syndrome (n=8), Lennox Gastaut syndrome (n=2), epilepsy attributed to malformation of cortical development (n=1), epilepsy of unknown cause (n=2), and epilepsy attributed to perinatal insult, encephalomalacia (n=1). The three non-responders had separate diagnoses of Lennox Gastaut syndrome, FIRES, and PCDH19 mutation. The response of one patient with seizures and encephalopathy was unknown.

Seven patients required no follow-up and for two patients no follow-up information was available. For the remaining 99 patients, the median length of follow-up was 10 months (range 1-36 months). Eighty-four patients had experienced further seizures at the time of follow-up including 23 with drug resistant (refractory) epilepsy.

32 patients had new deficits (other than epilepsy) including developmental delay, behavioural/ psychiatric impairment and motor deficits. All 108 patients with new onset seizures were classified according to the latest proposed ILAE organisation of seizures and epilepsies (Berg et al., 2010). Eighteen patients had seizures not traditionally diagnosed as a form of epilepsy; the remaining 90 patients had epilepsy, 32 with electroclinical syndromes, 30 with epilepsy attributed to structural-metabolic causes, and 28 with epilepsy of unknown cause (Table 3.2).

3.3.2 Antibodies and clinical features of positive patients and controls in Australian cohort

Eleven out of 112 (9.8%) patients with new onset seizures were positive for one or more of the tested antibodies; VGKC-complex (n=4), CASPR2 (n=3), NMDAR (n=2), VGKC-complex and NMDAR (n=2). None of the patients or controls samples were positive for GAD, AMPAR, $GABA_BR$, LGI1, or contactin-2 antibodies. The clinical features of all positive patients are summarized in Table 3.3. All antibody-positive patients were admitted to hospital on presentation with a mean duration of hospital stay of 3.72 days (median 3 days, range 2-11 days). None required admission to ITU. Two of the antibody positive patients had pre-existing developmental delay, which was severe in one. There was a positive family history of epilepsy in two patients. One of the patients (case eight) had status epilepticus of 45 minutes duration at presentation. Early seizure recurrence in the first 48 hours of presentation occurred in seven out of the 11 patients. Features associated with seizures on presentation are presented in Table 3.3. The timing of the samples for the positive patients was not significantly different to that of the antibody negative patients (mean 17.6; median 4, range 1 - 75 days vs. 43.5, 20 and 1 - 180 days respectively).

ILAE classification/ electro-clinical syndrome (n=90)		Patients (no)
Electroclinical syndrome (n=32) [b]		
Infancy		
	West syndrome	8[a]
	Benign infantile epilepsy	3
	Dravet Syndrome	3
	Myoclonic epilepsy in infancy (MEI)	1
Childhood		
	Lennox Gastaut Syndrome (LGS)	4[b]
	Febrile seizures plus (FS+)	2
	Panayiotopoulos syndrome	2
	Epilepsy with myoclonic atonic seizures	2
	Benign epilepsy with centrotemporal spikes (BECTS)	1
	Childhood absence epilepsy (CAE)	1
	Late onset Childhood occipital epilepsy (Gastaut type)	1
Adolescence		
	Autosomal dominant epilepsy with auditory features (ADEAF)	1
IGE		3
Epilepsy attributed to structural-metabolic causes (n= 30)		
	Infections/inflammation	
	Encephalitis	9[c]
	Malformation of cortical development (MCD)	10
	Perinatal insults	5
	Metabolic	3[d]
	Neurocutaneous syndrome	3
Epilepsies of unknown cause (n=28)		
Primary mode of seizure onset	Focal	16
	Generalised	8
	Spasms	2
	Undetermined	2

Conditions with epileptic seizures that are traditionally not diagnosed as a form of epilepsy (n=18)		Patients (no)
	Febrile seizures	7
	Acute symptomatic (provoked seizures)	
	Infection mediated	7[e]
	Posterior reversible encephalopathy syndrome (PRES) secondary to hypertension	1
	Asthma	1
	Single unprovoked seizure	2

Table 3-2 The epilepsy classification of the Australian cohort as per the new ILAE organisation of seizures and epilepsies (Berg et al., 2010).

Key for Table 3.2:

[a] 3 genetic, 2 metabolic (congenital glycosylation disorder), 1 structural (perinatal insult), 2 unknown

[b] 2 structural (malformation of cortical development, holoprosencephaly), 2 unknown

[C] Encephalitis patients include the following: five with potential infectious aetiology, 4 not otherwise specified.

[d] MELAS, propionic acidaemia, ornithine transcarbamylase deficiency.

[e] These patients had a systemic infection that was presumed to have provoked the seizure, but no evidence of CNS infection or inflammation, and either had no fever or were outside the age definition for febrile seizures. The precipitating infections were gastroenteritis (n=3), URTI (n=2), H1N1 influenza (n=1), fever alone (n=1).

EEG and MRI brain were performed in ten out of 11 antibody positive patients. The EEGs were abnormal in eight, and MRI abnormalities were recorded in four (Table 4). Routine CSF analysis revealed no abnormalities in 4/11 (36%) tested. CSF neopterin levels were tested in three, and elevated in one at 68 nmol/L (normal <30; case1) suggestive of CNS inflammation (Dale et al., 2009a).

Nine of the antibody positive patients received long term antiepileptic drugs, but none received immunotherapy during the disease course. Two antibody-positive cases were lost to follow up (cases 8 and non-epileptic case 6). The mean length of follow up for the remaining nine cases was 10.33 months (median 11 months, range 6-11 months), and was not different from the remaining antibody-negative cases. All of the nine patients with follow up had on-going seizures and one had drug resistant epilepsy (case 9). Five patients were on one AED, three were on two AEDs and one was on four AEDs. Two patients had a new neurological or developmental deficit (other than epilepsy) including speech impairment and hyperactivity (case 3), and motor deficit and behavioural alteration (case 5). Overall, there was no significant differences in the demographic and clinical features between antibody positive and negative patients (Table 3.4).

No.	Age and sex	Seizure type at onset/early seizure recurrence	Associated features	EEG [a]	MRI	Seizure type on follow up	Number of AED on follow up (in months)	ILAE classification	Ab positivity Titration**
1	2.5M	Focal dyscognitive/+	Nil	Epileptic: left fronto-temporal. Seizure: left temporal	Normal	Focal dyscognitive, atypical absence	1 (11)	Epilepsy of unknown cause (focal-temporal lobe)	VGKC (293)
2	4.9M	Focal versive/-	Nil	Epileptic: generalised with bifrontal lead	Normal	Generalised tonic clonic	1 (6)	Epilepsy of unknown cause (undetermined)	VGKC (193)
3	3.4M	Generalised tonic clonic/+	Nil	Slowing: right posterior	Normal	Generalised tonic clonic, atonic	2 (6)	Epilepsy of unknown cause (generalised)	VGKC (182)
4	1.5F	Focal dyscognitive/+	Motor deficit	Normal	Normal	Focal dyscognitive, atypical absence	1 (17)	Epilepsy of unknown cause (focal)	VGKC (133)
5	0.5F	Focal tonic with secondary generalisation/+	Intercurrent infection	Slowing: right temporal Epileptic: central.	Normal	Focal tonic with secondary generalisation	1 (11)	Epilepsy of unknown cause (focal)	CASPR2 (2) 1 in 200
6	7M	Focal tonic clonic/-	Intercurrent infection, fever	Not done	Not done	No follow up	-	Acute symptomatic (provoked) seizure	CASPR2 (1) 1 in 100
7	10M	Focal myoclonic/+	Encephalopathy, motor deficit (hemiparesis)	Slowing: generalised Epileptic: left parietal.	Left parietal hyperintensity	Focal	2 (13)	Epilepsy attributed to metabolic cause	CASPR2 (2.5) 1 in >400
8	4.5M	Focal dyscognitive/-	Nil	Slowing: right occipital.	Normal	No follow up	-	Epilepsy of unknown cause (focal-occipital lobe)	NMDAR (1.5) 1 in 100
9	3M	Generalised Myoclonic /+	Encephalopathy, behavioural alteration	Slowing: generalised Epileptic: right frontal.	Corpus callosal dygenesis, frontal heterotopia	Mixed (myoclonic, tonic, atonic)	4 (12)	Lennox- Gastaut syndrome	NMDAR (1.5) 1 in 100
10	8F	Generalised tonic/-	Preceding infliximab infusion	High voltage generalised spike and slow wave	Generous ventricles	Tonic/myoclonic	1 (10)	Epilepsy of unknown cause (generalised)	VGKC (368) NMDAR (1.5) 1 in 80
11	3F	Generalised tonic clonic/+	Intercurrent infection	Normal	Asymmetric hippocmpi	Generalised tonic clonic	2 (7)	Febrile seizure plus (FS+)	VGKC (233) NMDAR (1.5) 1 in 80

Table 3-3Demographic, clinical, electrographic and imaging features of the antibody positive patients in the Australian cohort

[a] EEG abnormal findings are described in the following order when present: slowing and location, epileptic activity and location, seizure and onset.
** CBA were scored on a visual scale: 0 (no binding), 1(low but specific binding)-4 (strong binding to all transfected cells) by 2 independent observers as described in the methods section 2.2.1. Titration values are highest dilution at which the sample remains positive compared to controls.

Demographics/Clinical Characteristics	Ab positive patients (%/ range) n=11	Ab negative patients (%/range) n= 97	P value (<0.05)
Median age	3.4 yrs (0.5-10)	2.1 yrs (0.1 -15.25)	
Sex M:F	7:4	45:52	
Past medical history			
Previously normal (n=78)	9 (81.8)	69 (71.0)	ns
First Seizure			
Focal	7 (63.6)	47 (48.5)	ns
Generalised	4 (36.4)	36 (37.1)	ns
Status epilepticus	1 (9.1)	17 (17.5)	ns
Early seizure recurrence	7(63.6)	70 (72)	ns
Hospitalisation	11 (100)	84 (86.5)	ns
Intensive care	0 (0)	13 (13.4)	ns
Associated features			
Fever	1(9.1)	16 (16.5)	ns
Encephalopathy	2 (18.2)	27 (27.8)	ns
Movement disorder	0 (0)	5 (5.2)	ns
Behavioural abnormality	1 (9.1)	21 (21.6)	ns
Cognitive abnormality	0 (0)	8 (8.2)	ns
Motor deficit	2 (18.2)	14 (14.4)	ns
Outcome			
Ongoing epilepsy	9 (81.8)	75 (77.3)	ns
New deficit	2 (18.2)	30 (30.9)	ns
Developmental delay	0 (0)	11 (11.3)	ns
Behavioural /psych impairment	2(18.2)	18 (18.5)	ns
Cognitive impairment	0 (0)	17 (16.5)	ns

Table 3-4 Comparison of demographic, clinical and paraclinical features of positive and negative cases in the Australian cohort.

Abbreviations; ns non-significant

Three of the 65 controls (4.6%) were positive for antibodies. Control 1 (VGKC-complex-Abs 497pM) was a 3 year old male with type 1 diabetes mellitus. Control 2 (VGKC-complex-Abs 200 pM) was a 2 year old male with vomiting illness and poor weight gain. Control 3 (NMDAR score 2, end point dilution 1 in 100) was a 8 year old male with acute lymphocytic leukaemia relapse treated with bone marrow transplant, complicated by chronic graft versus host disease. No neurological abnormality was noted in any of these controls; although no follow up was recorded in control 2.

3.3.3 Antibody positive new onset epilepsy patients categorised by the new ILAE organisation of seizures and epilepsies

The 11 antibody-positive patients with epilepsy had the following ILAE epilepsy classifications: electroclinical syndrome (n=2), epilepsy attributed to structural metabolic causes (n=1) and epilepsy of unknown cause (n=7). The eleventh patient had acute symptomatic seizures (which is not considered a form of epilepsy).

In the total cohort; only two out of 30 patients with electroclinical syndromes (6.7%) had positive antibodies (cases 9 and 11), which was not significantly different to the positive antibodies in the control group (3/65, 4.6%). Case 9 had Lennox-Gastaut Syndrome (LGS) and NMDAR-Abs, and case 11 had febrile seizures plus with antibodies to both the NMDAR and VGKC-complex.

Similarly, only one out of 33 patients with epilepsy attributed to a structural-metabolic cause (3%) had positive antibodies (case 7), again not significantly different to the controls. Case 7 had MELAS and was positive for CASPR2-Abs.

In comparison, seven out of 28 patients from the epilepsy cohort with epilepsy of unknown cause (25%) had positive antibodies, which was significantly different to the controls (4.6%; p=0.007, Fisher's exact test; Figure 3.3). Overall, the proportion of antibody positive patients classified with epilepsy of unknown cause (7/11; 63%) was

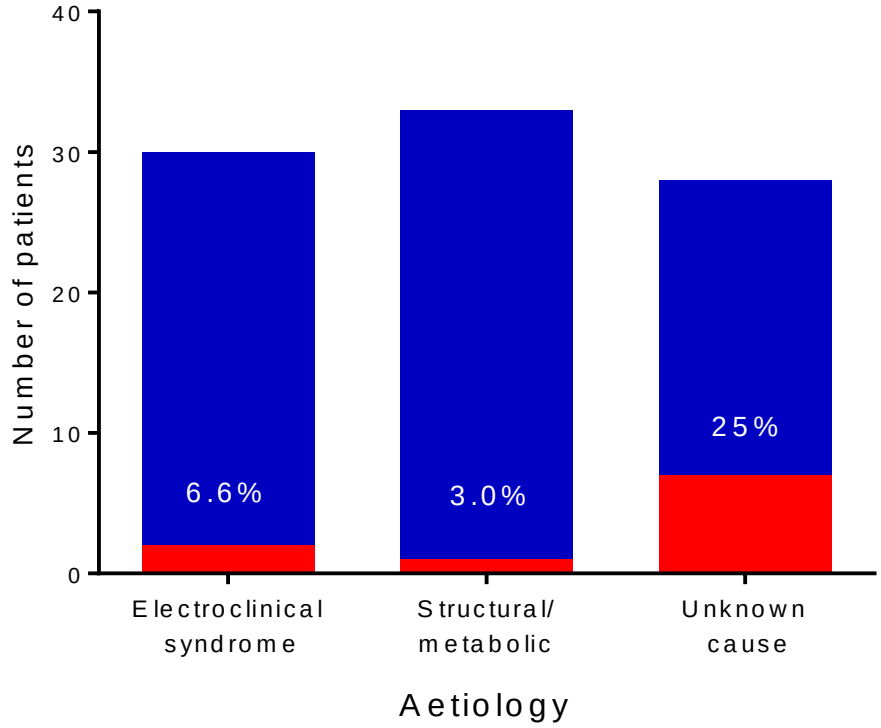

Figure 3-3 ILAE classifications for autoantibody positive patients in the Australian cohort

This graph shows the ILAE classifications of patients positive (coloured in red, antibody negative patients in blue) for one or more antibodies in the Australian cohort. The percentage of antibody positive patients in the 'unknown cause' group was significantly higher than controls (p=0.005, Fisher's exact test).

significantly higher than the remaining antibody negative epilepsy subjects (21/97; 26.7 %; p=0.006, Fisher's exact test). Furthermore, 4 of these 11 patients (36.4%) had focal epilepsy compared with 12 of the 97 antibody-negative patients (12.4%; p=0.057).

Of these seven antibody positive patients with epilepsy of unknown cause, four had VGKC-complex Abs only (cases 1-4), three of whom presented with focal seizures, and three had early seizure recurrence (cases 1, 3 and 4) (Table 2). Case 5, who had CASPR2 antibodies, presented with focal tonic/clonic seizures and had intercurrent infection. Case 8 was positive for NMDAR-Abs and had focal dyscognitive seizures and focal status epilepticus on presentation. Case 10 was positive for both NMDAR and VGKC-complex antibodies and had a number of co-morbidities. She presented with

seizures following an infliximab infusion given for her treatment resistant Crohn's disease. Infliximab is a monoclonal antibody against TNF-α used in the treatment of some autoimmune diseases and previously described to be associated with seizures (Brigo et al., 2011).

3.3.4 Summary of key findings from Australian epilepsy patients

The key finding in the Australian data was that autoantibodies were found more frequently in new-onset epilepsy patients of "unknown cause", often with focal epilepsies (Suleiman, Wright et al. 2013). This may therefore be the group that most benefits from autoantibody screening and consideration of immune therapy. However, follow-up data in these patients were limited. Long-term follow-up data were gathered from the Dutch cohort.

3.4 Dutch cohort and healthy controls results

The DSCE recruited 494 children aged one month to 16 years with new-onset epilepsy between 1988 and 1992. Children were enrolled from four participating centres in the Netherlands (Arts, Geerts et al. 1999). A total of 178 serum samples from newly-diagnosed paediatric patients with epilepsy from this cohort and 114 healthy controls were tested for autoantibodies to the VGKC-complex and associated proteins (CASPR2, Contactin-2 and LGI1), the NMDA and AMPA receptors, and GAD as before. 22 patients (22/178; 12.3%) were positive for one or more antibodies compared to 5 of the healthy controls (5/114; 4.3%, p=0.02; Fisher's exact test). Antibodies to the LGI1 protein, AMPA receptor or GAD were not identified in patients or controls. The five positive healthy controls had antibodies to the VGKC-complex (3), NMDAR (1) and both VGKC-complex and NMDAR (1).

3.4.1 Clinical features of antibody positive patients in Dutch cohort

The mean age of epilepsy onset was 5.5 years (median 5.1, range 0 - 15.5 years). Mean follow-up was 14.8 years (median 14.8, range 11.6-17.5 years). The clinical and paraclinical features, treatment responses and outcomes of the antibody positive patients are listed in Tables 3.5 and 3.6. Within the VGKC-complex Ab positive group (n=8), the two patients (cases 1 & 2) with the highest titres had cognitive impairment and focal epilepsy that was difficult to treat needing at least three AEDs for seizure control. Case 1 remained pharmacoresistant at long-term follow-up. Five out of the 6 remaining patients had good outcomes and required little treatment. Three out of the 5 NMDAR-Ab positive patients had learning difficulties ranging from mild (cases 11 and 13) to severe (case 12), although this was most likely related to a neonatal meningitis (Case 12). In all children the learning difficulties were present before seizure onset. No progressive changes were described in any of the patients. One NMDAR-Ab positive patient had classic childhood absence epilepsy (case 14) as well as two others who were also positive for VGKC-complex antibodies (cases 8, 9). Three patients were positive for Contactin-2 antibodies (cases 16, 17, 18); 1 had autistic features and 1 had a difficult to treat Benign Epilepsy with Centro-temporal Spikes (BECTS) requiring 3 anti-epileptic drugs (AEDs) for seizure control. Four patients were positive for CASPR2 antibodies and the two patients with the highest CASPR2 CBA titres had focal epilepsy with periods of intractability to AED treatment.

Case no/ Dutch code.	Age and sex	Seizure type at onset/FU	EEG and CT findings	Type of epilepsy/aetiology	Associated clinical features	Treatment history first 5 years /at end of follow-up (FU, yrs)	Assessment of patient outcome overall/TR (yrs)	Ab positivity (Titres)
1 KJ058	4F	CPS/ SPS, SE, unclear seizures	EEG: Focal epileptic abnormality left temporoparietal CT: left hemiatrophy, porencephaly	Localisation related symptomatic/remote symptomatic	Right hemiplegia Learning difficulties	4 AEDS: no fast response/ off AED at final FU (14.6)	Improving course TR = 10.2	VGKC (712)
2 KD227	1.7M	TC/TC, SPS, CPS, unclear seizures	EEG: Left occipital spikes CT not done	Localisation related symptomatic/ cryptogenic	MR, not progressive	3 AEDs: no fast response/on AED at final contact (14.7)	Poor course TR< 1 year, intractable	VGKC (480)
3 KJ075	7.4F	TC/TC, unclear seizures	EEG and CT: normal	Generalised idiopathic/ idiopathic	Mild DD	No AEDs; not on AED at final contact (15.3)	Improving course TR=1.5	VGKC (414)
4 KD290	4.8M	SE/ TC, unclear seizures	EEG: Generalised SWD CT : normal	Generalised idiopathic/ idiopathic	Mild DD-Attended special school and later regular education	No AEDs; not on AED at final contact (13)	Good course TR= 9.2	VGKC (299)
5 KJ157	3.6F	Minor motor and atonic/minor motor and atonic	EEG: Bilateral synchronised generalized SWD CT: normal	Generalised idiopathic myoclonic epilepsy of infancy/idiopathic	-	No AEDs; not on AED at final contact (12.3)	Good course TR= 12.3	VGKC (293)
6 KL168	3F	Absence/absence and MJ	EEG: Bilateral synchronised gereralised SWD CT: not done	Myoclonic epilepsy of infancy/idiopathic	-	1 AED: fast response/on AED at final contact (5)	Improving course TR = 1.5	VGKC (135)
7 KJ166	11.8F	Absence status/absences	EEG: 3 Hz generalised bilateral synchronised SWD CT: not done	Generalised idiopathic juvenile absence epilepsy/idiopathic	-	1 AED: fast response/off AED at final contact (13.4)	Good course TR=13.2	VGKC (104)
8 KD256	3.5F	Tonic clonic at onset and FU	EEG normal CT not done	Febrile convulsions during FU/idiopathic	-	1 AED: no fast response/off AED at final contact (5)	Improving course TR=3.6	VGKC (166)
9 KJ084	7.4M	Absences/absences	EEG: 3 Hz generalised bilateral synchronised SWD CT:normal	Generalised idiopathic CAE/idiopathic	-	2 AEDs:fast response/off AED at final contact (15.7)	Good course TR= 15.6	VGKC (182) NMDAR (2)
10 KJ190	1.5F	Minor motor and absences/minor motor and absences	EEG: 3 Hz generalised bilateral synchronised SWD CT:normal	Generalised idiopathic CAE/idiopathic	-	2 AEDs: no response (bad compliance)/on AED at final contact (13.5)	Improving course TR=1.7	VGKC (217) NMDAR (2)
11 KD336	12.6F	TC/ TC	EEG: photosensitivity and diffuse abnormalities CT: normal	Generalised idiopathic with photosensitivity/remote symptomatic	Mild LD – attended regular school	1 AED: fast response/on AED at final contact (13.1)	Good course TR=13.1	NMDAR (1.5)

Table 3-5 Demographic, clinical and paraclinical features, and long-term outcomes of CNS autoantibody positive patients (1 to 11) in the Dutch cohort

Abbreviations; CPS complex partial seizures, SPS simple partial seizures, EEG electroencephalogram, CT computed tomography, TCS tonic clonic seizure, FU follow-up, TR terminal remission, AED anti-epileptic drug, PS partial seizure, LGS Lennox Gastaut Syndrome, CAE childhood absence epilepsy, IGE idiopathic generalized epilepsy, RS remote symptomatic, MR mental retardation, SWD spikewave discharge, FS febrile seizures, BECTS Benign Epilepsy with Centrotemporal Spikes, MJ myoclonic jerks, SE status epilepticus

Case no/ Dutch code.	Age and sex	Seizure type at onset/FU	EEG and CT findings	Type of epilepsy/aetiology	Associated clinical features	Treatment history first 5 years /at end of follow-up (FU, yrs)	Assessment of patient outcome overall/TR (yrs)	Ab positivity (Titres)
12 KL125	12M	SE/SE, unclear small seizures	EEG:hypofunctional L temporal CT:normal	Loc related symptomatic/remote symptomatic	LD, IQ < 50 Tetraparesis	2 AEDs: no fast response/on AED at death (died 1.4yrs after enrollment)	TR= 1	NMDAR (1.5)
13 KD 376	3.6F	Atonic seizures/atonic seizures, TC	EEG: continuous bilateral synchronised generalized SWD CT: not done	Gen crypt LGS/remote symptomatic	Mild global delay	2 AEDs: no fast response/on AED at final FU (12.7)	Deteriorating course TR=0.5	NMDAR (1.5)
14 KD 221	6.6F	Absences/absences	EEG: 3 Hz generalized SWD CT: not done	CAE/idiopathic	-	1 AED: fast response/off AED at final FU (14.8)	Good course TR= 14.8	NMDAR (1.5)
15 KD 321	15.5F	TC/TC	EEG: focal abnormalities, not epileptic CT: normal	IGE/idiopathic	-	No AED/off AED at final FU (2)	Lost to follow-up after 2 years TR=2	NMDAR (1.5)
16 KW051	4.1M	SE/SE	EEG: multifocal epileptic abnormalities CT: large ventricles	Localisation related symptomatic/RS including MR	Mild LD, autism spectrum disorders	1 AED: fast response/off AED at final FU (15.9)	Good course TR 12.1	CONTACTIN-2 (1 in 100)
17 KW085	4.2M	Unclear seiz/TC with focal onset	EEG:normal CT:hypodense white matter	Remote symptomatic including MR	Global MR, spasticity, visual problems	1 AED: fast response/on AED at final FU (5)	Improving course TR>2	CONTACTIN-2 (1 in 100)
18 KW 052	8.8F	Atonic, astatic/SPS with generalisation	EEG: epileptic abnormalities (Rol.spikes) + abnormal background pattern CT: not done	BECTS/idiopathic	-	3 AED: no fast response/off AED at final FU (5)	Improving course TR>2	CONTACTIN-2 (1 in 100))
19 KW 080	12.5M	SPS/SPS with generalisation	EEG and CT normal	Benign partial epilepsy/idiopathic	-	Never used AED	Good course TR>5	CASPR2 (1 in 100)
20 KL141	8.9M	TCS/TCS	EEG: epileptiform, bilateral synchronised SWD CT:normal	IGE/idiopathic	-	1 AED: fast response/no AED at final FU (14)	Good course TR>5	CASPR2 (1 in 100)
21 KL173	10.5M	PS with secondary generalisation/clustered PS with gen leading to hospitalisation	EEG: epileptiform and focal abnormalities CT: normal	Localisation related cryptogenic/cryptogenic	-	3 AED: no fast response, polytherapy/on AED at final FU (13,3)	Poor course, intractable TR<0.1	CASPR2 (1 in 100)
22 KW019	0.6M	CPS,myoclonic, atonic/TCS	EEG: bilateral synchronised epileptiform abnormalities CT: abnormal, some atrophy	Secondary generalized multifocal with atonic and atypical absence seizures /RS including MR	Severe MR FS during FU	4 AED:no fast response/on AED at final FU (16.5)	Improving course. Period of intractability during first 5yrs FU, probably due to bad compliance. TR> 5	CASPR2 (> 1 in 100)

Table 3-6 Demographic, clinical and paraclinical features, and long-term outcomes of CNS autoantibody positive patients (12 to 22) in the Dutch cohort.

Abbreviations; as above (Table 3-5).

3.4.2 Comparison of clinical features and long-term outcomes between antibody positive and antibody negative patients in the Dutch cohort

Table 3.7 shows the comparisons of clinical features and long-term outcomes between the two groups. There was no difference in the sex distribution or age of onset of epilepsy, between autoantibody positive and negative patients. The autoantibody positive patients were more likely to present in SE (p=0.03; Fisher's exact test), but overall there was no difference in type of epilepsy at presentation or subsequent pattern and frequency of seizures. There was a higher rate of cognitive impairment/ learning difficulties in the autoantibody positive group (p=0.01; Fisher's exact test). However, as previously mentioned, in the autoantibody positive group these difficulties were present before the onset of epilepsy. In the antibody negative cohort 26 had cognitive impairment/learning difficulties at onset with six additional patients developing problems during their disease course. Epileptiform abnormalities were reported in 82% of standard EEGs in the antibody positive group, and 78% in the antibody negative group while CT abnormalities were seen in 18% of both groups. Two patients had febrile seizures in the antibody positive patients (9%; 2/22), compared to 31/156 (20%) of the remaining cohort.

At five year follow-up 73% of patients in both groups had been seizure free for more than 12 months. Approximately one third of patients in both groups were still on AEDs at final contact. The rate of intractability at last contact was similar in both groups (13.6% in autoantibody positive vs. 10% in autoantibody negative group). In the whole cohort, there were 10 patients intractable to AEDs with an unknown cause for their epilepsy (cryptogenic), two of these were antibody positive (20%).

Characteristic	Antibody positive (n=22)			Antibody negative (n=156)		
Sex	M:F 10:12			M:F 71:85		
Median age of presentation	5.7 years (range 0.9 – 15.5)			6.2 (range 0.2 -15.8)		
Type of epilepsy at enrolment	Generalised	12		Generalised	70	
	Focal	6		Focal	82	
	Other	2		Other	2	
Pattern of seizures	continuous	9		Continuous	67	
	intermittent	4		intermittent	55	
	bursts	0		bursts	21	
	unclear	1		unclear	3	
Frequency of seizures within first 6 months	1-3	9		1-3	68	
	4-25	4		4-25	34	
	Uncountable	9		Uncountable	55	
Aetiology at onset	Idiopathic	12		Idiopathic	84	
	RS incl MR	8		RS incl MR	41	
	Cryptogenic	2		Cryptogenic	31	
Pre-existing neurological signs/ abnormal neuro exam	4			17		
Mental retardation/cognitive impairment	10			32 p=0.01*		
History of febrile seizures before or after intake	2			31		
Family history	2			20		
Status epilepticus as presenting feature	4			7 p=0.03*		
Abnormal EEG	18			122		
CT	Normal	10		Normal	83	
	Abnormal	4		Abnormal	29	
	Not done	8		Not done	44	
Polytherapy	4/18			22/140		
On AED at final contact	6/18			43/140		
Intractable at last contact	3 (2 with late onset)			16 (8 with late onset)		
Terminal remission at 2 years: 5 years	Good	12	16	Good	84	114
	Fair	1	2	Fair	17	5
	Poor	8	2	Poor	48	30
	unknown	1	2	unknown	7	0

Table 3-7 Comparison of clinical features and outcomes of antibody positive and negative patients in the Dutch cohort.

(* analysed by Mann-Whitney)

Abbreviations: M male, F female, RS remote symptomatic, MR mental retardation, EEG electroencephalogram, AED anti-epileptic drug, CT computed topography

3.4.3 Testing of follow-up samples

Consecutive samples over a 12 month period were available from 9 patients (Figure 3.4). The 3 patients positive for NMDAR-Ab at initial presentation were all negative at 6 months (KD 376) and 12 months testing (KD221, KD 321). Two out of 3 (KD221, KD321) of these patients had a good overall outcome with generalised epilepsies responsive to treatment, suggesting the antibodies did not affect the disease course. The third patient had a deteriorating course with had multiple problems, including spastic diplegia and microcephaly.

Three out of the four patients initially positive for VGKC-complex antibody remained positive at 6 and 12 months (KJ166, KJ168, KD58), although in two patients the levels were consistently low (<150pmol/L). One patient became negative (KD227) and perhaps surprisingly, this was the patient with intractable epilepsy at long-term follow-up. The other patients all had a good or improving disease course. These changes in antibody positivity did not correlate with cognitive decline or seizure frequency. One of the two patients who were double positive for NMDAR-Abs and VGKC-complex antibodies showed an initial drop in VGKC-Abs at 6 months followed by an increase at 12 months. A similar change was seen in the NMDAR-Ab results. From clinical information available in the patient notes, these changes did not correlate with changes in seizure frequency or cognitive development.

Samples for the antibody negative patients available at 6 and 12 months were also tested for VGKC-complex antibodies and NMDAR-Abs to look for any positivity following the development of epilepsy. None of the patients that were initially VGKC-complex Ab negative became positive when tested at six or 12 months after the initial sample at enrolment, suggesting that these antibodies are not produced by the epileptic process itself. However, two six month and two 12 month samples were positive for NMDAR-Abs, all these had been negative at initial sample testing. The

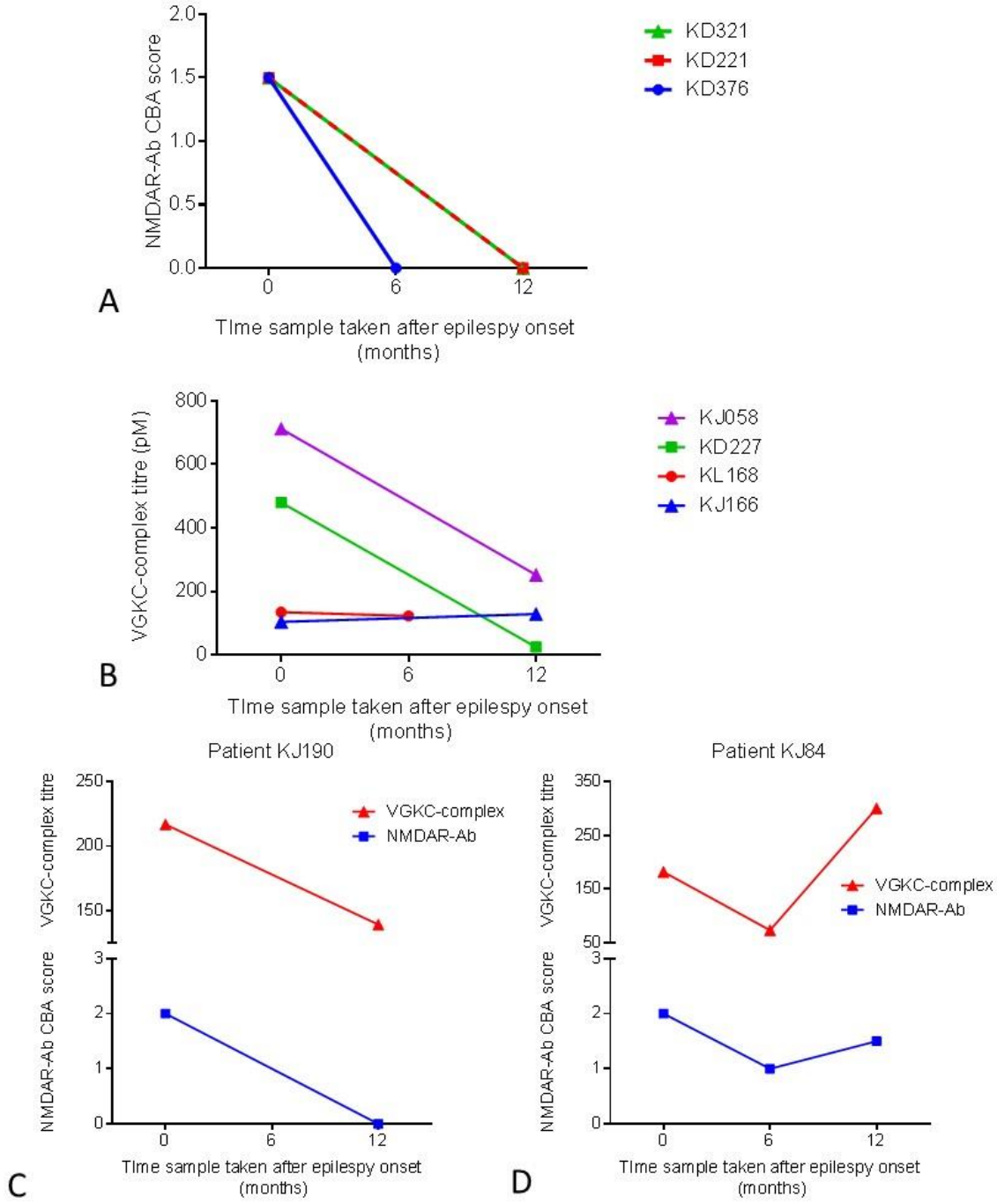

Figure 3-4 Antibody testing of consecutive serum samples in 9 antibody positive patients in the Dutch cohort.

A. The three NMDAR-Ab positive patients were all negative at either 6 months or 12 months post their first sample testing which was within 6 months of disease onset.
B. The 4 VGKC-complex patients also showed a reduction in titres over time.
C. One of the double antibody positive patients (patient KJ 190) showed a parallel reduction in both antibodies over time.
D. Patient KJ84 showed an initial reduction in antibody levels then increase over time. These antibody levels (C and D) did not correlate with developmental regression or seizure activity.

Patient	NMDAR-Ab positivity at:			Clinical and paraclinical features	Epilepsy course
	Intake	6 months	12 months		
131 KD 191	negative	**Low positive (CBA score 1.5)**	negative	1.5 yr Male Before intake tonic-clonic and absence seizure varying in intensity Abnormal EEG at intake, normal EEG after partial sleep deprivation, normal EEG at 6 months. Normal CT	No further seizures at 5 year F/U 2 AEDs, monotherapy, fast response Total FU 15.1 years TR 15.1 years, not intractable
136 KD 295	negative	No sample	**Positive (CBA score 2)**	0.5 yr Female Before intake, clusters of spasms 1/day Tuberous sclerosis, West syndrome, LD Abnormal EEG at intake (hypsarrythmia), and at 6 months Abnormal CT scan	After intake, several absence like events per day during period of one year 1 AED used, no fast response Total FU 13.7 yrs TR 1.5 years, not intractable
27 KJ 170	negative	No sample	**Low positive (CBA score 1.5)**	1.3 yr Male Before intake, 15 febrile convulsions clusters Behavioural problems, no LD, + FHx Normal EEGs at intake and 6 months Normal CT	During FU, monthly clusters of FSs, absences, CPS 1-6/week. 2 periods intractability >1 yr in first 5 yr FU Total FU 13.9 yrs TR 0, intractable at endpoint
124 KL 135	negative	**Low positive (CBA score 1.5)**	negative	4.2 yrs Male Before intake, 2 unclear seizures and febrile convulsions Normal EEG at intake, abnormal at 6 months. Normal CT	After intake, 5 seizures (type unknown) within 2 months One AED used, fast response Total FU 14.5 yrs, TR 14.3 yrs, not intractable

Table 3-8 Clinical features of NMDAR-Ab positive follow-up patients in Dutch cohort

Abbreviations: CBA cell based assay, EEG electroencephalogram, CT computed topography, LD learning difficulties, FHx family history, AED anti-epileptic drug, TR terminal remission, FU follow-up, FS febrile seizures, CPS complex partial seizures

clinical features of these patients are listed in Table 3.8. There was no common features or phenotype within this group of latent NMDAR-Ab positive patients. The patient with the highest titre of NMDAR-Abs (CBA score of 2; titre 1 in 500) developed these at 12 months following intake into the study. This patient had brain abnormalities as a result of Tuberous Sclerosis, learning difficulties and West syndrome.

3.4.4 Healthy controls testing

Five healthy controls were positive for autoantibodies. As described in the methods (section 2.1.1), these healthy controls were healthy sibling donors for bone marrow transplant patients, and were age and sex-matched. We were also provided with the serum samples from four of the bone marrow recipients of antibody positive healthy sibling donors. As seen in Figure 3.5, these recipient samples were all negative.

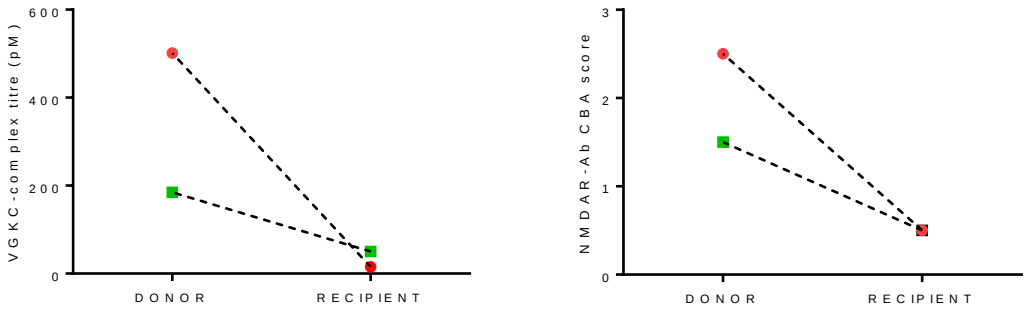

Figure 3-5 Antibody testing of bone marrow recipients from antibody positive healthy controls.

A. The healthy controls in the Dutch cohort were healthy sibling donors for bone marrow transplants. These graphs show the results of two positive VGKC-complex antibody healthy donors and the matching results (by dotted line) of their bone marrow recipients. Despite the positivity of the healthy donors, the recipients of their bone marrow were all negative for autoantibody screening post bone marrow transplant.
B. A similar results is seen for the two NMDAR-Ab positive healthy donors, with the bone marrow recipients testing negative.

3.4.5 Summary of key findings from Dutch epilepsy patients

Most autoantibody positive patients had a good outcome and responded to standard AEDs. Twenty per cent (2/10) of the intractable patients with an unknown aetiology for their epilepsy were found to be antibody positive. The first contactin-2 autoantibody positive paediatric epilepsy patients were identified within this cohort, and they shared language and developmental problems similar to some of the CASPR2 antibody patients. In view of this common association we tested a paediatric epilepsy cohort (French CSWS cohort) with these specific difficulties to see if this finding was replicable.

3.5 French CSWS cohort results

CSWS and the LKS are rare paediatric epileptic disorders that present with speech and language problems and regression as well as epileptic encephalopathy. Given the treatment response some patients show to steroids, and the finding of positive autoantibodies in patients with a similar phenotype, a role for autoimmunity in the pathophysiology of these disorders is possible.

Fifty-three patient and control samples collected by four French medical centres from 2009 for a CSWS/ LKS study investigating the genetics of this disorder (Lesca, Rudolf et al. 2012), were tested. Sample testing for autoantibodies to the cell adhesion proteins (CASPR2 and contactin-2) and the VGKC-complex, was performed, blinded to the identity of patient samples and clinical details. Additionally, given the subsequent discovery of mutations in the NR2A subunit in a significant proportion of these patients (Lesca, Rudolf et al. 2013), antibodies to NR1 and the NR2A subunit by CBA, and the standard NMDAR-Ab assay (NR1 and NR2B), were also tested. Eight samples were positive (8/53; 15%), four for CASPR2 antibodies and four for VGKC-complex

autoantibodies (Figure 3.6A-C). All samples were negative for antibodies to contactin-2 and the NMDAR including to the NR2A subunit. Testing on live cortical neurons was also negative.

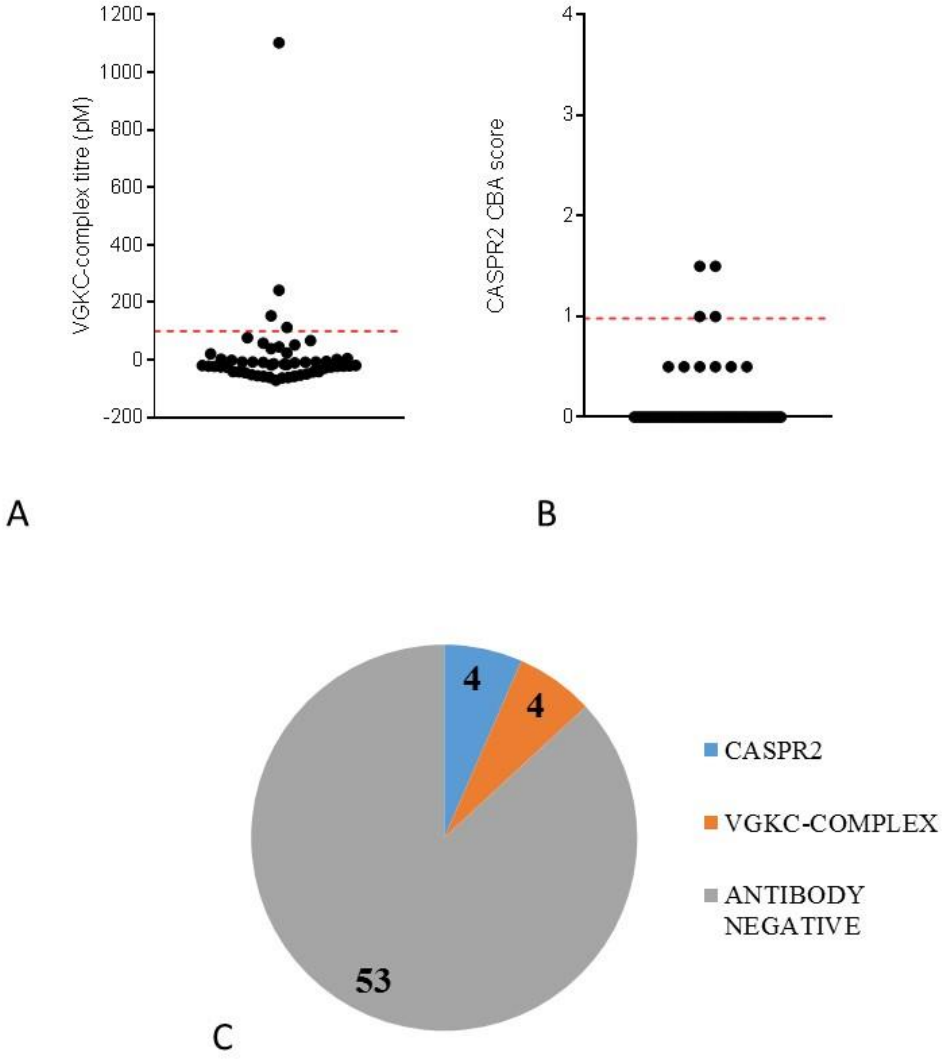

Figure 3-6 Antibody positivity in French cohort of CSWS/LKS patients and controls.

A. The titres of VGKC-complex antibody patients in the French CSWS cohort are shown here. The red dotted line represents the laboratory cut off for a positive result.
B. There were three positive CASPR2 antibody results in this cohort, separate from the VGKC-complex antibody positive patients. The red dotted line represents the laboratory cut off. The assay was performed at a serum dilution of 1:100.
C. Antibody positivity of the whole cohort was 15% (8/53).

3.5.1 Clinical correlation of French CSWS samples

Seven of the positive samples were from patients with CSWS (n=3; two VGKC-complex, one CASPR-Ab positive), Rolandic epilepsy (n=3; one VGKC-complex, two CASPR2-Ab positive), and a neurodevelopmental disorder (dyspraxia, CASPR2-Ab positive); the other positive case was an unaffected father of an antibody positive patient (Table 3.9). Three of the positive patients were from one family, two of whom had a GRIN2A mutations (Figure 3.7).

Overall, in terms of phenotype specificity, none of the four LKS patients in the cohort were positive; three out of 23 CSWS (13%) and three out of 12 Rolandic epilepsies (25%) were antibody positive. 16.3 % (7/43) patients in the CSWS group were positive for antibodies to the VGKC-complex , CASPR2, and contactin-2proteins compared to 7% of the new onset paediatric epilepsy cohorts (Dutch and Australian), (p=0.07,ns; Fisher's exact test).

3.6 Comparison of seizure semiology between autoimmune encephalitis (AE) and autoantibody positive paediatric epilepsy (PE) patients

CNS autoantibodies are found in both paediatric epilepsy and paediatric autoimmune encephalitis (AE). Examining the seizure semiology between both groups and looking for common features may give clues to the underlying pathogenesis.

For the AE cohort, paediatric patients presenting to five UK tertiary neurology centres with a new onset encephalopathy and seizures with positive CNS autoantibodies were studied (n=17) (Hacohen, Wright et al. 2013). Ten were positive for NMDAR-Ab and seven had antibodies to the VGKC-complex. In the new-onset

Serum/ Patient ID	Antibody result	Phenotype	Genetic mutation
DZ31 ★★	CASPR2 positive CBA score 1	atypical Rolandic epilepsy	GRIN2A
DZ27 ★	CASPR2 positive CBA score 1.5	Unaffected father of DZ31	no
A5	CASPR 2positive CBA score 1	CSWS	no
76D	CASPR2 positive CBA score 1	Dyspraxia	no
EC48	VGKC-Complex Titre 1102pM	Rolandic epilepsy	no
EF27 ★	VGKC-Complex Titre 242pM	CSWS	GRIN2A
A18	VGKC-Complex Titre 153pM	Rolandic epilepsy with ESES	no
A22	VGKC-Complex Titre 113pM	CSWS	no

Table 3-9 Positive results of CSWS cohort antoantibody screening.

Abbreviations: CBA cell-based assay, CSWS continuous slow-wave in sleep, ESES electrical status epilepticus in sleep

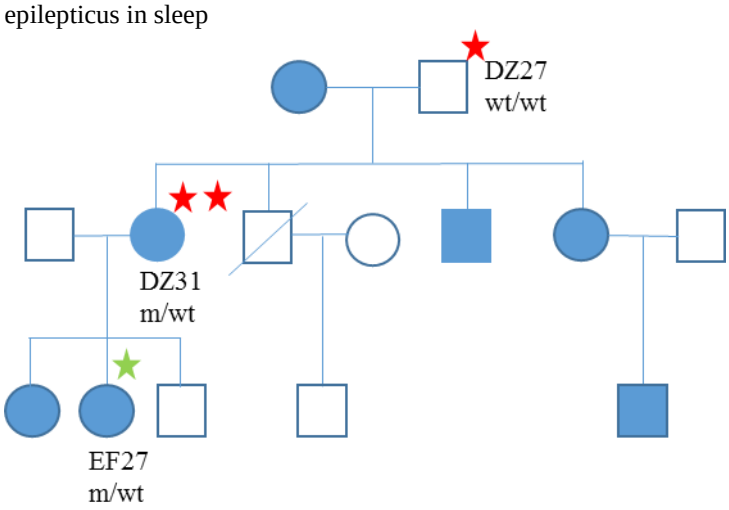

Figure 3-7 Antibody positivity in one GRIN2A mutation family

This is the family tree of Family 1 in the Lesca study (Lesca, Rudolf et al. 2013) with a number of family members affected with an inherited GRIN2A mutation (m/wt) associated with LKS, CSWS and atypical Rolandic epilepsy (coloured blue). Screening for CNS autoantibodies found CASPR2 antibodies in two (marked with red stars and corresponding to information in table 3.7) and VGKC-complex antibodies in one (green star). Interestingly, CNS autoantibodies and the GRIN2A mutation were both found in all three generations. Also similar to antibody positivity in an unaffected patient (DZ27) the NR2A genetic mutation was also present in one unaffected sibling (EF25).

paediatric epilepsy (PE) patients there were 12 VGKC-complex positive and seven NMDAR-Ab positive (Dutch and Australian cohort). The seizure semiology was similar between both groups, in that generalized seizures were the most common type of seizure seen. 15.7% of patients had status epilepticus which was not seen in the AE cohort. PE patients were more likely to have epileptiform discharges and were not encephalopathic. Therapy resistant seizures were seen in both groups at a rate of 20-40%. When antibody levels were compared between the two groups, the NMDAR-Ab levels were significantly higher in the autoimmune encephalitis patient group than those with epilepsy alone but VGKC-complex Ab titres were not significantly different between the two groups (Figure 3.8A-B).

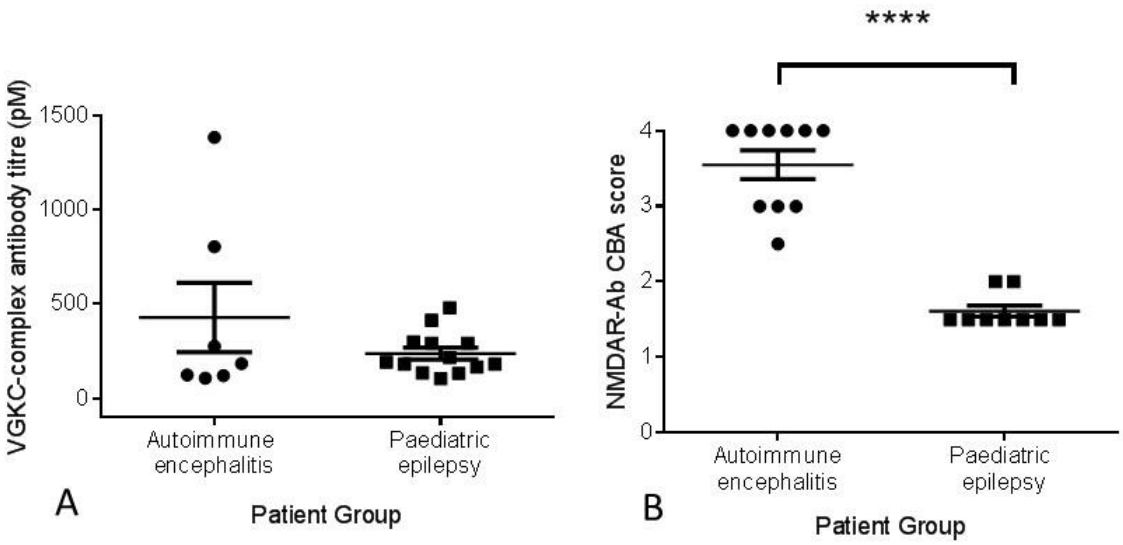

Figure 3-8 Comparison of VGKC-complex and NMDAR-Abs between autoimmune encephalitis (AE) and paediatric epilepsy (PE) patients.

A. There is no significant difference between the titres of VGKC-complex antibodies in the AE and PE groups, although the highest tire is in the AE group (mean +/- SEM).
B. The NMDAR-Ab CBA scores were significantly higher in those patients with NMDAR-Ab encephalitis compared to those with epilepsy alone (mean +/- SEM, $p = < 0.0001$, Mann-Whitney test).

3.7 Discussion and limitations

The importance of autoantibodies to neuronal proteins in a small but significant number of epilepsy patients (9-13%, McKnight et al., Majoie et al., 2006; Brenner et al., 2013) is increasingly recognized. However studies into paediatric epilepsy have been limited. Here we were able to test two separate cohorts of new-onset paediatric epilepsy patients for a range of autoantibodies, and correlate the positive and negative autoantibody results with type, aetiology and presentation of epilepsy, associated features including regression and autistic features, treatment responses and long and short term outcomes.

Overall antibody positivity in the two paediatric epilepsy cohorts combined was 11.4%, which was significantly different to control sample testing and similar to adult epilepsy patients (Brenner, Sills et al. 2013). In the Australian cohort, we found the antibodies were more common in children with epilepsy of "unknown cause", often with focal epilepsy, as also seen in the adult cohort studies. However in contrast to the adult studies and the Dutch paediatric epilepsy cohort, the patients in the Australian cohort represented an in-patient sample rather than a community out-patient sample group. The patients were younger and more complex, often requiring treatment in intensive care and with associated symptoms of infection, fever and additional underlying diseases. In some cases there was an overlap with encephalitis, although none of these were autoantibody positive.

The most frequently found antibody in both groups was to the VGKC-complex. All these patients were negative for VGKC-complex proteins LGI1, contactin-2 and CASPR2, and had relatively low titres (13/16, 81%, were <400pM). The lack of an identified complex protein has been previously reported in children (Haberlandt, Bast et al. 2011, Illingworth, Hanrahan et al. 2011, Suleiman, Brenner et al. 2011, Suleiman, Brenner et al. 2011). This is in contrast to adult patients in whom antibodies to LGI1,

and less commonly CASPR2 (Irani, Alexander et al. 2010, Lai, Huijbers et al. 2010) are found frequently in LE patients, although not when patients with a wide variety of clinical presentations are tested as in routine clinical practice (Paterson, Zandi et al. 2013). It is possible that in children, the VGKC-complex antibodies are binding to other, as yet unidentified extracellular antigens (Hacohen, Wright et al. 2013), or even intracellular targets (Hacohen et al. 2014, *submitted*). The lower titres seen in the paediatric epilepsy patients are also similar to those reported in the paediatric literature with most titres being less than 400 pM (Table 3.10). The pathological relevance of low levels of VGKC-complex antibodies is unknown. In adults, with mixed neurological diseases, levels less than 400pM were found to be less clinically relevant than those above 400 pM. It was suggested that low levels may be secondary to other disease pathologies and even part of a normal repertoire of autoantibodies found in healthy individuals (Paterson, Zandi et al. 2013). Our VGKC-complex antibody patients did not have concurrent diseases, but these antibodies were the most commonly found positive antibodies in both the healthy and disease controls. Interestingly, two out of three of the Dutch epilepsy patients with the highest VGKC-complex antibody levels (over 400 pM) did have a more severe epilepsy phenotype, needing more than three AEDs to treat their epilepsy with one becoming intractable to standard treatment.

Separate CBA testing of VGKC-complex associated proteins identified seven patients positive for CASPR2 antibodies and three positive for contactin-2 antibodies. These autoantibodies have not been previously identified in paediatric epilepsy patients. All seven patients were negative for VGKC-complex antibodies in the radioimmunoassay, so would have been missed with only standard VGKC-complex Ab testing. None of the VGKC-complex, CASPR2 or contactin-2 antibody positive patients had a phenotype typical of LE, although most of them presented with focal seizures. As previously mentioned, antibodies to the LGI1 protein, most commonly described in

Year of Publication	First author	Clinical features	No. of patients	VGKC-titres <400 pmol/L	VGKC-titres >400 pmol/L
2013	Suleiman	Epilepsy	3	1	2
2012	Hacohen	Autoimmune Encephalitis	7	4	3
2012	Iyer	Psychiatric features	1		1
2011	Suleiman	Encephalitis/Status epilepticus	9	8	1
2011	Suleiman	Epileptic spasms	1	1	
2011	Illingworth	FIRES	1	1	
2011	Haberblandt	Limbic Encephalitis	4	4	
2011	Dhamija	Various	12	8	4
Total			38	27 (71%)	11 (29%)

Table 3-10 Spectrum of paediatric VGKC-complex Ab associated neurological disease in relation to antibody titres

Abbreviations: FIRES febrile infection-related seizures

adult LE and FBDS, were not seen in these cohorts and have not previously been described in children. Despite the crucial role of the LGI1 protein in neuronal maturation, mouse CNS LGI1 gene expression is lower in intrauterine and early postnatal stages when compared to adult levels (Ribeiro, Sbragia et al. 2008) and patients with LGI1 related genetic epilepsy present mostly in early adulthood (Kalachikov, Evgrafov et al. 2002, Ottman, Winawer et al. 2004). This may explain the lack of paediatric patients with LGI1 antibodies in these and other paediatric autoantibody screening studies of epilepsy and encephalitis (Hacohen, Wright et al. 2013).

In the Dutch cohort, CASPR2 and Contactin-2 antibody positive patients were found to share cognitive and language problems. CASPR2 and Contactin-2 are both cell

adhesion molecules which play a crucial role at the synapse. Previously, CASPR2 antibodies have been mainly described in patients with Morvan syndrome, LE (Irani, Pettingill et al. 2012) and in two out of four adult epilepsy patients in a LE cohort (Irani, Alexander et al. 2010). Homozygous mutations in the CASPR2 gene (CNTNAP2) have been described in a group of Amish children with cortical dysplasia, focal epilepsy (CDFE) syndrome (Strauss, Puffenberger et al. 2006). These children present with intractable focal seizures beginning in early childhood with all developing autistic regression. A patient with a similar phenotype and CASPR2 antibodies was briefly described in another recent case series of LE (Lancaster, Huijbers et al. 2011). The CASPR2 knockout mouse model recapitulates the clinical features of patients with genetic mutations with severe epilepsy developing in the adult mouse (Penagarikano, Abrahams et al. 2011).

Contactin-2 antibodies are found rarely in LE, but have been described in some patients with multiple sclerosis (Boronat, Sepulveda et al. 2012) and are also present in a proportion with neuromyotonia or Morvans. Deletions in the Contactin-2 (CNTN2) gene have also been recently found in focal epilepsy (Stogmann, Reinthaler et al. 2013). Copy number variants in both CNTNAP2 and CNTN2 among other cell adhesion molecules, are found in 20% of patients with CSWS and LKS (Lesca, Rudolf et al. 2012). CSWS and LKS form part of the spectrum of childhood epileptic encephalopathies that present with or without overt clinical epileptic seizures, but neurodevelopmental regression which in LKS manifests as speech and language problems. These features were similar to those seen in the Contactin-2 antibody positive patients, suggesting a genetic and immunological link. Patients with Landau Kleffner syndrome can respond well to immunotherapy (Mikati, Saab et al. 2002), raising the possibility of an autoantibody mediated pathogenesis in some cases. We therefore tested a cohort of these patients and controls for antibodies and found a 15% positivity for the

relevant CNS autoantibodies. This was more than double the rate of antibody positivity in the unselected new-onset paediatric epilepsy patients. This suggests that some cases of CSWS can be associated with CNS autoantibodies and may be helpful in the management with regards to immunotherapy. This was also the first description of antibody testing within generations of the same family and in a cohort of genetically screened patients. Three positive CNS autoantibody results (out of eight in the total cohort), were found in three different generations of the same family, suggesting genetic factors may contribute to CNS autoantibody production. In the same family, there was also an unaffected sibling with the disease associated GRIN2A mutation similar to the unaffected father with a positive CNS autoantibody result. From this dual aetiology study of a subset of epilepsy patients, it appears that while genetic mutations and CNS autoantibodies may not always be directly causal, they should be considered as a risk factor for epilepsy.

Six patients with NMDAR-Abs had epilepsy without the other classically associated features of NMDAR-Ab encephalitis, i.e. neuropsychiatric features and movement disorder. This has also been described in adult patients with epilepsy (Niehusmann, Dalmau et al. 2009, Brenner, Sills et al. 2013). Two three year old patients (one each from Australian and Dutch cohort) had a similar phenotype with mixed seizure types, learning difficulties, and probable developmental structural brain abnormalities. Both were diagnosed with LGS and needed at least two AEDs for treatment. It has been suggested that the underlying pathogenesis of catastrophic epilepsies such as LGS may be neuronal damage caused by overexpression or excessive activation of glutamate receptors in development (Rho 2004). Whether this could also lead to the production of specific antibodies to the NMDAR in these patients is unknown. Additionally, felbamate, a drug that selectively acts on the NR1 and NR2B receptor have been shown to be particularly effective in LGS (Kleckner, Glazewski et

al. 1999). The reason for its effectiveness is thought to be due to the predominance of the NR2B subunit at this early developmental stage. As the brain develops however there is a change in composition to NR2A-containing NMDARs which may explain the later childhood presentation of NR2A associated genetic forms of Landau-Kleffner syndrome, also studied here (Dumas 2005, Lesca, Rudolf et al. 2013). However, despite this association and the response to immunotherapy seen in some of these patients, autoantibodies to the NR2A subunit were not found in LKS/ CSWS patients.

Four patients, all presenting with generalised epilepsies, were positive for both NMDAR and VGKC-complex antibodies; the finding of two or more neuronal antibodies has been previously described (Pellkofer, Kuempfel et al. 2010, Haberlandt, Bast et al. 2011, Brenner, Sills et al. 2013) and may reflect a wider activation of the immune system, perhaps by infections or possibly as a response to neuronal damage. In order to investigate this hypothesis further, we tested the follow-up samples of autoantibody negative Dutch epilepsy patients to see if neuronal changes or BBB permeability changes from epilepsy itself could stimulate autoantibody production. NMDAR-Abs, but not VGKC-complex Abs, were found in four patients between six and twelve months after the onset of epilepsy. Similarly, NMDAR-Abs have been described in relapsing herpes simplex virus (HSV) encephalitis patients who re-present after the initial phase of their disease with movement disorder and seizures and are found to be NMDAR-Ab positive (Hacohen, Deiva et al. 2014). The theory is that brain proteins become exposed during the destructive HSV encephalitis and autoantibodies develop to the exposed NMDAR proteins. Theoretically, this could also happen with epilepsy. This also means that timing of samples is crucial when trying to prove causality in the relationship between antibodies and epilepsy. Testing as soon as possible after the onset of the seizure disorders will reduce diagnostic doubt about aetiology if the test is positive for autoantibodies. Positive tests greater than six months

after onset may point to the antibodies being produced as a consequence of epilepsy rather than being the cause. However, we found that epilepsy serum samples that were initially negative for VGKC-complex antibodies remained negative for these antibodies at follow-up testing at six or 12 months, suggesting that in these cases, epilepsy had not stimulated production of new autoantibodies.

In terms of other investigations for epilepsy aetiology, the Dutch study was limited as there was a lack of MRI imaging data and CSF studies; both may have contributed additional evidence of CNS inflammation. Furthermore, other aetiological investigations (i.e. genetic screening) were limited given the historical nature of the cohort. MRI scans in the Australian cohort only identified abnormalities in four out of eleven positive patients, contributing to the diagnosis in one (case 9). CSF tested in four out of the Australian cohort patients was also normal apart from CSF neopterin which was elevated in one out of three tested at 68nmol/L (normal <30; case 1), suggestive of CNS inflammation. Unfortunately no CSF was available from any of the epilepsy patients to test for autoantibodies. This would have been important as the validity of low positive serum autoantibody results has been questioned (Gresa-Arribas, Titulaer et al. 2014), and may be due to differences in the CBA technique. Additional hippocampal neuronal testing was used in the Dutch epilepsy positive patients as a further confirmational test of autoantibody presence.

None of the 11 antibody positive patients in the Australian cohort received immunotherapy. Nine had ongoing epilepsy at the time of follow-up and two may have developed new cognitive or behavioural impairment. However the length of follow-up was short and detailed neuropsychology was not done. As this was a prospective observational cohort, we can only hypothesise that immunotherapy, if given, might have improved the epilepsy outcome.

Similarly in the Dutch cohort, no immunotherapy was given to the patients. Although, apart from West syndrome, it was not standard practice to treat many patients with immunotherapy in the 1980's and 1990's when the patients were recruited. Most autoantibody positive patients in the Dutch cohort had a good eventual outcome (up to 15 years follow-up) and responded to standard AEDs. This suggests that the autoantibodies were not the primary cause of the epilepsy, and many had been classified with a different aetiology, for example structural or genetic. However, the two patients who were classified as having an 'unknown cause' for their epilepsy prior to antibody testing did have long-term intractability with a poor epilepsy course. In these cases immunotherapy might also have been beneficial. Recently published guidelines suggest a trial of immunotherapy if autoimmune epilepsy is suspected in AED resistant cases (Toledano, Britton et al. 2014).

CNS autoantibodies are associated with seizures in both paediatric autoimmune encephalitis and epilepsy. There was no significant difference in seizure semiology between these two groups when compared, suggesting a common pathogenic mechanism. However, the NMDAR-Ab encephalitis patients had much higher antibody levels than those with epilepsy only, perhaps reflecting their disease severity and more complex symptomatology.

In summary, these observational prospective studies are the first to systematically test for autoantibodies in unselected paediatric epilepsy patients soon after disease onset, and as they were untreated with immunotherapy, serve as important controls for any prospective treatment trials. It can be recommended that as in adults, paediatric new onset focal epilepsy patients would be an appropriate group to routinely test for neuronal autoantibodies as a possible aetiological factor, particularly if a structural cause has been excluded on imaging (Suleiman, Wright et al. 2013). However given the positive autoantibody tests in the controls and the discovery of double

positives, it is also possible that the presence of neuronal antibodies are, in some circumstances, an epiphenomenon or secondary to structural damage or generalised immune activation.

The novel finding of Contactin-2 antibody positive epilepsy paediatric patients, further characterisation of CASPR2 antibody positive epilepsy and lack of LGI1 antibody positive cases suggests different antigenic targets may be more relevant in the paediatric population. Identification of novel antigens is therefore particularly important in these patients and identifying patients who positively stain live hippocampal neurons but are negative for known antigens is an important first step. A candidate antigen approach looking for previously undescribed NR2A antibodies was performed, but did not identify any new positive patients.

Pathogenic effects of some neuronal surface antibodies have been demonstrated *in vitro* but definitive *in vivo* epileptogenicity has yet to be demonstrated (Hughes, Peng et al. 2010, Manto, Dalmau et al. 2010, Lalic, Pettingill et al. 2011). Animal models disrupting the function of important neuronal proteins such as NMDARs (Duncan, Inada et al. 2010) and Contactin-2 (Fukamauchi, Aihara et al. 2001) can reduce seizure threshold as well as cause spontaneous seizures; autoantibodies may theoretically act to cause a similar effect in susceptible individuals. Further exploration of this hypothesis in our own animal studies is presented in the following chapters 4 and 5.

CHAPTER 4 - Seizure susceptibility and electrophysiology of NMDAR-Ab passive transfer mice

4.1 Introduction

Antibodies to neuronal surface proteins are found in some cases of paediatric epilepsy as presented in Chapter 3. Most of these patients do not have the associated clinical features of encephalitis. Given this observation, the question remains as to whether these antibodies are epileptogenic and could directly cause epilepsy? Alternatively, could they just be a biomarker of brain injury caused by the epilepsy that has a different aetiology, such as structural or metabolic?

In order to answer this question *in vivo* passive transfer experiments were performed using human IgG positive for NMDAR-Abs, the most commonly described neuronal surface antibodies in encephalitis and epilepsy, particularly in children. Most patients suffering from NMDAR-Ab *encephalitis* have seizures, and specific EEG findings have been described in these patients, emphasising the possible direct role of the antibodies on the neuronal network. Previous work from this laboratory successfully showed a cognitive deficit induced in mice injected in the cerebral lateral ventricle with NMDAR-Ab IgG (Pettingill et al., submitted). These mice also developed abnormal foot movements which may have represented a dystonia or focal epileptiform movements, reminiscent of NMDAR-Ab encephalitis.

In this chapter, data is presented from mice, implanted with experimental telemetric EEG devices that received passive transfer of NMDAR-Ab positive IgG by ICV injection. A seizure induction paradigm was designed, and used to test whether the seizure threshold was reduced in these mice. EEG analysis was optimised to include

epileptiform event detection. The analysis includes data from some experiments performed by Dr Louise Upton and Lucasz Stasiak and other contributors (see Table 4.1), but analysed by SW.

Expt. no.	Description of experiment	Surgery	Analysis of post-mortem tissue/EEG/data
1	Implantation of transmitter, PTZ (n=1)	LS LU	SW
2	Implantation of EEG transmitter and 2 ICV injections (n=8)	LS LU	SW
3	Implantation of EEG transmitter, ICV injections, seizure induction (n=6)	SW LU	SW
4	Implantation of EEG transmitter, ICV injections, seizure induction (n=15)	SW	SW
5	ICV injection of diluted IgG and seizure induction (n=4)	SW	SW
6	Implantation of transmitter, ICV injection, 3 seizure induction (n=4)	SW	SW
7	Injection of virus, ICV injection, ex-vivo patching (n=9)	SW Patching of cells: LM	SW, LM

Table 4-1 Experiments performed and contributors

Abbreviations; LS Lucasz Stasiak; LU Louise Upton; SW Sukhvir Wright; LM Lorenz Muller, ICV intracerebroventricular; PTZ pentylenetetrazol

4.2 Characterisation of NMDAR-Ab IgG used in experimental protocols

In order to select the most suitable samples for the experiments, all available NMDAR-Ab positive plasmas (n = 8) were screened on the NMDAR-Ab CBA, and on frozen

rodent brain sections. Samples from patients PB and RG were selected as they achieved the highest end point titration on the NMDAR–Ab CBA and were positive by immunohistochemistry. The IgG was purified from these two plasmas as described in the methods. The third IgG was provided by Philippa Pettingill (patient ME). The clinical details of all three patients from whom the IgG was purified, and final IgG CBA titrations are summarized in Table 4.2. In addition, the serum from two healthy individuals was used to prepare HC IgG. The purified IgG preparations were then tested on the CBA with cells transfected with NR1, NR2B and EFGP, live hippocampal neurons and WT mouse sections for NMDAR-Ab binding specificity. The NMDAR-Ab IgG preparations showed characteristic binding in all tests; HC IgG preparations were negative (Figure 4.1). NMDAR-Ab IgG from patient ME only was used in the preliminary experiments described below.

Patient code	Demographics	Purified IgG titre/concentration (mg/ml)	Clinical features
ME	Female, 25 yrs Caucasian	1 in 4000 25mg/ml	Severe agitation, confusion, hypersomnolence, movement disorder, reduced level of consciousness
RG	Female, 19 yrs Caucasian	1 in 500 8.82mg/ml	Seizures, movement disorder, fluctuating level of consciousness
PB	Female, 11yrs Caucasian	1 in 1500 40mg/ml	Seizures, movement disorder, neuropsychiatric features, dysautonomia

Table 4-2 Characteristics of clinical material used in experiments.

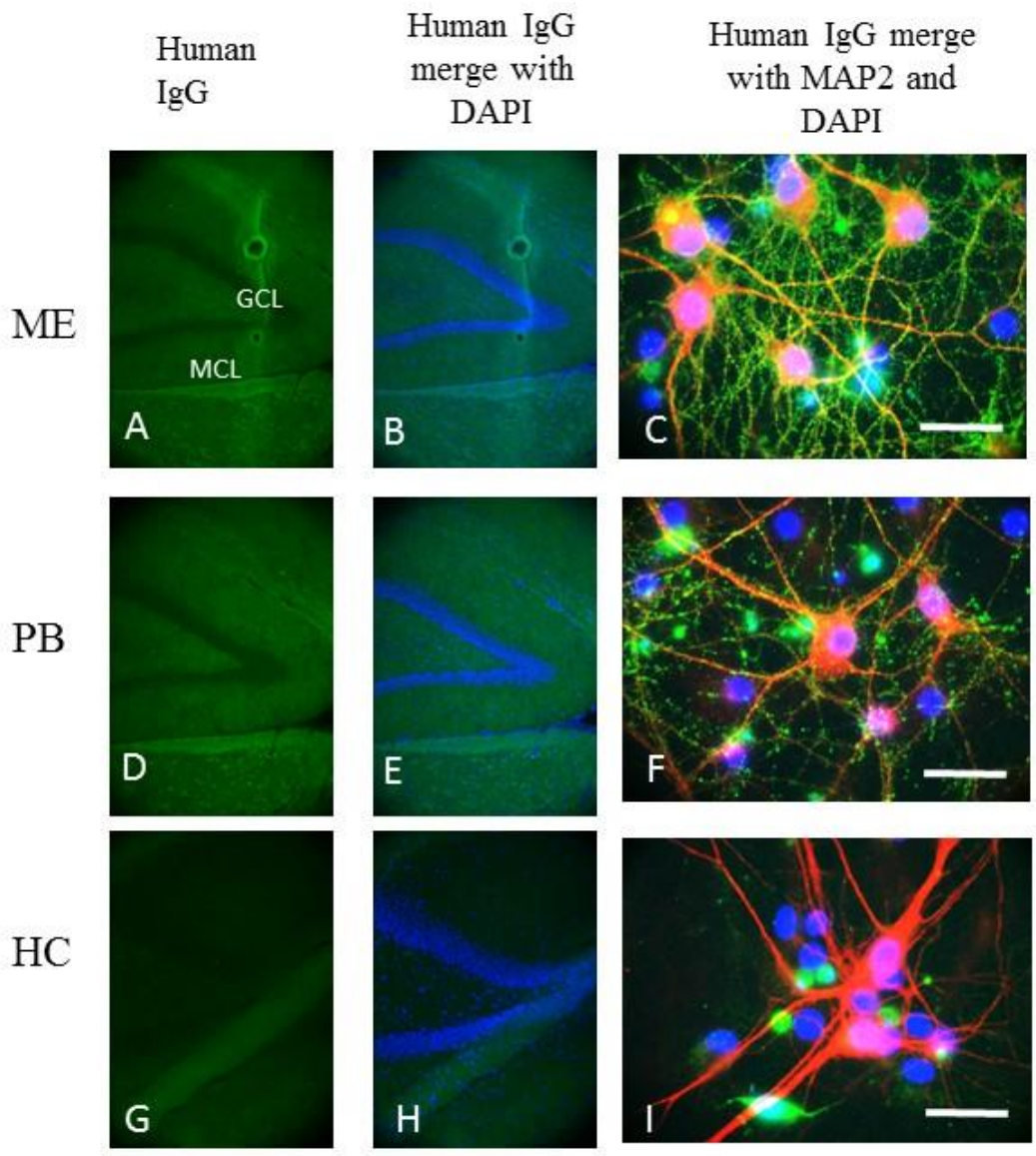

Figure 4-1 Characterisation of NMDAR-Ab positive IgG and HC IgG.

A-C. Patient "ME" IgG shows the characteristic binding of NMDAR-Ab IgG (green, A) of the dentate gyrus with sparing of the granule cell layer (GCL) and staining of the molecular cell layer (MCL) (B), on the hippocampus of a frozen rodent brain sagittal section. In C, binding of human IgG (green) to the surface of live hippocampal neurons (red, stained with MAP2) is shown in merge with DAPI (blue). Note the punctate human IgG binding indicating synaptic localisation of NMDARs. Scale bar 40µm.

D-F. Patient "PB" IgG shows a similar binding pattern as Patient ME on the frozen rodent brain section (D,E) and on the surface of hippocampal neurons (F).

G-I. The "HC" IgG however has no specific binding of the rodent section (G,H) and does not stain the surface of hippocampal neurons (I).

4.3 Experiment 1: Preliminary EEG recordings and analysis

To test the *in vivo* wireless telemetry system in C57BL/6 mice prior to the passive transfer of IgG into the left lateral cerebral ventricle, the preliminary experiment was performed by Dr Louise Upton and Lucasz Stasiak. Five days after implantation of the subcutaneous EEG transmitter, a 100 mg/kg i.p. injection of PTZ was administered to produce behavioural seizures that could be recorded.

The EEG recordings showed a stable baseline pre-injection (Figure 4.2A) as well as clear spike activity during the convulsive period (Figure 4.2B). Movement artefact was minimal despite the convulsions, confirming the stability of the wireless recording in freely moving mice. The power of oscillation in each of the seven frequency bands of the EEG (delta (1-4 Hz), theta (4-8 Hz), alpha (8-12 Hz), beta (12-30 Hz), gamma low (30-50 Hz), gamma high (50-70 Hz) and high frequency (70-160 Hz)) was determined using the Power Band Analysis (PBA) processor. This divides the EEG into 16 second intervals and determines the power in each of the seven wavebands defined above. The EEG showed increased power in the lower frequency ranges (1-4Hz, 4-8Hz, 8-12Hz, 12-30Hz) during the seizures after PTZ injection (Figure 4.2C, lower panel) compared to the time interval before the onset of convulsive seizure activity.

Having demonstrated the stability of recordings in convulsing and freely moving mice the battery life (operating life 3.6 weeks) of the wireless transmitters and the reliability of recordings following ICV injections was checked to ensure that the transmitter signal would not be disrupted by further intracranial surgery, and to optimize position of transmitters on the skull surface to enable access for ICV injections post implantation.

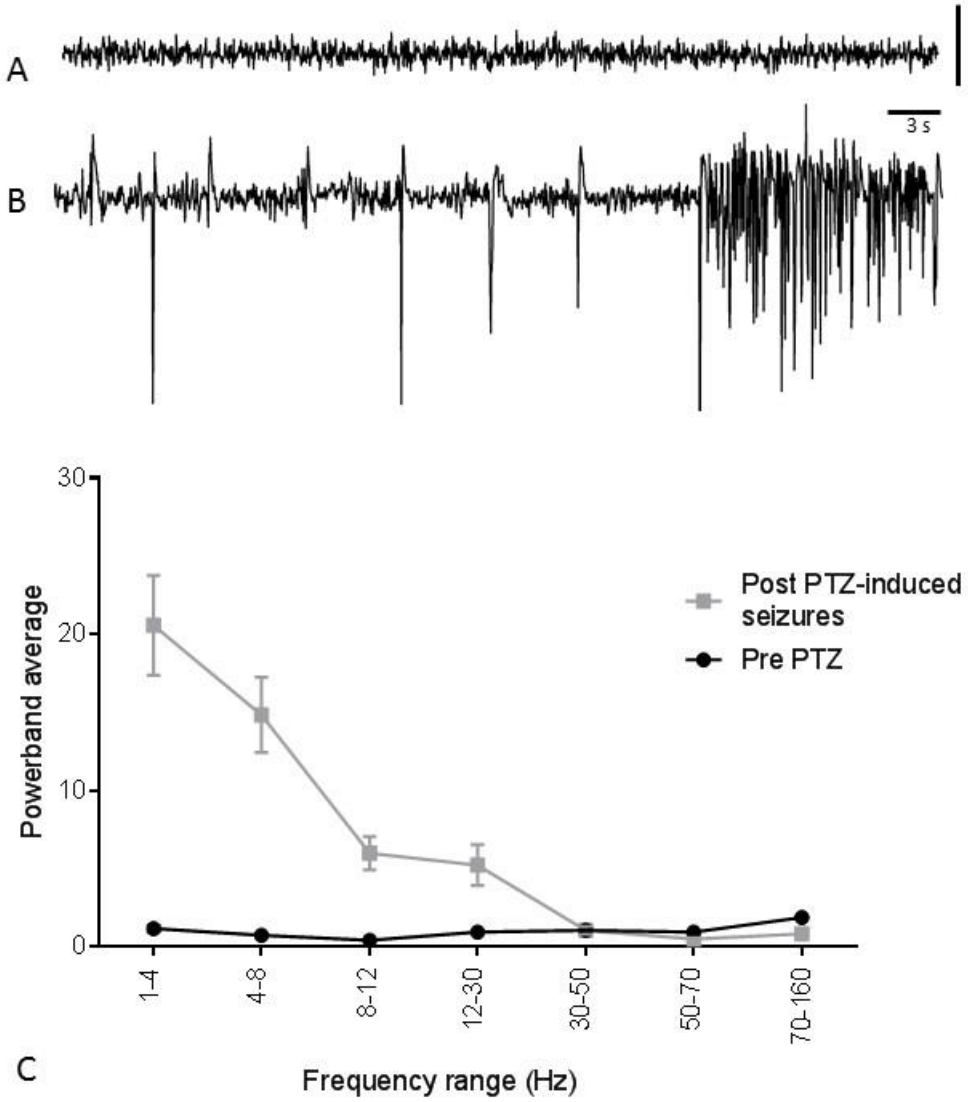

Figure 4-2 EEG telemetry and analysis of Experiment 1.

A. Example of EEG recording from cortex of mouse before the test dose of 100 mg/kg of PTZ. Note the stability of both the baseline EEG in a freely moving mouse, as well as when convulsive seizures are observed in B.
B. EEG recording example from mouse after PTZ induced seizures. Seizures started within 1 minute of PTZ injection with phenobarbital given after 14 minutes. The mouse had numerous (>15) Stage 3 seizures.
C. EEG power before the injection of PTZ (pre-PTZ) and after the onset of seizures induced by PTZ. There is an increase in power in the low frequency bands (delta 1-4Hz, theta 4-8Hz, alpha 8-12Hz, beta12-30Hz) reflecting the seizure activity observed.

4.4 Experiment 2: Long-term recordings of NMDAR-Ab and HC IgG injected mice to demonstrate stability and lifetime of implanted EEG transmitters

Eight C57BL/6 female mice were implanted with EEG transmitters and injected with NMDAR-Ab positive IgG (n=4) or HC IgG (n=4) ICV at Day 7 and 14 post implantation, with continuous recording of EEG over this period (Figure 4.3).

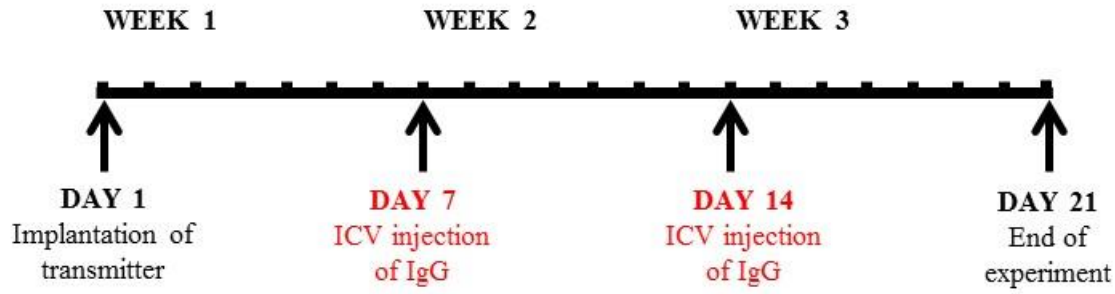

Figure 4-3 Experiment 2 animal weights and EEG recordings.
This schematic shows the timeline of procedures carried out in animals from Experiment 2.

In all IgG passive transfer experiments, the IgG was coded as "A" or "B" before injections so the experimenter was blinded. The procedures were well tolerated and there were no untoward effects in the mice, even after the ICV injections, as demonstrated by low distress scores using welfare score sheets (Appendix 2) throughout (<3/13). The mice showed stable weight gain over the three weeks, with any weight loss following a procedure regained over time (Figure 4.4).The screen shots of raw EEG taken from one animal in the HC IgG group (pink trace) in consecutive weeks of the experiment showed a reduction in the amplitude of the EEG recording over time (between Week 1 and Week 3, Figure 4.4 A,C). However this did not affect the analysis and reading of the raw EEG traces.

WEEK 1 WEIGHT EEG RECORDINGS

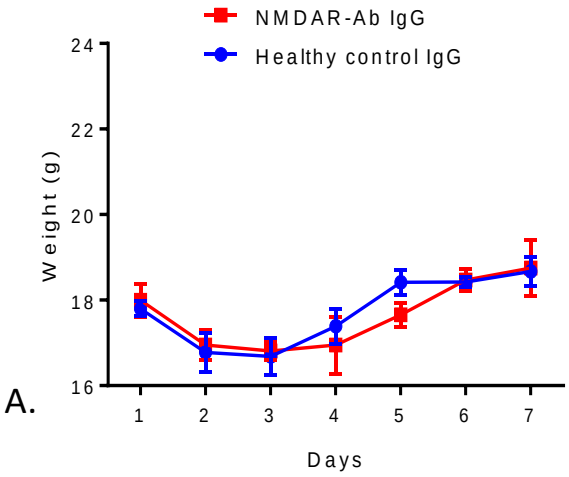

A.

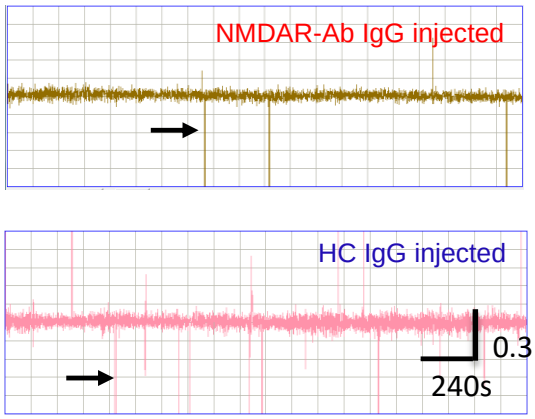

WEEK 2

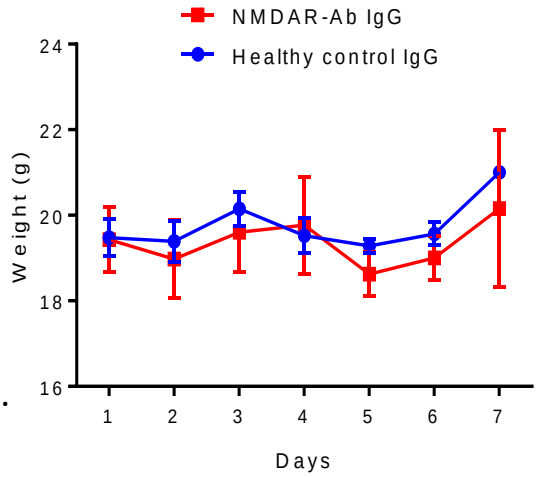

B.

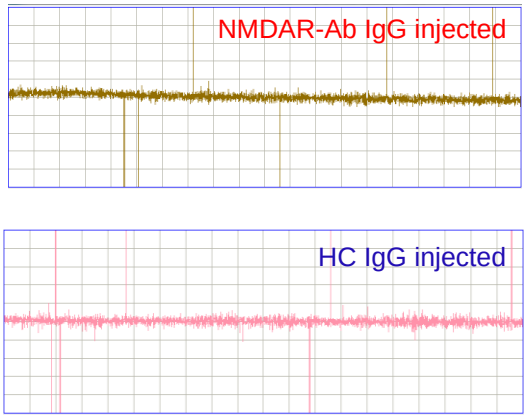

WEEK 3

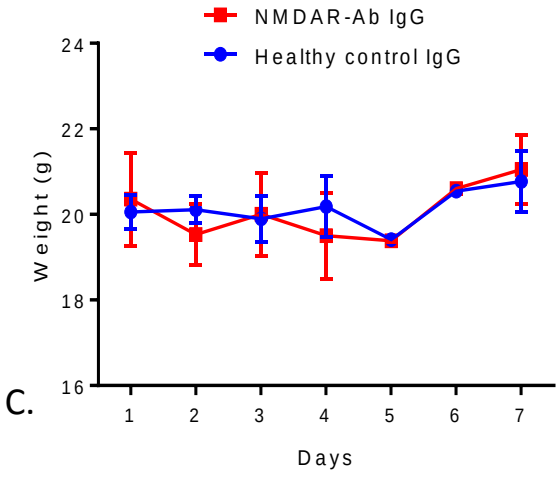

C.

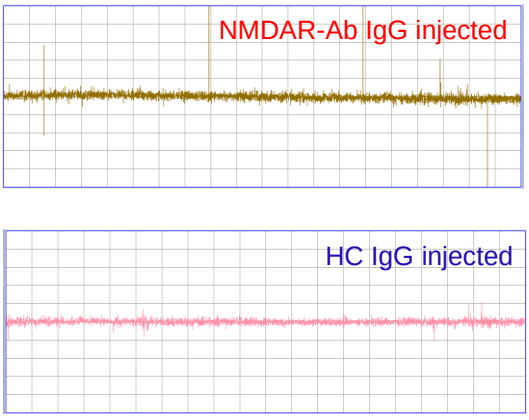

Figure 4-4 Experiment 2 animal weights (average of whole cohort) and EEG recordings.

A. In Week 1 the mice regain weight lost after transmitter implantation (Day 2-4). The initial raw EEG recording screenshots are taken from day 1 after implantation while the mice were still recovering from surgery, and show a larger overall amplitude of the EEG trace with some dropout of EEG signal (glitches, indicated by black arrows). All traces have the same time span and voltage calibration as shown.
B. In week 2 the animals recover weight lost after their ICV injection operation and the EEG has stabilised in terms of amplitude.
C. Week 3 is similar with continuing weight gain of the mice and stable EEG recordings. The brown trace is taken from a mouse that was injected with NMDAR-Ab in Week 2 and 3; the pink trace is from a HC IgG injected mouse.

Overall, the EEG recordings were stable in the freely moving mice of both groups with no deviations of the trace from the baseline. There was some signal dropout (glitches), indicated by the black arrows in the EEG recordings from Week 1 and Week 3 (Figure 4.4 A,C), despite this the reliability of the signal was very high.

In order to detect any effect the injection of NMDAR-Ab IgG may have had on the EEG recordings of the injected mice, the EEG was analysed initially for any changes in power within the seven different frequency wavebands. The lower frequency wavebands were of most interest as increased low frequency power was seen during the seizures induced by PTZ in Experiment 1. EEG power was averaged over 7 days (for Weeks 1, 2 and 3) for each transmitter used, and the two groups (NMDAR-Ab IgG vs. HC IgG) were then compared (Figure 4.5). In the first week post implantation of the transmitters there was no difference in the power band averages and all were low (Figure 4.5 A). Similarly, there was no difference in the power band averages in Week 2 (Figure 4.5 B). In Week 3, following the second ICV injection, both groups showed an increased power in the 1-4Hz frequency range compared to the preceding weeks (Figure 4.5 C). No spontaneous seizures were witnessed during Experiment 2. However, periods of observations were limited, with no continuous video and it is possible that occasional events were lost in the averaging.

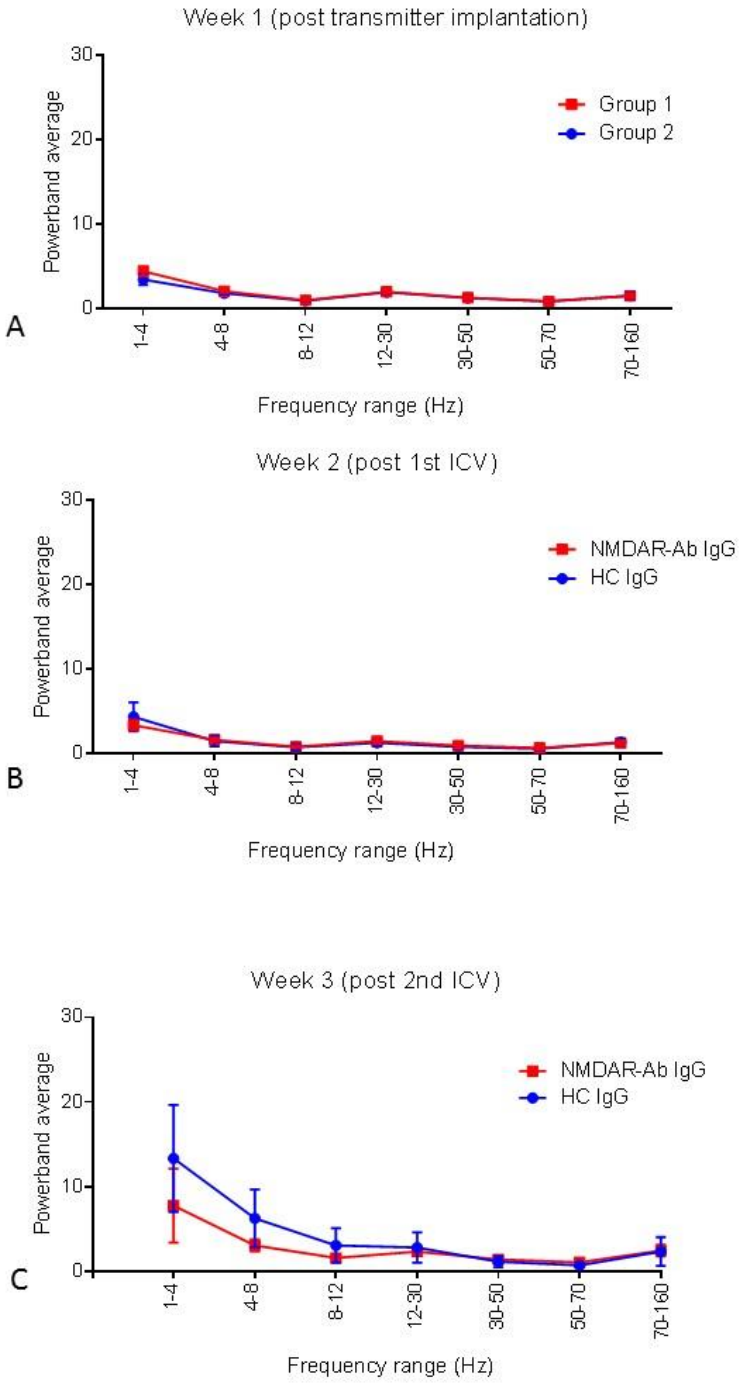

Figure 4-5 Power band analysis in Weeks 1 to 3 of animals in Experiment 2.

A. EEG power averaged over 7 days (week 1) following implantation of transmitters pre-injections of NMDAR-Ab IgG (Group 1) and HC IgG (Group 2).
B. EEG power averaged over 7 days following the first ICV injection of NMDAR-Ab IgG (red) and HC IgG (blue). There is no real change in the power spectrum in either group.
C. EEG power averaged over 7 days following the second injection of NMDAR-Ab IgG (red) and HC IgG (blue). There is increased power in the 1-4Hz frequency range in both groups after the second ICV compared to the previous two weeks.

4.5 Experiment 3: Optimisation of seizure susceptibility protocol

Given that spontaneous seizures might not be seen as C57BL/6 mice are relatively resistant to seizures (Ferraro, Golden et al. 1998, Ferraro, Golden et al. 1999), the next experiment looked at the seizure susceptibility of mice injected with NMDAR-Ab or HC IgG (coded as previously to reduce any observer bias) as a measure of neuronal excitability. PTZ at a subthreshold dose of 40 mg/kg was first tested as the proconvulsant for these experiments (Rajabzadeh, Bideskan et al. 2012). PTZ was injected into C57BL/6 mice that had no transmitters or ICV injections (n=2). The animals were then observed for 60 minutes and their behaviours were recorded (ethograms). Non-convulsive activity only, for example abdominal flattening and motionless staring (Stage 1), was seen following 40 mg/kg PTZ (Figure 4.6 A-B). The behavioural pattern was dose responsive as partial (Stage 2) and generalized (Stage 3) convulsive seizures were observed following injection of 50 mg/kg dose of PTZ (n=2, Figure 4.6 C-D). Therefore the 40 mg/kg dose of PTZ was an optimal subthreshold dose for seizure induction in experimental animals.

Six mice previously injected ICV with either NMDAR-Ab IgG (n=3) or HC IgG (n=3) were injected with 40-44 mg/kg PTZ and observed for 60 minutes by an observer blind to the IgG injected. As seen from the behavioural observations (Figure 4.7 A-D), after the unblinding, it appeared that implanted mice with either NMDAR-Ab or HC IgG injected were more seizure susceptible than the C57BL/6 mice who had not undergone surgery. Five of these mice (E4 to E8) had Stage 2 and Stage 3 seizures similar to, but even more severe than those seen in untreated C57BL/6 mice injected with 50mg/kg PTZ (Figure 4.6 C-D).

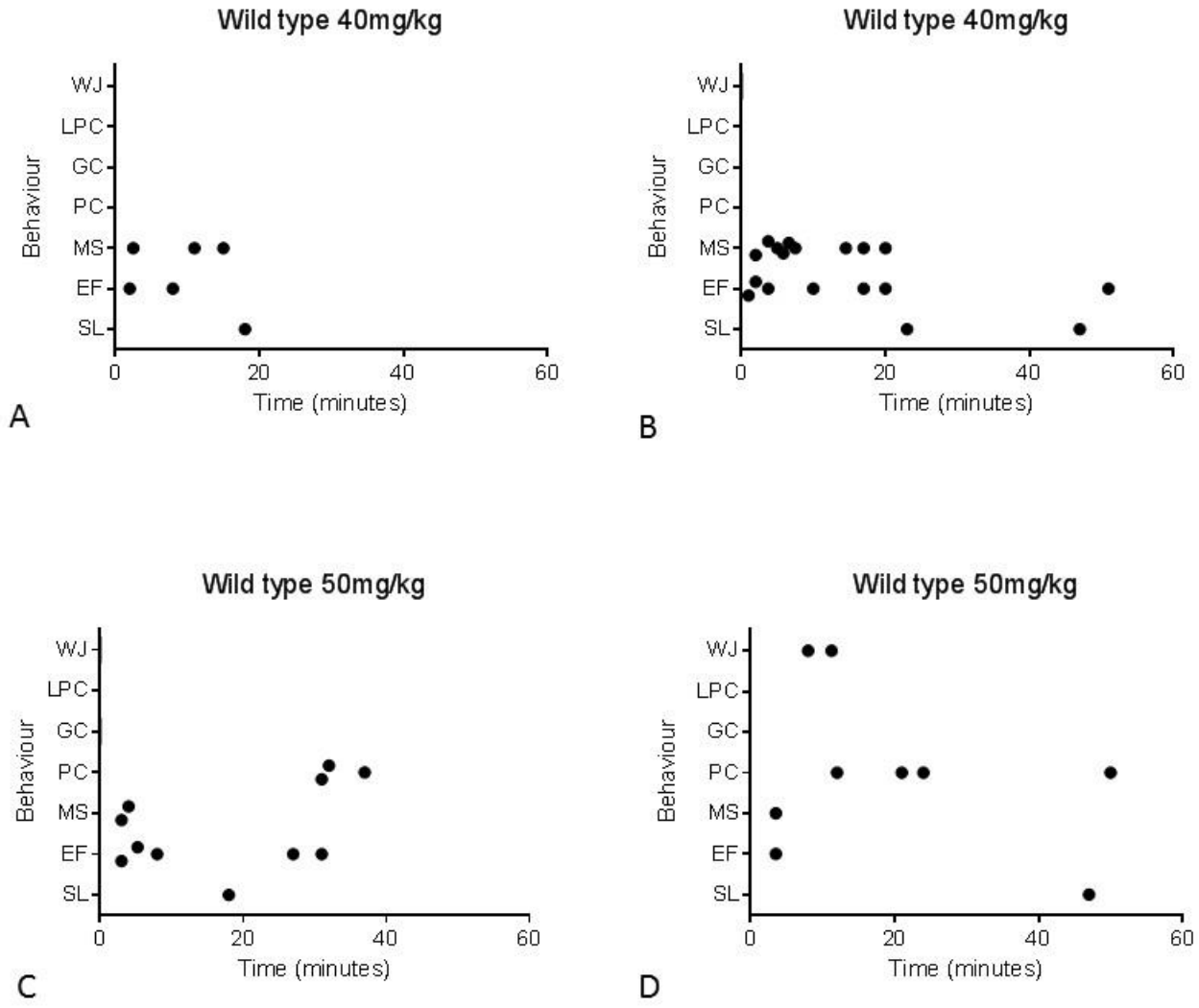

Figure 4-6 Ethograms of C57BL/6 mice post PTZ injections of 40-50mg/kg.

A-B. These ethograms show the seizures and behavioural change over the 60 minutes in two C57BL/6 mice following intraperitoneal (i.p.) injection of 40 mg/kg PTZ. Nonconvulsive activity (Stage 1) such as ear flattening (EF) and motionless staring (MS) associated with hypoactivity was seen followed by periods of sleeping (SL).

C-D. There were visible convulsive seizures seen (Stage 2) following a dose of 50 mg/kg PTZ in two C57BL/6 mice and these were mainly of the partial clonus (PC) type. Two Stage 3c seizures (WJ = wild jumping) were also seen in one mouse. Simple generalised convulsions (GC) and GC seizures associated with loss of postural control (LPC) were not seen.

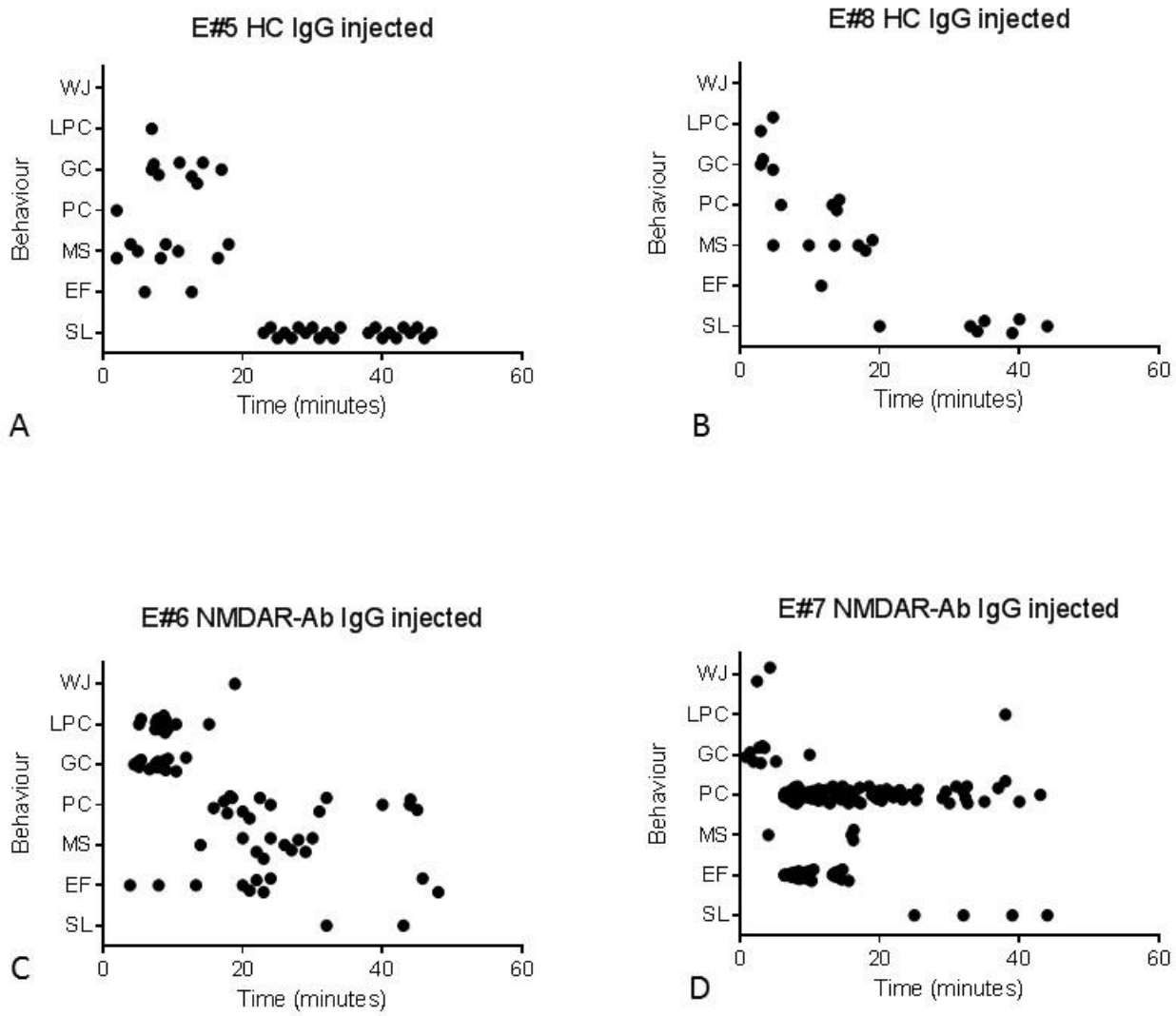

Figure 4-7 Ethograms of mice injected ICV with NMDAR-Ab or HC IgG before seizure induction with 40-44mg/kg PTZ

A-B. These two mice injected with HC IgG before seizure induction show Stage 2 and Stage 3 seizures similar to, but even more severe than untreated mice given 50 mg/kg PTZ.

C-D. Similarly, increased convulsive seizures are seen in NMDAR-Ab IgG injected mice as compared to mice with no prior surgery (Figure 4.6).

The median time latency to the first convulsive seizure was 1.5 minutes in the NMDAR-Ab group (range 0.9-4.5 mins); 2.5 mins in the HC IgG injected group (range 2-3mins) and 2 minutes in the un-injected mice given 50mg/kg PTZ (range 1-3 mins). Mice injected with NMDAR-Ab positive IgG had more stage 3 seizures (range 9-18) than the untreated mice and those injected with HC IgG (range 5-8) (Figure 4.8 A-B). The suggestion of increased epileptic activity induced in the NMDAR-Ab injected mice is illustrated in the raw EEGs shown in Figure 4.8 C-E. Here, the EEG recording for the hour following PTZ administration shows the increased spike activity in the NMDAR-Ab injected mouse (E#7) compared to the HC IgG injected mouse (E#8). These 'spikes' were seen with the convulsive seizures.

To determine whether the ICV injections had been correctly targeted, animals were culled 14 days after the last ICV injection, perfused with paraformaldehyde (PFA) and 50 micron sections were examined for the presence of long-lasting fluorescent beads injected with the patient IgG (Figure 4.9). The fluorescent beads were visible in the cortical tissue and corpus callosum with few beads lining the ventricle. Their position indicates a possible misplacement of the ICV injection. The same sections were stained with anti-human IgG antibodies to determine whether any human IgG remained bound to the brain tissue at the end of the experiment. Human IgG staining was minimal, which is not surprising given the time interval between passive transfer of human IgG and tissue analysis (14 days).

Table 4.3 gives a summary of the procedures and outcomes of the animals in Experiment 3, the first cohort of seizure susceptibility experiments.

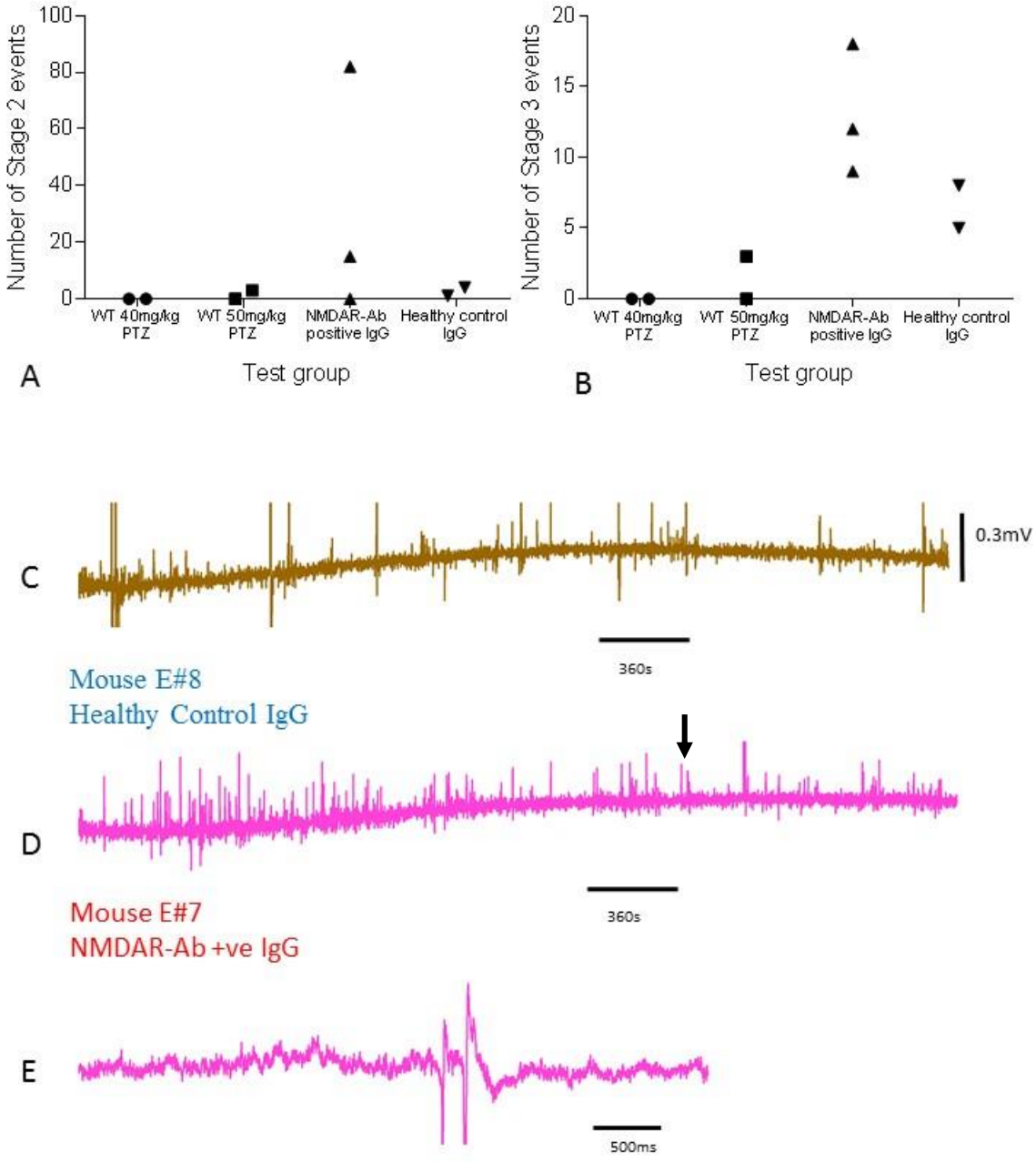

Figure 4-8 Comparison of seizure types and EEG traces in animals injected with NMDAR-Ab and HC IgG post PTZ

A-B. The first graph (A) shows that 2 out of 3 of the NMDAR-Ab injected mice had more Stage 2 seizures that those injected with HC IgG. The results for Stage 3 seizures (B) were similar.

C-E. 60 minute raw EEG recordings are shown from a HC IgG injected mouse (C, brown trace) and NMDAR-Ab injected mouse (D, pink trace) following an i.p. injection of 40mg/kg PTZ. There is increased spike activity in the NMDAR-Ab injected mouse compared to the HC IgG injected mouse. The black arrow indicates the expanded five second segment of EEG from mouse E#7 shown in E, clearly demonstrating the morphology of the spikes seen during the convulsive seizures.

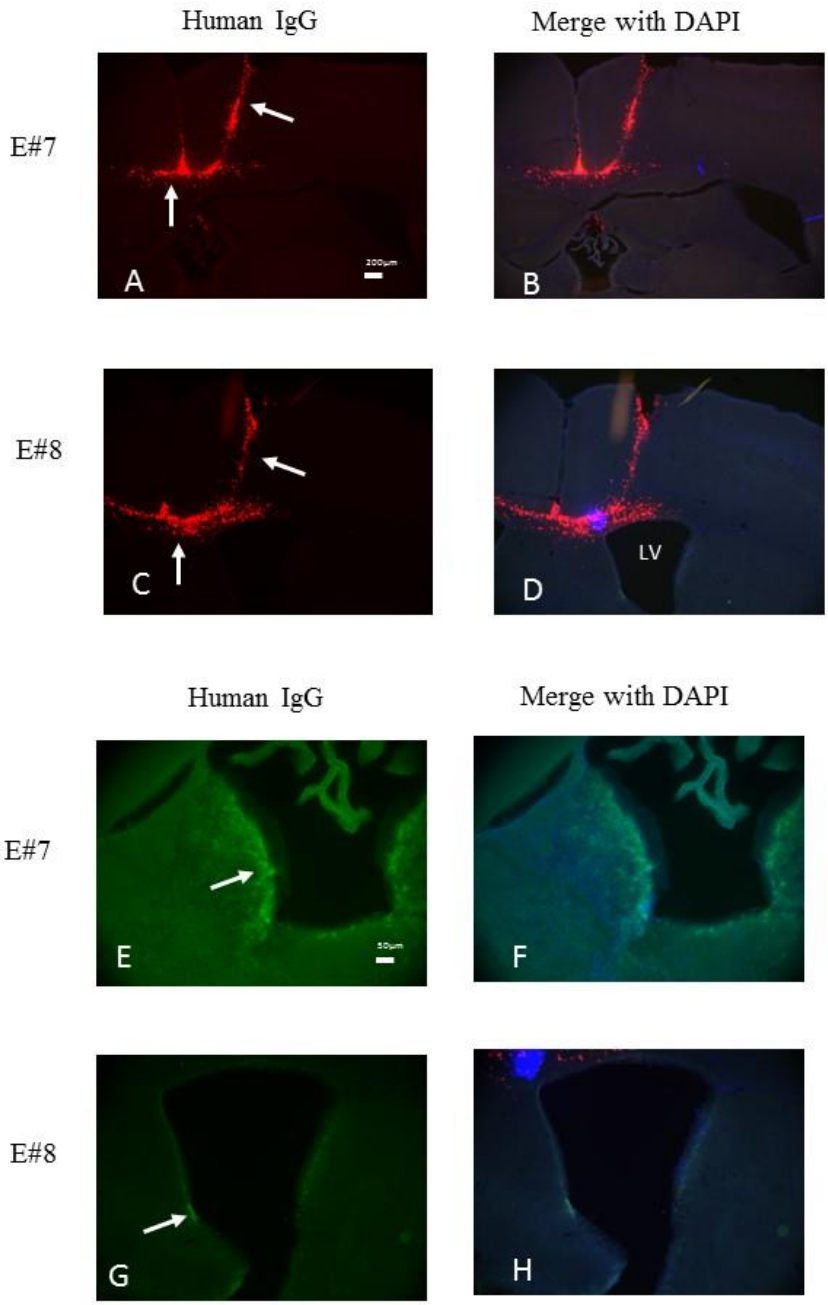

Figure 4-9 Preliminary immunostaining results of NMDAR-Ab and HC IgG injected mice.

A-D. The fixed 50 micron coronal sections of post-mortem tissue from the cortical injection site in mouse E#7 (HC IgG; A-B) and E#8 (NMDAR-Ab IgG; C-D) are shown. The fluorescent beads (red) are seen in the cortical tissue needle track and corpus callosum (white arrows) but not in the lateral ventricle (LV), the intended site of injection. At this magnification immunostaining with secondary anti-human IgG antibodies (green) is negative.

E-H. The periventricular regions of E#7 (E, F) and E#8 (G, H) are shown. There is some residual punctate positive anti- human IgG staining (green) in the periventricular region in both mice (white arrows).

Mouse ID	Date of transmitter implantation	Date of ICV	IgG injected	Date of seizure induction	Outcome of seizure induction	Problems identified
E#3	4/9/12	10/9/12 24/9/12	Healthy control	26/9/12	Death due to intra-abdominal bleed after PTZ	Animal died post PTZ injection due to intra-abdominal bleed (given higher dose of PTZ of 44mg/kg)
E#4	5/9/12	10/9/12 24/9/12	NMDAR-Ab positive	25/9/12	Increased seizure susceptibility SS 27	Only 24 hour interval between ICV injection and seizure induction
E#5	5/9/12	10/9/12	Healthy control	25/9/12	Increased seizure susceptibility SS 25	15 days between ICV injection and seizure induction
E#6	17/9/12	24/9/12	NMDAR-Ab positive	26/9/12	Increased seizure susceptibility SS 84	Given higher dose of 44mg/kg
E#7	18/9/12	24/9/12	NMDAR-Ab positive	26/9/12	Increased seizure susceptibility SS 200	?IgG injected into hippocampal tissue NOT ventricle
E#8	18/9/12	25/9/12	Healthy control	26/9/12	Increased seizure susceptibility SS 23	?IgG injected into hippocampal tissue NOT ventricle

Table 4-3 Details of procedures and outcomes of animals in Experiment 3.

Abbreviations; SS seizure score, PTZ Pentylenetetrazol, ICV intracerebroventricular, IgG immunoglobulin.

A number of problems were identified that required optimization;

- Two mice received a higher dose of PTZ (44mg/kg) than should have been administered as the weight of the transmitter (2.4g) was not subtracted from the total weight of the mouse when the dose of PTZ was calculated. One died post injection for unrelated reasons, the other had quite severe seizures.
- The interval between passive transfer of IgG and seizure susceptibility experiments was not consistent in this cohort of animals (range 24 hours to 15 days).
- The ICV injection may have been misplaced in some and when injected directly into tissue, a more severe phenotype was seen (E#7, Table 4.3).
- Prolonged interval between passive transfer and tissue analysis is likely to have hampered human IgG detection.
- PFA perfusion and 50 micron sections may not allow adequate penetration of secondary antibodies for detection of human IgG bound in vivo.

Given these inconsistencies it was difficult to compare the animals in each group (NMDAR-Ab IgG versus HC IgG) and for the next set of experiments an improved protocol was used (Figure 4.10A). Mice were implanted on Day 1, then injected with either NMDAR-Ab or HC IgG on Day 7. At least a 6 day interval was maintained between implantation of transmitter and ICV injection to allow the EEG recording to stabilise with enough battery life to cover the seizure induction period. Seizure induction was performed 48 hours after ICV injection in all animals. The dose of PTZ was kept strictly to 40mg/kg for each set of experiments. The observer for the 60 minute seizure induction period was always blind to the IgG injected. Fluorescent beads were used with each ICV injection to enable confirmation of injection site within the ventricle. Tissue was retrieved immediately after the seizure induction to preserve any

remaining bound human IgG for analysis and to preserve intracellular proteins that may be affected by increased neuronal excitability. Ice-cold PBS was used when culling at this stage to try and ensure only truly bound human IgG remained in the tissue not antibody that had been "fixed" in place. Processing of frozen tissue sections with the cryostat was used rather than the microtome to enable 12 micron section analysis to identify the intensity and spread of injected IgG.

The behavioural and EEG analysis results of these animals (Experiment 4), are presented in the following sections. Results of tissue analysis are contained in Chapter 5.

4.6 Experiment 4: Comparison of seizure susceptibility in NMDAR-Ab and HC IgG injected mice

Nine mice were injected with NMDAR-Ab IgG and six with HC IgG. In the NMDAR-Ab group, mice were divided into 3 groups each receiving a different patient NMDAR-Ab IgG (3 with RG; 3 with ME and 3 with PB). As previously, the procedures of transmitter implantation and ICV injection were well tolerated by the mice and after an initial drop their weights increased normally (Figure 4.10B). Analysis of the power spectrum revealed no change in EEG power of the seven different frequency bands pre and post ICV injection of IgG in both groups (NMDAR-Ab IgG versus HC IgG) (Figure 4.10C). It was therefore unlikely the mice were having multiple recurrent spontaneous seizures. Following this 48 hour period after ICV injection, seizure induction was carried out in line with the improved protocol (Figure 4.10A).

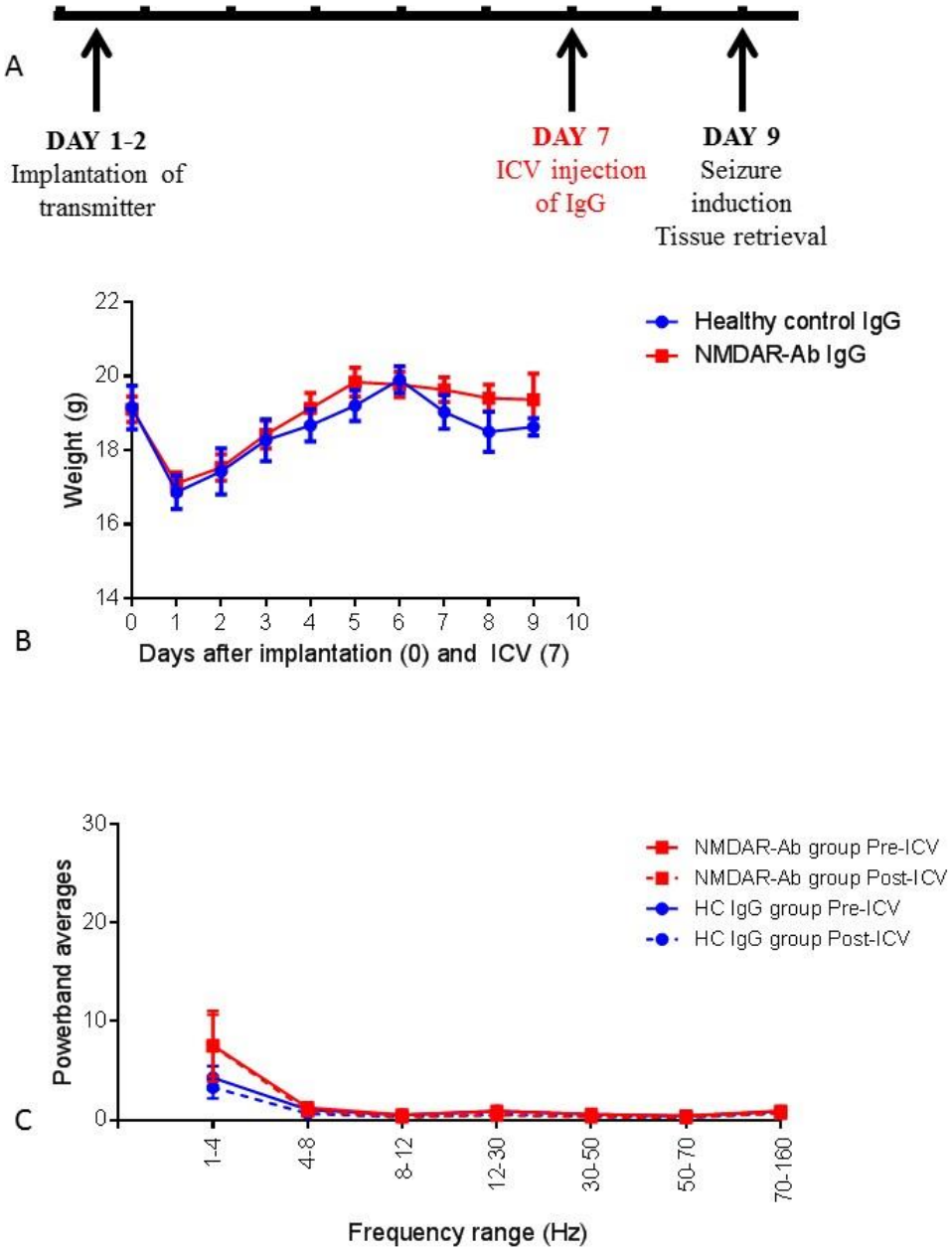

Figure 4-10 Experiment 4 protocol, animal weights and analysis of EEG power.

A. This schematic shows the improved protocol for implantation, ICV injection of IgG and seizure induction used in Experiment 4.
B. Despite the drops in weight gain following transmitter implantation (Day 0 on the graph) and ICV injection (Day 7 on the graph) the animals recovered their pre-operative weight by the end of the experimental period.
C. EEG power was averaged for the time period before ICV injection ('Pre-ICV', 5 days) and after the ICV injection of IgG ('Post-ICV', 2 days). There was no difference in either group (NMDAR-Ab and HC IgG injected) indicating multiple recurrent spontaneous seizures were not induced by ICV injection of IgG.

After 40 mg/kg of PTZ, all the mice, whether injected with NMDAR-Ab or HC IgG, experienced convulsive seizures as seen in the preliminary experiments (Figure 4.11 A-B). NMDAR-Ab injected mice showed a latency of 2.3 mins (range 0.97 – 6.18 mins) to the first convulsive seizure; in the HC-IgG injected mice, the latency was 7.45 mins (range 2.3 – 17.75 mins) which was not significantly different (p=0.09, ns) (Figure 4.11 C). However, significantly more NMDAR-Ab injected mice had Stage 3 seizures (the more severe): these were seen in *all* the NMDAR-Ab injected mice (9/9) compared to only 50% (3/6) of the HC IgG injected mice (Table 4.4; $p = 0.04$, Mann-Whitney).

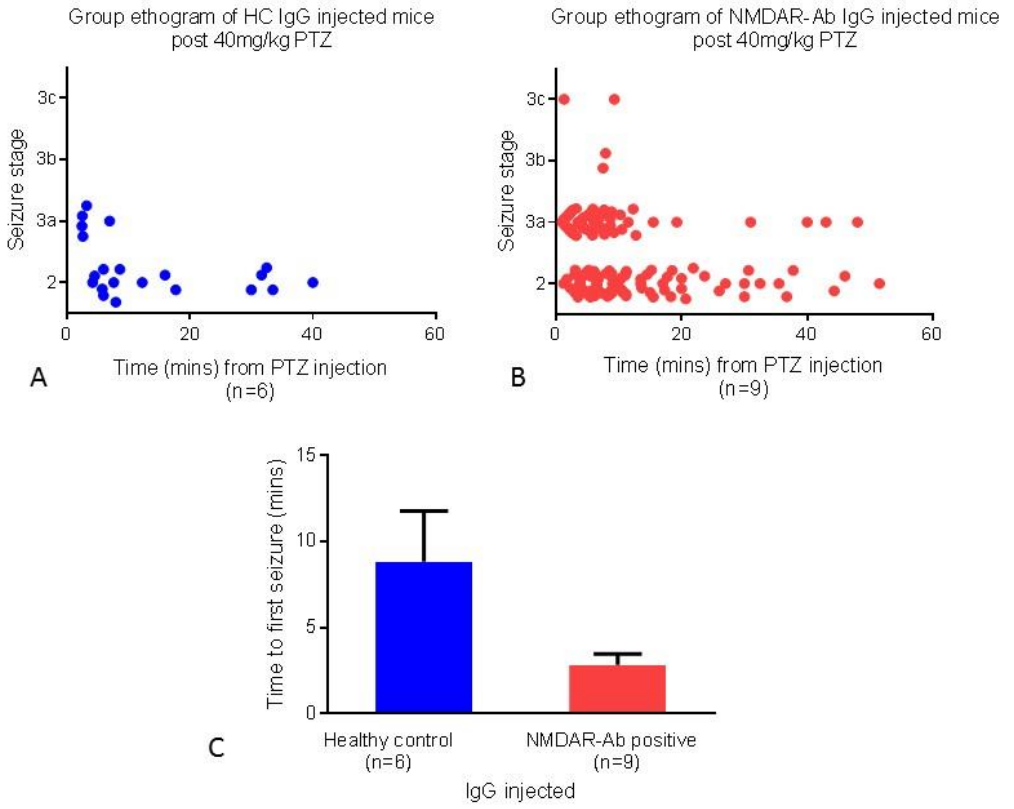

Figure 4-11 Group ethograms and seizure latency of animals in Experiment 4.

A-B. Group ethograms are shown for the mice injected with HC IgG (A; n=6)) and NMDAR-Ab IgG (B; n=9). There are more seizures seen over the 60 minute observation period in the NMDAR-Ab group, although there were also more mice in this group. Convulsive Stage 2 and Stage 3 seizures are seen in both groups (Seizure scale shown in Table 2.3)

C. The bar graph shows the time to the first convulsive seizure which is shorter in the NMDAR-Ab group, although this did not reach statistical significance (p=0.09).

Behavioural response to 40mg/kg PTZ	Healthy control IgG (n=6)	NMDAR-Ab IgG (n=9)
Stage 2 : partial clonus	4/6	6/9
Stage 3a: Generalised clonus with no loss of postural control	3/6	9/9*
Stage 3b: Generalised clonus with loss of postural control	0/6	1/9
Stage 3c: Wild jumping/running	0/6	2/9
Stage 4: Lethal seizure	0/6	0/9

Table 4-4 Comparison of behavioural response observed to 40mg/kg PTZ in NMDAR-Ab and HC IgG injected mice.

* p=0.04, Fisher's exact test

Mice injected with NMDAR-Ab IgG also had a significantly higher number of Stage 3 seizures (7.7 +/- 2.8 vs 0.8 +/- 0.4: p=0.003, Mann-Whitney; Figure 4.12 A) compared to mice injected with HC IgG. When analysed separately, the three NMDAR-Ab IgG groups (from patients ME/PB/RG) did show variability in the number of seizures seen (Figure 4.12 B-C). Overall, the NMDAR-Ab injected mice showed a significantly higher total seizure score (38 +/- 9.8 vs 7.5 +/- 1.7) calculated at the end of the 60 min observation period post PTZ injection, than the HC IgG injected mice (Figure 4.12 D; p=0.003, Mann-Whitney). Table 4.5 shows a summary of outcomes for this cohort and also illustrates the randomization of the mice to NMDAR-Ab (shaded rows) or HC IgG.

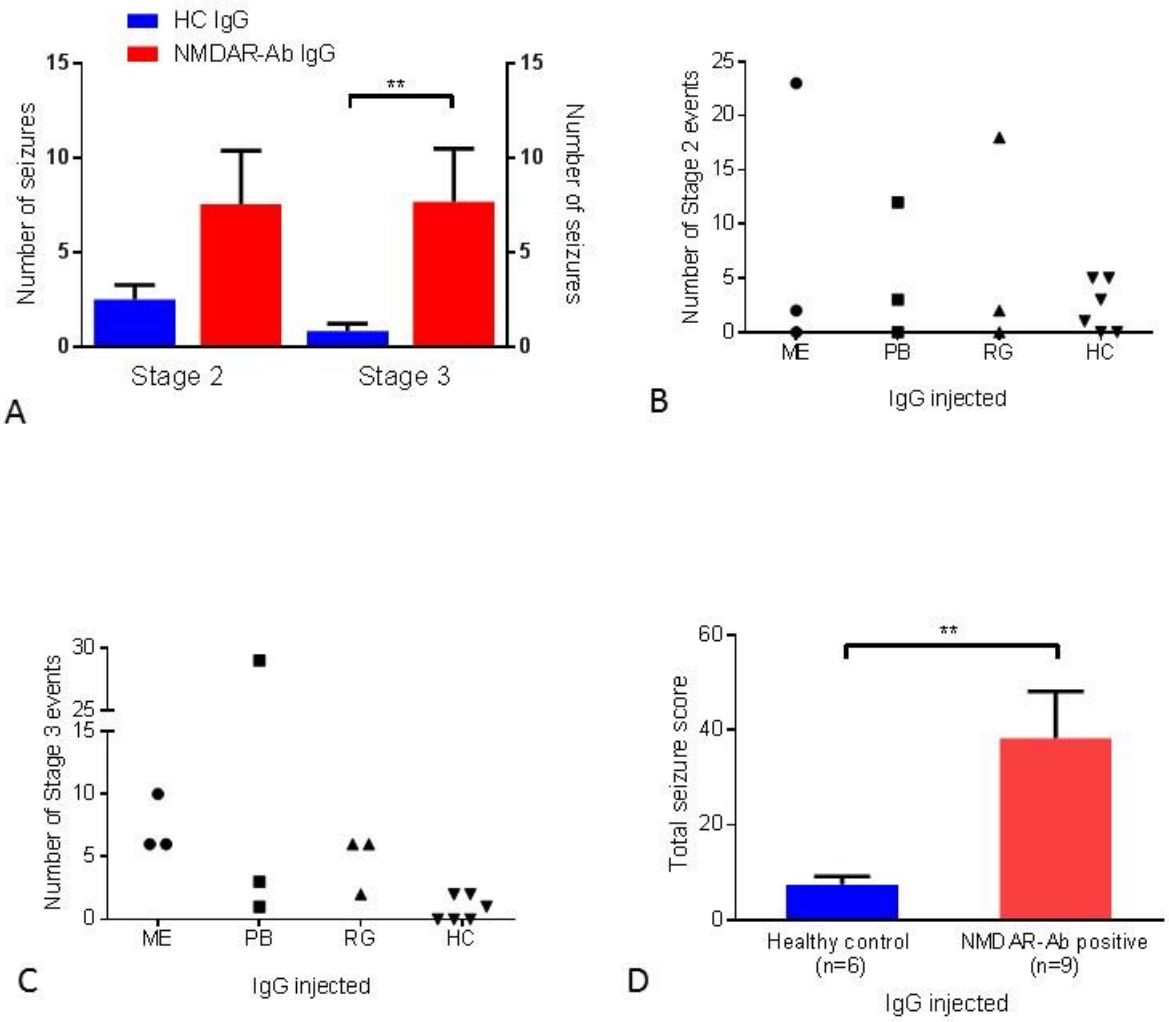

Figure 4-12 Comparison of seizure types and seizure scores between NMDAR-Ab and HC IgG injected mice in Experiment 4.

A. Graph of total number of Stage 2 and Stage 3 seizures in each group. Mice injected with NMDAR-Ab IgG (red) have more frequent and severe seizures compared to those injected with healthy control (HC) IgG injected mice (blue) following a sub-threshold dose of PTZ (40mg/kg).The number of Stage 3 seizures is significantly higher in the NMDAR-Ab IgG injected mice (p=0.0003, Mann-Whitney); a similar trend is seen with the number of Stage 2 seizures.

B-C. Plots to show number of Stage 2 and 3 seizures in relation to NMDAR-Ab IgG injected. The number of Stage 2 (B) and Stage 3 (C) seizures were variable with each NMDAR-Ab positive patient IgG Injected (ME/PB/RG); no single IgG proved more or less potent that the others overall. The number of seizures produced by the HC IgG was more consistent.

D. Graph to show comparison of total seizure score between the two groups. The total seizure score calculated over the 60 minute observation period following PTZ was significantly higher in the NMDAR-Ab IgG injected group (p=0.003, Mann-Whitney) compared to those injected with HC IgG.

Animal ID	Transmitter no.	Implanted	ICV injection	IgG	Seizure induction	No. of Stage 2 seizures	No. of Stage 3 seizures	Total SS
E#9	7	15/10/12	22/10/12	HC	24/10/12	0	2	6
E#11	10	16/10/12	22/10/12	NMDAR -Ab; ME	24/10/12	0	6	18
E#12	12	5/11/12	12/11/12	HC	14/11/12	1	0	2
E#13	10 (re-used)	5/11/12	12/11/12	NMDAR -Ab; ME	14/11/12	2	6	22
E#14	11	10/12/12	17/12/12	HC	19/12/12	4	1	11
E#15	12 (re-used)	10/12/12	17/12/12	NMDAR -Ab; ME	19/12/12	23	10	76
E#16	13	18/2/13	25/2/13	HC	27/2/13	2	0	4
E#17	14	18/2/13	25/2/13	NMDAR -Ab; RG	27/2/13	2	6	22
E#18	1	18/2/13	25/2/13	NMDAR -Ab; PB	27/2/13	9	1	21
E#19	2	4/3/13	11/3/13	NMDAR -Ab; PB	13/3/13	12	3	33
E#20	3	4/3/13	11/3/13	NMDAR -Ab; RG	13/3/13	18	6	54
E#21	4	4/3/13	11/3/13	HC	13/3/13	5	0	10
E#22	6	18/3/13	25/3/13	NMDAR -Ab; RG	27/3/13	0	2	6
E#23	5	18/3/13	25/3/13	NMDAR -Ab; PB	27/3/13	2	39	93
E#24	3 (re-used)	18/3/13	25/3/13	HC	27/3/13	3	2	12

Table 4-5 Details of procedures and outcomes of animals in Experiment 4.

Abbreviations: HC healthy control; ICV intracerebroventricular; ME/PB/RG patient IgG ID; SS seizure score.

4.7 Experiment 5: Pre-adsorption of NMDAR-Ab IgG

To confirm this increased seizure susceptibility was mediated solely by the NMDAR-Abs in the IgG preparation injected, an attempt was made to deplete the NMDAR-Abs by pre-adsorption. As a preliminary experiment to test the pre-adsorption protocol, before using the purified IgG that had been used in the ICV injections, the plasma (from which the IgG was initially purified) was used. Flasks of HEK cells transfected with

NR1 and NR2B were prepared as detailed in section 2.2.5. The NMDAR-Ab positive plasma was incubated with the NR1/ NR2B transfected cells to allow pre-adsorption of the specific antibodies to occur, as well as with un-transfected HEK cells as a control. There was a reduction in the retrieved plasma volume following the incubation with six aliquots of consecutive transfected NMDAR-Ab positive HEK cells, from 250 µl to 110 µl at the end of the experiment. Unfortunately, the pre-adsorption was unsuccessful (Table 4.6) and did not completely deplete the NMDAR antibodies in the plasma. Post pre-adsorption, the NMDAR-Ab positive plasma was still positive on the NMDAR-Ab CBA with a titre of 1 in 100.

CBA score at different titrations	Before pre-adsorption	NMDAR-Ab plasma POST pre-adsorption on NR1 transfected HEK cells	NMDAR-Ab plasma POST pre-adsorption on un-transfected HEK cells
1 in 20	2	2.5	2.5
1 in 100	1.5	1.0	1.5
1 in 500	1	0	0.5
1 in 2500	0.5	0	0

Table 4-6 CBA titrations of the NMDAR-Ab positive plasma on the NMDAR CBA before pre-adsorption, and post pre-adsorption on NR1/NR2B transfected and un-transfected and HEK cells.
Abbreviations; HEK human embryonic kidney, CBA cell-based assay.

The reduction in retrieved plasma volume was also a concern as the amount of purified IgG for ICV injection was limited. To address these problems, the in vivo effect of the NMDAR-Ab IgG was tested after dilution of the IgG tenfold. This would allow the pre-adsorption to be undertaken with more dilute IgG. The two mice injected with tenfold diluted NMDAR-Ab IgG showed no difference in seizure susceptibility from those injected ICV with tenfold diluted HC IgG (n=2) (Figure 4.13). The average seizure score of the mice injected with tenfold dilute NMDAR-Ab IgG was significantly lower

than the mice injected with undiluted NMDAR-Ab IgG, although the numbers in each group are small (4.5 +/- 1.5 vs 38 +/- 9.8); p = 0.05, Mann-Whitney).Therefore attempts to deplete diluted IgG preparations were abandoned.

In order to further prove the specificity of action of NMDAR-Abs, tissue staining techniques were used and shown in Chapter 5.

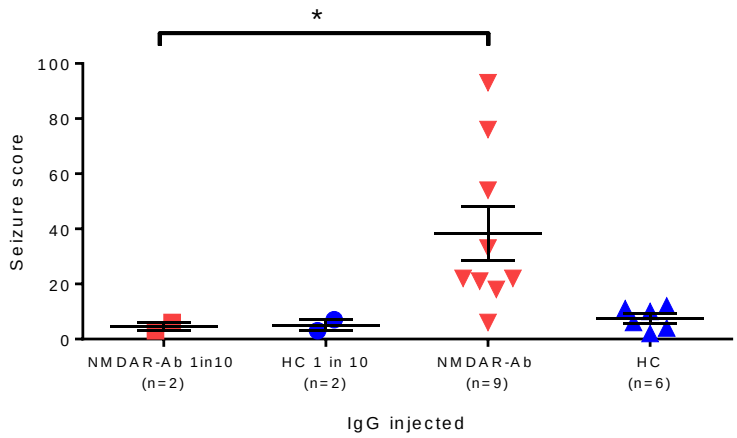

Figure 4-13 Effects of tenfold dilution of NMDAR-Ab IgG on seizure susceptibility.

The two animals injected with NMDAR-Ab IgG diluted tenfold (NMDAR-Ab 1 in 10) show a low average seizure score similar to the HC IgG injected mice from Experiment 4. There is a significant reduction in the average seizure score seen in the NMDAR-Ab IgG injected mice in Experiment 4 and those injected with the tenfold dilute preparation in Experiment 5 (p=0.05, Mann-Whitney).

4.8 Experiment 6: Effect of NMDAR-Abs over time in injected mice

In vitro work has shown that the internalization of NMDARs by NMDAR-Abs is reversible if the antibodies are removed (Hughes, Peng et al. 2010). Previous *in vivo* work carried out by Dr Phillippa Pettingill in this laboratory also showed a peak difference in cognitive testing between days 5-8 after ICV injection in mice injected

with NMDAR-Ab IgG, compared to HC IgG, with the cognitive deficit then returning to baseline by two weeks post ICV injection. In order to examine the time course of the effects of NMDAR-Abs on this model of seizure susceptibility, the Experiment 4 protocol was extended with two additional seizure susceptibility tests (Figure 4.14 A), seven and 14 days after the ICV injection. Four mice (E50, 51, 52, 53) were injected with NMDAR-Ab IgG (PB) and had seizure susceptibility testing with 40 mg/kg PTZ on Day 2, 7, and 14 post ICV injection. The animals tolerated the extended protocol well and regained weight lost after the two surgeries (Figure 4.14 B).

From seizure induction 1 (Day 2 post passive transfer) to seizure induction 2 (Day 7 post passive transfer), the median latency to Stage 2 seizures reduced from 7.2 mins (1-15.25 mins) to 2.28 mins (1.76-3.8 mins), although this was not statistically significant (p=0.49, Mann-Whitney; Figure 4.15A). The number of stage 2 seizures was not significantly different over time (Figure 4.15 B). However the number of stage 3 seizures significantly reduced by the third seizure induction (Figure 4.15C; p=0.02, Mann-Whitney). Overall, 3 out of four mice showed an increase in seizure score at Day 7 (Figure 4.15D). These results suggest the peak effect of the NMDAR-Ab IgG is most likely to be between 2 and 7 days post ICV passive transfer (Figure 4.15E). There could have been a contribution of a kindling effect at this stage after the second PTZ injection, even at the low dose of 40 mg/kg, but this is unlikely given that three out of the four mice showed a reduced seizure score after the third consecutive PTZ injection.

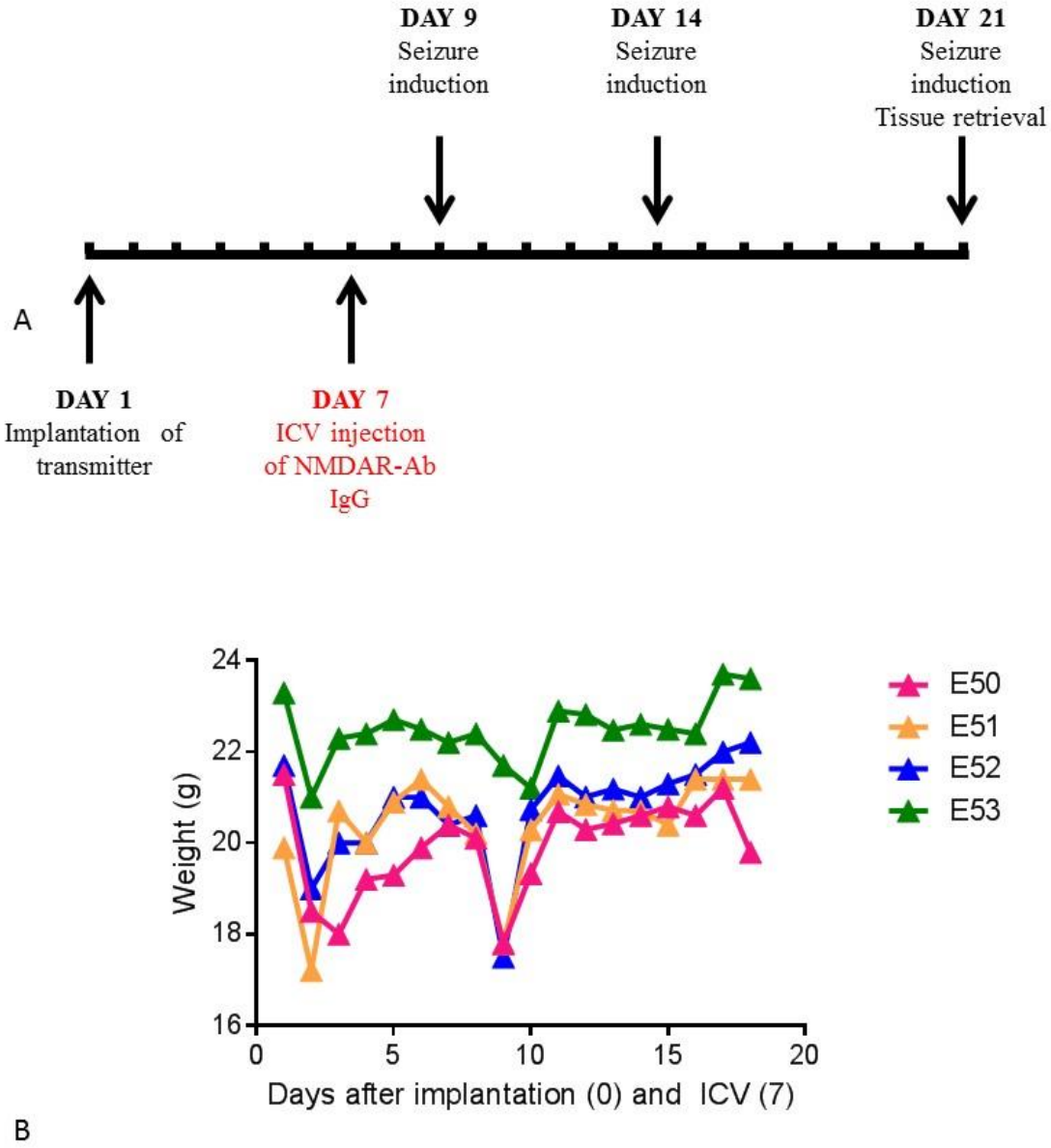

Figure 4-14 Experiment 6 protocol and animal weights throughout testing period.

A. Schematic showing the timeline of procedures for Experiment 6. The extension to this protocol from Experiment 4 is the two additional seizure induction tests at Day 14 and Day 21.
B. The graph shows the weight over time in the four animals tested in Experiment 6. The mice regained weight loss following the two procedures as seen previously in the other mice (transmitter implantation on Day 0; ICV injection on Day7). The additional seizure susceptibility testing did not appear to affect their overall well-being as weight gain continued to increase as expected in nearly all mice.

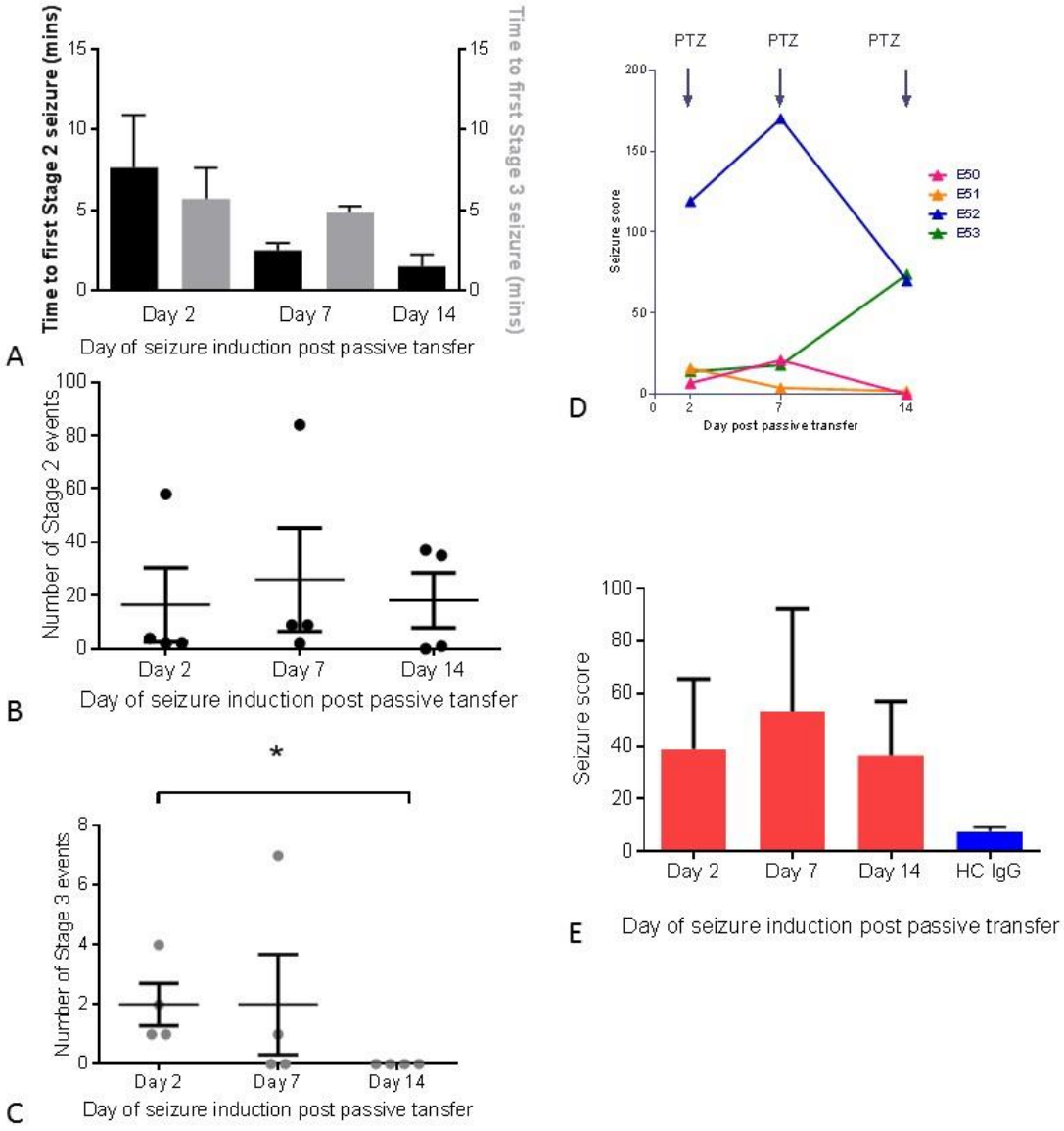

Figure 4-15 Seizure susceptibility of animals in Experiment 6.

A. Bar graph shows the time latencies to Stage 2 and Stage 3 seizures over consecutive seizure induction tests.
B. The number of Stage 2 events recorded in the observation period post 40mg/kg PTZ did not significantly change over time.
C. The number of Stage 3 events fell significantly between the 1st and 3rd seizure induction, with no animals having Stage 3 seizures in the 3rd seizure induction (p= 0.02, Mann-Whitney).
D. In this individual plot of subjects E50-53, three out of four mice showed an increase in seizure score at the second seizure induction. There was marked variability seen in the seizure scores within the group as seen with this IgG (PB) previously.
E. In the grouped bar chart (n=4), there is a peak of seizure score after the second seizure induction, the seizures scores of the HC injected mice (n=6) from Experiment 4 have been added as a comparison. This might correspond to the time of peak action of the NMDAR-Abs injected by ICV injection.

Analysis of EEG power in the seven different frequency wavebands showed a reduction in EEG power in the delta (1-4Hz) waveband in the 48 hour period following ICV injection of NMDAR-Abs (Figure 4.16A). The EEG power in this waveband was also averaged daily following the first seizure induction and showed a rise in power which peaked just before the second seizure induction (Figure 4.16B). This rise in power preceded the peak seizure score seen at the second seizure induction (Figure 4.15E). Power band averages are a fast but not very sensitive way to detect seizures and epilepsy as rare events will be lost in the averaging. The low frequency activity associated with seizures can also occur in normal behaviour. In order to further characterise the EEG and in particular to try and identify potentially epileptiform events, the Event Classification Processor (ECP) was used (section 2.2.5). The optimisation of this process and results of this analysis are detailed in section 4.9.

4.9 Optimisation of ECP and event libraries for seizure detection

To identify EEG patterns associated with particular behaviours EEG traces were manually screened looking for events/ EEG oscillations of potential interest. In some cases these correlated with observed behaviour from simultaneous EEG and video recording of experimental mice. Following this behaviour- EEG matching, we identified four main EEG patterns or “events” of interest (Figure 4.17) on which we based our first library. A “spikewave” was identified when the mouse was having a convulsive seizure. “Headshakes” were a behaviour frequently seen in mice injected with both NMDAR-Ab and HC IgG.

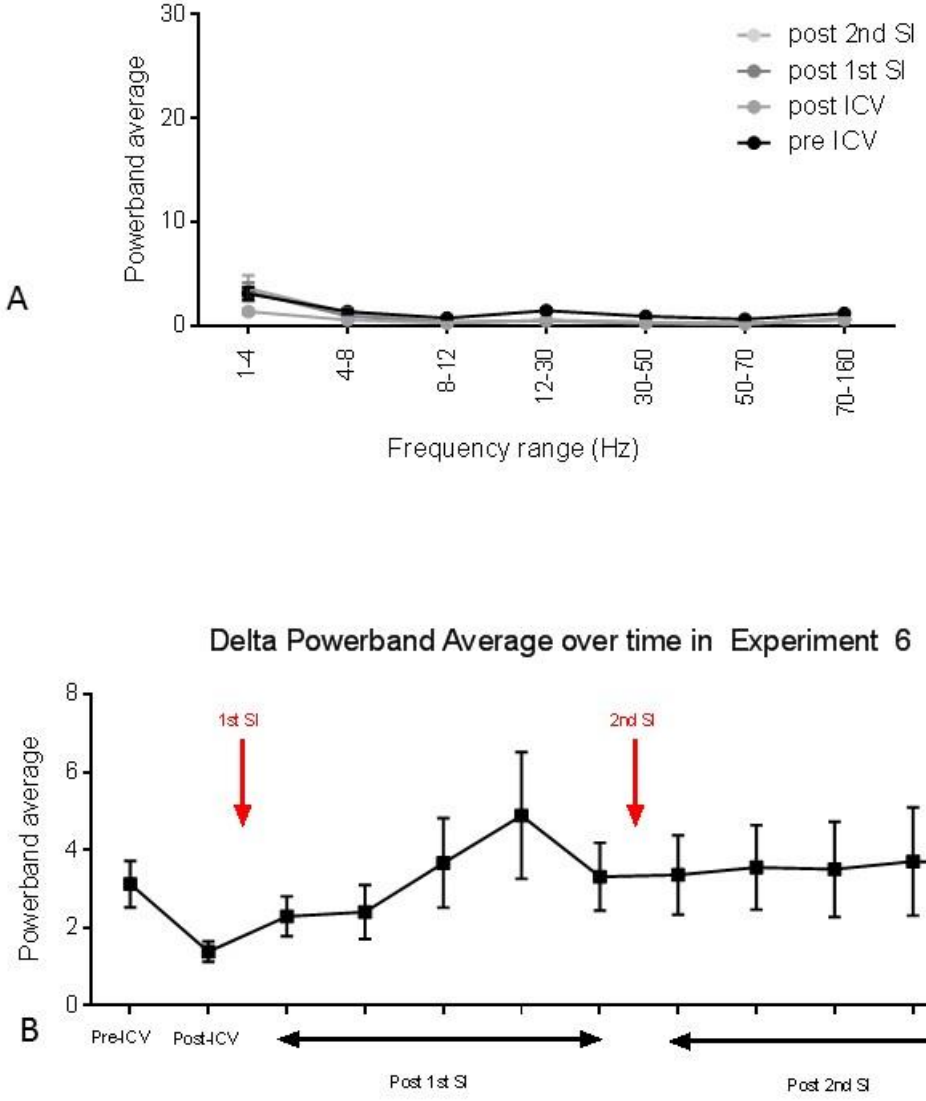

Figure 4-16 EEG power analysis for Experiment 6.

A. EEG power in all frequency wavebands averaged over experimental stage is shown here. There is a small drop in the EEG power of the low frequency band (1-4Hz) in the 48 hours following ICV injection (post-ICV). Following the first and second seizure induction (SI) there is no an overall change in EEG power in any of the wavebands analysed.

B. Separate analysis of the EEG power in the delta waveband (1-4Hz) is shown here. The Pre-ICV value is averaged over 5 days, the Post-ICV value over 2 days. The subsequent values represent average daily power in the delta waveband over time. There is a rise in the EEG power of the delta waveband following the first seizure induction which peaks just before the second seizure induction. Interestingly, 3 out of 4 animals were more seizure susceptible at this 2nd seizure induction.

"Delta" events were seen post-ictally in some mice but also when viewing interictal EEG. These were of interest due to the "extreme delta brush" pattern seen in some NMDAR-Ab encephalitis patients (section 1.3.2) and may have represented specific EEG changes induced by NMDAR-Abs in the injected mice. "Spikewave delta" was a spike wave within delta waves.

All these events were initially selected by visual morphology only and used to create a library (Figure 4.17 A). Six quantitative metrics were extracted for each segment of EEG containing an event by the Event Classification Processor (ECP): these were event power (EP); spikeyness (Sp); transient power (TP); high frequency power (HF); asymmetry (As) and Intermittency (Int). A full definition of these metrics is given in Table 2.2. Each event was therefore represented as a co-ordinate in 6-dimensional parameter space but plotted in 2D in Neuroarchiver for a visual representation (Fig 4.17 A). Similar events cluster together in these plots. In this initial approach many events were added to define boundary regions between event types. Some EEG intervals had an above-threshold event power and technically could be classified as an "event" but they did not have recognizable characteristic features and were deemed to be insignificant from simultaneously viewed video footage; they were classed as a 'no event'. Our final additional category named 'other' contained potential events that could not be matched to a particular behaviour. These were thought to be useful as general 'buffer' for all other categories of interest (Figure 4.17A). 'Events' files were then created for each hour of EEG data using the 'batch classification' tool in the ECP programme in Neuroarchiver. Each events file contained a list of 'events' detected for each transmitter within that hour.

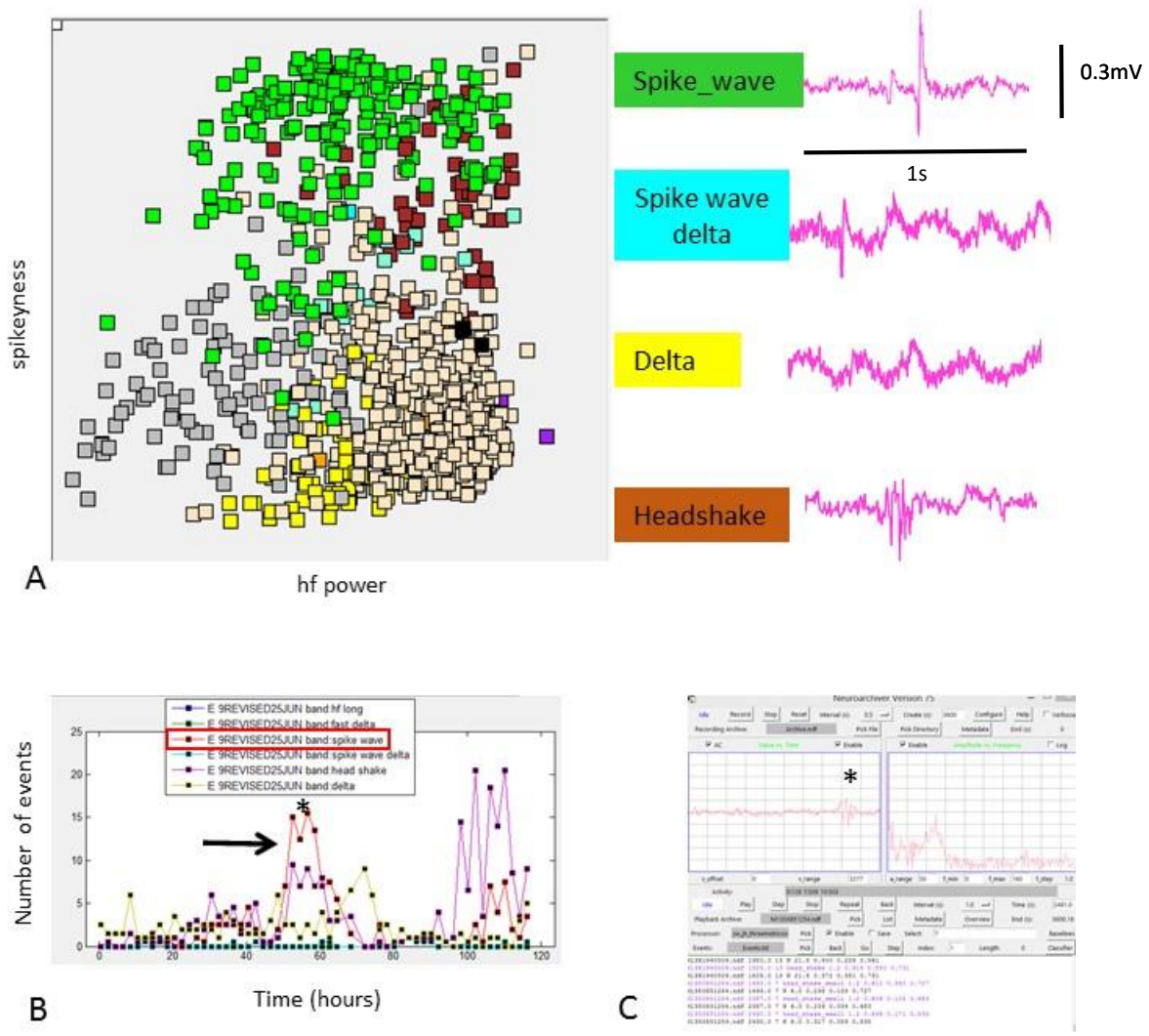

Figure 4-17 Library of events for seizure detection.

A. The plot shows a visual representation of the "event library", a screenshot taken from the Event Classification Programme (ECP) in Neuroarchiver. Each event type analysed are shown, i.e. spikewave (green), delta (yellow), spikewave delta (aquamarine) and headshake (brown), all are one second intervals. The additional categories are 'other' (grey squares) and 'no event' (peach squares). Each event represented by a small coloured square added to the library was defined by six metrics and plotted in 6 dimensional parameter space but shown with 2 metrics plotted (spikeyness vs hf power). Events of the same type cluster together as seen.
B. This shows the Matlab generated graph of number of events over time (hours). Each coloured line represents a different event. The red boxed event is 'spikewave' and in the graph it can be seen there is an unexpected peak of these events (black arrow*) *before* ICV injection (80-85 hours).
C. When the corresponding raw EEG data was analysed in the Neuroarchiver programme as see in this screenshot, these 'spikewave' events were headshakes (*). This indicates a high of risk of false positives in the detection of spikewave events with this library.

To facilitate analysis of these 'events' files, a group of Matlab routines developed by Joost Heeroma and K Zheng from UCL (Appendix 3) were used to define each animal, group animals according to the IgG injected and then compare events detected. The initial results were quite surprising in that many animals appeared to have 'spikewave' events identified even prior to the ICV injection (Figure 4.17B). However on interrogation of the raw EEG most of these spikewave events detected were headshakes (Figure 4.17B). This was concerning as a high false positive rate in the detection of potentially epileptiform events could lead to misinterpretation of the data.

To reduce the number of false positives identified as spikewave the metrics used to define these events were examined. There was a remarkable similarity between the metrics that defined the "spikewave" and "headshake" events (Figure 4.18A). The addition of many events to the library had also resulted in a huge overlap within metrics, thereby making it difficult to have specific defining metrics for each event. Both of these factors meant the detection of spikewave events, which was most important, was problematic with a high false positive rate. The results with the delta analysis also proved problematic and inconsistent. The event classifier was picking up mild rumbles of the baseline and not the delta waveform. In order to improve the accuracy of event detection, the metrics for the "best" examples of events were more strictly defined so that events that fell outside these boundaries could be eliminated. The "headshakes" were divided into "shakes_small" and "shakes_large" to help differentiate them from spikewave events. In terms of the metrics defining each event, we then found (Figure 4.18 B-E);

- "Delta" events have moderate EP (<0.6); low TP (<0.2); low spikeyness (<0.4)
- "Shakes large" have high EP (>0.8); high TP (>0.6); moderate spikeyness (0.2-0.7)

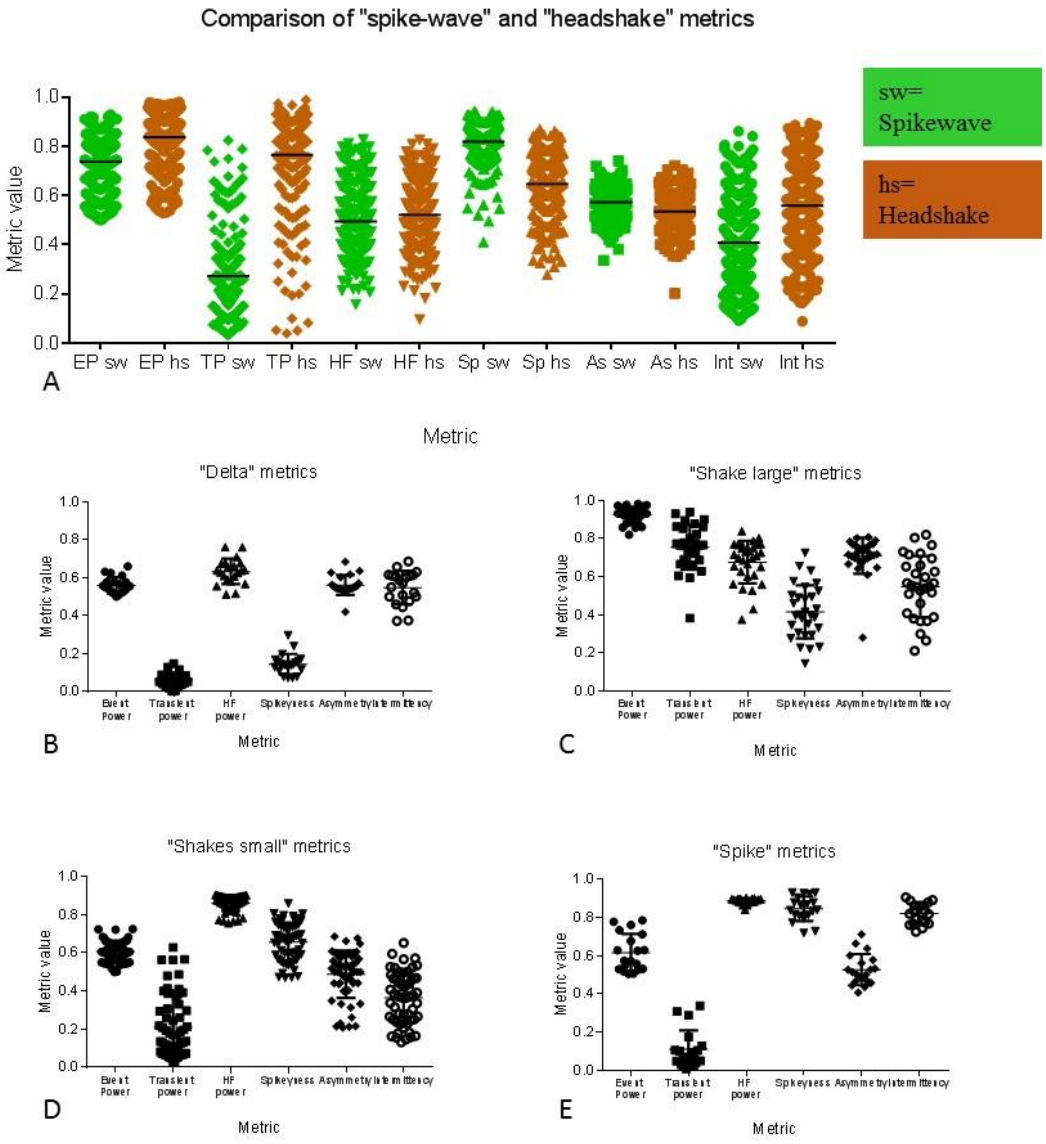

Figure 4-18 Optimisation of event detection.

A. This graph shows a comparison of the defining metrics used for two event types, spikewave and headshakes. The six metrics used to define an event are EP=event power, TP=transient power, HF= high frequency power, SP=spikeyness, AS=asymmetry, and INT=intermittency. The two events have very similar values and distributions of their metric values which made it difficult for the computer based programme to differentiate the two events clearly. This led to the high false positivity seen in detecting spikewave events.

B-E. These plots show the metrics for each event type when more carefully defined. The four events are now "delta", "shakes_small", "shakes_large" and "spikes" formally known as "spikewave". There is tighter clustering of the event metrics as those events on the boundaries of the defining metrics have been removed. There is still a similarity between small shakes and spikes but the intermittency metric is now the best differentiating metric.

- "Shakes small" have moderate EP (0.5-0.7); low TP (<0.6); high spikeyness (>0.5)
- "Spikes" have moderate EP (0.5-0.7); low TP (<0.3); high spikeyness (>0.8); high intermittency (>0.7)

The improved library with these selected events only is shown in Figure 4.19. Having the intermittency to differentiate the shakes small and spikes it was hoped that this would improve accuracy of event detection. The same EEG recordings were then run through the ECP again with this new library of events. Unfortunately the false positive rate remained high.

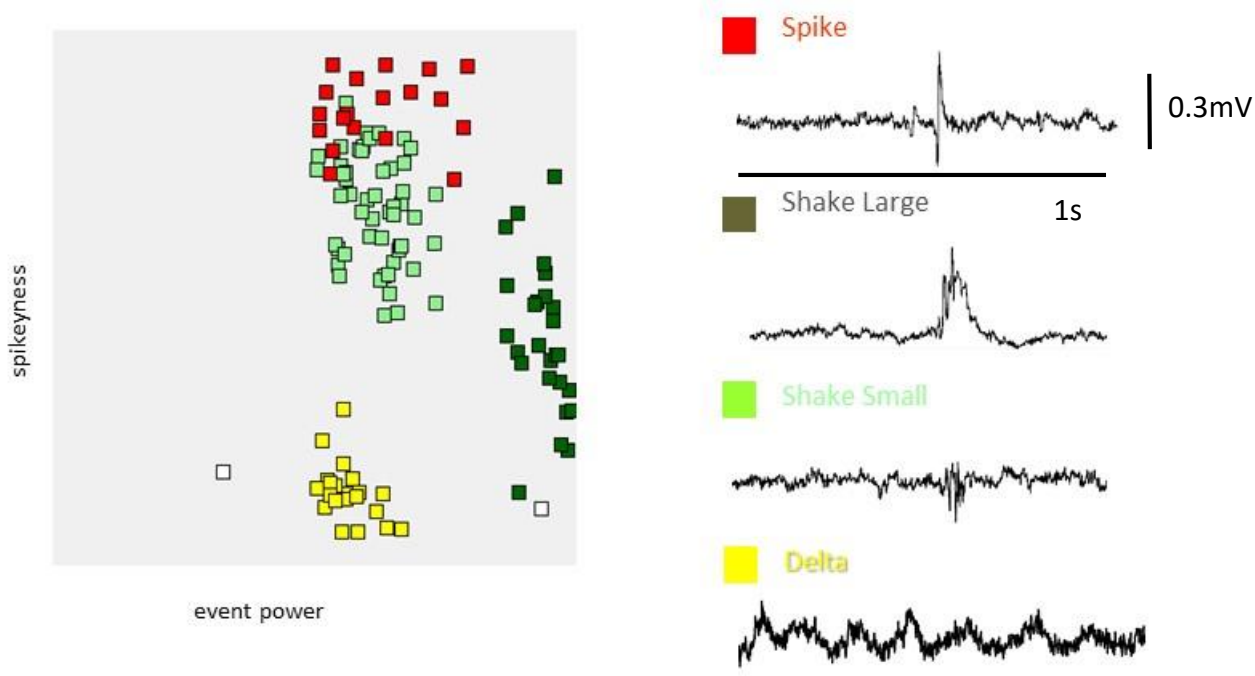

Figure 4-19 The improved library after optimisation of event detection.

This library (shown in the screenshot grey panel on the left) now has less but more well defined events. The groups of events are much smaller and cluster well. There is remaining overlap between shake small and spikes but spikes are now well differentiated from shakes_large.

The metrics were initially designed to pick up high frequency events as described in section 2.2.5. In this animal model, the EEG power in lower frequency bands seemed to be more important. With assistance from Kevan Hashemi (OSI), the ECP classifier was modified with the event power (EP) metric changed to measure the power between 2-100Hz rather than 4-160Hz. The high frequency (HF) metric was changed to detect band power within the 10-40Hz range as opposed to 60-160Hz. This processor was named ECP3. This processor gave more weight to the intermittency of high-frequency power which was the only metric that could separate the "shake_ small" events from the "spikes". These changes also meant that the metrics asymmetry, spikeyness and transient power became more useful in defining events. The border limits were reduced further and the 'match limit' function was used so that events that were within 0.1 distance of the best examples were included. If an event was more than a match limit (0.1) away from all other events in the library it was classified as 'unknown'. The risk of this strategy was the possibility that the unknowns would contain false negatives, but from previous analysis attempts, it was the false positives that needed to be avoided. The false positive rate was reduced to 10% which should enable detection of a 50% or 100% increase in spike rate, although more subtle spike events might be missed.

The delta wave detection was also modified with assistance from Dr Kevan Hashemi (OSI). Here, the detection of a delta event was based on the change in the power of low frequency oscillations over time and was processed in 8 second intervals as opposed to all the other events detected in one-second intervals of EEG (Figure 4.20). Previous attempts at detection of delta events contained many false positives of electrode problems and glitches. In this delta event processor (ECP4), a transient metric

Figure 4-20 Detection of delta events with ECP4.

The screen shot of the ECP4 library shows the delta events plotted as small yellow squares. Jumping to an event on the library list allows the user to see the event in the raw EEG panel as shown in the right sided screen shots. Two examples are shown (pink and green arrows). The EEG is seen with an 8 second interval within the viewer window containing the EEG traces. The Fourier transform of the EEG signal is displayed in the adjacent box of the EEG viewer panel. The black arrow indicates the peak of delta frequency resulting from the delta wave in the EEG. Detection of this signal in the 8 second interval formed the basis of the ECP4 processor.

was used to detect glitches and a periodicity metric to detect glitches and electrode problems at the same time. The results from ECP4 and ECP3 analysis of animals from Experiments 2, 4 and 6 are detailed below.

4.9.1 Headshake and delta events analysis of EEG data from Experiments 2, 4 and 6

The EEG data from animals in Experiment 2 (n=8; two ICV injections, no seizure induction), Experiment 4 (n=15; one ICV injection, one seizure induction), and Experiment 6 (n=4; one ICV injection, three seizure inductions) were processed using ECP3 and ECP4 to detect headshakes and delta events. The number of events were counted for each separate phase of the experimental protocol (for example Pre-ICV, Post-ICV) then averaged over the number of days to give an average daily event number. The numbers of 'shakes_small' and 'shakes_large' events were combined ('headshakes').

The average daily delta events in the animals of Experiment 2 were much higher in the NMDAR-Ab IgG injected group in all phases of the experimental protocol (pre-ICV, post 1st ICV, post 2nd ICV), although this difference was apparent in the animals even before the ICV injection of NMDAR-Ab IgG (Figure 4.21 A). The headshakes analysis in these mice showed an overall increase in event number over time in both groups, which may be a reflection of the increasing number of procedures carried out on the mice causing increased brain tissue irritability (Figure 4.21 B).

In the animals from Experiment 4, the analysis time between ICV injection and seizure induction was shorter, i.e. 36 hours. The baseline (Pre-ICV injection) average daily number of delta events was not significantly different between the NMDAR-Ab and HC IgG injected groups. There was a decrease in average daily delta events after the passive

transfer of IgG in both groups (Figure 4.21 C). The average daily number of headshakes showed a similar pattern to the animals in Experiment 2 with an increase after the second brain surgery (Figure 4.21 D).

Experiment 6 involved mice only injected with NMDAR-Ab IgG. In these mice, there was an initial decrease in delta events but this then increased in the interval between the first and second seizure induction (Figure 4.21 E); a similar pattern was seen with the average daily EEG power in the delta waveband rising between the first and second seizure induction (Figure 4.16 B). The average daily headshakes counts mirrored this pattern (Figure 4.21 F). Interestingly both values (average daily delta events and average daily headshakes) decreased between the 2nd and 3rd seizure inductions. This trend was also similar to the seizure scores over time in this group (Figure 4.15 E). Three out of the 4 mice tested had an increased seizure score in the second seizure induction on Day 7 post ICV. This seizure susceptibility had reduced by the 3rd seizure induction with a corresponding reduction in average daily headshake count and delta count.

4.9.2 Spike event detection as a measure of spontaneous seizure activity in Experiments 2, 4 and 6

In order to improve our detection of spontaneous seizures from power band analysis only, the ECP3 to detect ‘spike’ events as a marker of seizure activity was used. The batch classification tool as described in the methods was used to detect “spike” events in the periods before and after ICV injection but not including seizure induction periods.

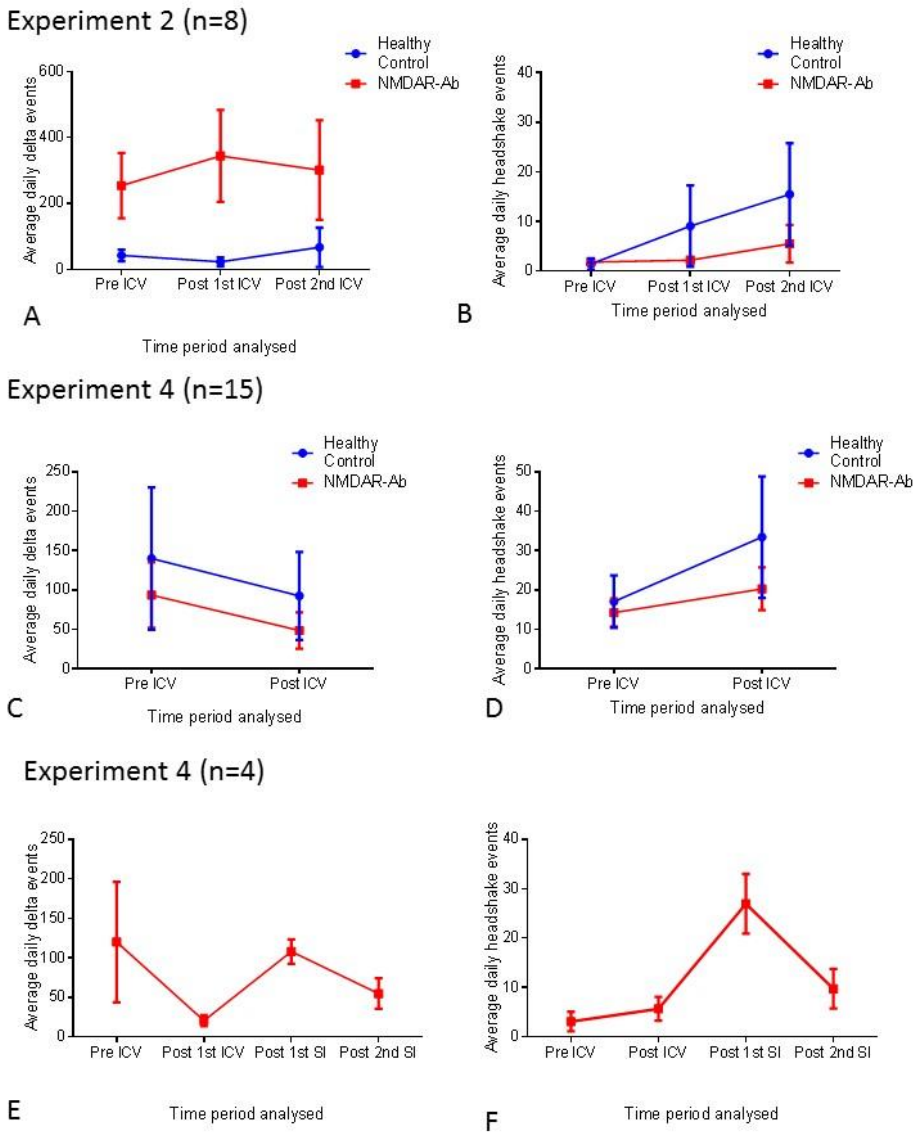

Figure 4-21 ECP3 and ECP4 analysis of headshake and delta events in Experiments 2, 4 and 6.

A-B. In Experiment 2 there seems to be a difference in the average daily delta events between the two groups even before the ICV injection; the headshakes increase over time in both groups.

C-D. Experiment 4 animals show a decrease in the average number of delta events before ICV compared to after the passive transfer. Headshakes increase over time as seen in Experiment 2.

E-F. Experiment 6 animals show similar changes in average daily headshake and delta events as the previous two Experiments (2 and 4).However, after the first seizure induction (SI) there is a steep increase in both delta and headshake events which is not sustained after the second seizure induction(SI).

(Pre-ICV is the time period between implantation of transmitter and before passive transfer. Post 1st ICV is the time period between the 1st ICV up to the 2nd ICV/PTZ seizure induction (SI). In cohort 3, post 1st SI is the time period between the 1st and 2nd seizure induction; Post 2nd SI is the time period between the 2nd seizure induction, up to the 3rd seizure induction.)

The results for Experiments 2, 4 and 6 using the ECP3 processor and event library were as follows;

- Spike detection revealed no recurrent spike events in the mice in Experiment 2, that received two ICV injections of either NMDAR-Ab or HC IgG. The only events picked up were, on visual inspection of the EEG trace, false positives, i.e. glitches in the EEG signal.
- In Experiment 4, there was the occasional spike event picked up outside the seizure induction period (Figure 4.22) in both groups of animals but these were rare and unlikely to represent recurrent spontaneous seizures.
- Experiment 6 revealed a similar pattern of detection as Experiment 4, with no spike events outside of the seizure induction times.

Given that very low numbers of spikes were detected by the processor, to check that it was picking up genuine events it was used to analyse the EEG recordings post PTZ of spike events in Experiment 4 mice. A combination, of computer-based detection and blinded observer counting, showed a significant difference in events between the NMDAR-Ab and HC IgG injected group: NMDAR-Ab IgG had a higher number of spike events (18 +/- 4.6 vs 7 +/- 2.8, p=0.02, Mann-Whitney; Figure 4.22 C).

From the experiments so far, it appears that passive transfer of NMDAR-Ab positive IgG caused an effect on neuronal excitability making the animals more seizure susceptible, but did not cause spontaneous seizures. The exact mechanism of this seizure susceptibility cannot be extrapolated simply from the *in-vivo* experiments. One possibility is that NMDARs on inhibitory interneurons are being selectively targeted by the antibodies, leading to a reduction in inhibition. To investigate this further, the techniques

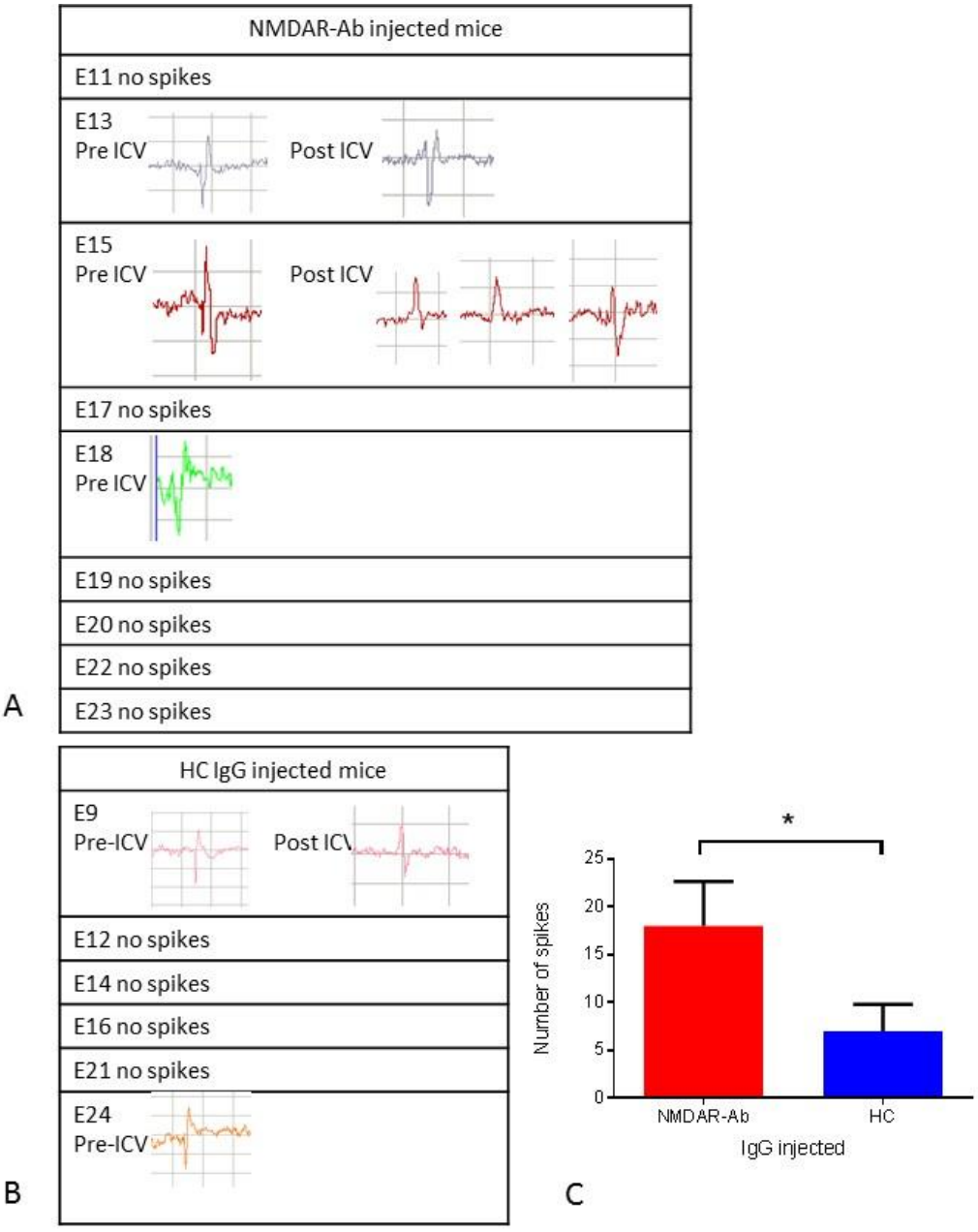

Figure 4-22 Spike event detection in Experiment 4 mice.

A. The number of spike events that were detected for each mouse injected with NDMAR-Ab IgG in Experiment 4 are presented here. The spikes in the seizure induction hours were not counted as we were specifically looking for evidence of recurrent spontaneous seizures. Three mice injected with NMDAR-Ab IgG had interictal spikes detected. Each animal had one pre-ICV injection and up to 3 post-ICV injection only.
B. Two mice in the HC IgG injected cohort also had spikes pre (2) and post ICV (1). These events are unlikely to represent recurrent spontaneous seizures.
C. This graph shows a comparison of the spike count in the seizure induction hours calculated by a combination of observer analysis and computer event detection. The NMDAR-Ab mice have a significantly higher number of spikes as reflected in their overall higher seizure scores (p=0.02, Mann-Whitney).

of optogenetics and *ex-vivo* electrophysiology were used. The results are presented in the following section.

4.10 Experiment 7: Optogenetic stimulation of recurrent networks as a test of interneuron NMDAR hypofunction

Previous work performed in the host laboratory (Dr Karri Lamsa; Dept of Pharmacology, University of Oxford) for this experiment had used the experimental paradigm described in section 2.2.9 for investigating interneuron NMDAR hypofunction and its effect on network-driven inhibition in the neuregulin overexpression mouse. It was hypothesised in our experiments that if there had been a "knockdown" of NMDAR receptors in the interneurons following injection of NMDAR-Ab IgG an impairment of recurrent inhibition might be seen.

A total of nine CAM-CreII $^{-/-}$ mice were first injected into CA1 with a viral vector encoding channelrhodopsin and YFP (AAV-ChR2-eYFP) (SW). Three weeks later to allow for viral infection and protein expression, ICV injections of NMDAR-Ab or HC IgG with fluorescent beads as previously, were performed (SW). These were coded IgG A and IgG B to ensure blinded ICV injections and patching of cells. Forty eight hours after ICV injection, mice were culled (SW) and brain sections harvested for *ex-vivo* electrophysiology (section 2.2.9)(LM). In 8/9 mice fluorescent beads were subsequently identified on postmortem visible in the lateral ventricle confirming correct position of the ICV. In 8/9 mice multiple cells expressing GFP were visible in the brain slices indicating that they had good levels of viral expression in the region of interest, CA1 (Figure 4.24 A). Successful cell recordings were obtained from 6/9 animals (all recordings performed by

LM). Recorded cells were filled with neurobiotin at the end of each experiment for visualisation of the cells with streptavidin-fluorophore. The exact morphology of all cells was examined using confocal microscopy to confirm they were pyramidal cells (Figure 4.24 B-C). On immunocytochemical analysis, two cells were not pyramidal cells, which gave a total of 5 cell recordings included from each group.

For the optogenetic experiments, the stimuli (5 pulses of fixed-spot 473 nm laser light stimulation in blue) were applied to activate glutamatergic axons in CA1, with recording of EPSCs and disynaptic IPSCs in CA1 pyramidal cells (section 2.2.9) (LW,SW). An example recording from an NMDAR-Ab IgG injected mouse is shown in Figure 4.25A. The NMDAR blocker DL-AP5 reduced the amplitude of the IPSCs but this was not completely abolished until the addition of NBQX which caused a full blockade, confirming their disynaptic origin (Figure 4.25B). The DL-AP5 suppressed the recurrent IPSCs in both the NMDAR-Ab and HC IgG injected mice as expected. However there was no difference in the magnitude of this reduction between the groups (0.79 +/- 0.04 versus 0.78 +/- 0.07, p=0.8; Figure 4.25 C-D). Similarly, there was no difference in the peak amplitude of the IPSCs between the two groups (0.82 +/- 0.04 versus 0.87 +/- 0.06, p=0.4; Figure 4.23H). These results, in limited cell numbers, show there was no difference in the NMDAR mediated component in recurrent inhibition between mice injected with NMDAR-Ab or HC IgG. This could be explained by the limited cell numbers resulting in the possibility of underpowered analysis, a lack of effect of NMDAR-Abs on interneuron function, or failure of passive transfer. The optogenetic stimulation protocol worked well. The lack of effect was disappointing given the neuronal network effect seen in vivo. The effectiveness of passive transfer by ICV injection was further explored by analysis and measurement of IgG

reaching the brain parenchyma by immunostaining of post-mortem sections. These results are contained in Chapter 5.

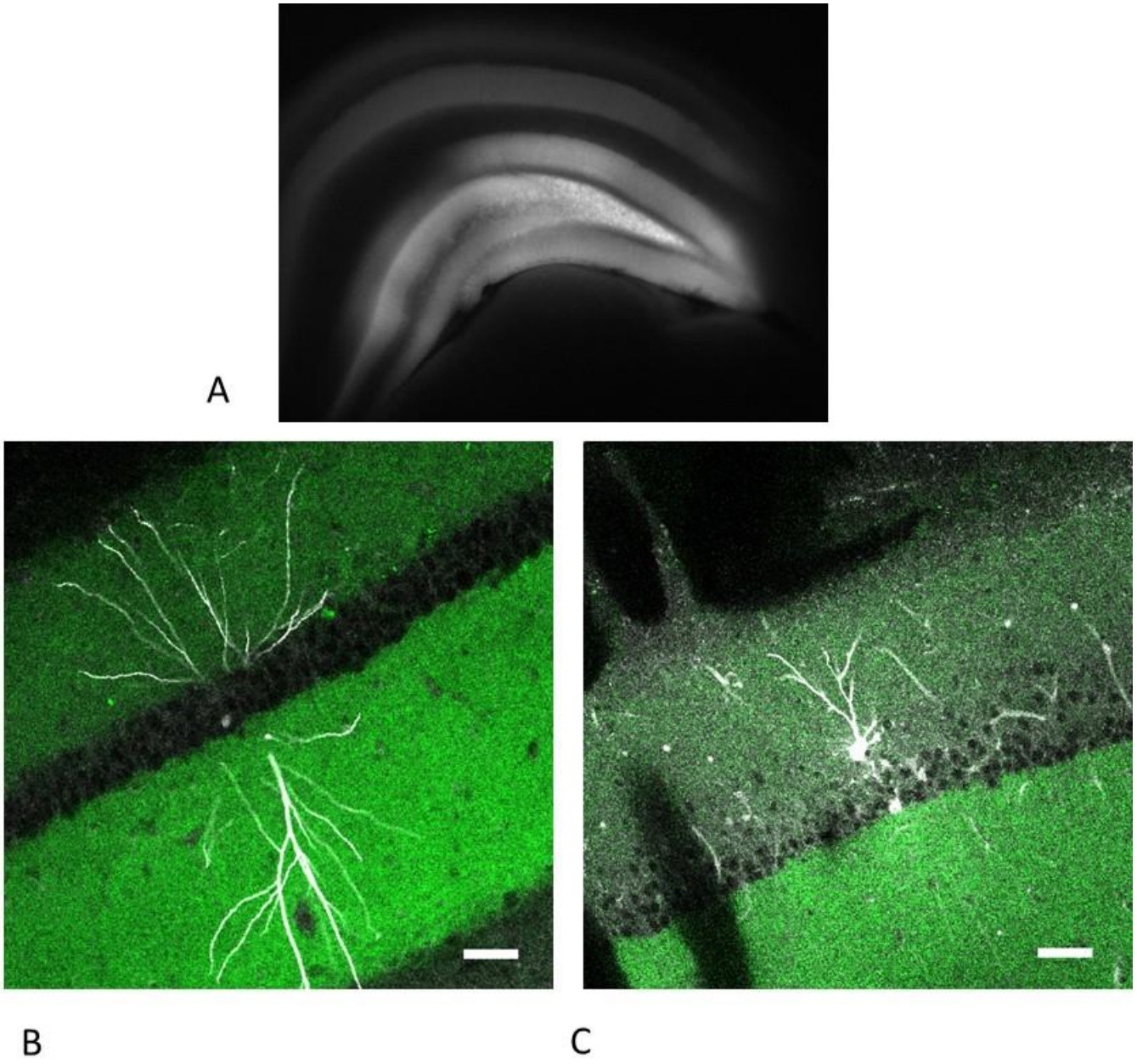

Figure 4-23 GFP expression and immunostaining of ex-vivo mouse brain slices

A. This sagittal 60 µm ex-vivo slice of the hippocampus show the expression of YFP expressing cells throughout the hippocampus, including in the CA1 region where the viral vector was injected (white staining).
B. A pyramidal cell confirmed by morphology in post-hoc analysis of neurobiotin filled recorded cell. Scale bar 50 µm.
C. A basket cell identified here was excluded from the analysis. Scale bar 50µm.

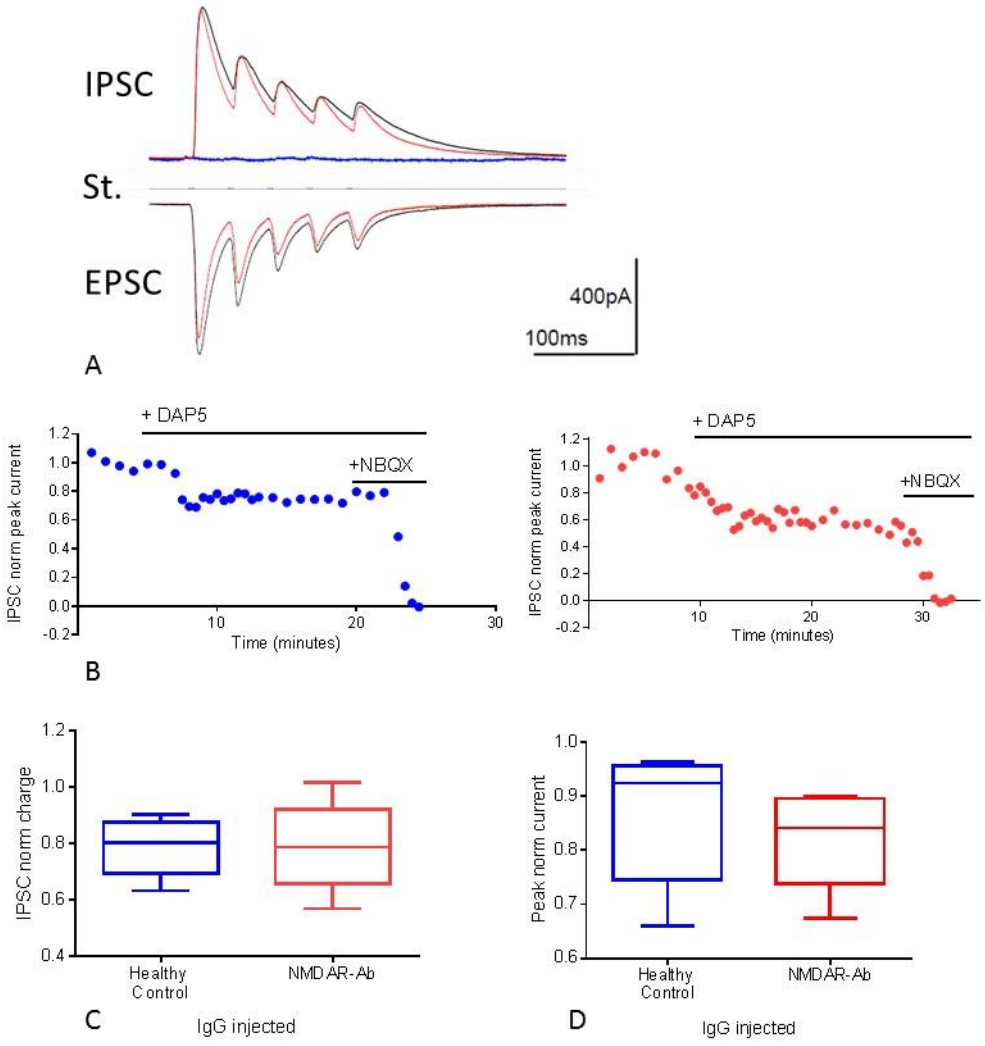

Figure 4-24 Optogenetic stimulation of recurrent networks used to test interneuron NMDAR hypofunction.

A. Averaged EPSCs (recorded at -70mV, black traces) and recurrent IPSCs (at the EPSCs reversal potential, black traces) in putative CA1 pyramidal cell from mouse injected with NMDAR-Ab IgG. Currents were evoked by optogenetic stimulation of pyramidal cells (St., 5 pulses, 20Hz). NMDAR blocker DAP5 suppressed recurrent IPSCs (red trace; blockade of IPSCs by NBQX shown in blue trace). In addition, EPSCs were also reduced by DAP5.

B. These scatter plots over time show disynaptic IPSCs throughout the optogenetic stimulation protocol. The red trace was from a AAV-ChR2-eYFP transfected CAMKII-Cre homozygous mouse injected ICV with NMDAR-A IgG; the blue trace from a HC IgG injected mouse. The wash-in of DL-AP5 shows suppression of the IPSCs which are completely abolished by the AMPAR blocker NBQX. This confirms the disynpatic nature of the IPSCs.

C-D. The blue box shows the baseline-normalized IPSC charge in cells from HC IgG injected (n=5 cells), and NMDAR-Ab injected mice (n= 5 cells) following application of DLAP5. There is no difference of the DL-AP5 effect between the groups. The peak current (baseline-normalized) following pulsed optogenetic simulation, also does not show a significant difference between the two groups (D). This confirms that NMDARs in GABAergic cells contribute significantly to recurrent inhibition during entrainment of glutamatergic fibres, but also that recurrent inhibition has not been altered in the mice injected with NMDAR-Abs.

4.11 Discussion and limitations

Optimisation of a novel wireless EEG telemetry system for use in mice was performed. This included optimising the surgical technique, as well as working with the manufacturers to improve both the design of the transmitters in terms of wire length and skull screw design, and the metrics of the software used for event detection and analysis. The system was then used to test the effect of NMDAR-Ab IgG passive transfer. Mice injected with NMDAR-Ab IgG did not have spontaneous seizures, but were found to be more seizure susceptible than those injected with HC IgG following a sub-threshold dose of the pro-convulsant PTZ. This was established by behavioural observation as well as the computer based detection programmes optimised to find specific epileptiform and behavioural events in the continuous EEG recordings.

Wireless EEG recording systems offer some advantages over the traditional "tethered' methods, including less movement artefact and reduction of distress to the animal. These experiments showed the devices were well tolerated by the mice, and produced long-lasting stable EEG recording even during convulsive episodes. The devices used in these experiments worked well with sufficient battery life for all experiments, even enabling multiple use of some transmitters, for "24/7" EEG recordings of all experimental mice.

The initial prolonged recordings from Experiment 2 were used to look for spontaneous seizures induced by passive transfer of NMDAR-Ab IgG. Disappointingly, spontaneous seizures were not detected in our EEG analysis. The mouse strain used in our experiments, C57BL/6, is generally regarded as the most resistant to electrical and chemical epileptic stimuli (Ferraro, Golden et al. 1998, Ferraro, Golden et al. 1999). Future

studies comparing epileptiform activity in different inbred mouse strains injected with NMDAR-Ab positive IgG, as performed in other epilepsy mouse models, may demonstrate further the epileptogenic potential of these antibodies (Aydin-Abidin, Yildirim et al. 2011). Additionally, there may have been technical reasons for the lack of spontaneous seizures recorded. The placement of only two electrodes (reference and recording) on the skull surface enabled further surgery to be performed for passive transfer of NMDAR-Ab and HC IgG into the lateral cerebral ventricle. However, this also meant there was only one channel of EEG recording and the occurrence of seizures might not be within the recording field of the electrode pair. Even though the IgG was always injected on the left side, with one channel the seizures could not be localised or seizure propogation studied. Multiple channel recording devices have now been developed by Dr Hashemi and it would be useful to test the advantages of multi-channel recording in this model. However, this would have to be offset against the reduction in battery life given the additional amount of data processing. Skull surface electrode placement was made through a craniotomy aiming for epidural electrode placement. While these “surface” electrodes have a lower signal to noise ratio they also do not allow accurate localization of seizures or interictal activity within deeper cortical structures. Intracranial electrodes are more likely to cause injury, but in this model may have been useful for recording from our hypothesized seizure-onset area near the lateral ventricle in the hippocampus.

A computer based event detection programme was used to analyse the EEG. Although there was an initial large investment of time in creating the algorithm for this method this made it possible to analyse large data sets. However, it needed to be regularly checked and refined. The seizures were defined by video-EEG matching and were mainly

of Stage 2 and Stage 3a type (Table 2.3). Spike events were identified here and used as a marker of epileptiform activity in the event library. The prolonged EEG recordings post passive transfer of NMDAR-Ab IgG did not reveal a significant number of spike events. However despite the optimization of this analysis there always remains the possibility that false negative events were missed and the occurrence of spontaneous seizures may have been underestimated. For spike analysis of the PTZ hours, a combination of observer counting and event detection was used, thereby providing a check on the specificity of event detection. However this would not be possible with hundreds of hours of EEG and the computer detection system was essential for long-term EEG analysis.

One major difficulty was knowing exactly the type of event to look out for in the EEG analysis as without examples of events it is not possible to train the computer detection system to find them. The PTZ induction hours with video gave us example spike events to use, but there may have been other important events missed. The other events the computer detection system was trained to find were “headshakes” and “delta”. We defined “headshakes” as the EEG oscillations associated with this movement in mice which were initially mistaken for ‘spike’ events. In rats, headshakes are a normal behaviour but are also seen in experimental epilepsy models associated with convulsive seizures in acute and kindling models, although this relationship is variable (Rodrigues et al., 2005). In all three Experiments analysed (2, 4 and 6) there was an increase in headshakes over time, and as the animals experienced more procedures. However in Experiment 6 where the mice were given three doses of PTZ, the headshakes peaked after the second dose and did not continue to rise. In addition intermittent delta wave oscillations were investigated as similar EEG features have been described in NMDAR-Ab encephalitis patients (Schmitt,

Pargeon et al. 2012). It is still not known if these changes represent a specific effect on neuronal oscillations caused by the NMDAR-Abs or are simply a manifestation of an acutely unwell encephalitis patient. Disappointingly, there was no consistent relationship in all three data sets analysed (Experiments 2, 4 and 6), between the passive transfer of IgG and number of delta events.

Although spontaneous seizures were not seen or recorded, the NMDAR-Ab injected mice were found to be highly seizure susceptible in comparison to the HC IgG injected mice. In our experiments, we chose a 48 hour window between ICV injection and testing as a starting point as NMDAR receptor internalisation is thought to occur quite quickly in vivo, i.e. 12-24 hours. Testing at 24 hours as shown in early experiments may not have been enough time for recovery from surgery, therefore 48 hours was chosen. Ideally a time course experiment would be useful, i.e. first seizure induction at Day 2, compared to different time intervals for first seizure induction, e.g. 4 days, 8 days and 12 days post ICV.

The increased seizure susceptibility seen in the mice injected with NMDAR-Ab IgG is comparable to the NR1 hypomorphic mouse model where all experienced lethal seizures compared to none in WT mice when given a 20 mg/kg dose of kainic acid (Duncan, Inada et al. 2010), although our phenotype was much less severe. This model has lost at least 80% of NMDA receptors and further electrophysiological characterisation has demonstrated altered excitatory-inhibitory (E/I) signalling with selective disruption of parvalbumin-expressing interneurons and pyramidal cell excitability (Gandal, Sisti et al. 2012) as a consequence. It was hypothesised in this model that NMDARs on inhibitory interneurons were more susceptible/accessible to NMDAR-Ab positive IgG binding in vivo, and were therefore preferentially targeted. This is similar to their disproportionate

sensitivity to NMDAR antagonists compared to pyramidal neurons (Grunze, Rainnie et al. 1996, Li, Clark et al. 2002). If the NMDARs on interneurons are 'knocked down' by antibody-mediated internalization, pyramidal cell excitability and seizure susceptibility will result. *In vitro*, while preferential binding to inhibitory interneurons was not seen, there was an overall reduction in GABAergic synaptic density onto excitatory neurons (Moscato, Peng et al. 2014) which may still have a profound network effect. This theory was tested by looking at recurrent inhibition and the effect of hypothesized NMDAR hypofunction on interneurons in ex-vivo slices.

Unfortunately no difference was seen between the NMDAR-Ab and HC IgG injected group with *ex-vivo* patching of cells in CA1. The ICV injection was not directed to a particular hippocampal area so the spread to specific areas, i.e. CA1, was not known. This area was selected for study as the circuits are relatively simple compared to CA3 thereby allowing a greater chance of isolating a recurrent circuit. Detailed analysis of IgG spread and localization (Chapter 5) would allow planning of future experiments to target the most physiologically relevant regions of the hippocampus. A possible reason for the lack of an effect on recurrent inhibition seen in the optogenetics experiments may have been because the injected NMDAR-Ab IgG failed to reach the CA1 region.

A number of novel techniques were used to demonstrate the epileptogenicity of NMDAR-Abs in vivo. Following passive transfer of NMDAR antibodies in mice, there was an increased seizure susceptibility compared to mice injected with HC IgG. The exact mechanism underlying this effect remains unknown, but further analysis of IgG passive transfer effects, in particular parenchymal IgG staining and specificity as shown in Chapter 5, may help explain the observed behavioural changes seen.

CHAPTER 5 - Post-mortem tissue analysis of NMDAR-Ab passive transfer mice

5.1 Introduction

Chapter Four demonstrated that there was increased seizure susceptibility in mice injected in the lateral ventricle with NMDAR-Ab IgG. The rationale for using ICV injection for passive transfer was to ensure maximal delivery of the human IgG to the brain parenchyma. In Experiment 4, the mice were culled 48 hours after seizure induction so that immunoflourescent staining could be used to detect the presence and extent of the passive transfer of IgG. The relationship between the pattern of IgG binding and seizure induction, and the effects on activity levels and potentially cell death in the brain were investigated, using c-fos expression as an indirect marker of neuronal activity and TUNEL staining for the detection of apoptotic cells.

5.2 Use of fluorescent tracer beads to confirm correct site of ICV injections

The initial analysis of sections was simply to determine whether the injections had been in the correct place as surgery based on the position of bregma is somewhat subjective. Fluorescent latex microspheres or 'beads' (Lumafluor Inc., USA) were injected with the patient IgG to allow us to identify the site of ICV injection on tissue analysis post-mortem. Originally designed for use as retrograde tracers, many beads remain bound to tissue at the site of injection and are therefore useful for confirmation of injection site. In 12 µm sections cut from injected mice brains the fluorescent beads were found lining the lateral ventricle in multiple sections. This confirmed that the injection had been correctly made in to the ventricle (Figure 5.1A). Beads lining the 4th ventricle were

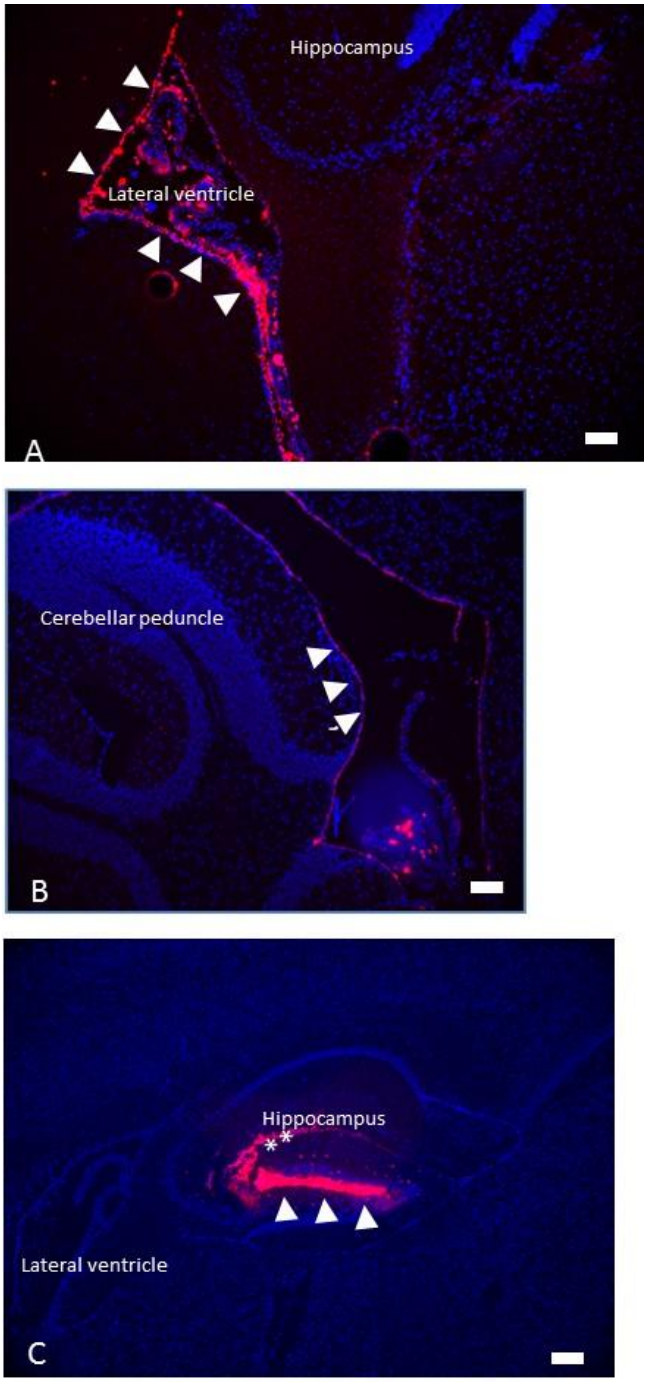

Figure 5-1 Fluorescent tracer beads used to identify site of IgG injection

A. The hippocampus and lateral ventricle in a sagittal brain section with DAPI staining (blue) of a mouse injected ICV with IgG and fluorescent beads (red). The beads are lining the lateral ventricle (white arrowheads) to confirm correct site of IgG injection post mortem. Scale bar 50µm.
B. The cerebellum in a sagittal brain section with DAPI staining (blue) of a mouse injected ICV with IgG and fluorescent beads (red). There are beads seen lining the 4th ventricle indicating (white arrowheads) full ventricular circulation of the IgG injected with beads. Scale bar 50µm.
C. The hippocampus in a sagittal brain section with DAPI staining (blue) of a mouse injected with IgG. The fluorescent beads (red) are seen within the hippocampus and not in the lateral ventricle indicating misplaced ICV injection (white arrowheads). There is evidence of retrograde transport of the fluorescent beads into the cell bodies within the granule cell layer (white **). Scale bar 200µm.

visible in some animals, indicating that the injected fluid was able to access the full ventricular system (Figure 5.1B). In one of the first trial animals injected where the ICV injection was misplaced, beads were seen within the hippocampus with none lining the lateral ventricle (Figure 5.1C). In these animals there was evidence of retrograde transport into the cell bodies as beads were identified within the granule cell layer of the hippocampus (figure 5.1C). Correct ICV injection placement in all animals injected in Experiment 4 with HC IgG (n=5/5 tested) and NMDAR-Ab IgG (n=7/7 tested) was seen, with the fluorescent beads in the lateral ventricle.

5.3 Human IgG binding in injected animals

To examine the extent of binding of human IgG to tissue in injected animals, post mortem tissue was stained with anti-human IgG antibodies. Sections from un-injected mice were used as controls for non-specific binding of the secondary antibody. Unfixed tissue was sectioned at 12 µm on a cryostat and incubated overnight with anti-human IgG conjugated to Alexa 488 at a dilution of 1 in 1000. The hippocampus and cerebellum were examined because of the ventricular circulation of the IgG. Animals E9,12, 14, 21, 24 from Experiment 4 injected with HC IgG had some remaining IgG within and around the injection site and/ or needle track (Figure 5.2 A-C), but there was no other staining in the cortex, hippocampus (Figure 5.2 D-E) or cerebellum (Figure 5.2 G-H) in any of the HC IgG injected mice tissue sections analysed. Staining in uninjected mouse tissue was negligible (Fig 5.2 F, I).

Tissue was available from 7/9 of the NMDAR-Ab injected mice from Experiment 4. As seen in the HC IgG injected mice, those injected with NMDAR-Ab IgG also showed human IgG within and around the needle track (Figure 5.3 A-B). There was also a lack of human IgG binding in the rest of the cortex (Figure 5.3 C-D) and

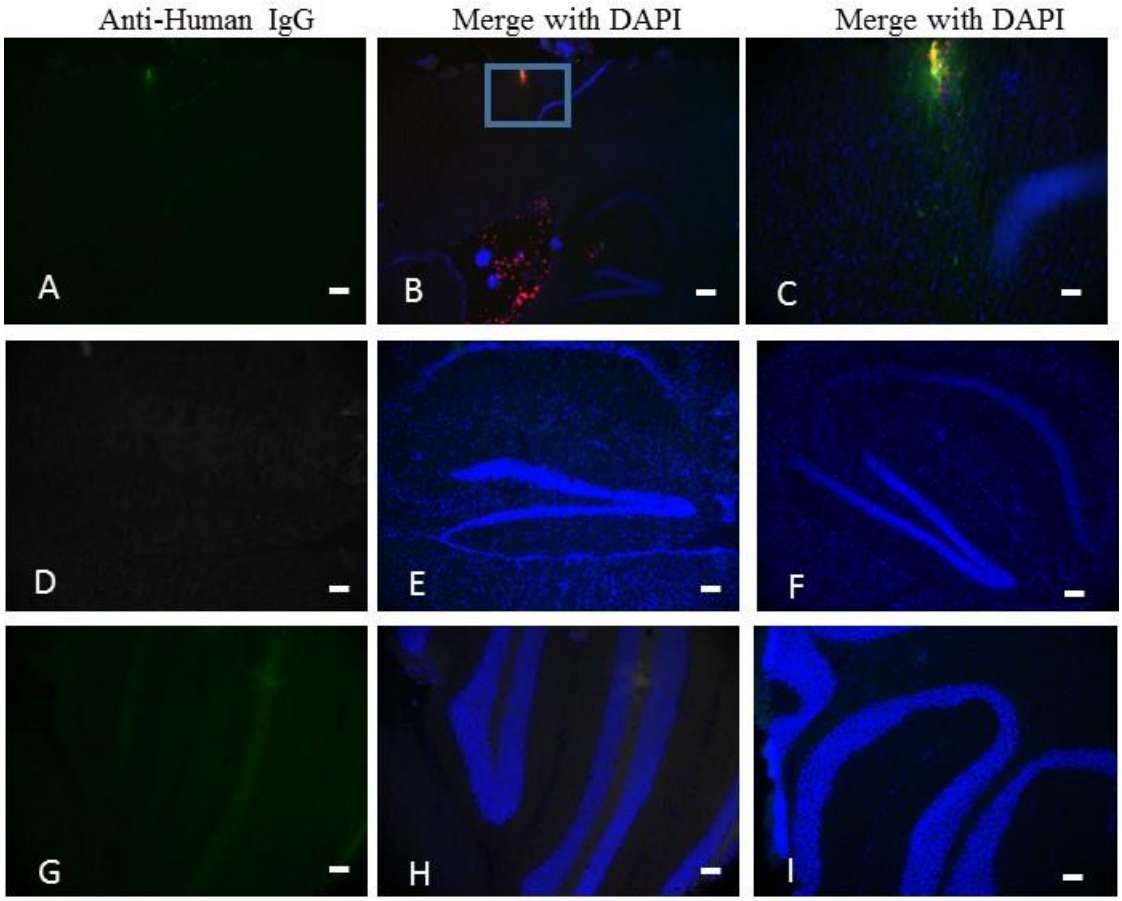

Figure 5-2 Human IgG binding in animals injected with HC IgG.

A-C. The first sagittal brain section (A,scale bar 200µm) of the cortex, hippocampus and lateral ventricle is from mouse E21 injected with HC IgG. The immunofluorescent staining (green) of anti-human IgG in the cortex at the injection site is the only residual IgG binding seen at 48 hours after ICV injection. In the merge with DAPI (blue, B, scale bar 200µm), the red fluorescent beads can be seen within the ventricle indicating correct placement of the ICV injection. The boxed area is magnified in C (scale bar 50µm) showing co-localisation of the tracer beads and human IgG staining (yellow) and some additional punctate human IgG staining around the injection site in the cortical tissue.

D-E. Sagittal hippocampal sections also taken from E21. In D and the merge with DAPI (blue, E) there is no human IgG staining despite confirmation above that the ICV injection did go into the lateral ventricle. All scale bars 100µm.

F. Sagittal mouse hippocampal section showing the background immunofluorescent staining with anti-human IgG 488 antibody (green) in a non-injected mouse merged with DAPI (blue).The level of non-specific binding of this secondary antibody is low.

G-I. Given the potential circulation of IgG into the fourth ventricle, cerebellar sections of mouse E21 were also examined. In G and the merge with DAPI (blue, H), no human IgG staining is seen. The control background staining of the anti-human IgG (green) in an un-injected mouse hippocampal section is again low (blue is DAPI staining as previously). All scale bars 100µm.

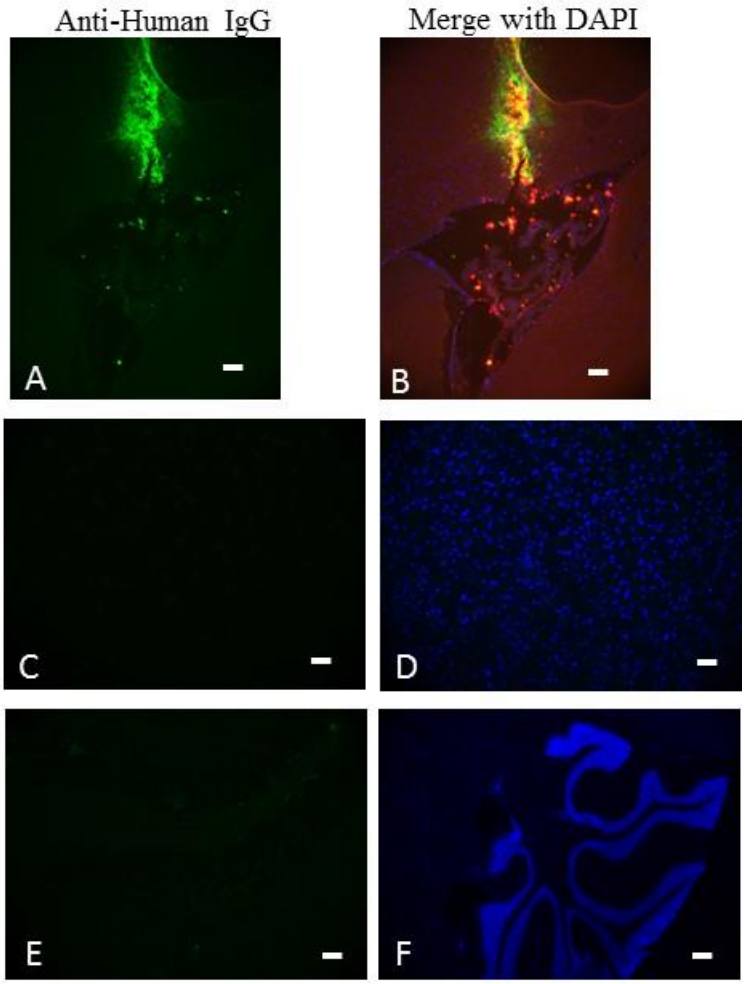

Figure 5-3 NMDAR-Ab IgG binding in cortex and cerebellum.

A-B. This sagittal brain section (A) of the lateral ventricle is from a mouse injected with NMDAR-Ab IgG where immunofluorescent staining (green) of anti-human IgG is seen in the cortex in and around the needle track of the ICV injection. In the merge with DAPI (blue, B) the red fluorescent beads can be seen within the ventricle and co-localising with human IgG staining in the needle track (yellow) similar to the HC IgG injected animals. Scale bars 50µm.

C-D. Apart from in the needle track there is no other green fluorescent human IgG staining in the cortical tissue as seen in this sagittal section of the cortex (C) and in the merge with DAPI (D, blue). Scale bars 50µm.

E-F. Similar to the HC IgG injected mice, in this sagittal section of the cerebellum (E) in an NMDAR-Ab injected mouse there is no human IgG staining seen, confirmed on the merge with DAPI (F, blue). Scale bars 100µm.

cerebellum (Figure 5.3E-F). However, in contrast to the HC IgG injected mice, there was specific hippocampal staining clearly visible in serial sections within the

hippocampus (Figure 5.4). Two animals had a more discrete binding pattern concentrated within the CA3 area of the hippocampus (Figure 5.5A-D), and relatively less in the dentate and CA1. The binding was seen within serial sections through the injected hemisphere and showed relative sparing of the granule cell layer (Figure 5.5A).

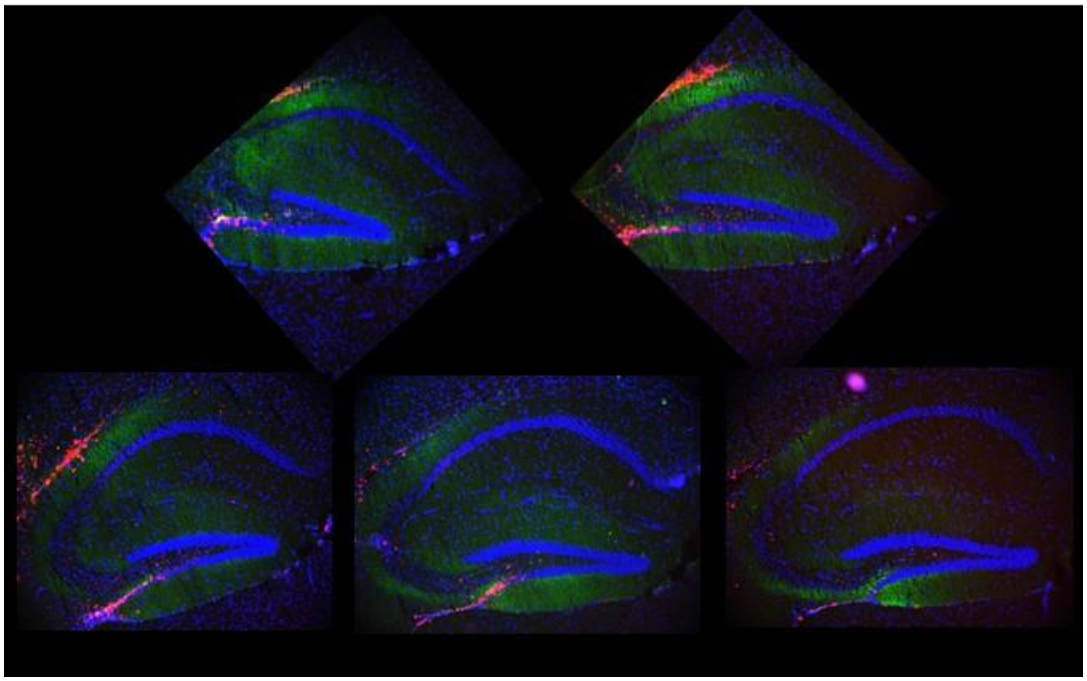

Figure 5-4 NMDAR-Ab IgG binding in the hippocampus.

In this series of sagittal sections of a mouse injected with NMDAR-Ab IgG (E15) starting with the top left photomicrograph, there is human IgG staining (green) seen throughout the hippocampus, with DAPI staining in blue, and red fluorescent tracer beads.

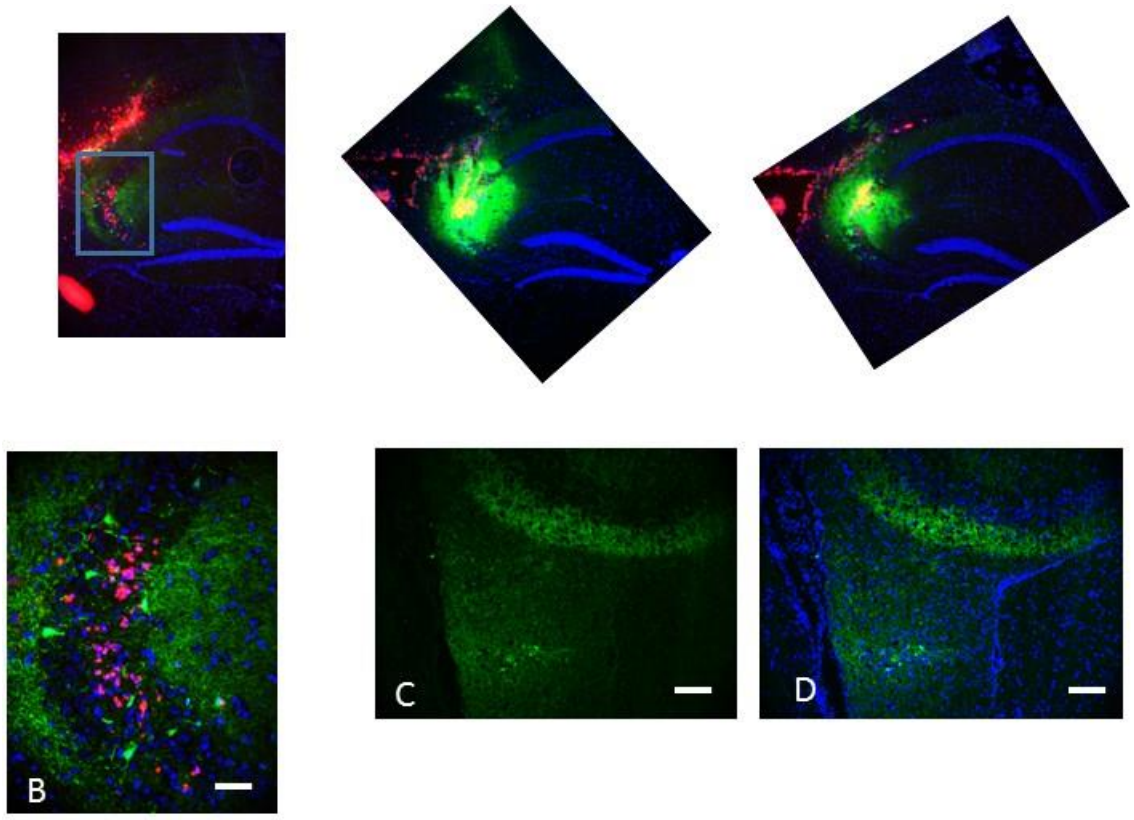

Figure 5-5 NMDAR-Ab IgG binding in the CA3 region of the hippocampus.

A. This sagittal brain section series of the left hippocampus is from a mouse injected with NMDAR-Ab IgG where immunofluorescent staining (green) of anti-human IgG is seen most intensely in the CA3 region of the hippocampus. The boxed area is magnified in picture B. Scale bar 100µm.
B. In this higher magnified picture of CA3 the punctate binding of the NMDAR-Ab IgG (green) can be seen primarily in the molecular layer with relative sparing of the granule cell layer. Additionally, red fluorescent beads are seen in the granule cell layer as a result of retrograde transport. Scale bar 50µm.
C. This pattern of NMDAR-Ab IgG staining (green) is also seen in this animal in the CA3/fimbria region of the hippocampus. In the merge with DAPI (D, blue) most of the binding is restricted to the molecular cell layer of the hippocampus as above. Scale bars 50µm.

5.4 The pattern of human NMDAR-Ab IgG hippocampal binding in injected mice

The common feature of the hippocampal human IgG binding seen in NMDAR-Ab injected mice was sparing of the granule cell layer both in CA3 and the dentate gyrus. This characteristic neuropil staining pattern of the injected NMDAR-AB IgG was similar to that seen in mouse sections incubated *in vitro* with NMDAR-Ab IgG

(Chapter 4; Figure 4.1 A-B) and NMDAR-Ab positive CSF (Figure 5.6 A-B). However, the characteristic cerebellar granule cell layer binding of NMDAR-Ab positive CSF was not seen in the injected animals, indicating that the IgG did not diffuse through the fourth ventricle into the cerebellum (Figure 5.6 A-B). These sections were all stained unfixed with no permeabilisation of the tissue.

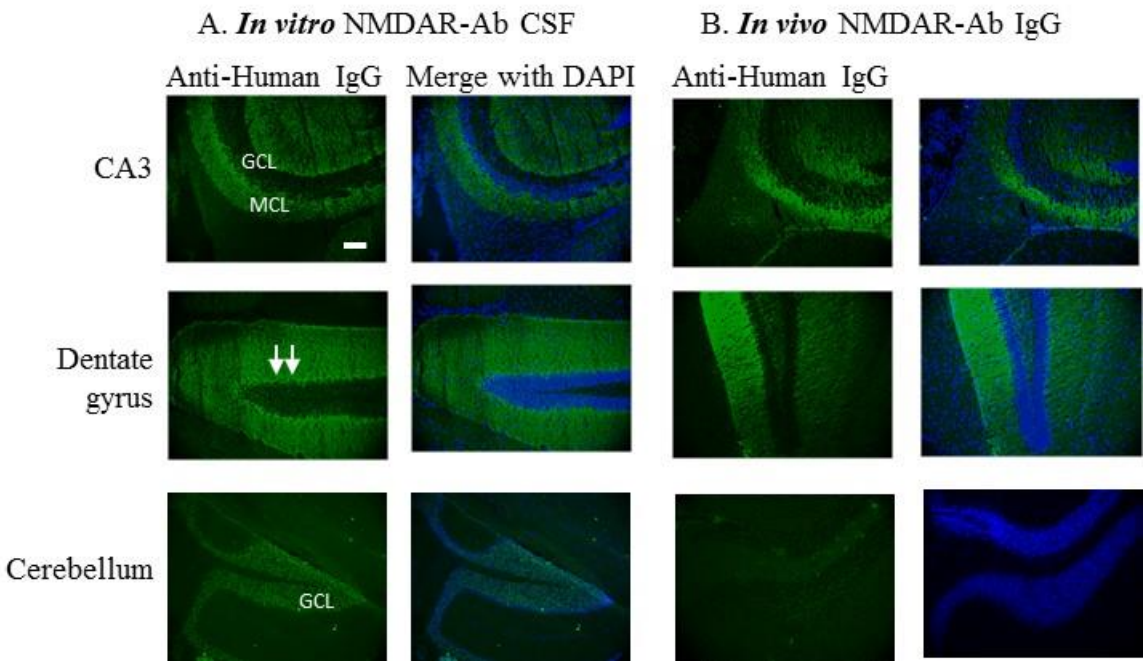

Figure 5-6 Hippocampal NMDAR-Ab binding *in vitro* and *in vivo.*

A. This vertical panel shows the NMDAR-Ab positive CSF binding on *in vitro* mouse hippocampal sections labelled with a anti-human IgG 488 secondary antibody (green) with no fixation. In CA3 there is characteristic sparing of the granule cell layer (GCL) and staining of the molecular cell layer (MCL). In the dentate gyrus of the hippocampus there is similar sparing of the GCL and some subtle increased staining of the inner molecular layer (white arrows). The staining of NMDAR-Abs in the cerebellum is restricted to the granular cell layer. Scale bar 50µm.
B. The post-mortem immunofluorescent staining of mice injected with NMDAR-Ab IgG *in vivo* (green) is also shown here to compare with the characteristic *in vitro* staining patterns seen in A. The hippocampal regional human IgG staining of CA3 and the dentate gyrus are similar to the *in vitro* sections with sparing of the GCL and staining of the MCL. There is no staining of the cerebellum indicating that little NMDAR-Ab IgG is found in the cerebellum under these conditions.

For further characterization of the injected NMDAR-Ab IgG binding pattern, and given that NMDAR-Abs bind to the extracellular surface of the NMDAR, an NR1 commercial antibody to an extracellular epitope of NR1 (Neuromab; USA) was then tested on

unfixed and unpermeabilised tissue sections as above. This produced a distinct staining pattern of discrete neuronal cells in CA3 (Figure 5.7A), the polymorphic layer of the dentate (Figure 5.7B) and throughout the cortical tissue (Figure 5.7C), this was very unlike the characteristic neuropil binding of human NMDAR-Abs. However, the granule layer of the cerebellum was stained similarly to NMDAR-Ab CSF in vitro (Figure 5.7D).Given the possibility from the morphology and location of the stained cells that these could represent NMDARs on interneurons, immunostaining for parvalbumin was performed alongside. There was some co-localisation of the NR1 stained cells and parvalbumin (Figure 5.8).

In a further attempt to compare the distribution of injected NMDAR-Ab IgG with a commercial antibody, a standard NR1 commercial directed towards the intracellular component of NR1 was used (BD Pharmingen; Oxford). Frozen sections from control mice were first fixed and permeabilised before application of the commercial NR1 antibody overnight at 4^{o}C. The familiar NR1 staining pattern with binding in the molecular cell layer in the hippocampus and sparing of the granule cell layer of the cerebellum was seen (Figure 5.9A-D). When compared with both *in vitro* NMDAR-Ab positive CSF staining and the intracellular NR1 commercial binding, the hippocampal binding of animals injected *in vivo* with NMDAR-Ab IgG does appear to be specific for the NMDA receptor/ NR1 subunit (Figure 5.9E-G). However, as demonstrated in the three different NMDAR-Ab IgG injected mice sections shown (Figure 5.4, 5.5), there was variability in region and intensity in the *in-vivo* hippocampal binding.

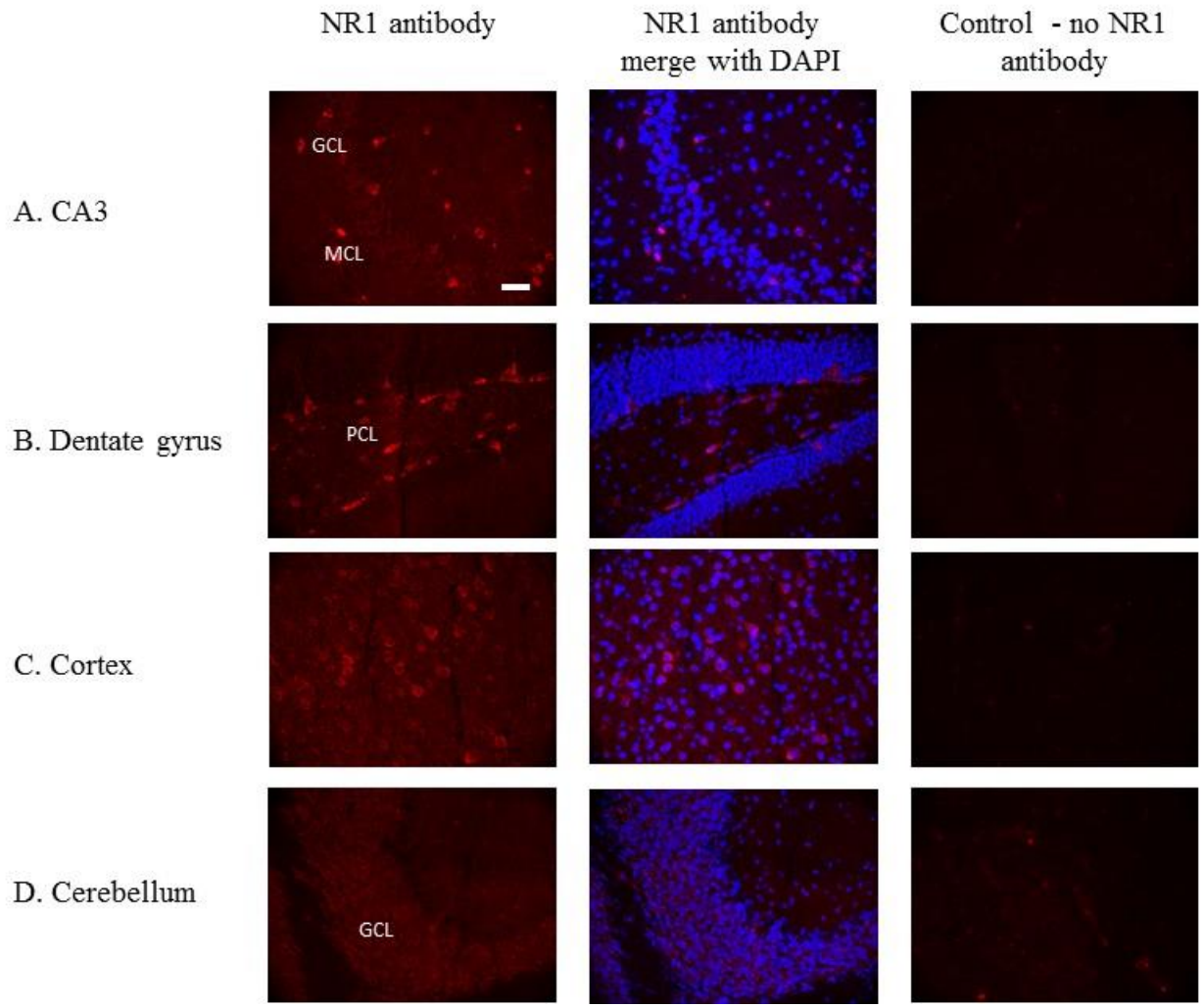

Figure 5-7 Extracellular NR1 commercial antibody binding to mouse hippocampus, cortex and cerebellum.

A. This horizontal panel shows the binding pattern of the NR1 commercial targeted to an extracellular epitope (red) in the CA3 region of the hippocampus. There is binding of many discrete neuronal cells throughout the CA3 region (GCL and MCL). This was thought to be specific as it was seen above the levels of background control staining (third picture). Scale bar 50µm.
B. In the dentate gyrus there was binding of the NR1 commercial restricted to the polymorphic (PCL) layer with sparing of the granule cell layer but no diffuse staining of the neuropil as seen with NMDAR-Ab IgG/ CSF.
C. There was widespread neuronal staining of the NR1 commercial antibody to the cortical tissue which was not seen with NMDAR-Ab IgG/CSF *in vivo/vitro*.
D. The granule layer (GCL) staining of the cerebellum with the NR1 commercial antibody is similar to the staining pattern seen with the NMDAR-Ab CSF *in vitro*.

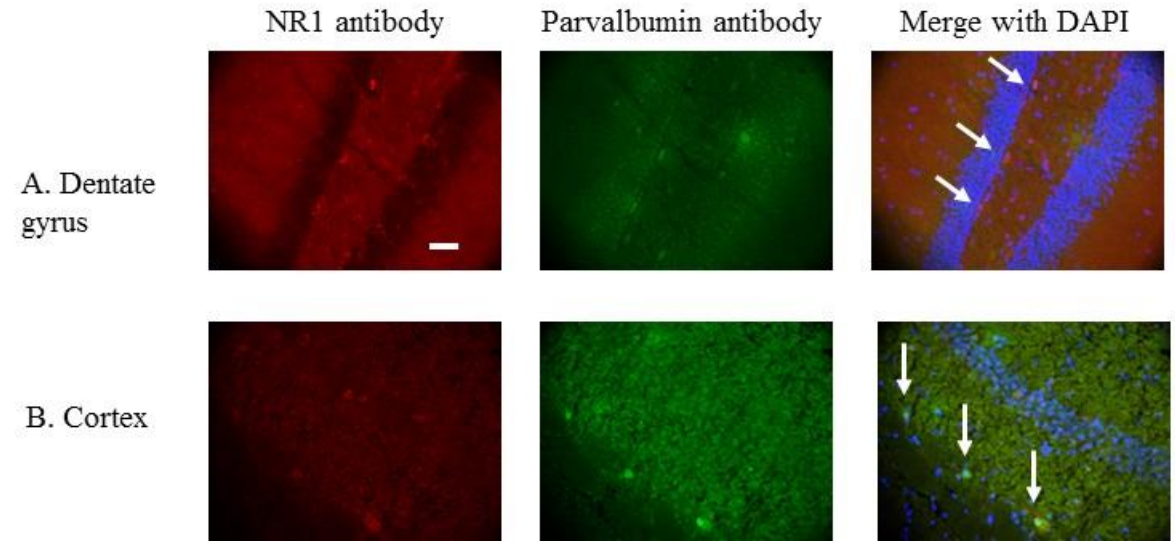

Figure 5-8 Double staining of extracellular NR1 commercial and parvalbumin antibodies.

A. This vertical panel shows the NR1 commercial antibody binding to discrete neuronal cells (red) in the dentate gyrus. Some of these cells are also positive for parvalbumin (green). The co-localisation is shown in the merge with DAPI (white arrows). Scale bar 50µm.
B. This area of cortex shown in panel B also has similarly stained red cells by the NR1 commercial antibody (red) which are also picked up with the parvalbumin staining (green). The co-localisation of these cells is indicated by the white arrows in the third merge with DAPI (blue) photomicrograph.

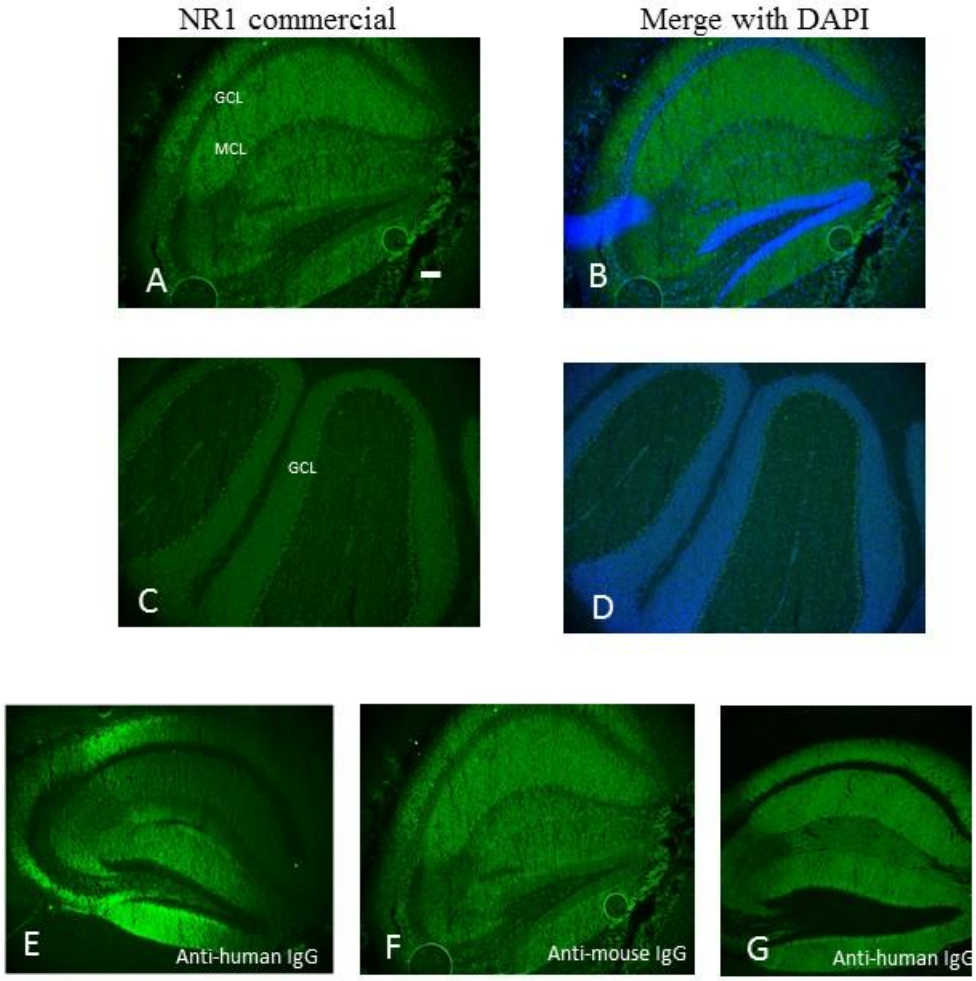

Figure 5-9 Intracellular NR1 commercial binding.

A-B**.** The binding of the intracellular NR1 commercial antibody to the mouse hippocampus is shown here (green). There is staining of the molecular cell layer (MCL) and relative sparing of the granule cell layer (GCL) which is seen on the merge image with DAPI (blue) (B). Scale bar 100µm.

C-D. There is staining of the granule cell layer (GCL) of the cerebellum (green) as seen with NMDAR-Ab CSF *in vitro*. This co-localises with the DAPI staining of the same region (blue) (D).

E-G. The pattern of hippocampal staining *in vivo* after passive transfer of NMDAR-Ab IgG (E) is similar to that seen both with the intracellular NR1 commercial antibody (F) and NMDAR-Ab positive CSF *in vitro* (G).

5.5 The intensity and regional variability of human NMDAR-Ab IgG hippocampal binding in injected mice

In order to examine the relationship between the IgG injected and the behavioural phenotype seen (seizure susceptibility), the mouse sections from Experiment 4 were used. Serial sections of the left hemisphere in four NMDAR-Ab and three HC IgG injected mice were stained for human IgG as previously (see Methods 2.2.6). Pictures at x40 magnification from three different regions of the hippocampus (CA1, CA3 and dentate) were taken from each section (at least 8 sections per animal). The sections were all coded for immunostaining and analysis so that analysis was blinded to treatment. The fluorescence intensity of each picture is represented as a distribution curve of pixel intensity. The first graph (Figure 5.10 A) shows the very low pixel intensity of a control WT mouse section stained with anti-human IgG secondary antibody. The fluorescence intensity of serial sections in three HC IgG injected mice (Figure 5.10 B,C,D) showed levels similar to the background staining in WT sections indicating no human IgG binding in the hippocampus. Figure 5.10 E, F and G, show the results from staining from E15, E20 and E23 respectively, three of the NMDAR-Ab IgG injected mice. In these mice, some of the sections show increased fluorescence intensity as seen with the shift of distribution curves to the right. The fourth NMDAR-Ab injected mouse examined (E22, Figure 5.10 H) showed levels of fluorescence intensity similar to WT and HC IgG injected mice. Interestingly, this mouse had the lowest seizure score, 6, similar to the scores seen in the HC IgG injected mice. This suggest a failure of passive transfer in this mouse, as there was no binding of NMDAR-Ab human IgG and the seizure score was low.

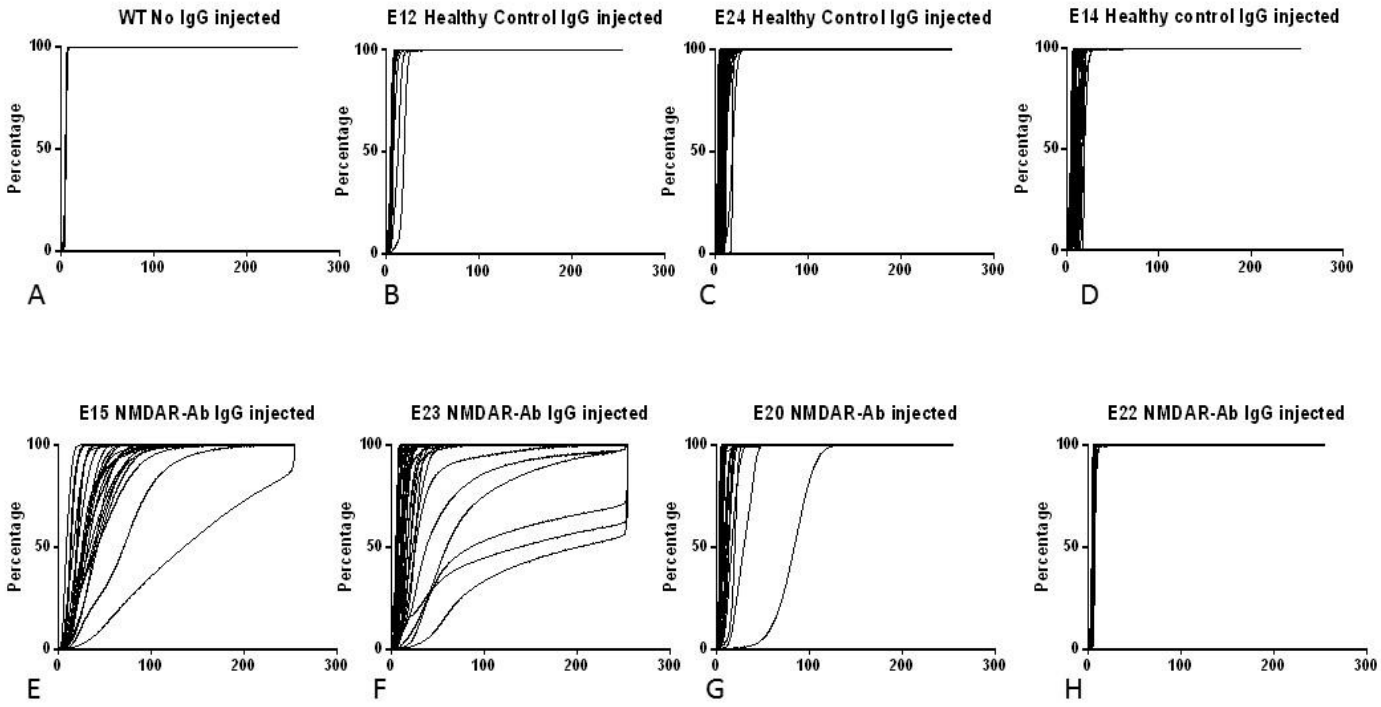

Figure 5-10 The intensity and variability of human IgG binding in vivo after passive transfer of NMDAR-Ab and HC IgG.

A-D. These graphs show human IgG fluorescence intensity measurement distribution curves (x-axis on all graphs) of CA3, CA1 and dentate gyrus in serial left hemisphere sections of WT (A) and healthy control injected mice (B,C,D). Each section analysed is represented by a line on the graph. The lack of human IgG binding is shown in the 3 HC IgG injected mice (B,C,D), as the distribution curves are similar to that of WT control sections (A) where background levels of anti-human IgG staining are negligible.

E-H. These graphs show human IgG fluorescence intensity measurement distribution curves of CA3, CA1 and dentate gyrus in serial left hemisphere sections of four NMDAR-Ab injected mice (E,F,G,H). The first 3 (E,F,G) show a shift of the distribution intensity curves to the right indicating positive binding of human IgG and therefore fluorescence intensity levels higher than that of the WT (A) and HC IgG injected mice (B,C,D). The fourth NMDAR-Ab injected mouse stained (E22, H) showed levels of fluorescence intensity similar to WT and HC IgG injected mice. This mouse had the lowest seizure score of 6 in the NMDAR-Ab IgG injected group, similar to the scores seen in the HC IgG injected mice. This suggest a failure of passive transfer in this mouse, as there was no binding of NMDAR-Ab human IgG and the seizure score was low.

When log values of serial sections were plotted against distance from the midline in E15 and E23 (the mice with highest seizure scores) and compared within hippocampal region, the levels peaked at the site of the injection and were highest in CA3 (Figure 5.11 A and B).

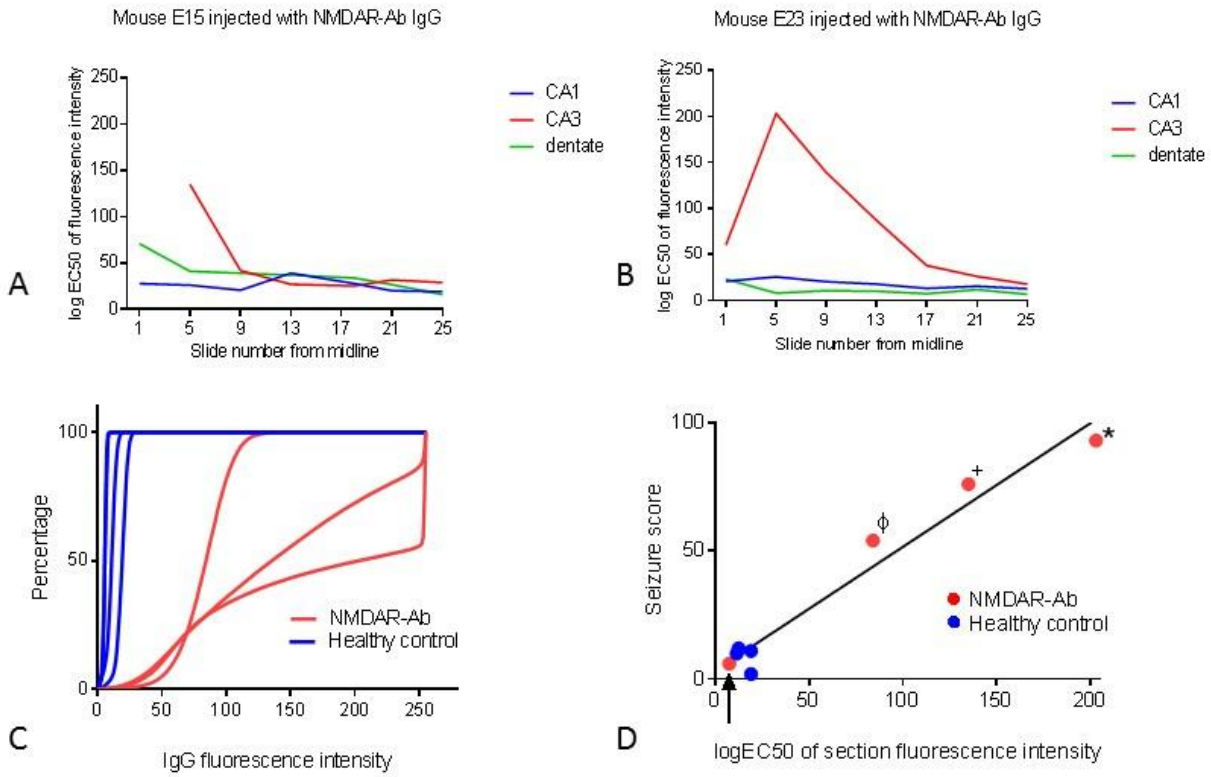

Figure 5-11 Regional hippocampal NMDAR-Ab IgG intensity, comparison with HC IgG injected mice and correlation with seizure susceptibility

A-B. These graphs are of log values of fluorescence intensity in serial numbered sections through the hemisphere from the midline in two NMDAR-Ab injected mice. In both, the highest IgG intensity is in CA3 peaking at the injection site region (slide 5-9).

C. Maximum fluorescence distribution curves for 3 animals from each group, NMDAR-Ab (red) and HC IgG injected (blue). The average distribution of the three representative NMDAR-Ab injected mice values for IgG intensity are significantly different from the distribution of the three representative HC injected mice values, (Kolmogorov-Smirnov test, $p < 0.0001$).

D. The fluorescence intensity of the IgG staining in NMDAR-Ab injected mice (n=4) and HC injected mice (n=4) when plotted as log values against seizure score show a significant correlation (R^2 0.9613; $p < 0.0001$), suggesting a dose-response effect between NMDAR-Ab IgG binding to mouse hippocampus and seizure susceptibility. The black arrow indicates mouse E22 which had a low seizure score of 6, indicating a failure of passive transfer (injected with patient PB IgG). (*) indicates animal injected with Patient 3 IgG, (+) Patient 1 IgG and (ϕ) Patient 2 IgG. The pathogenic effect of the antibodies appears to be proportional to the amount of IgG bound, and not related to the titre of the NMDAR-Ab positive IgG.

Overall the peak fluorescence intensity distribution curves from NMDAR-Ab injected mice were significantly different to WT and HC IgG injected mice (Figure 5.11C; Kolmogorov-Smirnov test, p=<0.0001) and when log values of the peak fluorescence intensities were compared to seizure score there was a strong correlation (Figure 5.11D; R=0.96, p=<0.0001). This suggests that when passive transfer of NMDAR-Ab IgG is successful, the pathogenic effect as measured by seizure susceptibility is proportional to the amount of IgG binding within the mouse brain.

5.6 Levels of NR1 expression in NMDAR-Ab injected mice

Other studies have shown reduced expression levels of NR1 consistent with antibody-mediated receptor internalization *in vivo* (Hughes, Peng et al. 2010). In order to explore this effect, sections from animals injected with NMDAR-Ab IgG were immunostained for human IgG and NR1 expression. Initial testing of NR1 staining in areas of intense human IgG binding in NMDAR-Ab injected mice showed a qualitative reduction of intensity of NR1 in these areas, in particular CA3 (Figure 5.12 A-D). Serial sections of two NMDAR-Ab IgG injected mice and two HC IgG injected mice were then stained for human IgG and NR1 expression. The CA3 region was initially analysed and compared in all sections (Figure 5.12 E-H). As seen previously, in the two NMDAR-Ab IgG injected mice (Figure 5.12 E, G) most of the IgG was bound in the medial sections, with some fluorescence intensity remaining in the lateral sections. The HC injected mice displayed no bound human IgG but the levels of NR1 intensity showed some variability (Figure 5.12 F, H). In mouse E23 (Figure 5.12 E), there was some reduction in NR1 expression when IgG intensity was highest, but this was not a consistent finding in the other NMDAR-Ab injected mouse, E15.

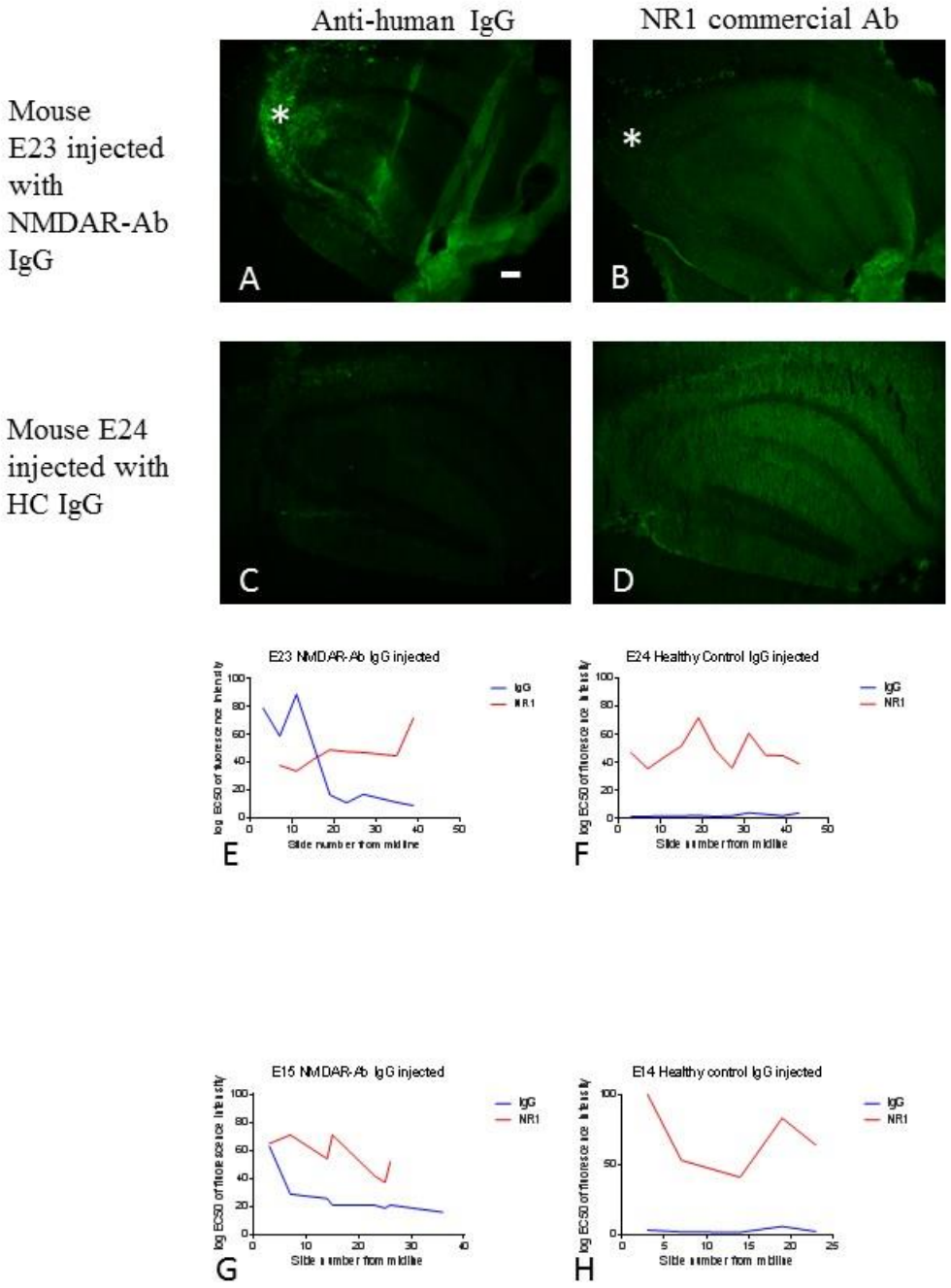

Figure 5-12 Levels of NR1 expression in NMDAR-Ab injected mice.

A-B. The photomicrographs of E23 injected with NMDAR-Ab IgG show intense binding of human IgG in the hippocampus (green, A, *). In the NR1 commercial immunostaining of an equivalent hippocampal frozen sagittal section (green, B) there is a reduction in NR1 binding in the area of most intense IgG binding, i.e. CA3 (*). Scale bar 100µm.

C-D. In the anti-human IgG immunostaining of mouse E24, injected with HC IgG, there is no bound IgG in the hippocampus (green, C). In an equivalent section, immunostaining with NR1 commercial antibody shows good levels of NR1 expression throughout the hippocampus (green, D).

E-H. These graphs show a comparison of log values of fluorescence intensity in serial sections of both human IgG (blue) and NR1 commercial antibody staining (red). In the HC IgG injected mice (F, H) the levels of IgG are negligible as expected; the levels of NR1 vary considerably. The NR1 levels in E23, injected with NMDAR-Ab IgG shows some reduction in NR1 expression when IgG intensity is highest in the medial sections (E). This finding is not replicated in the other NMDAR-Ab injected mouse, E15 (G).

In view of this variability the fluorescence intensity levels were compared between3 regions of the hippocampus of 5 individual slices within each of three animals (E24, E23, WT). NR1 expression varied within the regions of the hippocampus in the WT mouse (Figure 5.13A) and this variation was similar to that seen in the mouse injected with HC IgG (E24, Figure 5.13C). In mouse E23, injected with NMDAR-Ab IgG, there was a significant difference between the peak fluorescence intensity levels in CA1 compared to CA3 (Figure 5.13B). This suggested that NR1 levels had been altered in CA3 by the injection of patient IgG.

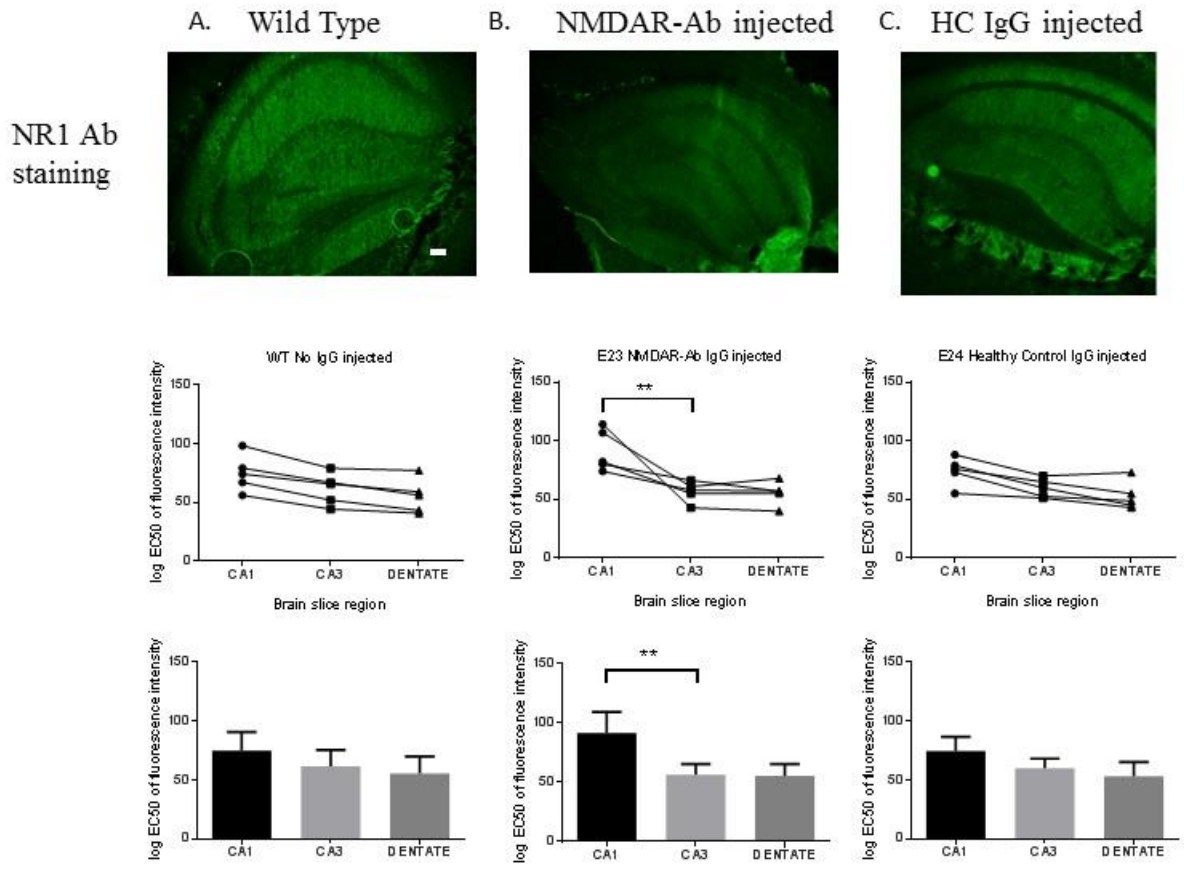

Figure 5-13 NR1 commercial immunostaining analysis in mice injected with human IgG.

A-C. The first vertical panel (A) of the WT mouse sections, shows the NR1 commercial binding pattern with immunofluorescence throughout the hippocampus (green). The line graph shows the individual log values of the fluorescence intensity in 3 different regions within the hippocampus (CA3, CA1, dentate gyrus) taken from five separate sections, which is summarised in the bar graph below it. There is no real difference in the intensity of NR1 expression within the 3 regions. This is similar to the results seen with analysis of sections taken from a mouse injected with HC IgG (E24, panel C). The NR1 levels in the mouse injected with NMDAR-Ab IgG (E23, B) however shows significantly higher levels in the CA1 compared to the other regions (p=0.0079, Mann-Whitney). Scale bar 100µm.

5.7 The diffusion distance of NMDAR-Ab IgG binding after passive transfer

To estimate the maximum lateral diffusion of NMDAR-Ab IgG through the hippocampus the fluorescence intensity distribution curves of sections immunostained for human IgG were compared between mice injected with NMDAR-Ab IgG and those of the HC injected mice (Figure 5.14). The maximum diffusion distance was taken to be the distance between the first and last sections of the series that had intensity of IgG levels no different from those of two HC IgG healthy control injected mice. An example for E23 is shown in Figure 5.14A. The estimated maximum lateral diffusion of E23 was to 2.76 mm and for E15 to 2.4 mm from the injection site. Representative images of the sections positive for human IgG in the NMDAR-Ab injected mice, medial and lateral to the injection site (Figure 5.14C-E) are shown with a schematic aerial view of the mouse brain indicating the spread of injected IgG (blue lines in 5.14B).

The same two animals (E23 and E15) were also analysed for spread of IgG through to the *right* hemisphere contralateral to the injection site in the left hemisphere. Analysis was restricted to CA3, as this was the region with the highest levels of IgG binding for both mice in the injected hemisphere, but IgG fluorescence intensity was negligible in the right hemisphere (Figure 5.14F,G). There was, in each animal in the right-sided cortical tissue, a small area of IgG binding at the level of the IgG injection, which may represent a small amount of IgG diffusion to the contralateral cortex, perhaps tracking through the corpus callosum (Figure 5.14H-J).

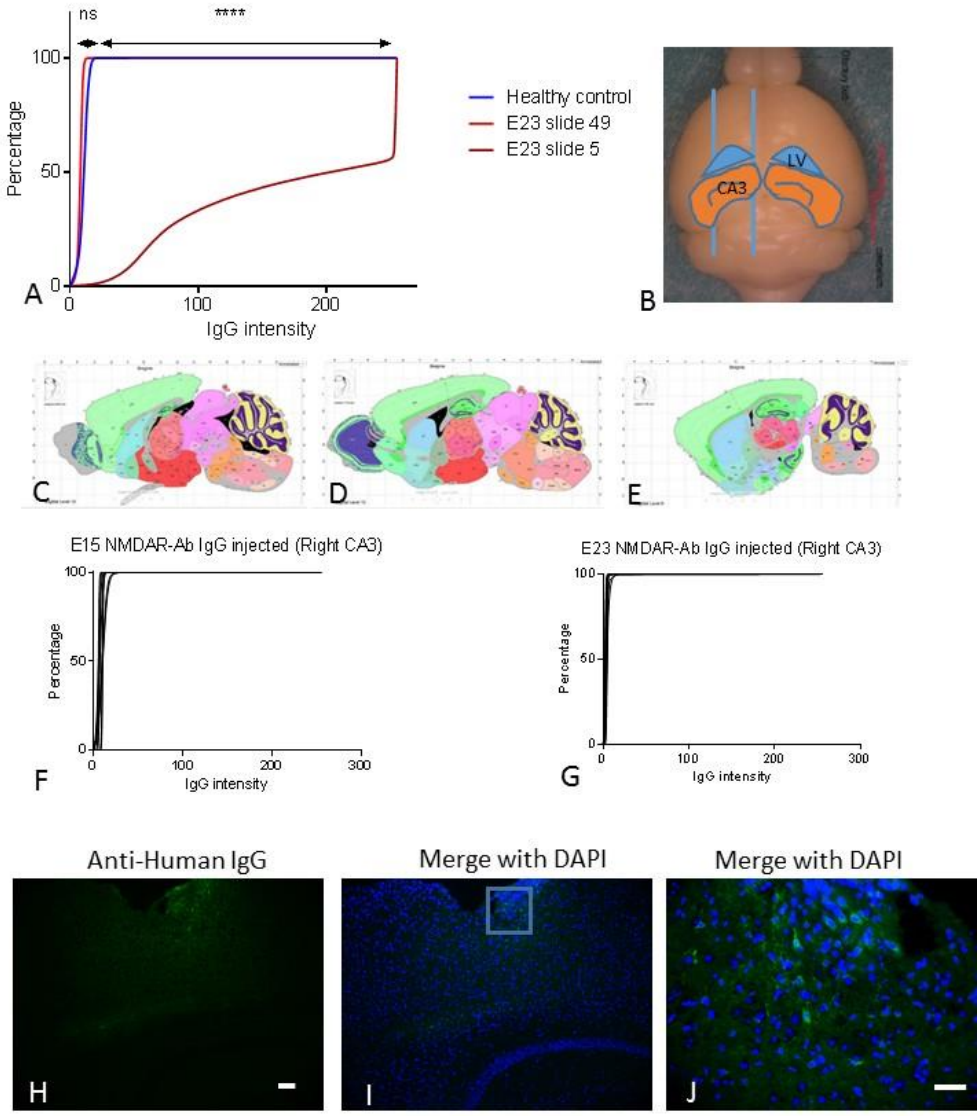

Figure 5-14 Diffusion distance of NMDAR-Ab binding after ICV injection in the right hemisphere.

A. This fluorescence intensity distribution curve demonstrates the method used to determine the maximum diffusion distance of the NMDAR-Ab IgG in injected mice. The first section of mouse E23, injected with NMDAR-Ab IgG (section 5, brown curve) had a significantly different distribution to the combined HC IgG injected distribution curve ($p<0.001$). The section on slide 49 of E23 (pink trace) was the first section in the series not significantly different to control/HC IgG injected fluorescence intensity distribution and therefore taken as the maximum horizontal diffusion distance.

B. This schematic shows the estimated maximum horizontal diffusion of IgG from an aerial perspective indicated by the two blue solid lines. The position of the lateral ventricle (LV) and CA3 region of the hippocampus (orange) are indicated on the graph.

C-E. These parasagittal mouse section diagrams are taken from loci corresponding to the first appearance medially of IgG immunofluorescent staining (C), the injection site region (D) and the most lateral serial section in which IgG immunostaining was detected (E).

F-G. Fluorescent distribution curves from sections of the contralateral hemisphere of mice E15 and E23. There is minimal IgG staining in the contralateral hemisphere to the ICV injection of NMDAR-Ab IgG in these two animals who had the highest intensity binding of IgG on the injected side (E15-F; E23-G); the diffusion of IgG appears to be restricted to the injected side.

H-J. These photomicrographs show a small area of discrete neuronal staining of human IgG (H; green) seen in the cortex of the contralateral hemisphere. The boxed area in I (merge with DAPI, blue) is magnified in J and single human IgG positive immunolabelled neurons (green) are seen within the cortical tissue. Scale bar H an I 100µm, in J scale bar 50µm.

5.8 The binding of injected NMDAR-Ab IgG in CA3 14 days post ICV injection from Experiment 6

Four animals E50-E53 were injected with NMDAR-Ab IgG and underwent repeated seizure inductions on D2, D7 and D14 post ICV injection (see Chapter 4). Animals were culled on day 14 and brains harvested, sectioned and photographed for determination of IgG binding. The fluorescence intensity distribution curves for human IgG staining for the hippocampal CA3 region are shown in Figure 5.15 A-D. There were negligible amounts of IgG remaining and the distribution curves are similar to background staining of human IgG on WT tissue and HC IgG injected mice. Figure 5.15 E also shows the log values of fluorescence intensity plotted throughout the hemisphere from slide 1 (medial) to the most lateral section (number 48). This confirms the lack of CA3 human IgG binding by this stage.

The only human IgG remaining was in and around the needle track. Figure 5.15 F-H shows some green fluorescence although this mainly localizes with the fluorescent tracer beads. There is some residual punctate IgG binding separate from the beads but this is very minimal (Figure 5.15 I-L) Therefore, the tissue appears to be cleared of human IgG within two weeks.

5.9 C-fos immunostaining in mice following seizure induction in Experiment 4

Immunostaining for c-fos expression was performed on brain sections from three mice in each group (NMDAR-Ab IgG and HC IgG injected) from Experiment 4 where the tissue was harvested immediately after the 60 minute observation period following seizure induction. The contralateral hemisphere to the ICV injection was used as this tissue had been immediately post-fixed after perfusion, thus conserving changes in intracellular protein expression (the injected hemisphere for all mice was PBS-perfused

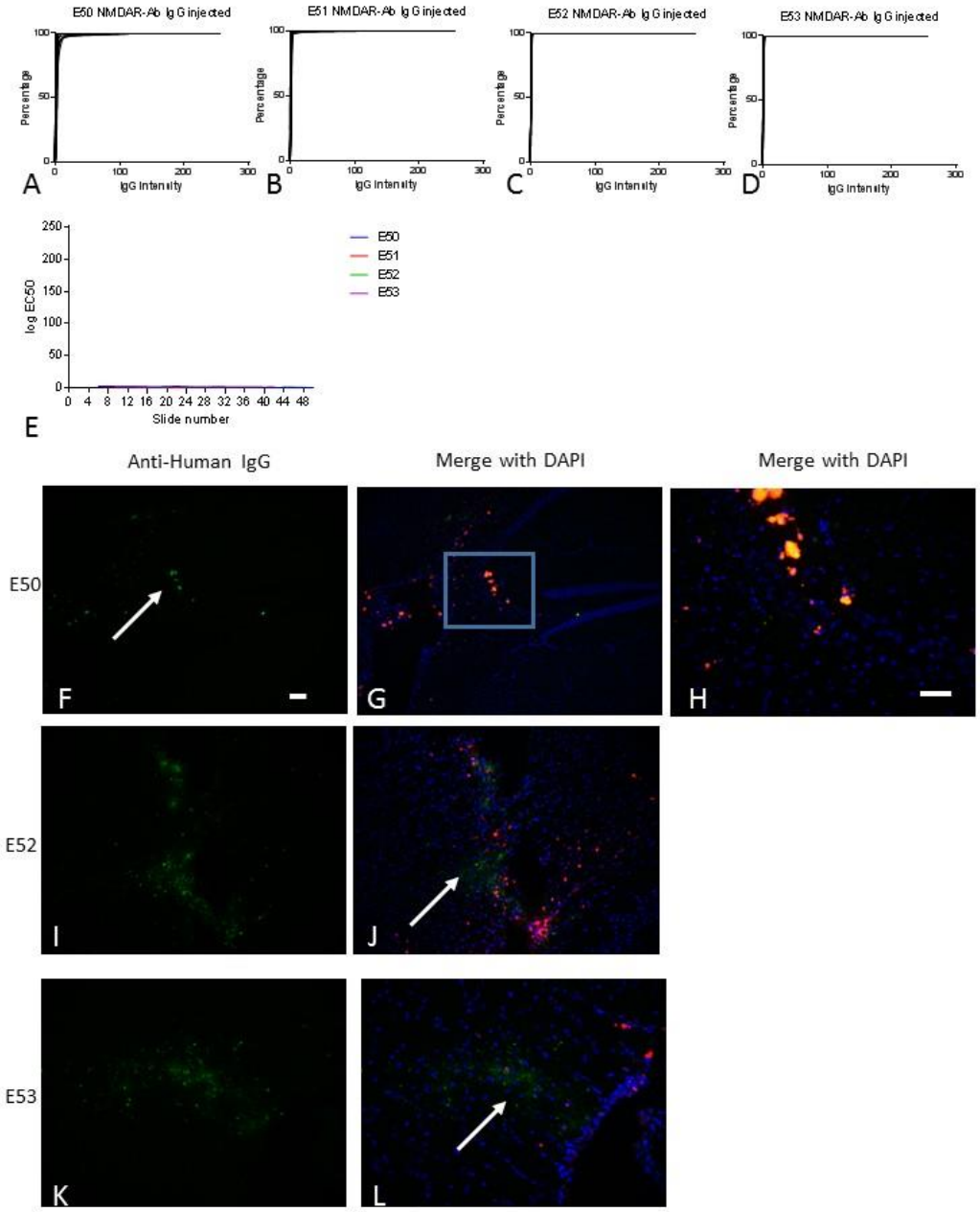

Figure 5-15 Binding of injected NMDAR-Ab in CA3 14 days post ICV injection.

A-D. These graphs show human IgG fluorescence intensity measurement distribution curves of CA3 in serial left hemisphere sections of E50-53 14 days after ICV injection of NMDAR-Ab IgG. There is no IgG binding 2 weeks post ICV passive transfer of NMDAR-Ab IgG.

E. The plot of fluorescence intensity log values against sections from medial to lateral also confirms no significant residual binding of human IgG throughout the injected hemisphere in the CA3 region of the same four animals (E50-53).

F-H. These sagittal sections near the lateral ventricle and hippocampus from mouse E50 show some residual binding above the lateral ventricle in the cortex (green, F, indicated with white arrow) but this all co-localises with the red fluorescent beads (seen in the merge image G, and magnified in H). Scale bar F,G,I,J,K,L 100µm; H scale bar 50µm.

I-J. In sagittal sections of mouse E52 shown here, there is some residual IgG binding (green, I) separate from the red fluorescent beads (indicated with white arrow in J) in the similar region near the injection site into the lateral ventricle.

K-L. Similarly in mouse E53, there is also some residual human IgG binding remaining (green, K) 14 days after ICV injection near the injection site into the lateral ventricle that does not co-localise with the red fluorescent beads (indicated with white arrow in L).

and then immediately frozen with no post-fixation for IgG immunostaining). Positive c-fos staining was confirmed with red intracellular staining of neuronal cell bodies (Figure 5.16 A-D). Additionally, c-fos positive sections of light stimulated mouse retina (donated kindly by Dr Steven Hughes from the Department of Ophthalmology) were used as a positive control. There was no difference in the c-fos expression between the HC and NMDAR-Ab IgG injected groups (Figure 5.16 E). One mouse was negative for c-fos expression and on analysis of behavior, only had stage 2 (partial) seizures. All the remaining mice tested had generalized seizures which we assume involve both sides of the brain and hence c-fos expression was seen on the contralateral side to the ICV injection.

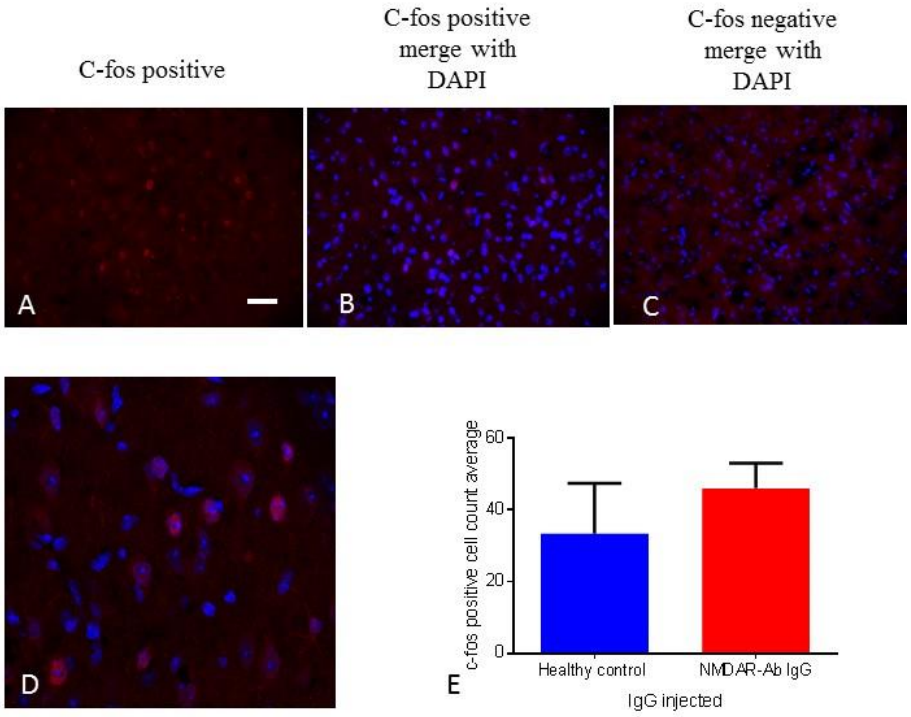

Figure 5-16 C-fos immunostaining in mice after passive transfer of NMDAR-Ab and HC IgG and seizure induction.

A. This sagittal section taken from the cortical tissue of a NMDAR-Ab IgG injected mouse after seizure induction shows positive intracellular c-fos immunostaining (red). Scale bar 50µm.
B. The merge with DAPI (blue) confirms the intracellular binding.
C. This section from a similar region in the cortex, shows a negative immunostaining result for c-fos antibody.
D. This confocal photomicrograph of the cortex shows a magnified image of the positively stained neurons.
E. There was no significant difference in the number of c-fos positive immunostained cells in NMDAR-Ab and HC IgG injected mice.

5.10 TUNEL staining in human IgG injected mice

There is tissue trauma following ICV injection as shown by DAPI staining in the normal brain parenchyma. TUNEL staining was used to detect if there had been any significant apoptosis of the cortical and hippocampal tissue as a result, which could have contributed to the pathogenic effect seen. A commercial TUNEL staining kit was used (Millipore) and protocol tested on frozen post-fixed mouse brain sections to ensure it was working (Figure 5.17 A-D). The ICV injection sites and needle tracks of five mice were stained with the TUNEL protocol and kit. One out of five (Figure 5.17 E-G) showed minimal positive TUNEL staining only, the others were negative. Two mice injected with NMDAR-Ab IgG in whom there was significant levels of IgG within the hippocampus were also analysed for apoptosis. Despite the high levels of IgG binding, particularly in CA3, there was no evidence of significant or widespread apoptosis (Figure 5.17 H-M).

5.11 Discussion and limitations

This chapter describes the histological analysis of the NMDAR-Ab and HC IgG injected mice described in Chapter 4. Purified IgG had been injected into the lateral ventricle to circumvent the BBB and increase the chances of parenchymal antibody binding, with minimal brain tissue damage. The use of fluorescent beads allowed accurate identification of the site of injections. With the post-mortem human IgG staining, it was found that, after ICV injection, human NMDAR antibodies can bind in a similar manner to the distribution of NMDARs in the hippocampus. Moreover there was a significant relationship between levels of NMDAR-Ab IgG bound and seizure scores, despite the small numbers of mice examined. This analysis also gives an explanation for the low seizure score in one of the NMDAR-Ab injected mice, E22, where some problem with

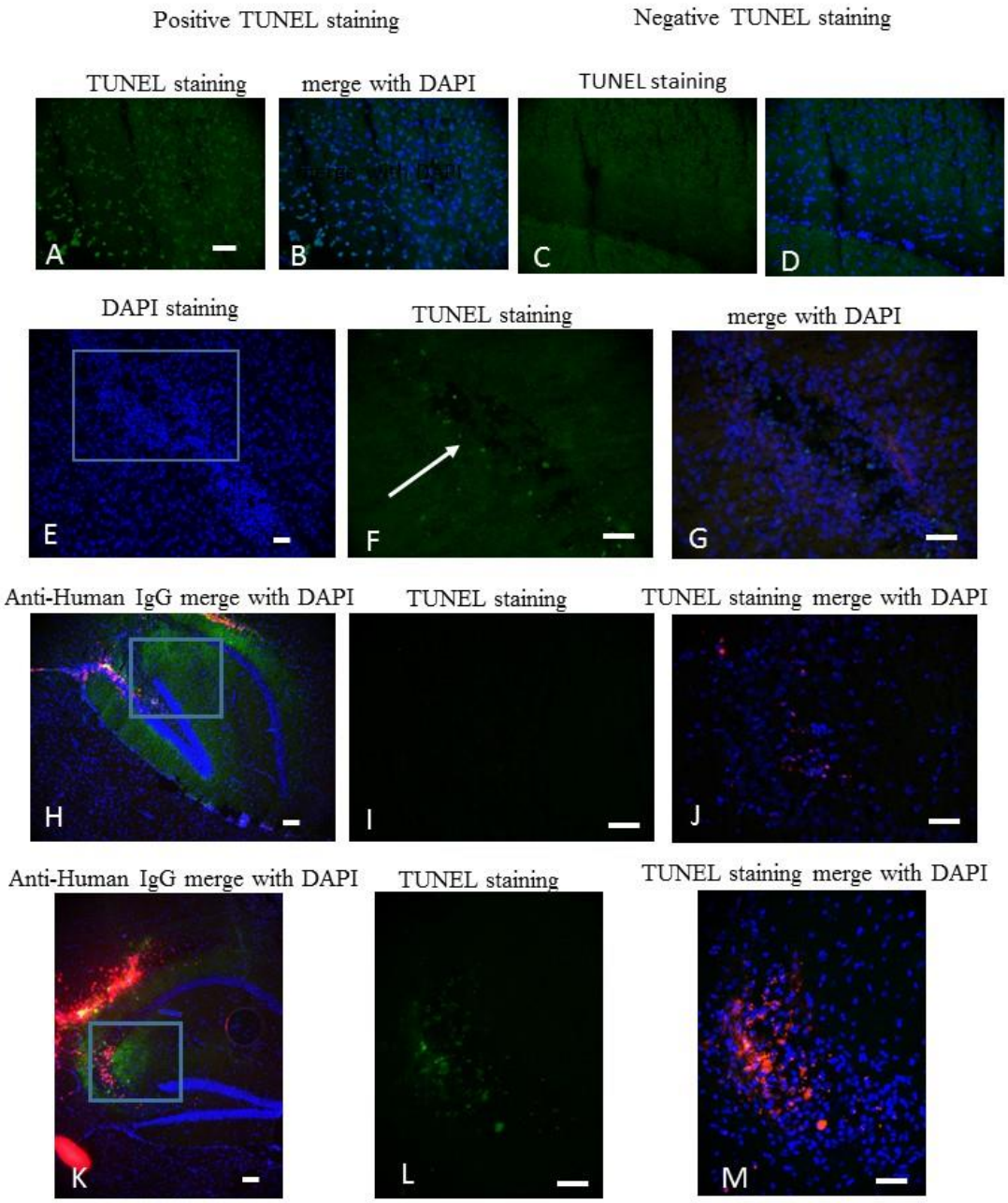

Figure 5-17 TUNEL staining of mice injected ICV with NMDAR-Ab and HC IgG.

A-D. Positivity for TUNEL staining in this cortical tissue (A) is indicated by green dotted staining throughout the affected tissue and on merge with DAPI (blue). Negative staining (C) does not have the characteristic green staining above levels of background (merge, D). Scale bar 50µm.

E-G. The disruption of the DAPI staining (blue, E) by the needle track in the cortex for the ICV injection is shown in the blue box. This area is magnified and shows some positive TUNEL staining (F, white arrow) along the needle track which does not co-localise with the injected red fluorescent beads on the merge image (G).Scale bar 50µm.

H-J. Human IgG binding of the hippocampus in mouse E15 injected with NMDAR-Ab positive IgG is positive (green, H, scale bar 100µm). The CA3 region, boxed in blue and magnified (I, scale bar 50µm) when only stained for apoptotic cells, does not show any positive TUNEL staining in this equivalent section despite the intensity of human IgG binding. This is also confirmed in the merge image with DAPI (blue) where the tracer beads are also seen (red, J, scale bar 50µm).

K-M. Human IgG binding of CA3 in mouse E23 injected with NMDAR-Ab positive IgG is positive (green, K, scale bar 100µm). The blue boxed area (K) is magnified (L, scale bar 50µm) to show no positive TUNEL staining in an equivalent section outside the intense fluorescence of the beads (red, M, scale bar 50µm) which when clumped in tissue was very strong.

the injection resulted in the lack of IgG binding. Thus, the NMDAR-Ab IgG is likely to have mediated the behavioural effects seen (Chapter 4).

Although we were able to show the binding of the NMDAR-Ab IgG was specific to regions known to express NR1, the intensity and distribution of the human IgG binding was variable. This may reflect the technical difficulties of the ICV injection following transmitter implantation, and explain the inconsistency in producing effective passive transfer of human IgG with each injection. Mouse CSF is recirculated more than 12 times a day, compared to the human rate of approximately 5 times a day. A single ICV injection, therefore, may not always produce adequate tissue penetration of the injected patient IgG. Targeted intrahippocampal injections (for example into CA3) or continuous intracerebral delivery of IgG via an osmotic pump may ensure a more consistent delivery of IgG for further experiments. However, the potential lesional effects of an intracerebral injection, and parallel placement of EEG transmitters alongside an osmotic pump device, may present additional challenges. Direct intracerebral passive transfer of IgG has been used successfully to demonstrate the pathogenicity of other neurologic antibodies in vivo, including aquaporin-4 antibodies found in NMO (Saadoun, Waters et al. 2010). Earlier passive transfer experiments in autoantibody mediated diseases were performed using repeated intraperitoneal injections of patient IgG which avoids the problem of damaging brain tissue (Toyka, Brachman et al. 1975, Lang, Molenaar et al. 1984), but are not generally considered relevant to CNS disease. Since serum levels of NMDAR-Ab are of higher titre than those in the CSF of affected patients, increasing peripheral levels of NMDAR antibodies through i.p. injections of patient IgG may be a more accurate model of the disease.

The most seizure susceptible animals showed the most intense binding in the CA3 region of the hippocampus and there was some alteration in NMDAR levels. A recent study showed mutant mice lacking NMDARs in the hippocampal CA3 pyramidal neurons were more susceptible to kainate-induced seizures and pharmacological blockade of CA3 NMDARs in adult WT mice produced similar results (Fukushima, Nakao et al. 2009). The exact mechanism for this remains unknown, but it suggests a role for NMDARs in exerting negative control over the CA3 recurrent network, and hence network excitability *in vivo*. The NMDAR-Abs seem to bind most strongly to this region. If NMDAR hypofunction occurs as a consequence of NMDAR-Ab mediated internalization of NMDARs in CA3, this may explain the seizure susceptibility.

It is unfortunate that the *ex-vivo* electrophysiology experiments detailed in Chapter 4, looking for a reduction in the inhibitory currents that would be associated with internalisation of NMDARs on inhibitory interneurons, were performed on the CA1 region. The relative lack of binding of human IgG in CA1 may explain why there was difficulty in showing an effect on recurrent inhibition electrophysiologically in this region. As the level of NMDAR-Ab IgG binding seems to be directly proportional to pathogenic effect of the antibody, a more targeted intracerebral injection of IgG directly into CA1 may demonstrate the hypothesized effect of NMDAR-Abs on the inhibitory interneurons influencing the neuronal network. In one study, targeted injections of NMDAR-Ab IgG into dorsal CA1 produced reduced expression levels of NMDARs (Mikasova, De Rossi et al. 2012). Alternatively the electrophysiology experiments could be attempted in the CA3 region.

It was found that hippocampal NMDAR IgG binding was not detectable 14 days after ICV injection. Despite this, one mouse (E53) of the four (E50-E52) who underwent repeated seizure induction after a single ICV injection, showed an increase of seizure susceptibility at this stage. There may have been a kindling effect of repeated

PTZ doses, although this is unlikely as it did not occur in the other three, and in rats, 12-14 doses of 40mg/kg PTZ given 48 hourly are needed for kindling (Rajabzadeh, Bideskan et al. 2012). In one study, pretreatment with the NMDAR antibody antagonist, MK-801, prevented the development of PTZ-induced kindling of rats (Giorgi, Orlandi et al. 1991).

Human IgG staining and analysis at D7 may be beneficial in future experiments, as two animals had their highest seizure score at this stage, and three animals showed a higher score than at day two. In previous behavioural work, Dr Pettingill has shown a maximal cognitive effect between days 5-8 after a single ICV injection (Pettingill et al.2014, *in preparation*).

The ICV injection and binding of NMDAR-Ab IgG do not appear to cause apoptosis; the results of TUNEL staining demonstrate no evidence of apoptosis either at the injection site or in areas of intense IgG binding. However TUNEL staining "kits" such as the one used here have been criticised for their limited specificity and ability to only detect some stages of apoptosis (Labat-Moleur, Guillermet et al. 1998). These problems are related to tissue processing and are encountered more frequently with heavily fixed paraffin-embedded archived sections, the results presented here were using flash frozen PBS –perfused post-fixed 12 micron sections. Further optimization of this TUNEL protocol specifically for these sections could be helpful for future analysis of experimental animals as it is possible apoptotic cells were missed.

Evidence of cell death caused by NMDAR-Ab IgG was not seen. It is possible that the antibody had a direct effect on the receptor as seen *in vitro*. In order to investigate NMDAR-hypofunction *in vivo* after a single ICV injection a commercial antibody specific for NR1 was used on sections from mice with NMDAR-Ab IgG and HC injected IgG and the results compared. The NR1 levels within the hippocampus of the most seizure susceptible mouse, E23, were altered. This preliminary results needs

further investigation with more animals and optimization of staining analysis. In previous experiments of continuous in vivo NMDAR-Ab IgG infusions into the hippocampus a reduction of NR1 levels in the hippocampus by western blot was shown (Hughes, Peng et al. 2010). Due to limited tissue availability after the staining analysis, it was not possible to perform this analysis. However, a single ICV injection does not always produce widespread IgG diffusion throughout the whole hippocampus, unlike that with continuous catheter infusion, and the method of protein analysis by Western blot of the whole hippocampus may not be as sensitive as studying each serial section of each animal as performed here.

In summary, injected NMDAR-Ab IgG was able to gain access to the brain parenchyma and bind specifically to the hippocampus *in vivo*. In the absence of apoptosis, the demonstration of a "dose-response" IgG effect, and a possibility of alteration of NR1 levels in the hippocampus, it seems likely the behavioural phenotype of seizure susceptibility seen in NMDAR-Ab IgG injected mice was caused directly by the pathogenic effects of NMDAR antibodies.

CHAPTER 6 - A potential novel treatment for NMDAR-Ab hypofunction mediated by NMDAR antibodies

6.1 Introduction

The mouse model of seizure susceptibility described in Chapters 4 and 5 demonstrated the pathogenicity of NMDAR-Abs *in vivo*. The underlying mechanism of NMDAR-Ab pathogenicity has been explored *in vitro* by others who showed loss of NMDAR surface expression on rodent hippocampal neurons in culture, resulting from cross-linking of the NMDARs by divalent antibody and subsequent internalization (Hughes, Peng et al. 2010, Moscato, Peng et al. 2014).

Standard medical treatments of patients with NMDAR-Abs concentrate on removal of circulating antibodies by plasma exchange, modifying inflammation (steroids) and reducing antibody production (Rituximab) (Titulaer, McCracken et al. 2013). In this chapter, a novel treatment hypothesis for NMDAR-Ab mediated neurological disease was investigated.

I hypothesised that if the expression of NMDAR could be increased, this might counteract the pathogenic effect of the NMDAR-Abs on the NMDAR and have therapeutic applications. Pregnenolone sulphate (PregS), is a neurosteroid, that has been shown to increase surface expression of NMDARs in primary rat neocortical cultures within ten minutes of application (Kostakis, Smith et al. 2013). I therefore set out to test this first on hippocampal neurons in culture, and then in our *in vivo* model.

6.2 Effect of PregS on NMDAR expression in untreated hippocampal neurons *in vitro*

In order to test the effect of PregS on surface expression of NMDARs *in vitro*, the drug was applied to cultured live hippocampal neurons on Day 13 *in vitro*. These were untreated hippocampal neurons and were assessed for level of surface expression of NMDARs pre- and post-application of PregS or vehicle alone. As the commercial NR1 antibodies used in chapter 5 did not bind to the NMDARs on the surface of hippocampal neurons *in vitro*, NMDAR-Ab positive plasma from patient PB was used as a 'primary antibody' to determine surface NMDAR expression.

Plasma from patient PB at a dilution of 1 in 500 was applied for one hour to;

1. Untreated hippocampal neurons
2. Hippocampal neurons that had been pre-treated for 10 minutes with 500 mM of PregS in 0.01% DMSO, and
3. Hippocampal neurons that had been pre-treated for 10 minutes with 0.01% DMSO only (vehicle).

At one hour, punctate human IgG binding was seen on the cell bodies and dendrites of untreated hippocampal neurons as expected (Figure 6.1A). The human IgG binding on the hippocampal neurons pre-treated with vehicle only showed a similar staining pattern (Figure 6.1B). However, pre-treatment with PregS increased the surface binding of the NMDAR-Ab IgG both on the cell bodies and dendrites (Figure 6.1C-F). The intensity and strength of surface binding was objectively measured by Dr Teresa Moloney rating the pictures taken of neurons in the three different conditions (blinded to the treatment), on a scale of 0-4 (where 0 was negative and 4 most intense binding). This revealed significantly higher scores in the PregS treated hippocampal neurons (n=5) compared to the DMSO and untreated cultures (n=3) (score 3.4 vs 1.3; p=0.03 Mann-Whitney).

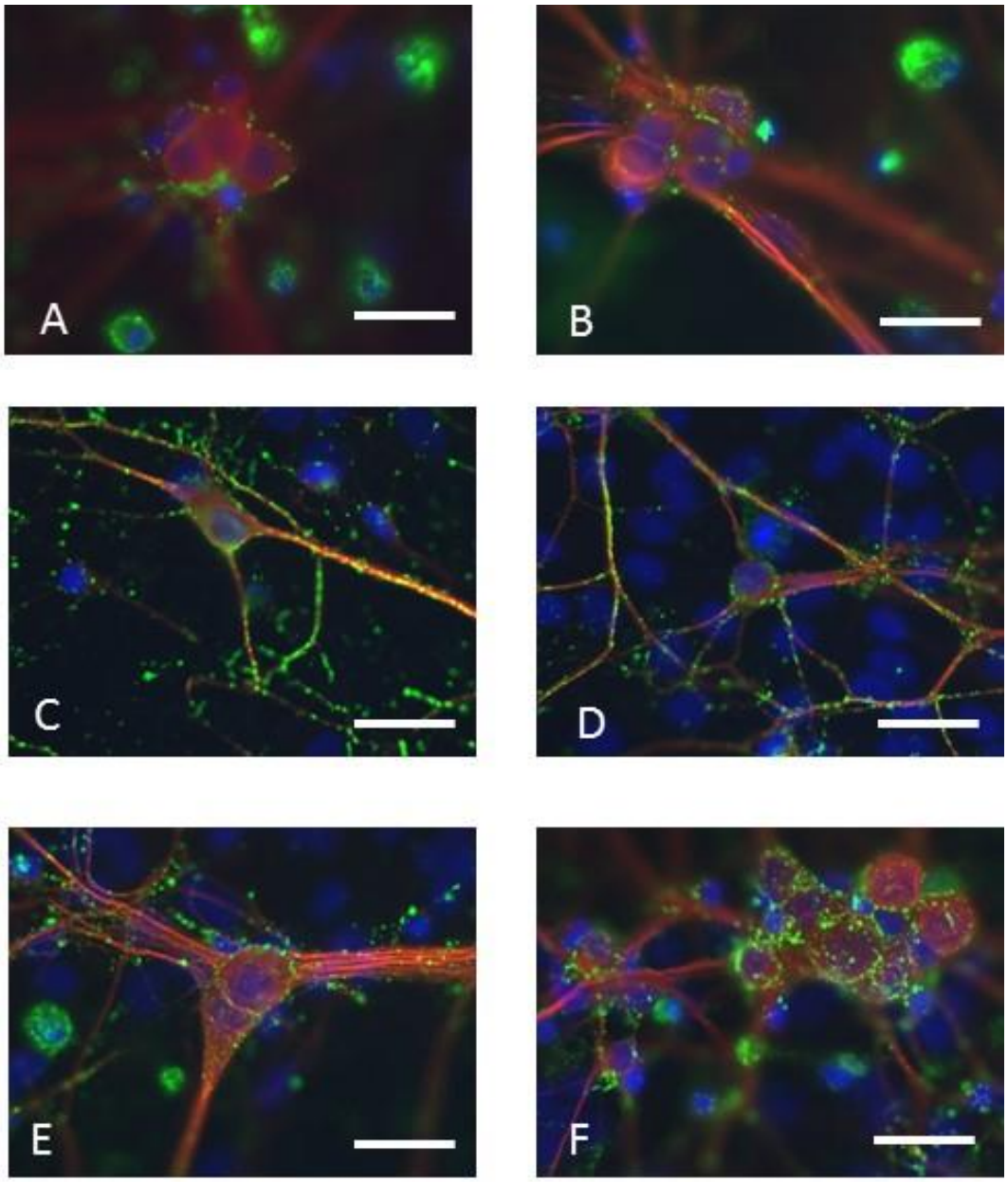

Figure 6-1 Effect of PregS treatment on Day 12 in vitro hippocampal neurons.

A. Hippocampal neurons *in vitro* stained with MAP2 (red) with human NMDAR-Ab IgG punctate binding on the cell body surface (green), (merge with DAPI, blue).These neurons were untreated before application of the NMDAR-Ab IgG used as the primary antibody. Scale bars 40µm.

B. Here, the neurons were pre-treated with the PregS vehicle only, DMSO. Similar to picture A, the neurons (stained with MAP2, red) have some cell body surface IgG binding (green) after incubation with NMDAR-Ab positive IgG.

C-F. These photomicrographs show the effect of pre-treatment of the hippocampal neurons (stained with MAP2, red) with PregS. There is an increase in the surface human IgG binding after application of NMDAR-Ab IgG used as the primary antibody (green). This punctate binding is seen on surface of the cell bodies (F) and along the dendrites (C,D). The pre-treatment with PregS has significantly increased the surface expression of NMDARs resulting in increased surface binding of the NMDAR-Ab IgG in the cell bodies and dendrites.

6.3 Effect of PregS treatment on internalisation of NMDARs in HEK cells

In order to demonstrate PregS could increase surface expression of NMDARs following internalization induced by antibody binding, an *in vitro* HEK cell assay was used. HEK cells were transfected with NR1/NR2B, similar to the cell-based assay (CBA) for NMDAR-Abs used routinely in the laboratory. The transfected HEK cells were incubated for one hour with NMDAR-Ab positive serum to stimulate internalization of the surface NMDAR-Abs. Strong human IgG surface binding (red) of HEK cells transfected with NR1 and NR2B was seen after a 1 hour incubation with NMDAR-Ab positive serum (Figure 6.3A). An extracellular mouse NR1 antibody at dilution 1:500 (Neuromab, USA) was used to demonstrate the NR1 surface expression after one hour incubation with the NMDAR-Ab positive serum. At this stage there was strong surface binding of the NR1 commercial, indicating good surface expression of NMDARs (Figure 6.3C). The cells were then washed to remove any unbound IgG and left at 37^0C with the bound NMDAR-Abs for a further 24 hours. Following this incubation, the transfected HEK cells were probed again for human IgG using an anti-human IgG secondary antibody, and the surface levels of human IgG were reduced (Figure 6.3B). The surface expression of NR1 when probed with the commercial antibody, was also reduced (Figure 6.3D). The CBA score of the NR1 commercial on the transfected HEK cells reduced from 3 to 1.5 when objectively scored by Dr Judith Cossins, blinded to the treatment conditions. These results suggest that the bound human NMDAR-Abs had caused an internalization of the surface NR1 receptors similar to previous *in vitro* experiments which have demonstrated this effect on hippocampal neurons (Hughes, Peng et al. 2010, Moscato, Peng et al. 2014).

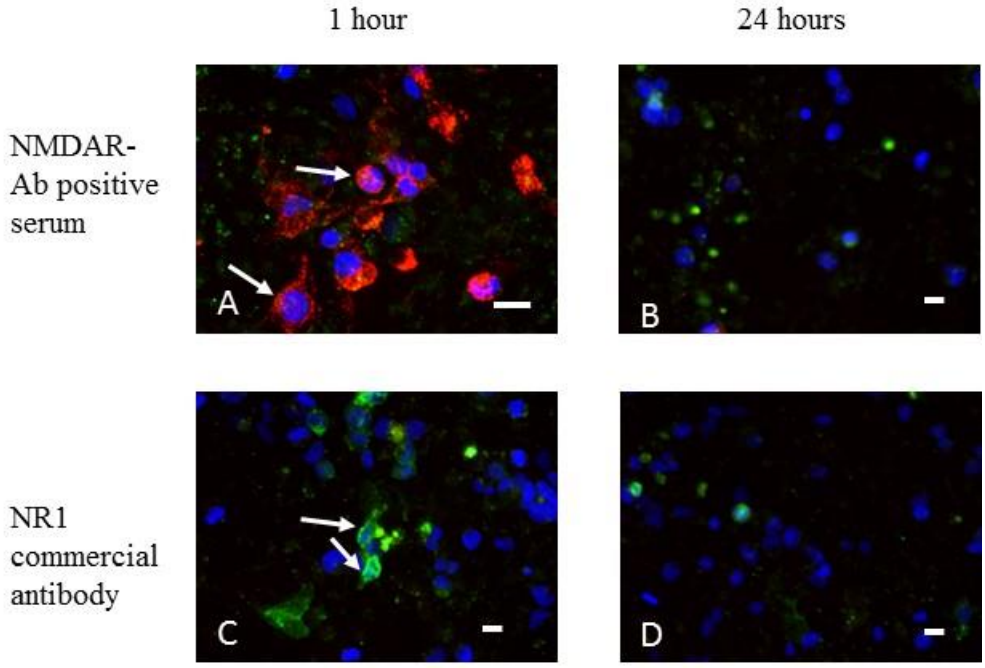

Figure 6-2 Internalisation of NMDARs in NR1/NR2B transfected HEK cells by NMDAR-Ab positive serum.

A. This shows the human IgG surface binding, detected with anti-human IgG 568 (red) after one hour incubation of the NR1/ NR2B transfected HEK cells (nuclei stained with DAPI, blue) with NMDAR-Ab positive serum. The binding is punctate and covers the surface of the cell (white arrows). Scale bars all 50µm.
B. This shows the same transfected HEK cells incubated with anti-human IgG secondary antibody (red) to detect surface human IgG binding 24 hours after application of NMDAR-Ab positive serum. There is no longer any surface human IgG detected (red) suggesting internalisation of the bound IgG-NMDAR complex.
C. Detection of surface binding of NR1 commercial antibody (green) at the beginning of the experiment, i.e. one hour after application of NMDAR-Ab positive serum. There is strong characteristic surface binding indicating good surface expression of NMDARs at this stage (indicated by white arrows).
D. At 24 hours after application of the NMDAR-Ab positive serum, re-probing of NR1 surface expression with the commercial antibody (green) reveals reduced surface expression of NMDARs on the transfected HEK cells (CBA score dropped from 3 to 1.5). This suggests internalisation of the NMDARs following incubation with the NMDAR-Ab positive serum.

Following the demonstration of reduced surface expression of NR1 after incubation with NMDAR-Ab positive serum, a ‘rescue’ treatment of this internalization was attempted using PregS. As PregS is thought to act very quickly (Kostakis, Smith et al. 2013), the internalized HEK cells were incubated for ten minutes with PregS or vehicle alone, twenty four hours after addition of the NMDAR-Ab IgG, then re-probed with the NR1 commercial. The surface expression of NMDARs was increased by PregS

treatment (Figure 6.4 B,C) but not with the vehicle alone (Figure 6.4 A). The CBA score of the transfected cells became more positive with PregS treatment to 2, in comparison to the transfected HEK cells treated with vehicle only, where the CBA score was 1, lower than following internalisation (Figure 6.4 D).

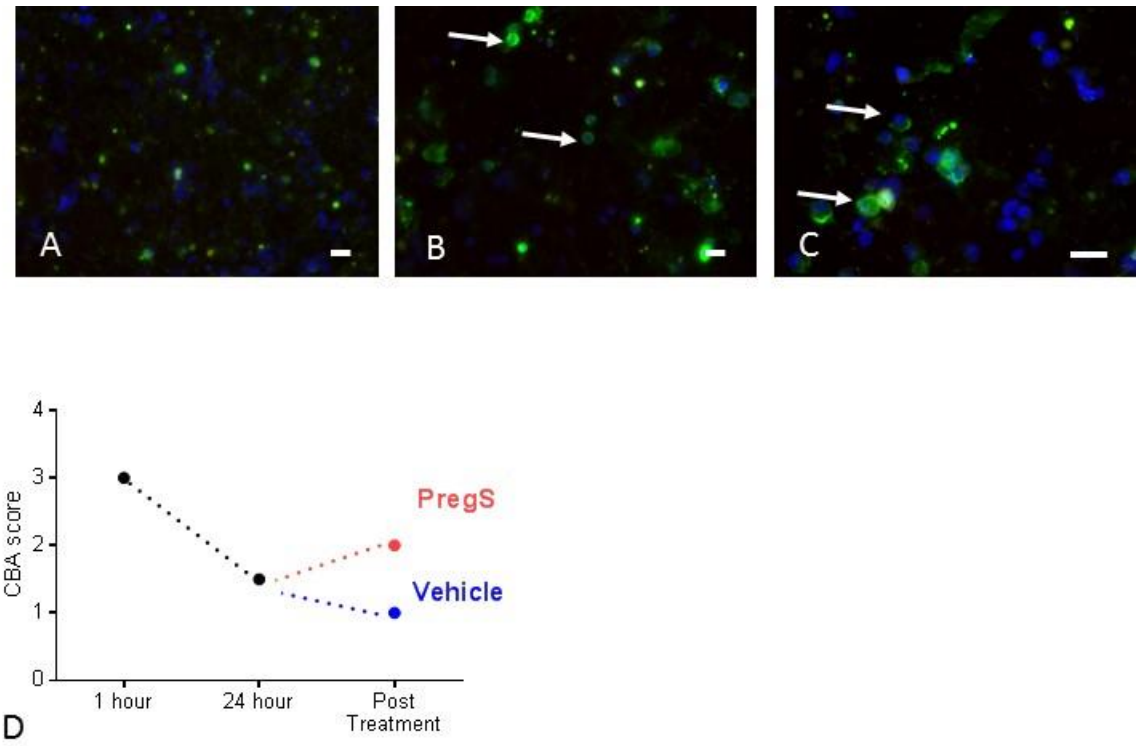

Figure 6-3 Rescue of internalisation of NMDARs by PregS treatment.

A. This shows the transfected HEK cells with internalised NMDARs after treatment with vehicle and re-probing with NR1 commercial. There is minimal characteristic surface binding of the commercial NR1 antibody in these NMDAR-Ab internalised HEK cells, suggesting the vehicle alone has had no effect on up-regulation of surface NMDAR expression. The green staining seen is background and binding to dead HEK cells. Scale bars all 50µm.
B. The results of re-probing with the NR1 commercial (green) following treatment of internalised HEK cells with PregS, are shown. There is a return of the characteristic surface binding (indicated by white arrows) although not quite to the levels seen at one hour.
C. A magnified photomicrograph of the same cells seen in B are shown here to emphasise the surface binding of NR1 (green, white arrows) following treatment of internalised HEK cells with PregS.
D. The CBA score of the transfected HEK cells following NR1 commercial antibody binding at 1 hour, 24 hours and post-treatment with either PregS or vehicle. The treatment of PregS has increased the CBA score to positive (2), the cells treated with vehicle reduced from 1.5 to 1 on the CBA scoring system.

6.4 *In vivo* treatment of NMDAR-Ab passive transfer mouse model with PregS/vehicle

After the successful *in vitro* demonstration of PregS treatment upregulating NMDAR surface expression in untreated neurons, and in internalized transfected HEK cells, further experiments were performed *in vivo* using the passive transfer mouse model (detailed in Chapters 4 and 5). NR1 expression was altered following passive transfer of NMDAR-Ab IgG in these animals and it was therefore hypothesised that reduced NR1 levels could be the cause of the increased seizure susceptibility seen with PTZ. In order to examine whether treatment to increase NMDAR expression could reduce seizure susceptibility, mice given patient Ab were then treated with PregS or vehicle alone to try and prevent the observed reduction in seizure threshold mediated by the injected NMDAR-Ab IgG.

As we were uncertain what the effects of PregS injection would be, a preliminary experiment prior to treatment with PregS in the passive transfer mouse model was carried out where unoperated C57BL/6 mice were injected i.p. with 60mg/kg of PregS dissolved in vehicle (n=2) and vehicle alone (n=2) i.p. for 3 days before seizure induction with PTZ. PregS was dissolved in 2-Hydroxypropyl-β-cyclodextrin (HP-β-CD) at 10mg/ml. These animals did not show any convulsive seizures after the 40mg/kg dose of PTZ, similar to the previous untreated C57BL/6 mice (section 4.5). Therefore, the additional treatment of PregS/vehicle did not alter the baseline seizure susceptibility.

The protocol for the first PregS *in vivo* experiment is shown in Figure 6.5 A. Six mice were injected ICV on Day 1 with NMDAR-Ab IgG (2 with patient RG, 4 with patient PB). On days 1 and 2 an i.p. injection of PregS/vehicle was given, with the third dose administered on Day 3 of the experiment, 15 minutes before seizure induction with PTZ. The observer for the 60 minute induction period was blinded to the treatment

(PregS/ vehicle) received by the mice in this and subsequent experiments. The two animals injected with RG NMDAR-Ab IgG had a seizure score (calculated at the end of 60 minute observation period post PTZ) of 9 in the vehicle treated and 3 in the PregS treated. In the mice injected with PB NMDAR-Ab IgG there was also a difference in the seizure scores between the two treatment groups. The two mice treated with PregS had seizure scores of 13 and 32 but the vehicle treated mice seizure scores were higher at 77 and 79 (Figure 6.5 B). This difference in seizure score was mainly due to the number of Stage 2 seizures which were higher in the vehicle treated group (31 and 35 in the vehicle treated group, versus 2 and 10 in the PregS treated group, Figure 6.5 C). The number of Stage 3 seizures was between 3-5 in both groups (Figure 6.5 C). On analysis of the post-mortem tissue sections there was evidence of human IgG immunofluorescent staining in all four animals injected with PB NMDAR-Ab IgG (Figure 6.5 D-G). The two mice treated with PregS both had high levels of human IgG binding in the dentate gyrus as well as CA3 with the tracer beads indicating that the ICV injection went mainly into tissue (intrahippocampal) rather than the lateral ventricle (Figure 6.5 D,E). The two mice treated with vehicle had correct placement of the ICV injection, with NMDAR-Ab IgG staining in the fimbriae and CA3 (Figure 6.5 F-G). Previously it was seen that animals with intrahippocampal injections of NMDAR-Ab IgG had a much higher seizure score than those injected ICV (Chapter 4, table 3, mouse E#7). Here, the two animals with possible intrahippocampal injected NMDAR-Ab IgG and treatment with PregS (E40 and E41) had lower seizure scores than those injected ICV and treated with vehicle (E42 and E43). Thus, there may have been a significant effect of PregS in lowering the seizure threshold in the mice that were injected with NMDAR-Ab IgG directly into the hippocampus.

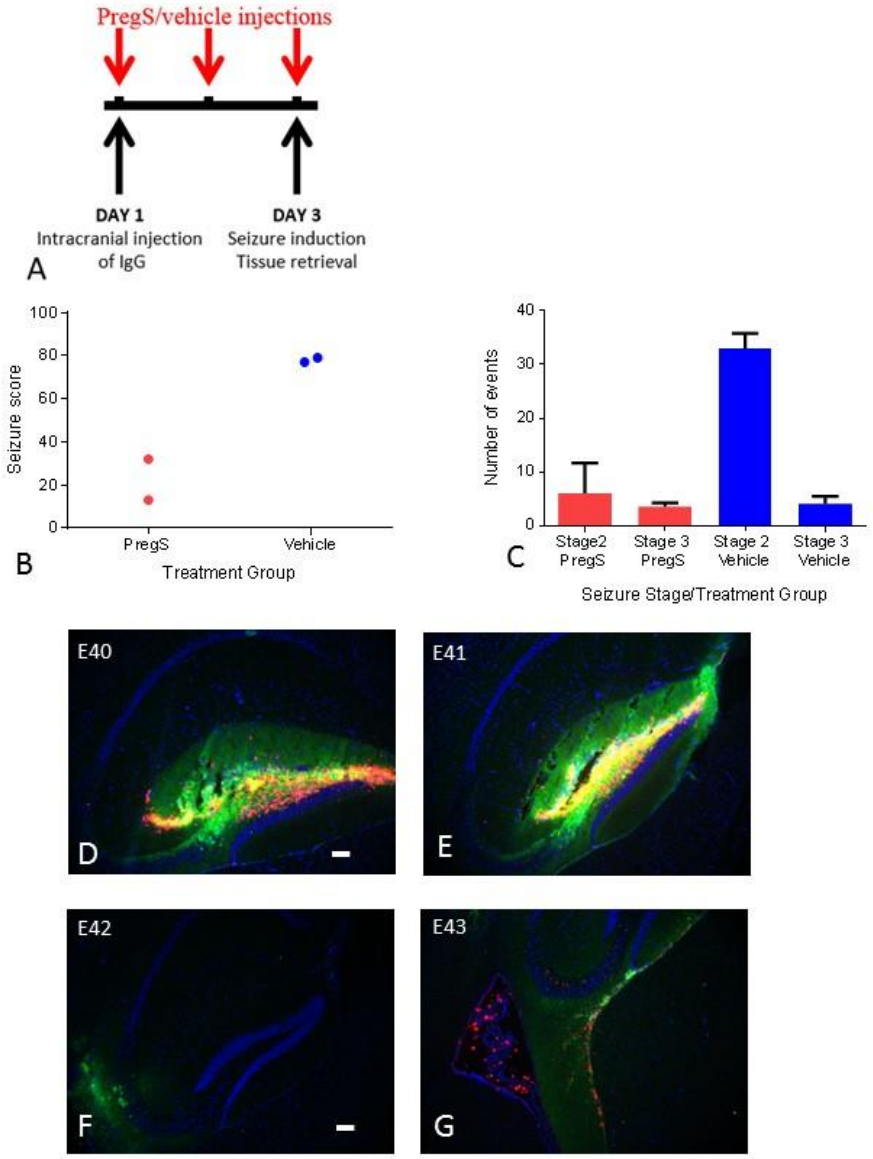

Figure 6-4 Effect of PregS/vehicle treatment on NMDAR-AB IgG passive transfer mice.

A. This schematic shows the experimental protocol followed for the first PregS/ vehicle treatment experiment on NMDAR-Ab IgG passive transfer mice. The mice received three treatment injections (red) before seizure induction on Day 3. Scale bars all 100µm.

B. The seizure scores of the four mice, injected with PB NDMAR-Ab IgG and treated with PregS/ vehicle, following seizure induction are shown in this graph. To calculate the total seizure score at the end of the 60 minute observation period post PTZ, a score of 2 is given for every Stage 2 seizure and 3 for every Stage 3 seizure, these are then totalled to give the final seizure score. The two mice treated with PregS (red) had a lower seizure score than the two treated with vehicle only (blue).

C. This graph compares the number of Stage 2 and Stage 3 seizures within each treatment group. The number of Stage 2 seizures is higher in the vehicle treated group, the number of Stage 3 seizures is similar in both groups.

D-E. These photomicrographs show the hippocampal sagittal sections of the two mice treated with PregS following passive transfer of NMDAR-Ab IgG from patient PB. They have been immunostained for human IgG (green), the pictures are merged with the DAPI (blue) image. There is human IgG binding to the molecular cell layer of the dentate and CA3. The tracer beads (red) indicate possible misplaced ICV injection.

F-G. These sections similar to D and E are from the mice treated with vehicle only. There is immunofluorescent staining of human IgG (green) in the CA3 regions in both mice. The ICV injection was into the lateral ventricle in both of these mice (red, G, E43).

6.5 *In vivo* treatment of transmitter-implanted NMDAR-Ab passive transfer mice with PregS/ vehicle

Although the number of mice used was too small for the effects to be statistically significant, there seemed to be an effect of PregS on NMDAR-Ab IgG injected animals and their seizure susceptibility. Therefore, the experiment was repeated in mice implanted with EEG transmitters (Figure 6.6). Following transmitter implantation on Day 1, the animals recovered for a week then had an ICV injection of NMDAR-Ab IgG (PB) on Day 7. PregS/ vehicle i.p. injections were given for three days with the last injection before seizure induction on Day 9.

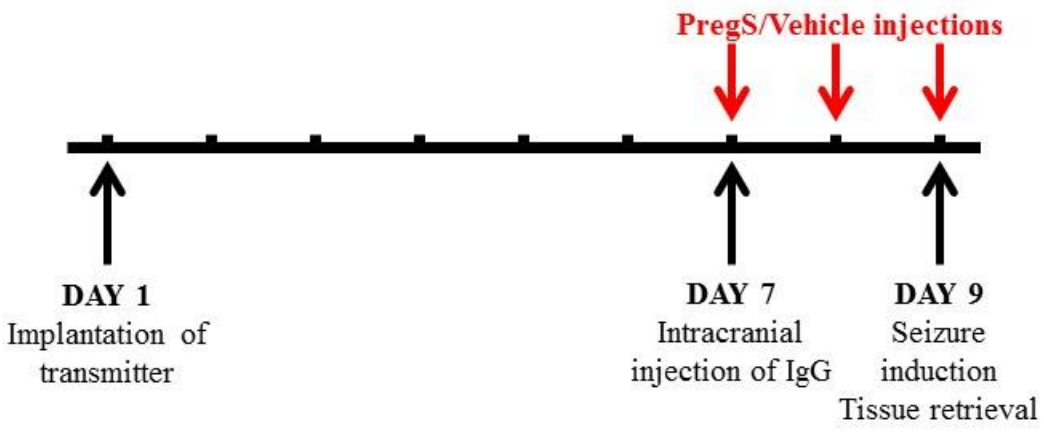

Figure 6-5 Experimental protocol for transmitter implanted mice NMDAR-Ab passive transfer mice.

This schematic shows the experimental protocol followed for the second PregS/ vehicle treatment experiment on NMDAR-Ab IgG passive transfer mice. The mice were implanted with EEG transmitters on Day 1, ICV injection on Day 7 and received three treatment injections (red) before seizure induction on Day 9.

Surprisingly, in contrast to the first passive transfer experiment, only two mice had a single Stage 2 seizure each (Table 6.1). The others showed no convulsive seizures after the sub-threshold dose of PTZ. When the mice were culled and brains examined for human IgG, there was no evidence of human IgG in CA3 of the hippocampus or any

other region in any of the six mice (Figure 6.7A-F). This was despite the fact that all ICV injections had been placed correctly into the lateral ventricle, as evidenced by the presence of red tracer beads within the lateral ventricle seen post-mortem. The failure of the NMDAR-Ab IgG to diffuse into the hippocampus from the lateral ventricle would explain why hardly any seizures were seen in these mice. Fluorescence intensity measurements of immunofluorescent staining in CA3 of all PregS/ vehicle treated passive transfer mice with or without transmitters, showed the first four mice (E40,41,42,43) had significantly higher levels of fluorescence intensity compared to the other six (p=0.016, Mann-Whitney, Figure 6.7G). Two of these had NMDAR-Ab IgG injected directly into the hippocampal tissue. As an effect of treatment was seen in these animals, a further experiment was performed in which the injection of NMDAR-Ab IgG was targeted directly into the hippocampus rather than the lateral ventricle.

Animal code number	E44	E45	E46	E47	E48	E49
Treatment	P	V	P	V	P	V
Seizure score	2	0	0	0	0	2
No. of Stage 2 seizures	1	0	0	0	0	1
No. of Stage 3 seizures	0	0	0	0	0	0

Table 6-1 The outcomes of all mice with transmitters implanted, NMDAR-Ab IgG passive transfer and PregS/vehicle treatment.

Abbreviations; P PregS; V vehicle.

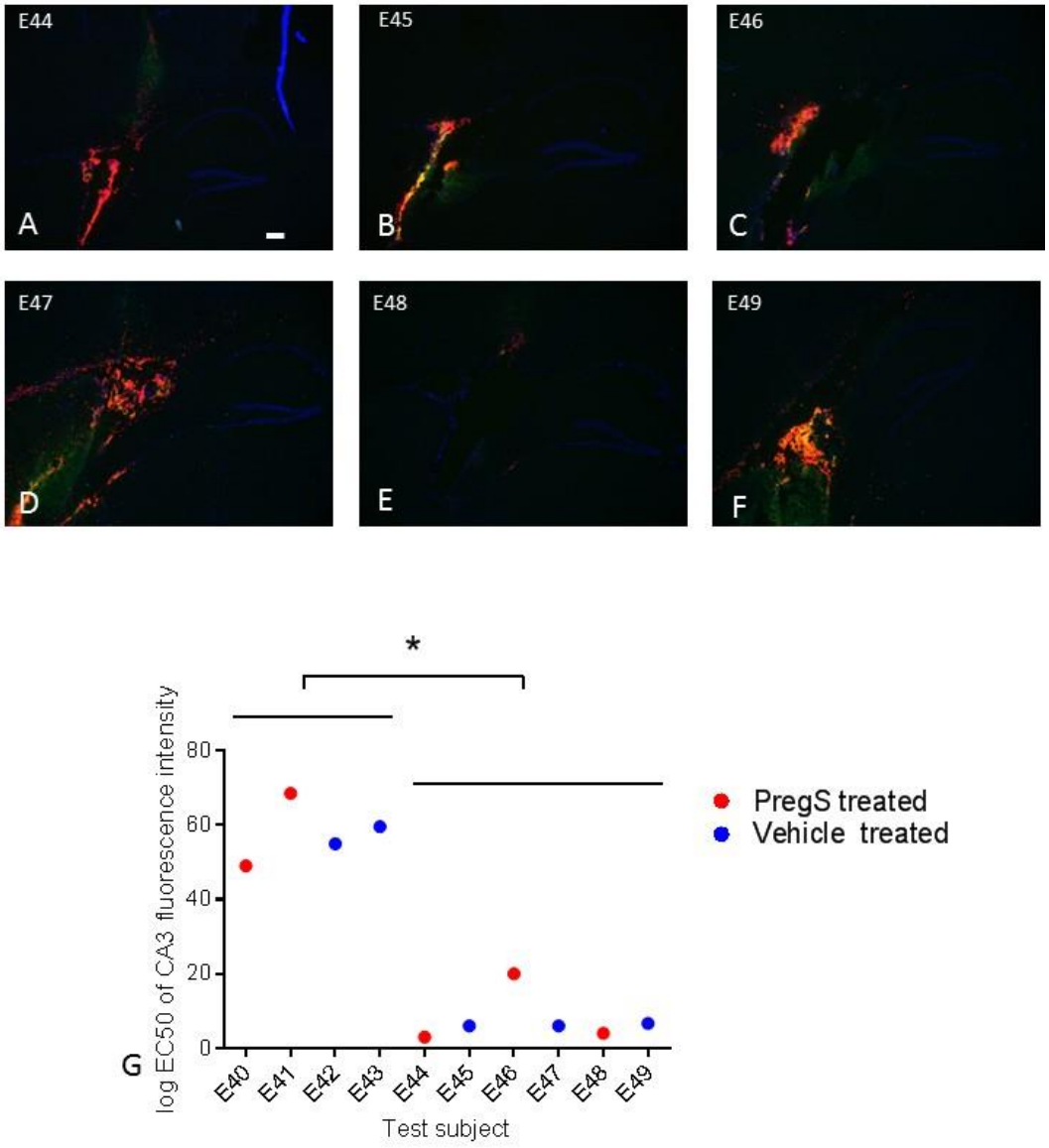

Figure 6-6 Histology and immunofluorescent staining analysis of NMDAR-Ab passive transfer mice treated with PregS/vehicle.

A-F. These photomicrographs show the hippocampal sagittal sections of all the transmitter implanted mice treated with PregS/vehicle following passive transfer of NMDAR-Ab IgG from patient PB. They have been immunostained for human IgG (green), the pictures are merged with the DAPI (blue) image. There is no human IgG binding in CA3 in any of the animals following passive transfer of NMDAR-Ab IgG. The ICV injection was into the lateral ventricle in all of the mice as indicated by the red tracer beads in the lateral ventricle. The failure of passive transfer of NMDAR-Ab IgG may explain the low seizure scores seen in the animals post-PTZ seizure induction. Scale bar 100µm.

G. In this graph, the log value of peak CA3 fluorescence intensity of human IgG immunoflourescent staining is plotted for each animal passively transferred with NMDAR-Ab IgG and treated with PregS (red dots) or vehicle (blue dots). The mice E40 to E43 show significantly higher levels of fluorescence intensity in CA3 (p=0.016, Mann-Whitney).

6.6 Intracerebral passive transfer of NMDAR-Ab IgG and treatment with PregS/ vehicle

The co-ordinates from bregma for the intracerebral injection of NMDAR-Ab IgG were revised for this set of experiments to target the dorsal CA3/fimbriae, the region in which high immunofluorescent staining levels were associated with high seizure scores in the seizure induction protocol with PTZ. Four mice were injected with NMDAR-Ab IgG on Day 1, no transmitters were implanted. Two mice received daily injections of PregS (E55, E56), the other two received vehicle injections only (E54, E57). Three injections were given, with seizure induction carried out 15 minutes after the 3rd i.p. treatment injection as previously. The number of seizures seen during the seizure induction observation period was low with two mice having no seizures at all, and no consistent pattern for PregS versus vehicle (Table 6.2).

Animal code	E54	E55	E56	E57
Treatment	V	P	P	V
Seizure score	0	9	0	4
No. of Stage 2 seizures	0	0	0	2
No. of Stage 3 seizures	0	3	0	0

Table 6-2 The outcomes of mice with intracerebral NMDAR-Ab IgG passive transfer and PregS/ vehicle treatment.

Abbreviations; P PregS, V vehicle.

To see if this lack of response to PTZ was due to failure of passive transfer, the mice were culled after PTZ induction, PBS-perfused and brain tissue harvested as previously for immunofluorescent analysis of anti-human IgG binding. Unfortunately, the brain

tissue from mouse E54, treated with vehicle, was not suitable for analysis as PBS perfusion was suboptimal due to sudden cardiac arrest of the animal with the euthatal injection. The brain tissue from mouse E56, treated with PregS, split during sectioning into pieces, and despite resectioning with these pieces re-embedded in Tissue-Tek® (Sakura), the landmarks were variable and difficult to compare to the others. This left one brain from each group to analyse (E55 and E57). Disappointingly, there was very little human IgG staining in these brains despite the injection of NDMAR-Ab IgG directly into the hippocampus (Figure 6.8).

Animal code	E54	E55	E56	E57
Treatment	V	P	P	V
Seizure score	0	9	0	4
No. of Stage 2 seizures	0	0	0	2
No. of Stage 3 seizures	0	3	0	0

Table 2. The outcomes of mice with intracerebral NMDAR-Ab IgG passive transfer and PregS/vehicle treatment.
Abbreviations; P PregS, V vehicle.

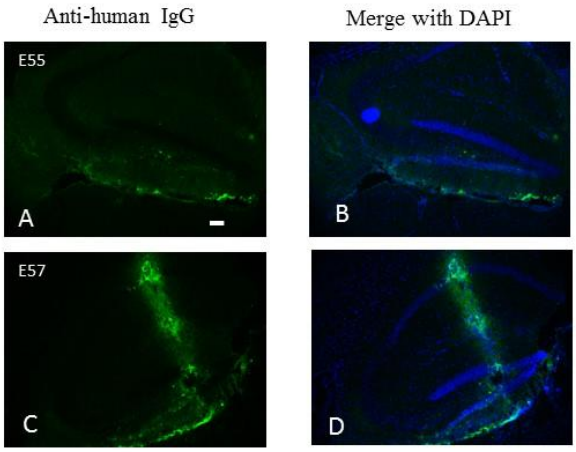

Figure 6-7 Intracerebral passive transfer of NMDAR-Ab IgG.

A-B. This sagittal section of the hippocampus of mouse E55 shows minimal human IgG immunostaining (green) despite the intrahippocampal injection of NMDAR-Ab IgG. This is confirmed on the merge with DAPI (blue, B). Scale bar 100µm.

C-D. This hippocampal sagittal section of mouse E57, similarly injected with NMDAR-Ab IgG into the hippocampus does not show diffuse binding of human IgG (green) throughout the hippocampus as was expected from the site of injection. D shows the merge with DAPI (blue).

6.7 Discussion and limitations

This chapter describes the results of preliminary *in vitro* and *in vivo* experiments exploring a novel treatment for NMDAR-Ab mediated neurological disease. PregS is a neurosteroid that has direct effects on the NMDAR at the membrane level. One of these particular effects, to increase the surface expression of NMDARs, was effective in NR1 transfected HEK cells *in vitro* where surface NMDARs had been internalized by NMDAR-Abs. Despite initial promising results *in vivo* demonstrating a potential rescue of the increased seizure susceptibility in NMDAR-Ab passive transfer mice, this effect was not reproducible.

Seizure susceptibility was seen to be increased in the mouse model of passive transfer of NMDAR-Ab IgG into the lateral ventricle (Chapter 4). There was a strong correlation between the amount of NMDAR-Ab IgG diffused into the hippocampus and seizure susceptibility (Chapter 5). However, there was also marked variability in the amount of IgG binding to tissue despite the same passive transfer process (ICV injection). Therefore, this mouse model may not be the most robust and reproducible model for trial of a therapeutic drug.

In the PregS/ vehicle treatment experiments, there was considerable failure of NMDAR-Ab IgG diffusion into the hippocampus even when the ICV injection was in the correct place, and when the IgG was injected directly into the tissue. Apart from standard experimental error, for example IgG not taken up correctly, the only difference in these set of experiments was the treatment with PregS/ vehicle following passive transfer. This raises the possibility that poor IgG diffusion was caused by the only common agent used which was the vehicle for PregS, 2-Hydroxypropyl-β-cyclodextrin (HP-β-CD). This cyclodextrin belongs to a family of cyclic oligosaccharides with a

hydrophobic interior cavity and relatively hydrophilic exterior surface. For this reason, cyclodextrins are widely used for their ability to increase the solubility of poorly water-soluble drugs (Davis and Brewster 2004). HP-β-CD is also known to form complexes with cholesterol and *in vitro* studies have shown it is highly efficient in extracting cholesterol cell membranes in various cell types (Ohtani, Irie et al. 1989, Liu, Cogny et al. 2003). This effect has been exploited therapeutically. HP-β-CD has proved an effective treatment in the genetic condition Niemann-Pick-C (NPC), a neurodegenerative rare disease with disruption to the intracellular trafficking of cholesterol and other lipids, leading to accumulation in the CNS and other organs (Ottinger, Kao et al. 2014). Interestingly, the first suggestion of this therapeutic effect was seen when HP-β-CD was used as the vehicle in a trial of allopregnanolone, another neurosteroid, as a therapeutic agent in a NPC mouse model (Griffin, Gong et al. 2004). The doubling of lifespan seen in the NPC mouse was subsequently shown to be due to the HP-β-CD alone rather than the allopregnanolone (Davidson, Ali et al. 2009). The exact mechanism of HP-β-CD's action in NPC is still unknown and the subject of ongoing research. However, the removal of cholesterol from cell membranes may also have unforeseen *negative* physiological effects. Cyclodextrins can cause loss of cell viability and cell morphology in endothelial cell lines (Kline, O'Connor Butler et al. 2010) and potentially disrupt membrane receptor function by affecting membrane fluidity (Sooksawate and Simmonds 2001). This could theoretically affect the diffusion of IgG across the BBB in view of HP-β-CD's effect on the vascular endothelial cell membrane, although given HP-β-CD does not cross the BBB (Pontikis, Davidson et al. 2013) there is unlikely to be a direct effect on neuronal cell membranes and receptors as it was delivered systemically by i.p. injection. This may also have limited the PregS delivery across the BBB. PregS has been shown to be acutely effective when given directly into the lateral cerebral ventricle in some animal experiments (Mathis, Paul et

al. 1994), which could offer an alternative route of administration in this model. However a different vehicle other than HP-β-CD would be appropriate.

As mentioned in the introduction, the main effects of PregS are reported to be on the NMDAR, however, it is also a negative allosteric modulator of the $GABA_AR$ and acute effects here and on other receptors may have affected the results.

The precursor to PregS, pregnenolone has also been used effectively in other animal models of NMDAR hypofunction, i.e. schizophrenia (Wong, Chang et al. 2012). Acute and chronic administration of pregnenolone effectively alleviated both positive and negative schizophrenia-like symptoms (Wong, Chang et al. 2012). It may be that delivery of pregnenolone could prove more effective than PregS in the passive transfer NMDAR-Ab IgG mouse model. In fact, it is pregnenolone that has been used safely and effectively in human patients in drug trials for schizophrenia (Marx, Lee et al. 2014). In this placebo-controlled trial, the number of participants experiencing treatment-emergent adverse events was comparable in the placebo and pregnenolone groups (58 vs 55%, respectively). Overall, pregnenolone was well tolerated in doses up to 500mg four times a day. There are currently six trials in the USA recruiting patients in treatment trials of pregnenolone for a variety of indications including autism, schizophrenia and traumatic brain injury (source: clinicaltrials.gov), no clinical trials have been published of the use of pregnenolone in children. Oral administration of pregnenolone results in elevated serum pregnenolone sulphate levels (Marx, Lee et al. 2014). In the USA, pregnenolone is considered a ‘dietary supplement’ and supplies for drug trials are provided with certificates of analysis. The supplement is also available to buy from on-line retailers, but there is no current UK medicines supplier or importer.

Despite the disappointing effect *in vivo*, the *in vitro* effect of the neurosteroid PregS points to a potential beneficial effect of these drugs in alleviating symptoms caused by NMDAR-Ab internalization in patients positive for NMDAR-Abs.

CHAPTER 7 - Final discussion

The results of this thesis have shown that CNS autoantibodies are present in approximately 11% of paediatric patients with new-onset epilepsy and seizures. The CNS autoantibodies are most commonly found in children with focal epilepsy of unknown cause, and in some cases can lead to long-term intractable epilepsy. Novel autoantibody associations were made in selected phenotypes, notably CSWS. However, none of the patients were treated with immunotherapy and a good outcome was seen in the majority with standard AED treatment.

With an *in vivo* mouse passive transfer model of NMDAR-Ab IgG, the epileptogenic properties of CNS autoantibodies were demonstrated. The effect on seizure susceptibility was directly proportional to the amount of NMDAR-Ab IgG bound in the hippocampus.

On confirmation *in vitro* of the underlying mechanism for epileptogenesis in NMDAR-Abs, i.e. NMDAR internalization and hypofunction, this effect was reversed by PregS, a neurosteroid proven to have specific NMDAR effects.
These findings have important implications for the field of CNS autoantibodies in neurological disease and are discussed below.

7.1 "Autoimmune epilepsy – is there a specific phenotype in children?"

Given the dramatic changes in brain maturation that take place between birth and 18 years of age, it is not unexpected that neurological diseases such as epilepsy are different in children compared to adults. Specific forms of epilepsies only occur in the developing brain, and some resolve completely before reaching adulthood. Therefore, it was surprising to find that the presence of CNS autoantibodies in paediatric epilepsy

patients was shown to be similar to that of adult epilepsy, with just over one in ten patients positive. Given the existence of immune therapy responsive epilepsy syndromes in childhood, one might have expected a higher rate of antibody positivity. However, the antigenic targets for these antibodies do show a difference. For example, LGI1 antibodies found in the adult "autoimmune epilepsy," FBDS, were not found in any paediatric epilepsy patients. Instead, antibodies to the other VGKC-complex proteins, CASPR2 and contactin-2, were found in more significant numbers. Human and animal data has shown that CASPR2 is integrally associated with neuronal connectivity, interneuron development/ function, synaptic organization and activity and neuronal migration in the developing brain (Rodenas-Cuadrado, Ho et al. 2014). The neurobiological effects of CASPR2 loss or dysfunction in animals models are spontaneous seizures, increased stereotyped and repetitive behaviour and decreased socialization; in effect, a similar phenotype seen in CSWS spectrum patients, some of whom are CASPR2 antibody positive.

In a recent study characterizing neuronal antibody positive epilepsy in adults, there was no difference in seizure semiology or characteristics between antibody negative and positive patients (Iorio, Assenza et al. 2014). This was similar to the findings in paediatric epilepsy, where the only significant difference was the higher frequency of status epilepticus in antibody positive patients. In the adults, there was a difference in the paraclinical investigations, with significantly higher frequency of T2-hyperintense lesions on brain MRI and in increased CSF IgG index (Iorio, Assenza et al. 2014). The authors suggested that the combination of neuronal autoantibodies and these positive investigations may lead to the recognition of autoimmune epilepsies. However, in some of these patients there were additional features, for example, mild cognitive impairment, visual hallucinations, pharmacoresistance seizures and tumours that may have contributed to the inflammatory changes seen, particularly in epilepsy associated

with an autoimmune encephalitis. In the paediatric epilepsy patients studied here, there was no consistent imaging or CSF biomarker to aid the diagnosis of paediatric "autoimmune epilepsy", and no specific phenotype.

There was, however, an increased number of antibody positive patients with focal epilepsy of unknown cause compared to epilepsies with a known aetiology, which was similar to a recent adult epilepsy study (Brenner, Sills et al. 2013). In routine paediatric epilepsy practice, these would be the target population to test in the future for autoantibodies (Suleiman, Wright et al. 2013).

Children are not just "little adults" and the autoantibody results in paediatric epilepsy reflect this. Different antigenic targets, some of which remain unknown, are more relevant in this population and future studies may define an 'autoimmune epilepsy' phenotype that is distinct from adults.

7.2 Serum testing of antibodies – is timing important?

Testing for CNS autoantibodies as soon as possible after disease onset is important when trying to prove an association that could be potentially pathogenic. This study, in contrast to previous studies, tested all the new-onset epilepsy patients in the early stages of disease (less than six months). Samples taken six and twelve months after the start of the epilepsy were also tested. It was found that neuronal antibodies to the VGKC-complex did not develop during the course of the epilepsy as only those patients positive at intake for VGKC-complex antibodies remained positive six to twelve months later. This is important as it suggests that VGKC-complex antibodies do not develop as a *consequence* of epilepsy and are unlikely to represent an epiphenomena in this group of patients. This result may also increase the "window of opportunity" in detecting a relevant positive VGKC-complex antibody result to a year after disease onset.

In contrast to this, NMDAR-Abs were detected during the course of epilepsy, even when patients initially tested negative. Recent studies have also shown the development of high levels of NMDARs post HSVE. The antibodies are thought to be pathogenic as patients display a neurological deterioration with movement disorder, behavioural change, seizures, and worsening of brain lesions on MRI, with no evidence of reactivation of the herpes simplex virus (Hacohen, Deiva et al. 2014). In our patients there was no definite clinical deterioration or phenotypic change suggestive of NMDAR-Ab encephalitis, although this was not specifically asked for at the time of the study in the 1990's. Patients would have been seen only in outpatient clinics, and no details were available of acute hospital admissions. In HSVE relapse, NMDAR-Ab positive patients improve with early immunotherapy (Mohammad, Sinclair et al. 2014), and this demonstrates the importance of testing for NMDAR-Abs if a patient presents with specific neurological features, even in the context of another illness, as they can be effectively treated.

Although a positive CNS autoantibody result late into a disease process may not represent a direct causation, in paediatric epilepsy it is unlikely to be irrelevant. As evidenced from the association with NMDAR-Ab mediated HSVE relapse, the pathogenic effects of neuronal antibodies may contribute to the clinical features, and are amenable to treatment.

7.3 Serum testing of antibodies – relevance of "low positives"?

Most of the serum samples tested in the paediatric epilepsy patients had lower levels of antibodies than those seen in autoimmune encephalitis patients, which may cast doubt on their clinical significance. This was particularly significant for NMDAR-Abs, where antibody levels were significantly lower in epilepsy compared to encephalitis (Figure

3.9). However, in the VGKC-complex antibody positive epilepsy patients (Dutch cohort), there was a “dose-response” effect; patients with the highest titres of antibody had the poorest outcomes suggesting that the Abs were significant factors in their disease.

A recent audit of NMDAR-Ab results in autoimmune diseases in the Oxford Laboratory looked at 1039 patients between 2008-2012 that had sera sent for NMDAR-Ab testing. A total of 56 patients had a “low positive” result. Analysis of the clinical records found these low levels of NMDAR-Abs present in “definite NMDAR-Ab non-paraneoplastic encephalitis” (7/16; 44%), “possible NMDAR-Ab mediated disease” (13/18; 72%) and in “unlikely NMDAR-Ab mediated or autoimmune disease” (11/13; 84%) (Zandi, Paterson et al. 2014). There were no “low positives” in the “definite NMDAR-Ab mediated paraneoplastic encephalitis” patients (n=9) which included eight females with ovarian teratomas, all of whom (with available clinical data) had four to six of the core clinical features (encephalopathy, psychiatric symptoms, cognitive symptoms, seizures, extrapyramidal movement disorder and inflammatory CSF).
As with the NMDAR-Ab positive paediatric epilepsy patients, who present with seizures only, the number of core features was significantly lower in the “low positive” group, suggesting a dose response effect. This would also explain the higher NMDAR-Ab levels seen in the paediatric NMDAR-Ab encephalitis as they have more symptoms than just epilepsy.

Importantly, the Oxford audit included NMDAR-Ab CBA test results that were scored 1 as “low positive”. From 2011 and in the assays performed for this thesis, a score of 1 was deemed negative, and 1.5 used as “low positive”. In the Oxford audit, using this cut-off would have decreased the number of “unlikely NMDAR-Ab mediated or autoimmune disease” cases from eleven to five, thus increasing the specificity (Zandi, Paterson et al. 2014). Response to immunotherapy was seen in all “low

positive" patients with "definite" disease (judged by the clinician) and this, most importantly, demonstrates that the clinical features and presentation of a patient outweigh the significance of antibody levels.

7.4 Serum or CSF testing of autoantibodies?

Controversy exists over the relative significance of CSF versus serum antibody levels (Gresa-Arribas, Titulaer et al. 2014). This may be due to assay technique; use of the live cell CBA in Oxford finds higher serum levels of antibody than CSF levels in paired samples; other laboratories using fixed and permeabilised cells in the assay report, on occasion, positive CSF antibodies with negative serum antibodies (Gresa-Arribas, Titulaer et al. 2014).

All antibody testing in this thesis was done on serum samples, no CSF samples were available. This was because the epilepsy patients tested (particularly the Dutch cohort) were an outpatient group with a stable neurological condition. In paediatric epilepsy, the main indication for a "routine" CSF would be to obtain a ratio of CSF to blood glucose for the diagnosis of glucose transporter-1 deficiency syndrome. This disorder, caused by mutations in the *SLC2A1* gene in most patients, results in impaired glucose transport into the brain (Leen, Klepper et al. 2010), and presents with epilepsy in 85% of patients. The diagnosis is crucial as the ketogenic diet can be effective in over 80% of affected patients. Apart from investigation for this aetiology, a lumbar puncture for CSF examination is not performed in the routine investigation of paediatric epilepsy, hence the lack of CSF samples for testing from this cohort. It is disappointing, however, that no CSFs were available from the Australian study as these patients were hospitalized and more severe; 101 out of the 112 patients were admitted to the hospital during their initial presentation or during the first six months after seizure onset. If

paired serum/ CSF samples had been available for these cohorts this may have increased the sensitivity and specificity of the positive serum neuronal autoantibody results. However, given that CNS autoantibody mediated diseases respond well (and sometimes completely) to early *systemic* removal of antibodies by PLEX (Wright, Hacohen et al., 2014), and peripheral production of antibodies is often stimulated by a *systemic* tumour (e.g. ovarian tumour), the pathogenicity and significance of serum neuronal autoantibodies is clear. Nevertheless, intrathecal synthesis of CNS autoantibodies is seen with most antibody-mediated diseases and is an important indicator of disease progress, particularly if serum levels have been abrogated by immunotherapy. For autoimmune encephalitis, the provision of both serum and CSF samples for testing is optimal because it can be an important guiding factor for the length and extent of immunotherapy treatment and help predict or assess relapses (Irani, Gelfand et al. 2014). For epilepsy patients however, this is not yet well established. Ideally, testing prospectively collected paired CSF and serum samples from epilepsy patients along with tissue-based and neuronal culture assays would help to determine the significance of serum testing alone. This may be more feasible in adults rather than children where a lumbar puncture is a more involved procedure often requiring sedation.

7.5 "Autoimmune epilepsy"- should the diagnosis be based on response to immunotherapy?

In the long-term outcomes of the Dutch paediatric epilepsy cohort, the antibody positive patients had the same rate of seizure freedom at five years (73%), and rate of intractability as the antibody negative patients. None of the antibody positive patients in either Dutch or Australian cohort were treated with immunotherapy so we cannot know

if immunotherapy would have helped further improve the outcome of antibody positive epilepsy patients. However, two out of ten patients intractable to AEDs with an unknown cause for their epilepsy were antibody positive and we can speculate that immunotherapy would have helped these. There is some evidence that in adults, antibody positive epilepsy patients are more likely to be AED resistant (Brenner, Sills et al. 2013). Another recent study showed that AED-resistant epilepsies in adults respond well to immunotherapy, a significant number of these were antibody positive (75% achieved greater than 50% seizure reduction) (Iorio, Assenza et al. 2014). Despite stating that that no patient had clinical characteristics of limbic encephalitis, the inclusion criteria for one of the groups was an associated clinical feature which included psychiatric disturbance, movement disorder, cognitive impairment- all symptoms of autoimmune encephalitis. The seizures may well have improved with immunotherapy in this group due to the clinical overlap with autoimmune encephalitis, an immunotherapy responsive condition.

Another study suggested that a trial of immunotherapy in suspected autoimmune epilepsy was useful in confirming the diagnosis (Toledano, Britton et al. 2014). This was a retrospective study and also included patients who had a significant clinical overlap with autoimmune encephalitis. The most likely to respond were those patients with neuronal autoantibodies (87.5%), although 33% (2/6) patients without detectable antibodies also responded. This is not surprising as it has been previously shown that clinically diagnosed autoantibody negative paediatric autoimmune encephalitis patients also respond to immunotherapy (Hacohen, Wright et al. 2013).

Historically, unlike paediatric epilepsy patients, adults have rarely been treated for epilepsy with immunotherapy. With the increased awareness of neuronal antibodies and the role of the immune system in the pathogenesis of epilepsy at any age, there is more acceptance that the use of immunotherapy may be beneficial in epilepsy. The

beneficial effects of treating adult "autoimmune epilepsy" may just be a result of treating the often accompanying autoimmune encephalitis or the neuroinflammation that is a sequelae of chronic epilepsy and and/or seizures, regardless of the suspected "autoimmune" aetiology. The two trials that have successfully treated "autoimmune epilepsy" with immunotherapy are small in number and have failed to consistently include other control groups that might respond just as well, i.e. medically intractable epilepsy with *no* evidence of antibodies, or a placebo arm.

In paediatrics, West syndrome and CSWS respond to immunotherapy though these are not labelled "autoimmune epilepsy". The concern is that this label, in adults and children, may lead the clinician to escalate immunotherapy to chronic immunosupression with secondary agents that have additional side effects. In some cases this may help if the correct component of the immune system is being targeted, if not the immunosuppression may actually cause harm.

A consensus on the definition of "autoimmune epilepsy" is urgently required. This definition will be different for adults and children. Adult patients with this diagnosis are more likely to have "autoimmune encephalitis with seizure predominance". This is a more descriptive term acknowledging the additional features so frequently described in autoimmune epilepsy patients and would ensure patients receive the correct management.

Notably, the ILAE have recently included "immune" as an aetiology in the ILAE Revised Terminology for Organisation of Seizures and Epilepsies 2011-2013 (Appendix 4). In the accompanying report, they state that;

"an immune aetiology can be conceptualized as where there is evidence of autoimmune-mediated central nervous system inflammation…..Examples include anti-NMDA receptor encephalitis and anti-LGI1 encephalitis. With the emergence of these entities,

this etiological subgroup deserves a special category particularly given the treatment implications with targeted immunotherapies".

From this it can be implied, as stated above, that targeted immunotherapies should be reserved for those patients who have recurrent seizures within the context of an autoantibody mediated encephalitis. The diagnosis of autoimmune encephalitis should be made first, prior to consideration of immunotherapy. Most of the antibody positive paediatric epilepsy patients in this study do not fulfil this criteria and immunotherapy is not justified, and this is confirmed by the fact that the majority improved with standard therapies.

The only caveat to this with regards to treatment is that some antibody mediated disease can naturally show a benign course with a monophasic illness and spontaneous resolution. This was first described in a VGKC–complex antibody positive patient with non-paraneoplastic LE, in whom antibodies fell spontaneously over two years, with almost complete recovery of function (Buckley, Oger et al. 2001). This patient received no immunotherapy. In a cohort of paediatric autoimmune encephalitis, four patients recovered without immunotherapy (Hacohen, Wright et al. 2013). More recently, two cases of LGI1-Ab positive LE (one with FBDS) also became seizure free and spontaneously recovered with only mild/moderate cognitive impairment, without immunotherapy (Szots, Marton et al. 2014). These cases were all retrospectively identified but are important to report, as it suggests a minority of "immunotherapy treatment responses" may actually represent natural spontaneous resolution of disease. However, as in our antibody positive patients, complete resolution of symptoms may have been achieved if these patients had been identified and treated early with immunotherapy.

Currently, in clinical practice there is no doubt that acute seizures as part of an autoimmune encephalitic illness should be treated with first and second line

immunotherapy regimes. As these seizures, even if recurrent, would be considered ‘provoked’, or ‘acute symptomatic’ they may not fulfil the recently revised ILAE criteria for the definition of epilepsy and hence “autoimmune epilepsy” (Fisher, Acevedo et al. 2014).

Patients who develop seizures following autoimmune encephalitis have an enduring risk for unprovoked seizures following the brain insult that accompanies autoimmune encephalitis, and would be considered ‘epileptic’. The treatment data for these patients is limited, but suggests that up to 50% continue to have pharmacoresistant seizures at long term follow-up (Sarkis, Nehme et al. 2014).

Finally, as demonstrated in this thesis, there appears to be a small subset of paediatric as well as adult epilepsy patients with “focal epilepsy of unknown cause” that are neuronal autoantibody positive suggesting an aetiological cause. Therefore the significance of the positive antibodies within the context of epilepsy aetiology was explored in the animal passive transfer experiments.

7.6 CNS autoantibodies – are they epileptogenic?

Passive transfer of NMDAR-Ab IgG into the lateral cerebral ventricle of C57BL/6 mice allowed diffusion of the NMDAR-Abs into the hippocampus where they bound specifically in CA3 and the dentate gyrus. These mice showed a lower convulsive seizure threshold when challenged with the chemoconvulsant PTZ. The mice with the highest hippocampal levels of NMDAR-Abs were the most seizure susceptible. However, although the NMDAR-Abs altered the seizure threshold in this model, no spontaneous seizures were seen, so they cannot be thought of as causing “epilepsy”. Epileptogenesis is a process where the previously normal brain is functionally altered and biased towards the generation of aberrant and abnormal electrical activity

predisposing to the development of chronic seizures (Goldberg and Coulter 2013). From the results of the passive transfer experiments, we have shown that NMDAR-Abs are pathogenic and 'epileptogenic', in terms of increased seizure susceptibility. The likely mechanism underlying this is NMDAR hypofunction; an identical effect of seizure susceptibility is seen in NR1 knockdown mice (Duncan, Inada et al. 2010). Even in these mice with 85% reduction of NR1 there are no spontaneous seizures. It appears that like some genetic mutations, NMDAR autoantibodies are a risk factor/ co-factor for the development of seizures and epilepsy but not directly causative alone. This is further suggested by the identification of both genetic mutations and NMDAR-Abs in "healthy controls" with no epilepsy. Additional factors are required to precipitate the disease state.

The pathogenic mechanisms of the NMDAR-Abs are directly related to receptor function and do not include the brain inflammation that is seen in patients with VGKC-complex/LGI1 antibodies (Bien, Vincent et al. 2012). As well as the association with autoimmune encephalitis, LGI1 antibodies are thought to mediate FBDS, an epilepsy characterized by brief, dystonic seizures (Irani, Michell et al. 2011). Here, as brain inflammation is seen with these antibodies, activation of the immune system may also be contributing to the epileptogenic process. To our knowledge, *in vivo* experiments of LGI1 antibodies similar to the model in this thesis have not yet been performed, but given the additive pathogenic effect of a neuronal autoantibody and brain inflammation this may result in an "autoimmune epilepsy" animal model with spontaneous seizures. In order to see spontaneous unprovoked seizures, i.e. epilepsy, in our NMDAR-Ab IgG passive transfer mouse model, some modifications to the protocol could be made. These include, the use of a genetically seizure susceptible mouse strain, peripheral injection of lipopolysaccharide to activate the endogenous immune system, or active immunization to purified native antigens. All of these measures may come closer to mimicking the

natural pathogenic effect of NMDAR-Abs seen in symptomatic NMDAR-Ab positive patients. Figure 7.1 shows the place of autoantibodies within the complex aetiological framework of epilepsy and the immune system and highlights the fact that epilepsy is unlikely to be caused by neuronal autoantibodies alone.

7.7 Treatment options – should we target the antigenic target?

Most neuronal autoantibody mediated diseases are treated through a similar algorithm, using first-line and second-line immunotherapy, and a good response is seen although the disease course is long often involving intensive care admission and associated co-morbidities (Titulaer, McCracken et al. 2013). However, we know that pathogenic mechanisms vary between the different neuronal autoantibodies, and alternative therapies more specific to the antigenic target may be useful. Hypothesising that the pathogenic effects of NMDAR-Abs could be overcome by increasing the number of cell surface NMDARs, we used a neurosteroid known to upregulate surface NMDAR expression: PregS. The use of pregnenolone (which metabolises to PregS) has been used as an adjunctive therapy in schizophrenia to counteract the proposed NMDAR hypofunction contributing to the symptomatology (Marx, Lee et al. 2014), and is safe and well-tolerated. In NMDAR-Ab mediated neurological disease, pregnenolone could theoretically be useful in providing symptomatic relief, with the immunotherapy working to remove the remaining NMDAR antibodies. Upregulation of NMDARs was successful *in vitro,* however the results of the *in vivo* experiments were disappointing. Further proof of neurosteroid actions in this disease, both *in vitro* and *in vivo* are required before a clinical trial could be justified in human subjects. Another very

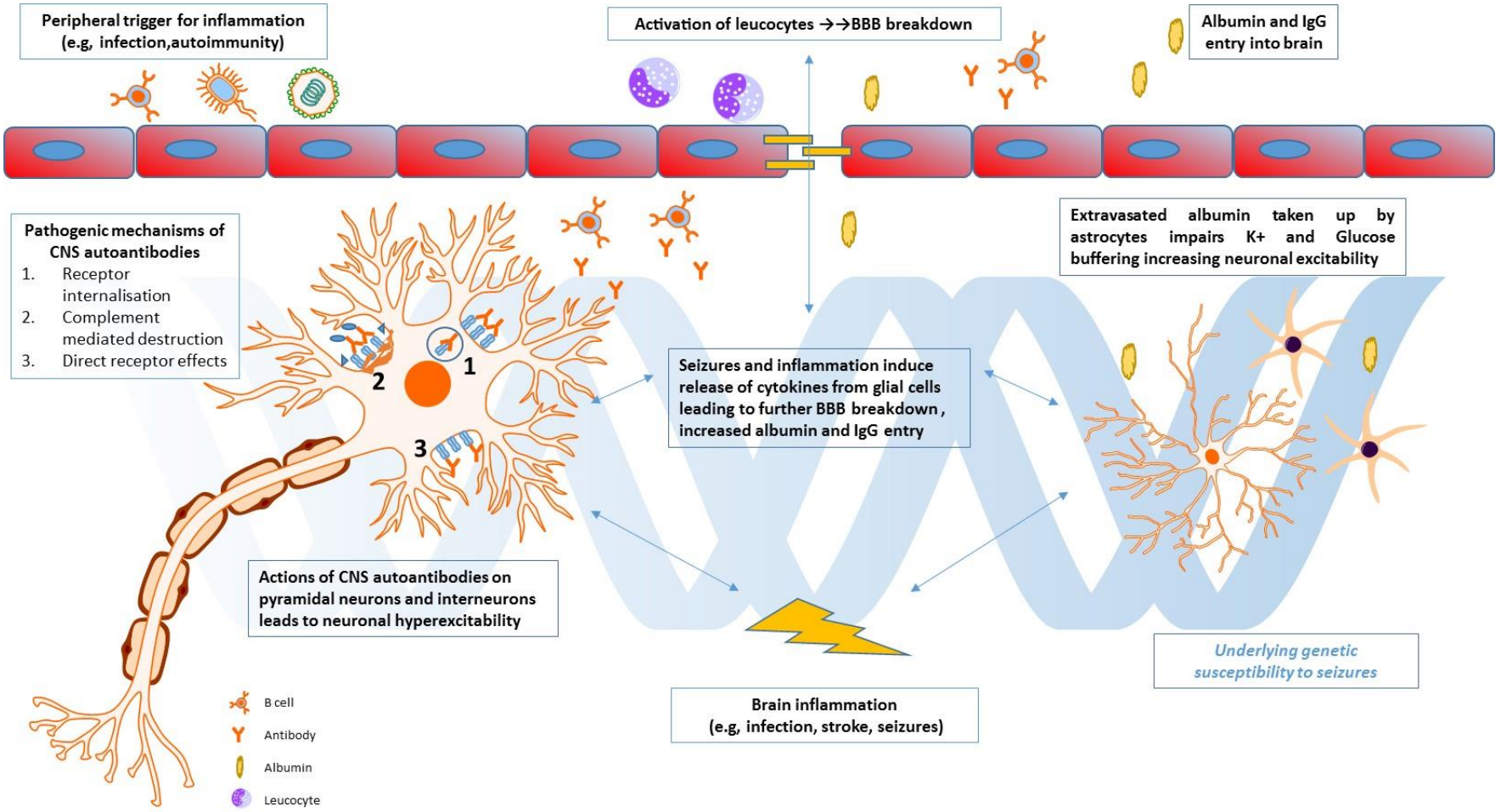

Figure 7-1 Schematic representing some of the complex interactions between the immune system, CNS autoantibodies and genetic susceptibility in the pathogenesis of epilepsy. Refs: Marchi, N., et al. (2014). "Inflammatory pathways of seizure disorders." Trends Neurosci **37**(2): 55-65.Vezzani, A., et al. (2011). "The role of inflammation in epilepsy." Nat Rev Neurol **7**(1): 31-40. Abbreviations: BBB blood-brain-barrier, K^+ potassium, CNS central nervous system, IgG immunoglobulins

recently described passive transfer model of NMDAR-Ab encephalitis infused NMDAR-Ab positive CSF into the lateral ventricles of mice over 14 days via osmotic pumps and the mice showed memory and behavioural deficits (Planaguma, Leypoldt et al. 2014). These effects were likely mediated by the binding of antibodies to NMDARs, as shown by immunohistochemical staining of the brains post-mortem, and reversal of behavioural deficits when the infusions were stopped. The reproducibility shown in the cognitive deficits would serve as an alternative model for testing of novel treatments such as PregS *in vivo*.

The idea of this drug working at the receptor level could also be explored in existing standard treatments. Do we know for example, if methylprednisolone also has acute actions on membrane receptors? There is some evidence for this: some patients do respond very quickly to this treatment and this is not in line with the accepted mode of action of steroids which is a slower, transcriptional effect. Knowledge of pathogenic mechanisms should be applied to the development of new therapies and may also increase our understanding of how current treatments work and can be optimised.

7.8 Future directions

In this thesis, the presence, relevance and pathogenicity of neuronal autoantibodies in paediatric epilepsy was investigated. During this process, future research questions were generated and discussed above.

New antigenic targets are regularly being discovered and the search is on for novel antigenic targets, in encephalitis and epilepsy patients. The recent reports of $GABA_A$ antibodies found in six patients with refractory seizures and status epilepticus present an exciting prospect of a relevant target antigen in epilepsy (Petit-Pedrol,

Armangue et al. 2014). The $GABA_A$ receptor mediates most of the fast inhibitory transmission in the brain and is the pharmacological target for many anti-epileptic drugs; internalization of synaptic $GABA_A$ receptors is thought to underlie the resistance seen to benzodiazepines in refractory status epilepticus (Goodkin, Yeh et al. 2005). Allopregnanlone, a positive allosteric modulator of synaptic and extrasynaptic $GABA_A$ receptors, has recently been shown to be effective in treating paediatric patients with refractory status epilepticus and provides the first report of neurosteroid use in paediatric neurological disease (Broomall, Natale et al. 2014). This may hopefully serve as a paradigm for future antigen specific neurosteroid treatments in autoantibody mediated neurological disease.

Given the hypothesis that CNS autoantibodies are only part of the inflammatory milieu involved in the pathogenesis of epilepsy, there is a pressing need for collaborative work between groups focused on these separate fields. Future pathogenesis studies need to take into account the intricacies of the human immune system and how these relate to and with CNS autoantibody pathogenesis. This is important for development of novel treatments, but also could be predictive of epilepsy "risk" in an individual. The discovery of predictive biomarkers in epilepsy that could indicate the likely progression of disease and treatment response would be invaluable to both patients and clinicians (Hegde and Lowenstein 2014), particularly the drug resistant, refractory cases with associated co-morbidities.

Given the pace of genetic advances and the proposed use of "personalised medicine" related to a person's genome (Chin, Andersen et al. 2011), the same doctrine may be applied to the treatment of CNS autoantibody mediated neurological disease in the future. With an increased understanding of the pathogenic mechanisms of CNS autoantibodies, the relationship to the immune system and genetic susceptibility, the time is ripe for fresh thinking on specific therapeutic options for the treatment of the

antibody mediated neurological diseases to improve patient recovery times and eventual outcome.

CHAPTER 8 - REFERENCES

Adamusova, E., O. Cais, V. Vyklicky, E. Kudova, H. Chodounska, M. Horak and L. Vyklicky, Jr. (2013). "Pregnenolone sulfate activates NMDA receptor channels." Physiol Res **62**(6): 731-736.

Armangue, T., M. J. Titulaer, I. Malaga, L. Bataller, I. Gabilondo, F. Graus and J. Dalmau (2013). "Pediatric anti-N-methyl-D-aspartate receptor encephalitis-clinical analysis and novel findings in a series of 20 patients." J Pediatr **162**(4): 850-856.e852.

Arts, W. F., F. K. Aarsen, M. Scheltens-de Boer and C. E. Catsman-Berrevoets (2009). "Landau-Kleffner syndrome and CSWS syndrome: treatment with intravenous immunoglobulins." Epilepsia **50 Suppl 7**: 55-58.

Arts, W. F., A. T. Geerts, O. F. Brouwer, A. C. Boudewyn Peters, H. Stroink and C. A. van Donselaar (1999). "The early prognosis of epilepsy in childhood: the prediction of a poor outcome. The Dutch study of epilepsy in childhood." Epilepsia **40**(6): 726-734.

Aydin-Abidin, S., M. Yildirim, I. Abidin, M. Akca and A. Cansu (2011). "Comparison of focally induced epileptiform activities in C57BL/6 and BALB/c mice by using in vivo EEG recording." Neurosci Lett **504**(2): 165-169.

Baulieu, E. E. (1997). "Neurosteroids: of the nervous system, by the nervous system, for the nervous system." Recent Prog Horm Res **52**: 1-32.

Beaudoin, G. M., 3rd, S. H. Lee, D. Singh, Y. Yuan, Y. G. Ng, L. F. Reichardt and J. Arikkath (2012). "Culturing pyramidal neurons from the early postnatal mouse hippocampus and cortex." Nat Protoc **7**(9): 1741-1754.

Belforte, J. E., V. Zsiros, E. R. Sklar, Z. Jiang, G. Yu, Y. Li, E. M. Quinlan and K. Nakazawa (2010). "Postnatal NMDA receptor ablation in corticolimbic interneurons confers schizophrenia-like phenotypes." Nat Neurosci **13**(1): 76-83.

Berg, A. T., S. F. Berkovic, M. J. Brodie, J. Buchhalter, J. H. Cross, W. van Emde Boas, J. Engel, J. French, T. A. Glauser, G. W. Mathern, S. L. Moshe, D. Nordli, P. Plouin and I. E. Scheffer (2010). "Revised terminology and concepts for organization of seizures and epilepsies: report of the ILAE Commission on Classification and Terminology, 2005-2009." Epilepsia **51**(4): 676-685.

Bien, C. G., A. Vincent, M. H. Barnett, A. J. Becker, I. Blumcke, F. Graus, K. A. Jellinger, D. E. Reuss, T. Ribalta, J. Schlegel, I. Sutton, H. Lassmann and J. Bauer (2012). "Immunopathology of autoantibody-associated encephalitides: clues for pathogenesis." Brain **135**(Pt 5): 1622-1638.

Bitanihirwe, B. K., M. P. Lim, J. F. Kelley, T. Kaneko and T. U. Woo (2009). "Glutamatergic deficits and parvalbumin-containing inhibitory neurons in the prefrontal cortex in schizophrenia." BMC Psychiatry **9**: 71.

Blaes, F., M. G. Pike and B. Lang (2008). "Autoantibodies in childhood opsoclonus-myoclonus syndrome." J Neuroimmunol **201-202**: 221-226.

Boronat, A., M. Sepulveda, S. Llufriu, L. Sabater, Y. Blanco, I. Gabilondo, N. Sola, P. Villoslada, J. Dalmau, F. Graus and A. Saiz (2012). "Analysis of antibodies to surface epitopes of contactin-2 in multiple sclerosis." J Neuroimmunol **244**(1-2): 103-106.

Boscolo, S., V. Baldas, G. Gobbi, L. Giordano, G. Cioni, T. Not, A. Ventura and E. Tongiorgi (2005). "Anti-brain but not celiac disease antibodies in Landau-Kleffner syndrome and related epilepsies." J Neuroimmunol **160**(1-2): 228-232.

Boyden, E. S., F. Zhang, E. Bamberg, G. Nagel and K. Deisseroth (2005). "Millisecond-timescale, genetically targeted optical control of neural activity." Nat Neurosci **8**(9): 1263-1268.

Brenner, T., G. J. Sills, Y. Hart, S. Howell, P. Waters, M. J. Brodie, A. Vincent and B. Lang (2013). "Prevalence of neurologic autoantibodies in cohorts of patients with new and established epilepsy." Epilepsia **54**(6): 1028-1035.

Broomall, E., J. E. Natale, M. Grimason, J. Goldstein, C. M. Smith, C. Chang, S. Kanes, M. A. Rogawski and M. S. Wainwright (2014). "Pediatric super-refractory status epilepticus treated with allopregnanolone." Ann Neurol.

Buckley, C., J. Oger, L. Clover, E. Tuzun, K. Carpenter, M. Jackson and A. Vincent (2001). "Potassium channel antibodies in two patients with reversible limbic encephalitis." Ann Neurol **50**(1): 73-78.

Buzatu, M., C. Bulteau, C. Altuzarra, O. Dulac and P. Van Bogaert (2009). "Corticosteroids as treatment of epileptic syndromes with continuous spike-waves during slow-wave sleep." Epilepsia **50 Suppl 7**: 68-72.

Callenbach, P. M., C. M. Jol-Van Der Zijde, A. T. Geerts, W. F. Arts, C. A. Van Donselaar, A. C. Peters, H. Stroink, O. F. Brouwer, M. J. Van Tol and C. Dutch Study of Epilepsy in (2003). "Immunoglobulins in children with epilepsy: the Dutch Study of Epilepsy in Childhood." Clin Exp Immunol **132**(1): 144-151.

Carvill, G. L., B. M. Regan, S. C. Yendle, B. J. O'Roak, N. Lozovaya, N. Bruneau, N. Burnashev, A. Khan, J. Cook, E. Geraghty, L. G. Sadleir, S. J. Turner, M. H. Tsai, R. Webster, R. Ouvrier, J. A. Damiano, S. F. Berkovic, J. Shendure, M. S. Hildebrand, P. Szepetowski, I. E. Scheffer and H. C. Mefford (2013). "GRIN2A mutations cause epilepsy-aphasia spectrum disorders." Nat Genet **45**(9): 1073-1076.

Chabrol, E., V. Navarro, G. Provenzano, I. Cohen, C. Dinocourt, S. Rivaud-Pechoux, D. Fricker, M. Baulac, R. Miles, E. Leguern and S. Baulac (2010). "Electroclinical characterization of epileptic seizures in leucine-rich, glioma-inactivated 1-deficient mice." Brain **133**(9): 2749-2762.

Chang, C. (2014). "Autoimmunity: from black water fever to regulatory function." J Autoimmun **48-49**: 1-9.

Chang, P., K. S. Hashemi and M. C. Walker (2011). "A novel telemetry system for recording EEG in small animals." J Neurosci Methods **201**(1): 106-115.

Chin, L., J. N. Andersen and P. A. Futreal (2011). "Cancer genomics: from discovery science to personalized medicine." Nat Med **17**(3): 297-303.

Connolly, A. M., M. Chez, E. M. Streif, R. M. Keeling, P. T. Golumbek, J. M. Kwon, J. J. Riviello, R. G. Robinson, R. J. Neuman and R. M. Deuel (2006). "Brain-derived neurotrophic factor and autoantibodies to neural antigens in sera of children with autistic spectrum disorders, Landau-Kleffner syndrome, and epilepsy." Biol Psychiatry **59**(4): 354-363.

Connolly, A. M., M. G. Chez, A. Pestronk, S. T. Arnold, S. Mehta and R. K. Deuel (1999). "Serum autoantibodies to brain in Landau-Kleffner variant, autism, and other neurologic disorders." J Pediatr **134**(5): 607-613.

Coyle, J. T. (1996). "The glutamatergic dysfunction hypothesis for schizophrenia." Harv Rev Psychiatry **3**(5): 241-253.

Dahm, L., C. Ott, J. Steiner, B. Stepniak, B. Teegen, S. Saschenbrecker, C. Hammer, K. Borowski, M. Begemann, S. Lemke, K. Rentzsch, C. Probst, H. Martens, J. Wienands, G. Spalletta, K. Weissenborn, W. Stocker and H. Ehrenreich (2014). "Seroprevalence of autoantibodies against brain antigens in health and disease." Ann Neurol **76**(1): 82-94.

Dalakas, M. C. (2005). "The role of IVIg in the treatment of patients with stiff person syndrome and other neurological diseases associated with anti-GAD antibodies." J Neurol **252 Suppl 1**: I19-25.

Dalmau, J., A. J. Gleichman, E. G. Hughes, J. E. Rossi, X. Peng, M. Lai, S. K. Dessain, M. R. Rosenfeld, R. Balice-Gordon and D. R. Lynch (2008). "Anti-NMDA-receptor encephalitis: case series and analysis of the effects of antibodies." Lancet Neurol **7**(12): 1091-1098.

Dalmau, J., E. Tuzun, H. Y. Wu, J. Masjuan, J. E. Rossi, A. Voloschin, J. M. Baehring, H. Shimazaki, R. Koide, D. King, W. Mason, L. H. Sansing, M. A. Dichter, M. R. Rosenfeld and D. R. Lynch (2007). "Paraneoplastic anti-N-methyl-D-aspartate receptor encephalitis associated with ovarian teratoma." Ann Neurol **61**(1): 25-36.

Davidson, C. D., N. F. Ali, M. C. Micsenyi, G. Stephney, S. Renault, K. Dobrenis, D. S. Ory, M. T. Vanier and S. U. Walkley (2009). "Chronic cyclodextrin treatment of murine Niemann-Pick C disease ameliorates neuronal cholesterol and glycosphingolipid storage and disease progression." PLoS One **4**(9): e6951.

Davies, G., S. R. Irani, C. Coltart, G. Ingle, Y. Amin, C. Taylor, J. Radcliffe, N. P. Hirsch, R. S. Howard, A. Vincent and D. M. Kullmann (2010). "Anti-N-methyl-D-aspartate receptor antibodies: a potentially treatable cause of encephalitis in the intensive care unit." Crit Care Med **38**(2): 679-682.

Davis, M. E. and M. E. Brewster (2004). "Cyclodextrin-based pharmaceutics: past, present and future." Nat Rev Drug Discov **3**(12): 1023-1035.

DeFelipe-Mimbrera, A., J. Masjuan, I. Corral, L. M. Villar, F. Graus and N. Garcia-Barragan (2014). "Opsoclonus-myoclonus syndrome and limbic encephalitis associated with GABAB receptor antibodies in CSF." J Neuroimmunol **272**(1-2): 91-93.

Deonna, T. and E. Roulet-Perez (2010). "Early-onset acquired epileptic aphasia (Landau-Kleffner syndrome, LKS) and regressive autistic disorders with epileptic EEG abnormalities: the continuing debate." Brain Dev **32**(9): 746-752.

Di Paolo, G., S. Sankaranarayanan, M. R. Wenk, L. Daniell, E. Perucco, B. J. Caldarone, R. Flavell, M. R. Picciotto, T. A. Ryan, O. Cremona and P. De Camilli (2002). "Decreased synaptic vesicle recycling efficiency and cognitive deficits in amphiphysin 1 knockout mice." Neuron **33**(5): 789-804.

Dogan Onugoren, M., H. Rauschka and C. G. Bien (2014). "Conjoint occurrence of GABAB receptor antibodies in Lambert-Eaton myasthenic syndrome with antibodies to the voltage gated calcium channel." J Neuroimmunol **273**(1-2): 115-116.

Dube, C. M., T. Ravizza, M. Hamamura, Q. Zha, A. Keebaugh, K. Fok, A. L. Andres, O. Nalcioglu, A. Obenaus, A. Vezzani and T. Z. Baram (2010). "Epileptogenesis provoked by prolonged experimental febrile seizures: mechanisms and biomarkers." J Neurosci **30**(22): 7484-7494.

Dumas, T. C. (2005). "Developmental regulation of cognitive abilities: modified composition of a molecular switch turns on associative learning." Prog Neurobiol **76**(3): 189-211.

Duncan, G. E., K. Inada, B. H. Koller and S. S. Moy (2010). "Increased sensitivity to kainic acid in a genetic model of reduced NMDA receptor function." Brain Res **1307**: 166-176.

Ellis, T. M. and M. A. Atkinson (1996). "The clinical significance of an autoimmune response against glutamic acid decarboxylase." Nat Med **2**(2): 148-153.

Evergren, E., M. Marcucci, N. Tomilin, P. Low, V. Slepnev, F. Andersson, H. Gad, L. Brodin, P. De Camilli and O. Shupliakov (2004). "Amphiphysin is a component of clathrin coats formed during synaptic vesicle recycling at the lamprey giant synapse." Traffic **5**(7): 514-528.

Ferraro, T. N., G. T. Golden, G. G. Smith, P. St Jean, N. J. Schork, N. Mulholland, C. Ballas, J. Schill, R. J. Buono and W. H. Berrettini (1999). "Mapping loci for pentylenetetrazol-induced seizure susceptibility in mice." J Neurosci **19**(16): 6733-6739.

Ferraro, T. N., G. T. Golden, R. Snyder, M. Laibinis, G. G. Smith, R. J. Buono and W. H. Berrettini (1998). "Genetic influences on electrical seizure threshold." Brain Res **813**(1): 207-210.

Fisher, R. S., C. Acevedo, A. Arzimanoglou, A. Bogacz, J. H. Cross, C. E. Elger, J. Engel, Jr., L. Forsgren, J. A. French, M. Glynn, D. C. Hesdorffer, B. I. Lee, G. W. Mathern, S. L. Moshe, E. Perucca, I. E. Scheffer, T. Tomson, M. Watanabe and S. Wiebe (2014). "ILAE official report: a practical clinical definition of epilepsy." Epilepsia **55**(4): 475-482.

Florance, N. R., R. L. Davis, C. Lam, C. Szperka, L. Zhou, S. Ahmad, C. J. Campen, H. Moss, N. Peter, A. J. Gleichman, C. A. Glaser, D. R. Lynch, M. R. Rosenfeld and J. Dalmau (2009). "Anti-N-methyl-D-aspartate receptor (NMDAR) encephalitis in children and adolescents." Ann Neurol **66**(1): 11-18.

Fujii, H., S. Kubo, T. Yunoki, K. Sato, K. Takamatsu, K. Tanaka, Y. Takahashi and M. Kuriyama (2013). "Glioblastoma with ovarian teratoma having N-methyl-D-aspartate receptor (NMDAR) antibody in CSF--a case report." Rinsho Shinkeigaku **53**(9): 712-715.

Fukamauchi, F., O. Aihara, Y. J. Wang, K. Akasaka, Y. Takeda, M. Horie, H. Kawano, K. Sudo, M. Asano, K. Watanabe and Y. Iwakura (2001). "TAG-1-deficient mice have marked elevation of adenosine A1 receptors in the hippocampus." Biochem Biophys Res Commun **281**(1): 220-226.

Fukata, Y., H. Adesnik, T. Iwanaga, D. S. Bredt, R. A. Nicoll and M. Fukata (2006). "Epilepsy-related ligand/receptor complex LGI1 and ADAM22 regulate synaptic transmission." Science **313**(5794): 1792-1795.

Fukushima, F., K. Nakao, T. Shinoe, M. Fukaya, S. Muramatsu, K. Sakimura, H. Kataoka, H. Mori, M. Watanabe, T. Manabe and M. Mishina (2009). "Ablation of NMDA receptors enhances the excitability of hippocampal CA3 neurons." PLoS One **4**(1): e3993.

Gable, M. S., H. Sheriff, J. Dalmau, D. H. Tilley and C. A. Glaser (2012). "The frequency of autoimmune N-methyl-D-aspartate receptor encephalitis surpasses that of individual viral etiologies in young individuals enrolled in the California Encephalitis Project." Clin Infect Dis **54**(7): 899-904.

Gandal, M. J., J. Sisti, K. Klook, P. I. Ortinski, V. Leitman, Y. Liang, T. Thieu, R. Anderson, R. C. Pierce, G. Jonak, R. E. Gur, G. Carlson and S. J. Siegel (2012). "GABAB-mediated rescue of altered excitatory-inhibitory balance, gamma synchrony and behavioral deficits following constitutive NMDAR-hypofunction." Transl Psychiatry **2**: e142.

Ganor, Y., H. Goldberg-Stern, R. Cohen, V. Teichberg and M. Levite (2014). "Glutamate receptor antibodies directed against AMPA receptors subunit 3 peptide B (GluR3B) can be produced in DBA/2J mice, lower seizure threshold and induce abnormal behavior." Psychoneuroendocrinology **42**: 106-117.

Geerts, A., O. Brouwer, H. Stroink, C. van Donselaar, B. Peters, E. Peeters and W. F. Arts (2012). "Onset of intractability and its course over time: the Dutch study of epilepsy in childhood." Epilepsia **53**(4): 741-751.

Geis, C., A. Weishaupt, B. Grunewald, T. Wultsch, A. Reif, M. Gerlach, R. Dirkx, M. Solimena, D. Perani, M. Heckmann, K. V. Toyka, F. Folli and C. Sommer (2011). "Human stiff-person syndrome IgG induces anxious behavior in rats." PLoS One **6**(2): e16775.

Geis, C., A. Weishaupt, S. Hallermann, B. Grunewald, C. Wessig, T. Wultsch, A. Reif, N. Byts, M. Beck, S. Jablonka, M. K. Boettger, N. Uceyler, W. Fouquet, M. Gerlach, H. M. Meinck, A. L. Siren, S. J. Sigrist, K. V. Toyka, M. Heckmann and C. Sommer (2010). "Stiff person syndrome-associated autoantibodies to amphiphysin mediate reduced GABAergic inhibition." Brain **133**(11): 3166-3180.

Giorgi, O., M. Orlandi, D. Lecca and M. G. Corda (1991). "MK-801 prevents chemical kindling induced by pentylenetetrazol in rats." Eur J Pharmacol **193**(3): 363-365.

Gitiaux, C., H. Simonnet, M. Eisermann, D. Leunen, O. Dulac, R. Nabbout, M. Chevignard, J. Honnorat, S. Gataullina, L. Musset, E. Scalais, A. Gauthier, M. Hully, N. Boddaert, M. Kuchenbuch, I. Desguerre and A. Kaminska (2013). "Early electro-clinical features may contribute to diagnosis of the anti-NMDA receptor encephalitis in children." Clin Neurophysiol **124**(12): 2354-2361.

Gleichman, A. J., J. A. Panzer, B. H. Baumann, J. Dalmau and D. R. Lynch (2014). "Antigenic and mechanistic characterization of anti-AMPA receptor encephalitis." Ann Clin Transl Neurol **1**(3): 180-189.

Goldberg, E. M. and D. A. Coulter (2013). "Mechanisms of epileptogenesis: a convergence on neural circuit dysfunction." Nat Rev Neurosci **14**(5): 337-349.
Goldberg, E. M., M. Titulaer, P. M. de Blank, A. Sievert and N. Ryan (2014). "Anti-N-methyl-D-aspartate receptor-mediated encephalitis in infants and toddlers: case report and review of the literature." Pediatr Neurol **50**(2): 181-184.

Goodkin, H. P., J. L. Yeh and J. Kapur (2005). "Status epilepticus increases the intracellular accumulation of GABAA receptors." J Neurosci **25**(23): 5511-5520.
Granata, T., H. Cross, W. Theodore and G. Avanzini (2011). "Immune-mediated epilepsies." Epilepsia **52 Suppl 3**: 5-11.

Granerod, J., H. E. Ambrose, N. W. Davies, J. P. Clewley, A. L. Walsh, D. Morgan, R. Cunningham, M. Zuckerman, K. J. Mutton, T. Solomon, K. N. Ward, M. P. Lunn, S. R. Irani, A. Vincent, D. W. Brown and N. S. Crowcroft (2010). "Causes of encephalitis and differences in their clinical presentations in England: a multicentre, population-based prospective study." Lancet Infect Dis **10**(12): 835-844.

Gresa-Arribas, N., M. J. Titulaer, A. Torrents, E. Aguilar, L. McCracken, F. Leypoldt, A. J. Gleichman, R. Balice-Gordon, M. R. Rosenfeld, D. Lynch, F. Graus and J. Dalmau (2014). "Antibody titres at diagnosis and during follow-up of anti-NMDA receptor encephalitis: a retrospective study." Lancet Neurol **13**(2): 167-177.

Griffin, L. D., W. Gong, L. Verot and S. H. Mellon (2004). "Niemann-Pick type C disease involves disrupted neurosteroidogenesis and responds to allopregnanolone." Nat Med **10**(7): 704-711.

Grunze, H. C., D. G. Rainnie, M. E. Hasselmo, E. Barkai, E. F. Hearn, R. W. McCarley and R. W. Greene (1996). "NMDA-dependent modulation of CA1 local circuit inhibition." J Neurosci **16**(6): 2034-2043.

Gultekin, S. H., M. R. Rosenfeld, R. Voltz, J. Eichen, J. B. Posner and J. Dalmau (2000). "Paraneoplastic limbic encephalitis: neurological symptoms, immunological findings and tumour association in 50 patients." Brain **123 (Pt 7)**: 1481-1494.

Haberlandt, E., T. Bast, A. Ebner, H. Holthausen, G. Kluger, R. Kravljanac, J. Kroll-Seger, G. Kurlemann, C. Makowski, K. Rostasy, E. Tuschen-Hofstatter, G. Weber, A. Vincent and C. G. Bien (2011). "Limbic encephalitis in children and adolescents." Arch Dis Child **96**(2): 186-191.

Hacohen, Y., K. Deiva, P. Pettingill, P. Waters, A. Siddiqui, P. Chretien, E. Menson, J. P. Lin, M. Tardieu, A. Vincent and M. J. Lim (2014). "N-methyl-D-aspartate receptor antibodies in post-herpes simplex virus encephalitis neurological relapse." Mov Disord **29**(1): 90-96.

Hacohen, Y., N. Dlamini, T. Hedderly, E. Hughes, M. Woods, A. Vincent and M. Lim (2014). "N-methyl-D-aspartate receptor antibody-associated movement disorder without encephalopathy." Dev Med Child Neurol **56**(2): 190-193.

Hacohen, Y., S. Wright, P. Waters, S. Agrawal, L. Carr, H. Cross, C. De Sousa, C. Devile, P. Fallon, R. Gupta, T. Hedderly, E. Hughes, T. Kerr, K. Lascelles, J. P. Lin, S. Philip, K. Pohl, P. Prabahkar, M. Smith, R. Williams, A. Clarke, C. Hemingway, E. Wassmer, A. Vincent and M. J. Lim (2013). "Paediatric autoimmune encephalopathies: clinical features, laboratory investigations and outcomes in patients with or without antibodies to known central nervous system autoantigens." J Neurol Neurosurg Psychiatry **84**(7): 748-755.

Hammer, C., B. Stepniak, A. Schneider, S. Papiol, M. Tantra, M. Begemann, A. L. Siren, L. A. Pardo, S. Sperling, S. Mohd Jofrry, A. Gurvich, N. Jensen, K. Ostmeier, F. Luhder, C. Probst, H. Martens, M. Gillis, G. Saher, F. Assogna, G. Spalletta, W. Stocker, T. F. Schulz, K. A. Nave and H. Ehrenreich (2014). "Neuropsychiatric disease relevance of circulating anti-NMDA receptor autoantibodies depends on blood-brain barrier integrity." Mol Psychiatry **19**(10): 1143-1149.

Hancock, E. C., J. P. Osborne and S. W. Edwards (2013). "Treatment of infantile spasms." Cochrane Database Syst Rev **6**: Cd001770.

Hansen, N., B. Grunewald, A. Weishaupt, M. N. Colaco, K. V. Toyka, C. Sommer and C. Geis (2013). "Human Stiff person syndrome IgG-containing high-titer anti-GAD65 autoantibodies induce motor dysfunction in rats." Exp Neurol **239**: 202-209.

Hart, I. K., P. Maddison, J. Newsom-Davis, A. Vincent and K. R. Mills (2002). "Phenotypic variants of autoimmune peripheral nerve hyperexcitability." Brain **125**(Pt 8): 1887-1895.

Hart, I. K., C. Waters, A. Vincent, C. Newland, D. Beeson, O. Pongs, C. Morris and J. Newsom-Davis (1997). "Autoantibodies detected to expressed K+ channels are implicated in neuromyotonia." Ann Neurol **41**(2): 238-246.

Harteneck, C. (2013). "Pregnenolone sulfate: from steroid metabolite to TRP channel ligand." Molecules **18**(10): 12012-12028.

Hegde, M. and D. H. Lowenstein (2014). "The search for circulating epilepsy biomarkers." Biomark Med **8**(3): 413-427.

Hoftberger, R., M. J. Titulaer, L. Sabater, B. Dome, A. Rozsas, B. Hegedus, M. A. Hoda, V. Laszlo, H. J. Ankersmit, L. Harms, S. Boyero, A. de Felipe, A. Saiz, J. Dalmau and F. Graus (2013). "Encephalitis and GABAB receptor antibodies: novel findings in a new case series of 20 patients." Neurology **81**(17): 1500-1506.

Honnorat, J., A. Saiz, B. Giometto, A. Vincent, L. Brieva, C. de Andres, J. Maestre, N. Fabien, A. Vighetto, R. Casamitjana, C. Thivolet, B. Tavolato, J. Antoine, P. Trouillas and F. Graus (2001). "Cerebellar ataxia with anti-glutamic acid decarboxylase antibodies: study of 14 patients." Arch Neurol **58**(2): 225-230.

Hughes, E. G., X. Peng, A. J. Gleichman, M. Lai, L. Zhou, R. Tsou, T. D. Parsons, D. R. Lynch, J. Dalmau and R. J. Balice-Gordon (2010). "Cellular and synaptic mechanisms of anti-NMDA receptor encephalitis." J Neurosci **30**(17): 5866-5875.

Hussain, S. A., S. Shinnar, G. Kwong, J. T. Lerner, J. H. Matsumoto, J. Y. Wu, W. D. Shields and R. Sankar (2014). "Treatment of infantile spasms with very high dose prednisolone before high dose adrenocorticotropic hormone." Epilepsia **55**(1): 103-107.

Illingworth, M. A., D. Hanrahan, C. E. Anderson, K. O'Kane, J. Anderson, M. Casey, C. de Sousa, J. H. Cross, S. Wright, R. C. Dale, A. Vincent and M. A. Kurian (2011). "Elevated VGKC-complex antibodies in a boy with fever-induced refractory epileptic encephalopathy in school-age children (FIRES)." Dev Med Child Neurol **53**(11): 1053-1057.

Iorio, R., G. Assenza, M. Tombini, G. Colicchio, G. Della Marca, A. Benvenga, V. Damato, P. M. Rossini, C. Vollono, D. Plantone, A. Marti, A. P. Batocchi and A. Evoli (2014). "The detection of neural autoantibodies in patients with antiepileptic-drug-resistant epilepsy predicts response to immunotherapy." Eur J Neurol.

Irani, S. R., S. Alexander, P. Waters, K. A. Kleopa, P. Pettingill, L. Zuliani, E. Peles, C. Buckley, B. Lang and A. Vincent (2010). "Antibodies to Kv1 potassium channel-complex proteins leucine-rich, glioma inactivated 1 protein and contactin-associated protein-2 in limbic encephalitis, Morvan's syndrome and acquired neuromyotonia." Brain **133**(9): 2734-2748.

Irani, S. R., K. Bera, P. Waters, L. Zuliani, S. Maxwell, M. S. Zandi, M. A. Friese, I. Galea, D. M. Kullmann, D. Beeson, B. Lang, C. G. Bien and A. Vincent (2010). "N-methyl-D-aspartate antibody encephalitis: temporal progression of clinical and paraclinical observations in a predominantly non-paraneoplastic disorder of both sexes." Brain **133**(Pt 6): 1655-1667.

Irani, S. R., C. Buckley, A. Vincent, O. C. Cockerell, P. Rudge, M. R. Johnson and S. Smith (2008). "Immunotherapy-responsive seizure-like episodes with potassium channel antibodies." Neurology **71**(20): 1647-1648.

Irani, S. R., J. M. Gelfand, A. Al-Diwani and A. Vincent (2014). "Cell-surface central nervous system autoantibodies: Clinical relevance and emerging paradigms." Ann Neurol.

Irani, S. R., A. W. Michell, B. Lang, P. Pettingill, P. Waters, M. R. Johnson, J. M. Schott, R. J. Armstrong, S. Z. A, A. Bleasel, E. R. Somerville, S. M. Smith and A. Vincent (2011). "Faciobrachial dystonic seizures precede Lgi1 antibody limbic encephalitis." Ann Neurol **69**(5): 892-900.

Irani, S. R., P. Pettingill, K. A. Kleopa, N. Schiza, P. Waters, C. Mazia, L. Zuliani, O. Watanabe, B. Lang, C. Buckley and A. Vincent (2012). "Morvan syndrome: clinical and serological observations in 29 cases." Ann Neurol **72**(2): 241-255.

Irani, S. R., C. J. Stagg, J. M. Schott, C. R. Rosenthal, S. A. Schneider, P. Pettingill, R. Pettingill, P. Waters, A. Thomas, N. L. Voets, M. J. Cardoso, D. M. Cash, E. N. Manning, B. Lang, S. J. Smith, A. Vincent and M. R. Johnson (2013). "Faciobrachial dystonic seizures: the influence of immunotherapy on seizure control and prevention of cognitive impairment in a broadening phenotype." Brain **136**(Pt 10): 3151-3162.

Ito, D., T. Komatsu and K. Gohara (2013). "Measurement of saturation processes in glutamatergic and GABAergic synapse densities during long-term development of cultured rat cortical networks." Brain Research **1534**(0): 22-32.

Jantzen, S. U., S. Ferrea, C. Wach, K. Quasthoff, S. Illes, D. Scherfeld, H. P. Hartung, R. J. Seitz and M. Dihne (2013). "In vitro neuronal network activity in NMDA receptor encephalitis." BMC Neurosci **14**: 17.

Jeffery, O. J., V. A. Lennon, S. J. Pittock, J. K. Gregory, J. W. Britton and A. McKeon (2013). "GABAB receptor autoantibody frequency in service serologic evaluation." Neurology **81**(10): 882-887.

Kaech, S. and G. Banker (2006). "Culturing hippocampal neurons." Nat Protoc **1**(5): 2406-2415.

Kalachikov, S., O. Evgrafov, B. Ross, M. Winawer, C. Barker-Cummings, F. Martinelli Boneschi, C. Choi, P. Morozov, K. Das, E. Teplitskaya, A. Yu, E. Cayanis, G. Penchaszadeh, A. H. Kottmann, T. A. Pedley, W. A. Hauser, R. Ottman and T. C. Gilliam (2002). "Mutations in LGI1 cause autosomal-dominant partial epilepsy with auditory features." Nat Genet **30**(3): 335-341.

Kayser, M. S., M. J. Titulaer, N. Gresa-Arribas and J. Dalmau (2013). "Frequency and characteristics of isolated psychiatric episodes in anti-N-methyl-d-aspartate receptor encephalitis." JAMA Neurol **70**(9): 1133-1139.

Kim, T. J., S. T. Lee, J. W. Shin, J. Moon, J. A. Lim, J. I. Byun, Y. W. Shin, K. J. Lee, K. H. Jung, Y. S. Kim, K. I. Park, K. Chu and S. K. Lee (2014). "Clinical manifestations and outcomes of the treatment of patients with GABAB encephalitis." J Neuroimmunol **270**(1-2): 45-50.

Klang, A., P. Schmidt, S. Kneissl, Z. Bago, A. Vincent, B. Lang, T. Moloney, C. G. Bien, P. Halasz, J. Bauer and A. Pakozdy (2014). "IgG and complement deposition and

neuronal loss in cats and humans with epilepsy and voltage-gated potassium channel complex antibodies." J Neuropathol Exp Neurol **73**(5): 403-413.

Kleckner, N. W., J. C. Glazewski, C. C. Chen and T. D. Moscrip (1999). "Subtype-selective antagonism of N-methyl-D-aspartate receptors by felbamate: insights into the mechanism of action." J Pharmacol Exp Ther **289**(2): 886-894.

Kline, M. A., E. S. O'Connor Butler, A. Hinzey, S. Sliman, S. R. Kotha, C. B. Marsh, R. M. Uppu and N. L. Parinandi (2010). "A simple method for effective and safe removal of membrane cholesterol from lipid rafts in vascular endothelial cells: implications in oxidant-mediated lipid signaling." Methods Mol Biol **610**: 201-211.

Kostakis, E., C. Smith, M. K. Jang, S. C. Martin, K. G. Richards, S. J. Russek, T. T. Gibbs and D. H. Farb (2013). "The neuroactive steroid pregnenolone sulfate stimulates trafficking of functional N-methyl D-aspartate receptors to the cell surface via a noncanonical, G protein, and Ca2+-dependent mechanism." Mol Pharmacol **84**(2): 261-274.

Kramer, U., C. S. Chi, K. L. Lin, N. Specchio, M. Sahin, H. Olson, R. Nabbout, G. Kluger, J. J. Lin and A. van Baalen (2011). "Febrile infection-related epilepsy syndrome (FIRES): pathogenesis, treatment, and outcome: a multicenter study on 77 children." Epilepsia **52**(11): 1956-1965.

Labat-Moleur, F., C. Guillermet, P. Lorimier, C. Robert, S. Lantuejoul, E. Brambilla and A. Negoescu (1998). "TUNEL apoptotic cell detection in tissue sections: critical evaluation and improvement." J Histochem Cytochem **46**(3): 327-334.

Lahti, A. C., B. Koffel, D. LaPorte and C. A. Tamminga (1995). "Subanesthetic doses of ketamine stimulate psychosis in schizophrenia." Neuropsychopharmacology **13**(1): 9-19.

Lai, M., E. G. Hughes, X. Peng, L. Zhou, A. J. Gleichman, H. Shu, S. Mata, D. Kremens, R. Vitaliani, M. D. Geschwind, L. Bataller, R. G. Kalb, R. Davis, F. Graus, D. R. Lynch, R. Balice-Gordon and J. Dalmau (2009). "AMPA receptor antibodies in limbic encephalitis alter synaptic receptor location." Ann Neurol **65**(4): 424-434.

Lai, M., M. G. Huijbers, E. Lancaster, F. Graus, L. Bataller, R. Balice-Gordon, J. K. Cowell and J. Dalmau (2010). "Investigation of LGI1 as the antigen in limbic encephalitis previously attributed to potassium channels: a case series." Lancet Neurol **9**(8): 776-785.

Lalic, T., P. Pettingill, A. Vincent and M. Capogna (2011). "Human limbic encephalitis serum enhances hippocampal mossy fiber-CA3 pyramidal cell synaptic transmission." Epilepsia **52**(1): 121-131.

Lancaster, E., M. G. Huijbers, V. Bar, A. Boronat, A. Wong, E. Martinez-Hernandez, C. Wilson, D. Jacobs, M. Lai, R. W. Walker, F. Graus, L. Bataller, I. Illa, S. Markx, K. A. Strauss, E. Peles, S. S. Scherer and J. Dalmau (2011). "Investigations of caspr2, an autoantigen of encephalitis and neuromyotonia." Ann Neurol **69**(2): 303-311.

Lancaster, E., M. Lai, X. Peng, E. Hughes, R. Constantinescu, J. Raizer, D. Friedman, M. B. Skeen, W. Grisold, A. Kimura, K. Ohta, T. Iizuka, M. Guzman, F. Graus, S. J. Moss, R. Balice-Gordon and J. Dalmau (2010). "Antibodies to the GABA(B) receptor in limbic encephalitis with seizures: case series and characterisation of the antigen." Lancet Neurol **9**(1): 67-76.

Lavoie, S., M. M. Murray, P. Deppen, M. G. Knyazeva, M. Berk, O. Boulat, P. Bovet, A. I. Bush, P. Conus, D. Copolov, E. Fornari, R. Meuli, A. Solida, P. Vianin, M. Cuenod, T. Buclin and K. Q. Do (2008). "Glutathione precursor, N-acetyl-cysteine, improves mismatch negativity in schizophrenia patients." Neuropsychopharmacology **33**(9): 2187-2199.

Leen, W. G., J. Klepper, M. M. Verbeek, et al. (2010). "Glucose transporter-1 deficiency syndrome: the expanding clinical and genetic spectrum of a treatable disorder." Brain **133**(Pt 3): 655-670.

Leite, M. I., S. Jacob, S. Viegas, J. Cossins, L. Clover, B. P. Morgan, D. Beeson, N. Willcox and A. Vincent (2008). "IgG1 antibodies to acetylcholine receptors in 'seronegative' myasthenia gravis." Brain **131**(Pt 7): 1940-1952.

Lemke, J. R., D. Lal, E. M. Reinthaler, et al. (2013). "Mutations in GRIN2A cause idiopathic focal epilepsy with rolandic spikes." Nat Genet **45**(9): 1067-1072.
Lennon, V. A., T. J. Kryzer, S. J. Pittock, A. S. Verkman and S. R. Hinson (2005). "IgG marker of optic-spinal multiple sclerosis binds to the aquaporin-4 water channel." J Exp Med **202**(4): 473-477.

Lesca, G., G. Rudolf, N. Bruneau, et al. (2013). "GRIN2A mutations in acquired epileptic aphasia and related childhood focal epilepsies and encephalopathies with speech and language dysfunction." Nat Genet **45**(9): 1061-1066.

Lesca, G., G. Rudolf, A. Labalme, E. Hirsch, A. Arzimanoglou, P. Genton, J. Motte, A. de Saint Martin, M. P. Valenti, C. Boulay, J. De Bellescize, P. Keo-Kosal, N. Boutry-Kryza, P. Edery, D. Sanlaville and P. Szepetowski (2012). "Epileptic encephalopathies of the Landau-Kleffner and continuous spike and waves during slow-wave sleep types: genomic dissection makes the link with autism." Epilepsia **53**(9): 1526-1538.

Li, Q., S. Clark, D. V. Lewis and W. A. Wilson (2002). "NMDA receptor antagonists disinhibit rat posterior cingulate and retrosplenial cortices: a potential mechanism of neurotoxicity." J Neurosci **22**(8): 3070-3080.

Lilleker, J. B., V. Biswas and R. Mohanraj (2014). "Glutamic acid decarboxylase (GAD) antibodies in epilepsy: Diagnostic yield and therapeutic implications." Seizure **23**(8): 598-602.

Lilleker, J. B., M. S. Jones and R. Mohanraj (2013). "VGKC complex antibodies in epilepsy: diagnostic yield and therapeutic implications." Seizure **22**(9): 776-779.

Liu, S. M., A. Cogny, M. Kockx, R. T. Dean, K. Gaus, W. Jessup and L. Kritharides (2003). "Cyclodextrins differentially mobilize free and esterified cholesterol from primary human foam cell macrophages." J Lipid Res **44**(6): 1156-1166.

Luttjohann, A., P. F. Fabene and G. van Luijtelaar (2009). "A revised Racine's scale for PTZ-induced seizures in rats." Physiol Behav **98**(5): 579-586.

Lux, A. L., S. W. Edwards, E. Hancock, A. L. Johnson, C. R. Kennedy, R. W. Newton, F. J. O'Callaghan, C. M. Verity and J. P. Osborne (2005). "The United Kingdom Infantile Spasms Study (UKISS) comparing hormone treatment with vigabatrin on developmental and epilepsy outcomes to age 14 months: a multicentre randomised trial." Lancet Neurol **4**(11): 712-717.

Mackay, I. R. (2010). "Travels and travails of autoimmunity: a historical journey from discovery to rediscovery." Autoimmun Rev **9**(5): A251-258.

Majoie, H. J., M. de Baets, W. Renier, B. Lang and A. Vincent (2006). "Antibodies to voltage-gated potassium and calcium channels in epilepsy." Epilepsy Res **71**(2-3): 135-141.

Malter, M. P., C. Frisch, J. C. Schoene-Bake, C. Helmstaedter, K. P. Wandinger, W. Stoecker, H. Urbach, R. Surges, C. E. Elger, A. V. Vincent and C. G. Bien (2014). "Outcome of limbic encephalitis with VGKC-complex antibodies: relation to antigenic specificity." J Neurol **261**(9): 1695-1705.

Malter, M. P., C. Helmstaedter, H. Urbach, A. Vincent and C. G. Bien (2010). "Antibodies to glutamic acid decarboxylase define a form of limbic encephalitis." Ann Neurol **67**(4): 470-478.

Manto, M., J. Dalmau, A. Didelot, V. Rogemond and J. Honnorat (2010). "In vivo effects of antibodies from patients with anti-NMDA receptor encephalitis: further evidence of synaptic glutamatergic dysfunction." Orphanet J Rare Dis **5**: 31.

Marchi, N., T. Granata and D. Janigro (2014). "Inflammatory pathways of seizure disorders." Trends Neurosci **37**(2): 55-65.

Martín-García, E., F. Mannara, J. Gutiérrez-Cuesta, L. Sabater, J. Dalmau, R. Maldonado and F. Graus (2013). "Intrathecal injection of P/Q type voltage-gated calcium channel antibodies from paraneoplastic cerebellar degeneration cause ataxia in mice." Journal of Neuroimmunology **261**(1–2): 53-59.

Marx, C. E., J. Lee, M. Subramaniam, A. Rapisarda, D. C. Bautista, E. Chan, J. D. Kilts, R. W. Buchanan, E. P. Wai, S. Verma, K. Sim, J. Hariram, R. Jacob, R. S. Keefe and S. A. Chong (2014). "Proof-of-concept randomized controlled trial of pregnenolone in schizophrenia." Psychopharmacology (Berl) **231**(17): 3647-3662.

Mathis, C., S. M. Paul and J. N. Crawley (1994). "The neurosteroid pregnenolone sulfate blocks NMDA antagonist-induced deficits in a passive avoidance memory task." Psychopharmacology (Berl) **116**(2): 201-206.

McKnight, K., Y. Jiang, Y. Hart, A. Cavey, S. Wroe, M. Blank, Y. Shoenfeld, A. Vincent, J. Palace and B. Lang (2005). "Serum antibodies in epilepsy and seizure-associated disorders." Neurology **65**(11): 1730-1736.

Mikasova, L., P. De Rossi, D. Bouchet, F. Georges, V. Rogemond, A. Didelot, C. Meissirel, J. Honnorat and L. Groc (2012). "Disrupted surface cross-talk between NMDA and Ephrin-B2 receptors in anti-NMDA encephalitis." Brain **135**(Pt 5): 1606-1621.

Mikati, M. A., R. Saab, M. N. Fayad and R. N. Choueiri (2002). "Efficacy of intravenous immunoglobulin in Landau-Kleffner syndrome." Pediatr Neurol **26**(4): 298-300.

Mohammad, S. S., K. Sinclair, S. Pillai, V. Merheb, T. D. Aumann, D. Gill, R. C. Dale and F. Brilot (2014). "Herpes simplex encephalitis relapse with chorea is associated with autoantibodies to N-Methyl-D-aspartate receptor or dopamine-2 receptor." Mov Disord **29**(1): 117-122.

Mohn, A. R., R. R. Gainetdinov, M. G. Caron and B. H. Koller (1999). "Mice with reduced NMDA receptor expression display behaviors related to schizophrenia." Cell **98**(4): 427-436.

Monjauze, C., H. Broadbent, S. G. Boyd, B. G. Neville and T. Baldeweg (2011). "Language deficits and altered hemispheric lateralization in young people in remission from BECTS." Epilepsia **52**(8): e79-83.

Moscato, E. H., X. Peng, A. Jain, T. D. Parsons, J. Dalmau and R. J. Balice-Gordon (2014). "Acute mechanisms underlying antibody effects in anti-N-methyl-D-aspartate receptor encephalitis." Ann Neurol **76**(1): 108-119.

Nabbout, R., M. Mazzuca, P. Hubert, S. Peudennier, C. Allaire, V. Flurin, M. Aberastury, W. Silva and O. Dulac (2010). "Efficacy of ketogenic diet in severe refractory status epilepticus initiating fever induced refractory epileptic encephalopathy in school age children (FIRES)." Epilepsia **51**(10): 2033-2037.

Newsom-Davis, J. (2005). "Neuromuscular junction channelopathies: a brief overview." Acta Neurol Belg **105**(4): 181-186.

Newsom-Davis, J., A. Vincent, S. G. Wilson, C. D. Ward, A. J. Pinching and C. Hawkey (1978). "[Plasmapheresis for myasthenia gravis]." N Engl J Med **298**(8): 456-457.

Niehusmann, P., J. Dalmau, C. Rudlowski, A. Vincent, C. E. Elger, J. E. Rossi and C. G. Bien (2009). "Diagnostic value of N-methyl-D-aspartate receptor antibodies in women with new-onset epilepsy." Arch Neurol **66**(4): 458-464.

Nosadini, M., C. Boniver, L. Zuliani, L. de Palma, E. Cainelli, P. A. Battistella, I. Toldo, A. Suppiej and S. Sartori (2014). "Longitudinal Electroencephalographic (EEG) Findings in Pediatric Anti-N-Methyl-D-Aspartate (Anti-NMDA) Receptor Encephalitis: The Padua Experience." J Child Neurol.

Ohkawa, T., Y. Fukata, M. Yamasaki, T. Miyazaki, N. Yokoi, H. Takashima, M. Watanabe, O. Watanabe and M. Fukata (2013). "Autoantibodies to epilepsy-related LGI1 in limbic encephalitis neutralize LGI1-ADAM22 interaction and reduce synaptic AMPA receptors." J Neurosci **33**(46): 18161-18174.

Ohtani, Y., T. Irie, K. Uekama, K. Fukunaga and J. Pitha (1989). "Differential effects of alpha-, beta- and gamma-cyclodextrins on human erythrocytes." Eur J Biochem **186**(1-2): 17-22.

Ong, M. S., I. S. Kohane, T. Cai, M. P. Gorman and K. D. Mandl (2014). "Population-Level Evidence for an Autoimmune Etiology of Epilepsy." JAMA Neurol.

Ottinger, E. A., M. L. Kao, N. Carrillo-Carrasco, N. Yanjanin, R. K. Shankar, M. Janssen, M. Brewster, I. Scott, X. Xu, J. Cradock, P. Terse, S. J. Dehdashti, J. Marugan, W. Zheng, L. Portilla, A. Hubbs, W. J. Pavan, J. Heiss, H. V. C, S. U. Walkley, D. S. Ory, S. A. Silber, F. D. Porter, C. P. Austin and J. C. McKew (2014). "Collaborative development of 2-hydroxypropyl-beta-cyclodextrin for the treatment of Niemann-Pick type C1 disease." Curr Top Med Chem **14**(3): 330-339.

Ottman, R., M. R. Winawer, S. Kalachikov, C. Barker-Cummings, T. C. Gilliam, T. A. Pedley and W. A. Hauser (2004). "LGI1 mutations in autosomal dominant partial epilepsy with auditory features." Neurology **62**(7): 1120-1126.

Pakozdy, A., P. Halasz, A. Klang, J. Bauer, M. Leschnik, A. Tichy, J. G. Thalhammer, B. Lang and A. Vincent (2013). "Suspected limbic encephalitis and seizure in cats associated with voltage-gated potassium channel (VGKC) complex antibody." J Vet Intern Med **27**(1): 212-214.

Palace, J. and B. Lang (2000). "Epilepsy: an autoimmune disease?" J Neurol Neurosurg Psychiatry **69**(6): 711-714.

Partridge, L. D. and C. F. Valenzuela (2001). "Neurosteroid-induced enhancement of glutamate transmission in rat hippocampal slices." Neurosci Lett **301**(2): 103-106.

Paterson, R. W., M. S. Zandi, R. Armstrong, A. Vincent and J. M. Schott (2013).

"Clinical relevance of positive voltage-gated potassium channel (VGKC)-complex antibodies: experience from a tertiary referral centre." J Neurol Neurosurg Psychiatry.
Patterson, J. L., S. A. Carapetian, J. R. Hageman and K. R. Kelley (2013). "Febrile seizures." Pediatr Ann **42**(12): 249-254.

Pellkofer, H. L., T. Kuempfel, L. Jacobson, A. Vincent and T. Derfuss (2010). "Non-paraneoplastic limbic encephalitis associated with NMDAR and VGKC antibodies." J Neurol Neurosurg Psychiatry **81**(12): 1407-1408.

Peltola, J., P. Kulmala, J. Isojarvi, A. Saiz, K. Latvala, J. Palmio, K. Savola, M. Knip, T. Keranen and F. Graus (2000). "Autoantibodies to glutamic acid decarboxylase in patients with therapy-resistant epilepsy." Neurology **55**(1): 46-50.

Penagarikano, O., B. S. Abrahams, E. I. Herman, K. D. Winden, A. Gdalyahu, H. Dong, L. I. Sonnenblick, R. Gruver, J. Almajano, A. Bragin, P. Golshani, J. T. Trachtenberg, E. Peles and D. H. Geschwind (2011). "Absence of CNTNAP2 leads to epilepsy, neuronal migration abnormalities, and core autism-related deficits." Cell **147**(1): 235-246.

Petit-Pedrol, M., T. Armangue, X. Peng, L. Bataller, T. Cellucci, R. Davis, L. McCracken, E. Martinez-Hernandez, W. P. Mason, M. C. Kruer, D. G. Ritacco, W. Grisold, B. F. Meaney, C. Alcala, P. Sillevis-Smitt, M. J. Titulaer, R. Balice-Gordon, F. Graus and J. Dalmau (2014). "Encephalitis with refractory seizures, status epilepticus, and antibodies to the GABAA receptor: a case series, characterisation of the antigen, and analysis of the effects of antibodies." Lancet Neurol **13**(3): 276-286.

Planaguma, J., F. Leypoldt, F. Mannara, J. Gutierrez-Cuesta, E. Martin-Garcia, E. Aguilar, M. J. Titulaer, M. Petit-Pedrol, A. Jain, R. Balice-Gordon, M. Lakadamyali, F. Graus, R. Maldonado and J. Dalmau (2014). "Human N-methyl D-aspartate receptor antibodies alter memory and behaviour in mice." Brain.

Poliak, S., L. Gollan, R. Martinez, A. Custer, S. Einheber, J. L. Salzer, J. S. Trimmer, P. Shrager and E. Peles (1999). "Caspr2, a new member of the neurexin superfamily, is localized at the juxtaparanodes of myelinated axons and associates with K+ channels." Neuron **24**(4): 1037-1047.

Poliak, S., D. Salomon, H. Elhanany, H. Sabanay, B. Kiernan, L. Pevny, C. L. Stewart, X. Xu, S. Y. Chiu, P. Shrager, A. J. Furley and E. Peles (2003). "Juxtaparanodal clustering of Shaker-like K+ channels in myelinated axons depends on Caspr2 and TAG-1." J Cell Biol **162**(6): 1149-1160.

Pontikis, C. C., C. D. Davidson, S. U. Walkley, F. M. Platt and D. J. Begley (2013). "Cyclodextrin alleviates neuronal storage of cholesterol in Niemann-Pick C disease without evidence of detectable blood-brain barrier permeability." J Inherit Metab Dis **36**(3): 491-498.

Quek, A. M., J. W. Britton, A. McKeon, E. So, V. A. Lennon, C. Shin, C. Klein, R. E. Watson, Jr., A. L. Kotsenas, T. D. Lagerlund, G. D. Cascino, G. A. Worrell, E. C. Wirrell, K. C. Nickels, A. J. Aksamit, K. H. Noe and S. J. Pittock (2012). "Autoimmune epilepsy: clinical characteristics and response to immunotherapy." Arch Neurol **69**(5): 582-593.

Rajabzadeh, A., A. E. Bideskan, A. Fazel, M. Sankian, H. Rafatpanah and H. Haghir (2012). "The effect of PTZ-induced epileptic seizures on hippocampal expression of PSA-NCAM in offspring born to kindled rats." J Biomed Sci **19**: 56.

Rasmussen, T., J. Olszewski and D. Lloydsmith (1958). "Focal seizures due to chronic localized encephalitis." Neurology **8**(6): 435-445.

Rho, J. M. (2004). "Basic science behind the catastrophic epilepsies." Epilepsia **45 Suppl 5**: 5-11.

Ribeiro, P. A., L. Sbragia, R. Gilioli, F. Langone, F. F. Conte and I. Lopes-Cendes (2008). "Expression profile of Lgi1 gene in mouse brain during development." J Mol Neurosci **35**(3): 323-329.

Riikonen, R. (2014). "Recent advances in the pharmacotherapy of infantile spasms." CNS Drugs **28**(4): 279-290.

Rivers, T. M. and F. F. Schwentker (1935). Encephalomyeltis accompanied by myelin destruction experimentally produced in monkeys. J Exp Med **61**(5): 689-702.

Rodenas-Cuadrado, P., J. Ho and S. C. Vernes (2014). "Shining a light on CNTNAP2: complex functions to complex disorders." Eur J Hum Genet **22**(2): 171-178.

Rogers, S. W., P. I. Andrews, L. C. Gahring, T. Whisenand, K. Cauley, B. Crain, T. E. Hughes, S. F. Heinemann and J. O. McNamara (1994). "Autoantibodies to glutamate receptor GluR3 in Rasmussen's encephalitis." Science **265**(5172): 648-651.

Roitt, I. M., D. Doniach, P. N. Campbell and R. V. Hudson (1956). "Auto-antibodies in Hashimoto's disease (lymphadenoid goitre)." Lancet **271**(6947): 820-821.

Rose, N. R. and C. Bona (1993). "Defining criteria for autoimmune diseases (Witebsky's postulates revisited)." Immunol Today **14**(9): 426-430.

Rosenfeld, M. R., M. J. Titulaer and J. Dalmau (2012). "Paraneoplastic syndromes and autoimmune encephalitis: Five new things." Neurol Clin Pract **2**(3): 215-223.

Saadoun, S., P. Waters, B. A. Bell, A. Vincent, A. S. Verkman and M. C. Papadopoulos (2010). "Intra-cerebral injection of neuromyelitis optica immunoglobulin G and human complement produces neuromyelitis optica lesions in mice." Brain **133**(Pt 2): 349-361.

Saiz, A., Y. Blanco, L. Sabater, F. Gonzalez, L. Bataller, R. Casamitjana, L. Ramio-Torrenta and F. Graus (2008). "Spectrum of neurological syndromes associated with glutamic acid decarboxylase antibodies: diagnostic clues for this association." Brain **131**(Pt 10): 2553-2563.

Sanchez Fernandez, I., K. E. Chapman, J. M. Peters, C. Harini, A. Rotenberg and T. Loddenkemper (2013). "Continuous Spikes and Waves during Sleep: Electroclinical Presentation and Suggestions for Management." Epilepsy Res Treat **2013**: 583531.

Sarkis, R. A., R. Nehme and Z. N. Chemali (2014). "Neuropsychiatric and seizure outcomes in nonparaneoplastic autoimmune limbic encephalitis." Epilepsy Behav **39c**: 21-25.

Sayyah, M., M. Javad-Pour and M. Ghazi-Khansari (2003). "The bacterial endotoxin lipopolysaccharide enhances seizure susceptibility in mice: involvement of proinflammatory factors: nitric oxide and prostaglandins." Neuroscience **122**(4): 1073-1080.

Schmitt, S. E., K. Pargeon, E. S. Frechette, L. J. Hirsch, J. Dalmau and D. Friedman (2012). "Extreme delta brush: a unique EEG pattern in adults with anti-NMDA receptor encephalitis." Neurology **79**(11): 1094-1100.

Schulte, U., J. O. Thumfart, N. Klocker, C. A. Sailer, W. Bildl, M. Biniossek, D. Dehn, T. Deller, S. Eble, K. Abbass, T. Wangler, H. G. Knaus and B. Fakler (2006). "The epilepsy-linked Lgi1 protein assembles into presynaptic Kv1 channels and inhibits inactivation by Kvbeta1." Neuron **49**(5): 697-706.

Shimada, T. and T. Takemiya (2014). "Role of Inflammatory Mediators in the Pathogenesis of Epilepsy." **2014**: 901902.

Singh, S. P. and V. Singh (2011). "Meta-analysis of the efficacy of adjunctive NMDA receptor modulators in chronic schizophrenia." CNS Drugs **25**(10): 859-885.

Smith, C. C., T. T. Gibbs and D. H. Farb (2014). "Pregnenolone sulfate as a modulator of synaptic plasticity." Psychopharmacology (Berl) **231**(17): 3537-3556.

Solimena, M., F. Folli, R. Aparisi, G. Pozza and P. De Camilli (1990). "Autoantibodies to GABA-ergic neurons and pancreatic beta cells in stiff-man syndrome." N Engl J Med **322**(22): 1555-1560.

Sommer, C., A. Weishaupt, J. Brinkhoff, L. Biko, C. Wessig, R. Gold and K. V. Toyka (2005). "Paraneoplastic stiff-person syndrome: passive transfer to rats by means of IgG antibodies to amphiphysin." Lancet **365**(9468): 1406-1411.

Sooksawate, T. and M. A. Simmonds (2001). "Influence of membrane cholesterol on modulation of the GABA(A) receptor by neuroactive steroids and other potentiators." Br J Pharmacol **134**(6): 1303-1311.

Stogmann, E., E. Reinthaler, S. Eltawil, M. A. El Etribi, M. Hemeda, N. El Nahhas, A. M. Gaber, A. Fouad, S. Edris, A. Benet-Pages, S. H. Eck, E. Pataraia, D. Mei, A. Brice, S. Lesage, R. Guerrini, F. Zimprich, T. M. Strom and A. Zimprich (2013). "Autosomal recessive cortical myoclonic tremor and epilepsy: association with a mutation in the potassium channel associated gene CNTN2." Brain **136**(Pt 4): 1155-1160.

Strauss, K. A., E. G. Puffenberger, M. J. Huentelman, S. Gottlieb, S. E. Dobrin, J. M. Parod, D. A. Stephan and D. H. Morton (2006). "Recessive symptomatic focal epilepsy and mutant contactin-associated protein-like 2." N Engl J Med **354**(13): 1370-1377.

Sukhotinsky, I., A. M. Chan, O. J. Ahmed, V. R. Rao, V. Gradinaru, C. Ramakrishnan, K. Deisseroth, A. K. Majewska and S. S. Cash (2013). "Optogenetic delay of status epilepticus onset in an in vivo rodent epilepsy model." PLoS One **8**(4): e62013.

Suleiman, J., T. Brenner, D. Gill, F. Brilot, J. Antony, A. Vincent, B. Lang and R. C. Dale (2011). "VGKC antibodies in pediatric encephalitis presenting with status epilepticus." Neurology **76**(14): 1252-1255.

Suleiman, J., T. Brenner, D. Gill, C. Troedson, A. J. Sinclair, F. Brilot, A. Vincent, B. Lang and R. C. Dale (2011). "Immune-mediated steroid-responsive epileptic spasms and epileptic encephalopathy associated with VGKC-complex antibodies." Dev Med Child Neurol **53**(11): 1058-1060.

Suleiman, J., F. Brilot, B. Lang, A. Vincent and R. C. Dale (2013). "Autoimmune epilepsy in children: case series and proposed guidelines for identification." Epilepsia **54**(6): 1036-1045.

Suleiman, J., S. Wright, D. Gill, F. Brilot, P. Waters, K. Peacock, P. Procopis, A. Nibber, A. Vincent, R. C. Dale and B. Lang (2013). "Autoantibodies to neuronal

antigens in children with new-onset seizures classified according to the revised ILAE organization of seizures and epilepsies." Epilepsia **54**(12): 2091-2100.

Szots, M., A. Marton, F. Kover, T. Kiss, T. Berki, F. Nagy and Z. Illes (2014). "Natural course of LGI1 encephalitis: 3-5 years of follow-up without immunotherapy." J Neurol Sci **343**(1-2): 198-202.

Titulaer, M. J. and J. Dalmau (2014). "Seizures as first symptom of anti-NMDA receptor encephalitis are more common in men." Neurology **82**(7): 550-551.

Titulaer, M. J., B. Lang and J. J. Verschuuren (2011). "Lambert-Eaton myasthenic syndrome: from clinical characteristics to therapeutic strategies." Lancet Neurol **10**(12): 1098-1107.

Titulaer, M. J., L. McCracken, I. Gabilondo, T. Armangue, C. Glaser, T. Iizuka, L. S. Honig, S. M. Benseler, I. Kawachi, E. Martinez-Hernandez, E. Aguilar, N. Gresa-Arribas, N. Ryan-Florance, A. Torrents, A. Saiz, M. R. Rosenfeld, R. Balice-Gordon, F. Graus and J. Dalmau (2013). "Treatment and prognostic factors for long-term outcome in patients with anti-NMDA receptor encephalitis: an observational cohort study." Lancet Neurol **12**(2): 157-165.

Toledano, M., J. W. Britton, A. McKeon, C. Shin, V. A. Lennon, A. M. Quek, E. So, G. A. Worrell, G. D. Cascino, C. J. Klein, T. D. Lagerlund, E. C. Wirrell, K. C. Nickels and S. J. Pittock (2014). "Utility of an immunotherapy trial in evaluating patients with presumed autoimmune epilepsy." Neurology.

Tonnesen, J., A. T. Sorensen, K. Deisseroth, C. Lundberg and M. Kokaia (2009). "Optogenetic control of epileptiform activity." Proc Natl Acad Sci U S A **106**(29): 12162-12167.

Toyka, K. V., D. B. Brachman, A. Pestronk and I. Kao (1975). "Myasthenia gravis: passive transfer from man to mouse." Science **190**(4212): 397-399.

Toyka, K. V., D. B. Drachman, D. E. Griffin, A. Pestronk, J. A. Winkelstein, K. H. Fishbeck and I. Kao (1977). "Myasthenia gravis. Study of humoral immune mechanisms by passive transfer to mice." N Engl J Med **296**(3): 125-131.

Tsiotra, P. C., D. Karagogeos, K. Theodorakis, T. M. Michaelidis, W. S. Modi, A. J. Furley, T. M. Jessell and J. Papamatheakis (1993). "Isolation of the cDNA and chromosomal localization of the gene (TAX1) encoding the human axonal glycoprotein TAG-1." Genomics **18**(3): 562-567.

Turkay, S., E. Baskin, S. Dener, A. Gultekin, F. Tanzer and E. Sekreter (1996). "Immune globulin treatment in intractable epilepsy of childhood." Turk J Pediatr **38**(3): 301-305.

van Baalen, A., M. Hausler, B. Plecko-Startinig, J. Strautmanis, S. Vlaho, B. Gebhardt, A. Rohr, A. Abicht, G. Kluger, U. Stephani, C. Probst, A. Vincent and C. G. Bien (2012). "Febrile infection-related epilepsy syndrome without detectable autoantibodies and response to immunotherapy: a case series and discussion of epileptogenesis in FIRES." Neuropediatrics **43**(4): 209-216.

van Campen, J. S., F. E. Jansen, O. F. Brouwer, J. Nicolai and K. P. Braun (2013). "Interobserver agreement of the old and the newly proposed ILAE epilepsy classification in children." Epilepsia **54**(4): 726-732.

Varadkar, S., C. G. Bien, C. A. Kruse, F. E. Jensen, J. Bauer, C. A. Pardo, A. Vincent, G. W. Mathern and J. H. Cross (2014). "Rasmussen's encephalitis: clinical features, pathobiology, and treatment advances." Lancet Neurol **13**(2): 195-205.

Veri, K., O. Uibo, T. Talvik, I. Talvik, K. Metskula, A. Napa, U. Vaher, E. Oiglane-Slik, R. Rein, A. Kolk, A. Traat and R. Uibo (2013). "Newly-diagnosed pediatric epilepsy is associated with elevated autoantibodies to glutamic acid decarboxylase but not cardiolipin." Epilepsy Res **105**(1-2): 86-91.

Vezzani, A., J. French, T. Bartfai and T. Z. Baram (2011). "The role of inflammation in epilepsy." Nat Rev Neurol **7**(1): 31-40.

Viaccoz, A., V. Desestret, F. Ducray, G. Picard, G. Cavillon, V. Rogemond, J. C. Antoine, J. Y. Delattre and J. Honnorat (2014). "Clinical specificities of adult male patients with NMDA receptor antibodies encephalitis." Neurology **82**(7): 556-563.
Vincent, A. (2002). "Unravelling the pathogenesis of myasthenia gravis." Nat Rev Immunol **2**(10): 797-804.

Vincent, A., C. Buckley, J. M. Schott, I. Baker, B. K. Dewar, N. Detert, L. Clover, A. Parkinson, C. G. Bien, S. Omer, B. Lang, M. N. Rossor and J. Palace (2004). "Potassium channel antibody-associated encephalopathy: a potentially immunotherapy-responsive form of limbic encephalitis." Brain **127**(Pt 3): 701-712.

Vincent, A., P. Waters, M. I. Leite, L. Jacobson, I. Koneczny, J. Cossins and D. Beeson (2012). "Antibodies identified by cell-based assays in myasthenia gravis and associated diseases." Ann N Y Acad Sci **1274**: 92-98.

Waters, P. and A. Vincent (2008). "Detection of anti-aquaporin-4 antibodies in neuromyelitis optica: current status of the assays." Int MS J **15**(3): 99-105.

Watson, R., Y. Jiang, I. Bermudez, L. Houlihan, L. Clover, K. McKnight, J. H. Cross, I. K. Hart, A. Roubertie, J. Valmier, Y. Hart, J. Palace, D. Beeson, A. Vincent and B. Lang (2004). "Absence of antibodies to glutamate receptor type 3 (GluR3) in Rasmussen encephalitis." Neurology **63**(1): 43-50.

Weiergraber, M., M. Henry, A. Krieger, M. Kamp, K. Radhakrishnan, J. Hescheler and T. Schneider (2006). "Altered seizure susceptibility in mice lacking the Ca(v)2.3 E-type Ca2+ channel." Epilepsia **47**(5): 839-850.

Witebsky, E., N. R. Rose, K. Terplan, J. R. Paine and R. W. Egan (1957). "Chronic thyroiditis and autoimmunization." J Am Med Assoc **164**(13): 1439-1447.

Wong, P., C. C. Chang, C. E. Marx, M. G. Caron, W. C. Wetsel and X. Zhang (2012). "Pregnenolone rescues schizophrenia-like behavior in dopamine transporter knockout mice." PLoS One **7**(12): e51455.

Wright S., Y. Hacohen, L. Jacobson, S. Agrawal, R. Gupta, S. Philip, M. Smoith, M. Lim, E. Wassmer, A. Vincent (2014). N-methyl-D-aspartate antibody-mediated neurological disease: results of a UK-based surveillance study in children. Arch Dis Child *in press*

Wykes, R. C., J. H. Heeroma, L. Mantoan, K. Zheng, D. C. MacDonald, K. Deisseroth, K. S. Hashemi, M. C. Walker, S. Schorge and D. M. Kullmann (2012). "Optogenetic and potassium channel gene therapy in a rodent model of focal neocortical epilepsy." Sci Transl Med **4**(161): 161ra152.

Xiong, Z. Q., W. Qian, K. Suzuki and J. O. McNamara (2003). "Formation of complement membrane attack complex in mammalian cerebral cortex evokes seizures and neurodegeneration." J Neurosci **23**(3): 955-960.

Yang, R., L. Chen, H. Wang, B. Xu, H. Tomimoto and L. Chen (2012). "Anti-amnesic effect of neurosteroid PREGS in Abeta25-35-injected mice through sigma1 receptor- and alpha7nAChR-mediated neuroprotection." Neuropharmacology **63**(6): 1042-1050.

Yoshimoto, T., M. Doi, N. Fukai, H. Izumiyama, T. Wago, I. Minami, I. Uchimura and Y. Hirata (2005). "Type 1 diabetes mellitus and drug-resistant epilepsy: presence of high titer of anti-glutamic acid decarboxylase autoantibodies in serum and cerebrospinal fluid." Intern Med **44**(11): 1174-1177.

Zandi, M. S., S. R. Irani, G. Follows, A. M. Moody, P. Molyneux and A. Vincent (2009). "Limbic encephalitis associated with antibodies to the NMDA receptor in Hodgkin lymphoma." Neurology **73**(23): 2039-2040.

Zandi, M. S., R. W. Paterson, M. A. Ellul, L. Jacobson, A. Al-Diwani, J. L. Jones, A. L. Cox, B. Lennox, M. Stamelou, K. P. Bhatia, J. M. Schott, A. J. Coles, D. M. Kullmann and A. Vincent (2014). "Clinical relevance of serum antibodies to extracellular N-methyl-d-aspartate receptor epitopes." J Neurol Neurosurg Psychiatry.

Zhang, Q., K. Tanaka, P. Sun, M. Nakata, R. Yamamoto, K. Sakimura, M. Matsui and N. Kato (2012). "Suppression of synaptic plasticity by cerebrospinal fluid from anti-NMDA receptor encephalitis patients." Neurobiol Dis **45**(1): 610-615.

Zheng, P. (2009). "Neuroactive steroid regulation of neurotransmitter release in the CNS: action, mechanism and possible significance." Prog Neurobiol **89**(2): 134-152.

Zuliani, L., F. Graus, B. Giometto, C. Bien and A. Vincent (2012). "Central nervous system neuronal surface antibody associated syndromes: review and guidelines for recognition." J Neurol Neurosurg Psychiatry **83**(6): 638-645.

CHAPTER 9 - APPENDICES

9.1 APPENDIX 1

ImageJ Macro for fluorescence intensity measurements

```
getRawStatistics(area, mean, min, max, std, h);
  for (i=1; i< h.length; i++)
     h[i] = h[i-1]+h[i];
  Plot.create("Cumulative Histogram of "+getTitle, "Value", "Sum of pixel count", h);
Plot.show();
//end
```

9.2 APPENDIX 2

Animal Welfare Score Sheet

9.3 APPENDIX 3

MATLAB Manual for neuroarchiver written by J Heeroma and K Zheng (UCL)

9.4 APPENDIX 4

ILAE Revised Terminology for Organisation of Seizures and Epilepsies 2011-2013